

**ATTACHMENT 2Q
DERIVATION OF SSLs FOR RADIOLOGICAL SRCs
USDOE/NNSA PANTEX PLANT
AMARILLO, TEXAS**

TABLE OF CONTENTS

2Q.0 SOIL SCREENING LEVELS FOR THE MIGRATION TO GROUNDWATER PATHWAY..	2Q-1
2Q.1 INTRODUCTION.....	2Q-1
2Q.2 EPA SOIL SCREENING LEVELS.....	2Q-1
2Q.2.1 EPA Generic SSLs.....	2Q-1
2Q.2.2 EPA SSLs with Site-Specific Input Parameters.....	2Q-1
2Q.3 CALCULATION OF SITE-SPECIFIC SSLs.....	2Q-5
2Q.3.1 Vadose Zone Attenuation Factor Modeling.....	2Q-7
2Q.3.2 Site-Specific SSLs	2Q-12
2Q.4 SUMMARY AND CONCLUSIONS	2Q-13

List of Tables

Table 2Q-1. K_d Values for Blackwater Draw and Upper Ogallala Sediments.....	2Q-3
Table 2Q-2. EPA PRG Calculator Method 2 Site-Specific Input Values	2Q-3
Table 2Q-3. EPA Activity-Based SSLs for Migration to Groundwater	2Q-4
Table 2Q-4. EPA Mass-Based SSLs for Migration to Groundwater	2Q-4
Table 2Q-5. Analytic Model Conceptual Discretization (SWMU 39).....	2Q-11
Table 2Q-6. Calculation of Water Saturation	2Q-11
Table 2Q-7. Average Saturation	2Q-11
Table 2Q-8. Water Travel Time.....	2Q-11
Table 2Q-9. Model Results (Playa Recharge Scenario).....	2Q-12
Table 2Q-10. Alternative Analysis Comparison (Playa Recharge Scenario)	2Q-12
Table 2Q-11. Calculation of Site-Specific SSLs (Playa Recharge Scenario).....	2Q-13
Table 2Q-12. SSLs for Migration to Groundwater (Playa Recharge Scenario).....	2Q-13

List of Equations

Equation 2Q-1. Soil/Water Partition Equation	2Q-6
Equation 2Q-2. Vadose Zone Attenuation Factor.....	2Q-7
Equation 2Q-3. Analytic Model for Calculating the Vadose Zone Attenuation Factor.....	2Q-8
Equation 2Q-4. Width of Source Pulse	2Q-9
Equation 2Q-5. Van Genuchten-Mualem Model of Relative Permeability and Effective Saturation.....	2Q-9
Equation 2Q-6. Total Saturation	2Q-10
Equation 2Q-7. Advective Travel Time.....	2Q-10
Equation 2Q-8. Retardation Factor	2Q-10

List of Supplemental Information

Analytical Solution to the One-Dimensional Advection Dispersion Equation
Sorption of Uranium on Blackwater Draw Sediments

2Q.0 SOIL SCREENING LEVELS FOR THE MIGRATION TO GROUNDWATER PATHWAY

2Q.1 INTRODUCTION

This attachment documents the calculation of SSLs to be used as PRGs for evaluation of the soil to groundwater pathway (methods for evaluation are included in Section 4.4 of the Main Text). EPA's Soil Screening Guidance for Radionuclides provides generic SSLs for use where site-specific data are limited and also provides a methodology for calculation of risk-based, site-specific SSLs. As stated in *Soil Screening Guidance for Radionuclides: Technical Background Document* (EPA/540-R-00-006 October 2000), the methodology for calculating SSLs for the migration to groundwater pathway was developed with flexibility to allow adjustments for site-specific conditions when adequate information is available. This flexibility allows for the use of unsaturated zone fate and transport models to extend the applicability of SSLs to subsurface conditions that are not adequately addressed by the simple, standardized equations.

The SSL methodology was designed for use during the early stages of site evaluation when information about subsurface conditions may be limited. Therefore, conservative simplifying assumptions about the release and transport of contaminants in the subsurface have been incorporated into EPA's default calculations. Because site investigations at Pantex Plant have been completed, much more detailed site-specific information is available, and many of the simplifying assumptions built into the SSL methodology are not applicable.

Unsaturated zone analytic fate and transport models were used to calculate site-specific SSLs for the migration to groundwater pathway for Pantex Plant. The procedures outlined in *Soil Screening Guidance for Radionuclides: Technical Background Document* were implemented to determine site-specific SSLs that are conservative and representative of site conditions, such as the thick vadose zones found at Pantex Plant. For comparison purposes, generic SSLs were obtained from the PRGs for Radionuclides website (<http://epa-prgs.ornl.gov/radionuclides/>), and site-specific SSLs based on the default SSL methodology were calculated using EPA's Radionuclide PRGs for Superfund Electronic Calculator.

The SSLs developed here are proposed for use as PRGs for evaluation of the soil to groundwater pathway. The Soil Screening Guidance for Radionuclides states that SSLs can be used as PRGs provided that conditions found at a specific site are similar to conditions assumed in developing SSLs (EPA, 2000).

2Q.2 EPA SOIL SCREENING LEVELS

2Q.2.1 EPA Generic SSLs

EPA provides generic SSLs derived using default input parameters in the standardized equations established for the SSL methodology described in the *Soil Screening Guidance for Radionuclides*. For the migration to groundwater pathway, the generic SSLs are back-calculated from the promulgated MCL for each contaminant. MCLs and generic SSLs for the Pantex Plant radiological site-related contaminants (SRCs) were obtained from the PRGs for Radionuclides website (<http://epa-prgs.ornl.gov/radionuclides/>).

2Q.2.2 EPA SSLs with Site-Specific Input Parameters

SSLs based on the default SSL methodology with site-specific input values were calculated using EPA's Radionuclide PRGs for Superfund Electronic Calculator (<http://risk.lsd.ornl.gov/rad-ssg/radssl1.shtml>). The PRG Calculator provides two methods for calculation of SSLs. The first method employs the

partitioning equation used to calculate the generic SSLs, but allows use of site-specific distribution coefficients. The second method uses a mass-limit equation with site-specific input values. For a complete description of the two calculation methods, refer to the *Soil Screening Guidance for Radionuclides: Technical Background Document* (EPA, 2000).

2Q.2.2.1 Site-Specific Distribution Coefficients

For method 1, site-specific distribution coefficient (K_d) values were used in place of the default values to represent partitioning of the radionuclide between water and soil. K_d is the ratio of the mass of radionuclide in the soil to the mass in the water. Laboratory flow-through column studies have recently been completed to provide site-specific measurements of uranium sorption. Results of these laboratory studies are documented in *Sorption of Uranium on Blackwater Draw Sediments* (Rainwater, et al. 2006). This document is provided as Attachment 2Q. Site-specific K_d values for the other SRCs were estimated from the values presented in the guidance document (EPA, 2000) and *Understanding Variation in Partition Coefficient, K_d , Values* (EPA 402-R-99-004B August 1999). Conservative values at the low end of the published K_d s that are representative of Pantex Plant site conditions were selected for use according to the following methodology.

Soils with higher clay content tend to have higher affinity for metals and radionuclides when compared to sands. This increased affinity translates into higher K_d values and slower migration of radionuclides. The Blackwater Draw material comprises primarily silts and clays with some very fine sands. Based on the analysis of 283 samples from the Blackwater Draw, the average soil texture is 36 percent clay, 48 percent silt, and 15 percent sand (note the totals only add up to 99 percent due to rounding errors in the average calculations for each grain size). The Blackwater Draw Formation soils are USDA classified as silty clay loam based on the average soil texture.

The upper Ogallala Formation sediments comprise primarily very fine-grained eolian sands. Based on the analysis of 27 samples from the upper Ogallala Formation sediments, the average soil texture is 6 percent clay, 26 percent silt, and 67 percent sand (note the totals only add up to 99 percent due to rounding errors in the average calculations for each grain size). The upper Ogallala Formation soils are USDA classified as sandy loam based on the average soil texture.

Soil pH is also an important consideration in the selection of appropriate K_d values. The pH observed in the shallow soils (i.e., upper 10 ft) range from 5 to 9. Measurements from greater depths in the Blackwater Draw and upper Ogallala sediments are not available. pH measurements are available for perched groundwater samples and typically range from slightly acidic to slightly basic with most measurements in the 6 to 8 range.

Table 2Q-1 presents the selected values and rationale. In this analysis, lower than expected, conservative K_d values were used for calculating SSLs. Lower K_d values result in higher groundwater concentrations.

Table 2Q-1. K_d Values for Blackwater Draw and Upper Ogallala Sediments

SRC	K_d (L/Kg)			Source	Rationale
	EPA Default	Blackwater Draw	Upper Ogallala		
³ H	0	0	0	EPA 2000	Default value from Table 5-3.
²³² Th	20	1,700	1,700	EPA 2000	Lowest published value from Table 5-8 for pH of 5 to 8.
²³⁹ Pu	5	380	5	EPA 2000	Lowest values published in Table 5-6 based upon the clay content of the Blackwater Draw (36%) and upper Ogallala sediments (6%).
Uranium	0.4	22	0.4	Rainwater, et al. 2006, EPA 2000	Blackwater Draw: Rainwater, et al. (2006) present an average value for uranium based on the results of laboratory flow-through column experiments using Blackwater Draw soils. Upper Ogallala Formation: Default value from Table 5-3 (EPA, 2000).

2Q.2.2.2 Method 1. Partitioning Equation for Migration to Groundwater

Using method 1, SSLs were calculated using the PRG Calculator with default input values for dilution factor, water-filled soil porosity, and dry soil bulk density and site-specific K_{ds} presented in Table 2Q-1.

2Q.2.2.3 Method 2. Mass-Limit Equation for Migration to Groundwater

Using method 2, SSLs were calculated using the PRG Calculator with site-specific input values and site-specific K_{ds} . Method 2 requires that the user input site-specific values for infiltration rate, average source depth, aquifer hydraulic conductivity, hydraulic gradient, source length parallel to groundwater flow, and aquifer thickness.

Because of the semi-arid climate and flat topography, recharge (or infiltration) rates at Pantex Plant vary greatly depending on water availability. Recharge is focused beneath areas of the Plant that collect surface water runoff, specifically ditches and playas. Recharge beneath upland, or interplaya, areas is negligible because of evapotranspiration processes and runoff. Because recharge is the primary transport mechanism for the movement of radionuclides through the soil column, SSLs were developed for the highest and lowest recharge rates estimated at Pantex Plant. For this analysis, recharge rates were obtained from the calibrated site-wide flow model. A recharge rate of 35 inches/year was used for areas of focused recharge (e.g., ditches and playas), and a recharge rate of 0.13 inch/year was used for upland areas.

Site-specific values for the other Method 2 parameters were obtained from data for FS-5. FS-5 is contaminated with depleted uranium, and the highest-measured concentrations of uranium were observed at FS-5. Therefore, source term values for FS-5 are conservative for other radiological sites at Pantex Plant. The site-specific input values for method 2 are presented in Table 2Q-4.

Table 2Q-2. EPA PRG Calculator Method 2 Site-Specific Input Values

Parameter	Site-Specific Value
Infiltration Rate (m/yr)	0.0033 (upland) 0.889 (playa)
Average Source Depth (m)	0.61
Aquifer Hydraulic Conductivity (m/yr)	3,660
Hydraulic Gradient	0.0031
Source Length Parallel To Groundwater Flow (m)	229
Aquifer Thickness (m)	79

2Q.2.2.4 Summary of EPA Generic SSLs and SSLs with Site-Specific Input Parameters

MCLs, EPA generic SSLs, and SSLs calculated using the PRG Calculator with site-specific input parameters are given in Table 2Q-3 in activity-based units and Table 2Q-4 in mass-based units.

Table 2Q-3. EPA Activity-Based SSLs for Migration to Groundwater

SRC	MCL (pCi/L)	Generic (pCi/g)	Method 1 (pCi/g)	Method 2	
				Upland Recharge (pCi/g)	Playa Recharge (pCi/g)
Tritium ^a	20,000	165	165	3,800	9,100
²³⁹ Pu ^b	15	1.56	110	1.4	3.3
²³² Th ^b	15	6.06	510	1.4	3.3
²³⁴ U ^c	19,000	2,240	83,000	17,000	41,000
²³⁵ U+D ^c	65	0.777	29	6.0	14
²³⁸ U+D ^c	10	0.121	4.5	0.93	2.2

^aThe MCL for tritium is derived from the MCL for beta particle and photon radioactivity of 4 millirem per year.

^bThe MCLs for ²³⁹Pu and ²³²Th are derived from the MCL for gross alpha particle radioactivity of 15 pCi/L.

^cThe MCL for uranium isotopes is derived from the MCL for total uranium of 30 µg/L.

Table 2Q-4. EPA Mass-Based SSLs for Migration to Groundwater

SRC	MCL (mg/L)	Generic (mg/kg)	Method 1 (mg/kg)	Method 2	
				Upland Recharge (mg/kg)	Playa Recharge (mg/kg)
Tritium ^a	2.10×10 ⁻⁹	8.40×10 ⁻⁹	8.40×10 ⁻⁹	1.9×10 ⁻⁷	4.6×10 ⁻⁷
²³⁹ Pu ^b	2.4×10 ⁻⁷	2.50×10 ⁻⁵	0.0018	2.2×10 ⁻⁵	5.3×10 ⁻⁵
²³² Th ^b	0.14	56.6	4,800	13	31
²³⁴ U ^c	0.030	0.360	13	2.8	6.6
²³⁵ U+D ^c	0.030	0.360	13	2.8	6.6
²³⁸ U+D ^c	0.030	0.360	13	2.8	6.6

^aThe MCL for tritium is derived from the MCL for beta particle and photon radioactivity of 4 millirem per year.

^bThe MCLs for ²³⁹Pu and ²³²Th are derived from the MCL for gross alpha particle radioactivity of 15 pCi/L.

^cThe MCL for uranium isotopes is derived from the MCL for total uranium of 30 µg/L.

Comparison of the SSLs calculated using EPA’s PRG Calculator illustrates how EPA’s standardized equations may not adequately address the subsurface conditions at Pantex Plant. Factors that are not applicable to Pantex Plant are discussed below.

- All of the SSLs calculated using method 1 (partitioning) are greater than SSLs calculated using method 2 (mass-limit) for all SRCs except tritium. However, method 1 is intended to provide more conservative SSLs than method 2 because EPA derived method 2 to address comments regarding the conservatism of the infinite source assumption used in method 1.
- The playa recharge SSLs calculated using method 2 are higher than the upland recharge SSLs for all SRCs. The extremely low upland recharge at Pantex Plant is a primary factor limiting migration of SRCs in the subsurface. Chemical contaminants, such as RDX, have migrated to perched groundwater beneath areas of focused recharge, such as ditches and playas. Therefore, it is apparent that the mass-limit model (method 2) is not applicable for the subsurface conditions at Pantex Plant, and SSLs derived using this method for the Plant may not be protective.

- The MCL for uranium is set at 30 µg/L for total uranium based on kidney toxicity. The National Primary Drinking Water Standards also recommend that total uranium activity in drinking water should not exceed 30 pCi/L based on cancer risk. Because uranium only occurs as a mixture of at least three isotopes, the total uranium concentration or activity is always greater than the concentration or activity of an individual isotope. Therefore, derivation of SSLs for uranium isotopes should include consideration of the expected isotopic abundance of uranium. However, the EPA SSLs are back-calculated by applying the MCL to each isotope separately rather than applying the MCL for total uranium concentration. As an example, consider the generic SSL for ²³⁴U. This isotope accounts for only 0.0054% by mass of total natural uranium, but accounts for 48.9% of the total activity. Because of the high specific activity of ²³⁴U, when the MCL of 30 µg/L is converted to activity, it becomes 19,000 pCi/L. This activity greatly exceeds EPA's recommended limit of 30 pCi/L. This example illustrates the need to consider the isotopic abundance of uranium when applying the MCL.

Because EPA's standardized equations may not adequately address the subsurface conditions at Pantex Plant and do not account for isotopic abundance of uranium, generic SSLs and SSLs obtained using the PRG Calculator are not applicable for use at Pantex Plant. Therefore, unsaturated zone fate and transport models were used to calculate site-specific SSLs for the migration to groundwater pathway in accordance with the methodology described in the Soil Screening Guidance for Radionuclides.

2Q.3 CALCULATION OF SITE-SPECIFIC SSLS

EPA's methodology for calculating SSLs for the migration to groundwater pathway considers two fate and transport mechanisms for the migration of radionuclides from soil to groundwater. The first mechanism is the release of the contaminant in soil leachate, and the second mechanism is the transport of the contaminant through the underlying soil and aquifer to a receptor well. The SSL methodology incorporates a standard linear equilibrium soil/water partition equation to estimate radionuclide release in soil leachate. This same methodology for contaminant release in soil leachate is incorporated into site-specific calculation of SSLs with the use of site-specific, rather than default, partition coefficients.

To represent the process of contaminant transport through the soil column and aquifer, the SSL methodology makes use of a dilution factor. This factor is applied to account for the fact that the contaminated water draining from the vadose zone does not comprise the entire flow in the saturated zone and, consequently, the drainage is diluted upon entry. This dilution factor only accounts for "dilution in groundwater;" it "does not consider processes that attenuate radionuclides in the subsurface (i.e., adsorption and degradation processes)" (EPA, 2000). The dilution factor is expressed as the ratio of leachate concentration to groundwater concentration at the receptor well. The receptor well is conservatively assumed to be located at the downgradient edge of the source area. For this analysis, the EPA default dilution factor of 10 for a 30-acre source was used as recommended in the 1996 *Soil Screening Guidance: Technical Background Document*.

Various transport processes, such as adsorption and dispersion, are neglected in the simple, standardized equations presented in the Soil Screening Guidance for Radionuclides. However, these phenomena are important considerations for contaminant transport in the unsaturated zone at Pantex Plant because of the thick unsaturated zones (e.g., approximately 257 ft from ground surface to the perched water table). Therefore, a vadose zone attenuation factor (VAF) was calculated for each SRC to represent these processes occurring in the unsaturated zone above perched groundwater. The VAF accounts for retardation (sorption), dispersion, and radioactive decay in the unsaturated zone. In simple terms, the VAF is equal to the ratio of the contaminant concentration when it is first mobilized in the vadose zone to its concentration just prior to entering the saturated zone. If this factor were derived from a column

experiment, it would be defined as the ratio of the concentration at the top of the column to the concentration at the bottom. For the purposes of this work, the VAF was derived by application of a vadose zone transport model that accounts for retardation, dispersion, and radioactive decay in the unsaturated zone.

The soil/water partition equation for migration to groundwater for inorganic contaminants presented in the *Soil Screening Guidance for Radionuclides: Technical Background Document* was modified to include the vadose zone attenuation factor as follows:

Equation 2Q-1. Soil/Water Partition Equation

$$SSL = C_t = C_{MCL} \cdot DAF_{EPA} \cdot VAF \cdot \left(K_d + \frac{n \cdot S}{\rho_s(1-n)} \right)$$

where:

Parameter/Definition (units)	Value	Remarks
SSL/soil screening level (mg/kg)	calculated	
C _t /total concentration measured in a soil sample (mg/kg)	calculated	
C _{MCL} /MCL (mg/L)	MCL	see Tables 2Q-3 and 2Q-4
DAF _{EPA} /dilution factor for mixing in groundwater	10	EPA default for 30-acre source area (1996 Soil Screening Guidance)
VAF/vadose zone attenuation factor	model-calculated	vadose zone attenuation resulting from sorption, dispersion, and radioactive decay processes
K _d /site-specific partition coefficient (L/kg)	contaminant-specific	see Table 2Q-1
n/total soil porosity	0.3	value for fine sand
S/soil saturation	model-calculated	average saturation in soil column under specific recharge conditions
ρ _s /soil particle density (kg/L)	2.65	typical value for soil mineral material

If the MCL is provided in units of pCi/L, a conversion factor of 10⁻³ kg/g is used to convert the SSL into units of pCi/g.

The final term in equation 2Q-1, $\left(K_d + \frac{nS}{\rho_s(1-n)} \right)$, transforms the MCL from a groundwater concentration into what would be measured with a soil sample collected during site characterization. This transformation is necessary since a soil sample includes solid soil particles, void spaces, and moisture. Each of these needs to be accounted for to change from the MCL units of mg contaminant per liter of water to the corresponding units of mg contaminant per kg of soil. EPA provides a detailed step-by-step derivation of this equation in Part 2 of the *Soil Screening Guidance for Radionuclides: Technical Background Document*.

Several conservative, simplifying assumptions from the EPA SSL methodology were retained for this analysis and are highlighted below.

- No chemical or biological degradation occurs in the unsaturated zone.
- Radioactive decay in the unsaturated zone is simulated, but daughter products are not included.

- Equilibrium soil/water partitioning is instantaneous and linear.
- The receptor well is located at the downgradient edge of the source (i.e., no dilution occurs downgradient of the source area) and is screened within the plume.
- The aquifer is unconsolidated and unconfined.
- Aquifer properties are isotropic. Heterogeneities in the soil profile are considered.
- Chelating or complexing agents are not present.
- Facilitated transport (e.g., colloidal transport) of inorganic contaminants does not occur.

Additionally, SSLs were conservatively calculated for migration to perched groundwater rather than to the Ogallala Aquifer. Because perched groundwater is not used at Pantex Plant, contaminants reaching perched groundwater would have to migrate offsite in perched groundwater or migrate to the Ogallala Aquifer to reach a potential point of exposure. This additional transport would result in further attenuation of contaminant concentrations, and therefore, higher SSLs than reported here.

Although radioactive decay was included in this analysis, daughter products were not. In EPA's PRG tables, the same screening levels for the soil to groundwater pathway are provided for ^{235}U and $^{235}\text{U}+\text{D}$ and also for ^{238}U and $^{238}\text{U}+\text{D}$ indicating daughter products for these isotopes are not important considerations in calculating screening levels for this pathway.

2Q.3.1 Vadose Zone Attenuation Factor Modeling

The VAF represents the decrease in contaminant mass caused by sorption, dispersion, and radioactive decay occurring during transport through the vadose zone. The VAF factor is calculated according to the following equation:

Equation 2Q-2. Vadose Zone Attenuation Factor

$$VAF = \left(\frac{C_{bottom}}{C_{source}} \right)$$

where:

- VAF = vadose zone attenuation factor
- C_{bottom} = peak concentration at the water table
- C_{source} = source concentration

An analytic model based on the one-dimensional advection-dispersion equation was used to determine the attenuation of radionuclides during transport through the unsaturated zone as a result of dispersion, sorption, and radioactive decay processes.

VAFs were developed by modeling the transport of SRCs through a conservative soil column representative of Pantex Plant subsurface conditions. Two primary hydrostratigraphic units comprise the soil column: an upper unit of approximately 80 ft of silty clay loam representing the Blackwater Draw Formation and a lower unit of approximately 170 ft of sandy loam representing the upper Ogallala

sediments. The caprock caliche was not simulated as a low permeability unit, but was assigned hydraulic properties consistent with the upper Ogallala Formation sediments. Site-specific K_d values for each hydrostratigraphic unit, presented in Table 2Q-1, were used in the VAF modeling.

The hydraulic conductivities of subsurface materials at Pantex Plant have been established using lithologic descriptions from boring logs and data from field and laboratory test results. The sediments beneath all potential radionuclide source areas at Pantex Plant were evaluated to identify the soil column having the highest overall hydraulic conductivity. This column occurred beneath SWMU 39, a landfill site at the Burning Ground. The soils at this SWMU were the sandiest and most conductive of the soils at the units considered and were therefore expected to serve for conservative estimation of SRC transport at all units. Therefore, the hydraulic properties beneath SWMU 39 were used in the VAF modeling.

Transport of radionuclides was considered for a period of 1,000 years. If SRC breakthrough was not calculated to occur at the bottom of the soil column within 1,000 years, then the SRC was assumed to be immobile under Pantex Plant conditions, and the VAF is infinity. If SRC breakthrough was calculated to occur at the bottom of the soil column within 1,000 years, then the peak breakthrough concentration was used to calculate the VAF, even if the peak occurred after 1,000 years. Release of SRCs was simulated as a constant concentration soil leachate applied to the recharge flux at the ground surface for a period of 50 years corresponding to the operational history of the Plant.

As described above, recharge rates at Pantex Plant vary greatly depending on water availability because of the semi-arid climate and flat topography. Because recharge is the primary transport mechanism for the movement of radionuclides through the soil column, SSLs were developed for the highest and lowest recharge rates estimated at the Plant to bracket the expected range of conditions. For this analysis, recharge rates were obtained from the calibrated site-wide flow model. A recharge rate of 35 inches/year was used for areas of focused recharge (e.g., ditches and playas), and a recharge rate of 0.13 inch/year was used for upland areas.

2Q.3.1.1 Analytic Model

An analytic model was derived from the one-dimensional advection-dispersion equation to calculate the VAF for each SRC. The model is presented below:

Equation 2Q-3. Analytic Model for Calculating the Vadose Zone Attenuation Factor

$$VAF = \frac{C_{source}}{C_{bottom,max}} = (L/\Delta L)\sqrt{4\pi\beta(1-(\Delta L/L)/2)} \cdot 2^{(T/T_{0.5})}$$

where:

L = length of the soil column

ΔL = width of source pulse

β = 0.1 = dispersion factor (consistent with EPA guidance for longitudinal dispersion)

T = advective travel time through soil column

$T_{0.5}$ = radioactive half-life

The complete derivation of this equation is provided as an appendix to this document. This derivation was provided by Dr. Randall Charbeneau of the University of Texas. This equation can be applied for

steady state flow in the unsaturated zone, but requires the use of water saturations and partition coefficients averaged over the length of the soil column. An analysis of the use of these average values is provided below.

The contaminant source is modeled as a constant flux boundary condition at the ground surface for 50 years. After 50 years, the mass flux drops to zero while infiltration continues at the same rate. Therefore, after 50 years, the upper part of the soil profile has a uniform concentration C_{source} over the depth ΔL , defined as the width of the source pulse. This depth is calculated by the following equation:

Equation 2Q-4. Width of Source Pulse

$$\Delta L = \frac{i_f \Delta t}{n S + \rho_b K_d}$$

where:

i_f = infiltration rate

Δt = source period

$n = 0.3$ = total soil porosity

S = average water saturation in soil profile

ρ_b = bulk density of soil matrix

To apply this equation, the average water saturation of the soil profile is calculated using the van Genuchten-Mualem model of unsaturated flow. Given a constant (steady state) infiltration rate, the water saturation in the soil adjusts to allow passage of the infiltration under unit hydraulic gradient such that $i_f = k_r K$, where k_r is the water relative permeability, and the vertical hydraulic gradient is $I_z = 1$. Thus $k_r = i_f/K$. For the van Genuchten-Mualem model, the relative permeability, effective saturation, and corresponding water saturation are related through the following equations:

Equation 2Q-5. Van Genuchten-Mualem Model of Relative Permeability and Effective Saturation

$$k_r = \sqrt{S_e} \left(1 - \left(1 - S_e^{1/M} \right)^M \right)^2$$

where:

S_e = effective saturation

$M = 1 - 1/N$ = van Genuchten-Mualem model parameter

N = van Genuchten-Mualem model power

Equation 2Q-6. Total Saturation

$$S = S_r + (1 - S_r)S_e$$

where:

S_r = residual water saturation

The relative permeability is calculated for each hydrostratigraphic unit in the soil column using the site-specific infiltration rate and saturated hydraulic conductivity. Then the effective saturation is obtained using Equation 2Q-5, and the total saturation is calculated from Equation 2Q-6.

The advective travel time through the soil column is given by the following equation:

Equation 2Q-7. Advective Travel Time

$$T = \frac{nSL}{i_f} R$$

where:

R = retardation factor, given by:

Equation 2Q-8. Retardation Factor

$$R = 1 + \frac{\rho_b K_d}{n S}$$

2Q.3.1.2 Application of Analytic Model

Table 2Q-5 provides the conceptual discretization and saturated hydraulic conductivities of the soil column beneath SWMU 39. The bottom of the model is set at a depth representative of the perched water table from the surface. The peak concentration at the bottom of the model, at a depth of 257 ft, represents the leachate concentration in the vadose zone immediately above the perched water table. For simplification, the Caprock caliche layer, approximately 10-ft thick, was not differentiated from the upper Ogallala formation materials.

Table 2Q-5. Analytic Model Conceptual Discretization (SWMU 39)

Layer	Unit	Depth (ft bgs)	K _z (ft/day)	Van Genuchten-Mualem Parameters
1	Blackwater Draw	0 - 90	0.30	Inverse air entry head: $\alpha = 2.2 \text{ ft}^{-1}$ Power in formula: N = 1.8 Residual saturation = 0.15
2	Caliche	90 - 257	4.46	Inverse air entry head: $\alpha = 3.0 \text{ ft}^{-1}$ Power in formula: N = 2.0 Residual saturation = 0.10
	Upper Ogallala			

Application of Equation 2Q-5 and 2Q-6 gives the water saturation results in Table 2Q-6.

Table 2Q-6. Calculation of Water Saturation

Recharge	Unit	k _r	S _e	S
Upland	Blackwater Draw	0.000098	0.22	0.34
	Upper Ogallala	0.000068	0.10	0.19
Playa	Blackwater Draw	0.026	0.64	0.69
	Upper Ogallala	0.0018	0.33	0.40

The average water saturation for each recharge condition is calculated using a weighted average based on the thickness of each hydrostratigraphic unit. Average saturations for the different recharge rates are shown in Table 2Q-7.

Table 2Q-7. Average Saturation

Recharge	Average Saturation
Upland	0.24
Playa	0.50

2Q.3.1.3 Model Results

The water travel time T through the vadose zone is found using the calculated average saturations in Equation 2Q-7 with R = 1. The advective travel times are given in Table 2Q-8.

Table 2Q-8. Water Travel Time

Recharge	Travel Time (years)
Upland	1,680
Playa	13

The difference in the water travel time presented in Table 2Q-8 illustrates the importance of recharge in subsurface contaminant migration. Under upland recharge, the water travel time is more than 1,000 years, but the water travel time is only 13 years under playa recharge. Because tritium is non-sorbing, it is the only SRC with the potential to migrate to the depth of perched groundwater within 1,000 years under upland recharge. However, any source of tritium would decay before reaching the depth of perched groundwater because of tritium's relatively short half-life (the advective travel time under upland recharge is more than 134 times the half-life). All other SRCs are strongly sorbed to Pantex Plant soils resulting in advective travel times much greater than 1,000 years. Thus, under upland recharge

conditions, no Pantex Plant SRCs have the potential to migrate to the depth of perched groundwater within several thousand years.

Model results and calculated VAFs for each SRC are presented in Table 2Q-9 for the playa recharge scenario. The contaminant travel times presented in this table are calculated by applying Equation 2Q-7 to each layer separately.

Table 2Q-9. Model Results (Playa Recharge Scenario)

SRC	Half-Life (years)	Average K_d (L/kg)	Width of Source Pulse (ft)	Advective Travel Time (years)	VAF
Tritium	12.5	0	972	13.2	2.1 ^a
²³⁹ Pu	2.44E+04	136	0.58	22,300	NC ^b
²³² Th	1.41E+10	1700	0.046	278,000	NC ^b
²³⁴ U	2.48E+05	7.96	9.8	1,320	29.3
²³⁵ U+D	7.13E+08	7.96	9.8	1,320	29.2
²³⁸ U+D	4.49E+09	7.96	9.8	1,320	29.2

^aBecause tritium is non-sorbing, the VAF only accounts for radioactive decay using the equation: $VAF = 2^{\frac{t}{T_{1/2}}}$.

^bBecause the advective travel times for ²³⁹Pu and ²³²Th are much greater than 1,000 years, these constituents are considered immobile, and VAFs are not calculated.

Under the playa recharge scenario, the advective travel time of tritium is about 13 years. Attenuation of tritium occurs solely because of radioactive decay resulting in a VAF for tritium of 2.1. Although the advective travel time for uranium is greater than 1,000 years, uranium breakthrough is expected within 1,000 years and VAFs are calculated. ²³⁹Pu and ²³²Th are strongly sorbed to Pantex Plant soils resulting in extremely long travel times. Therefore, these constituents are considered immobile, and VAFs are not calculated.

As noted above, application of the analytic model requires the use of average values of water saturation and partition coefficient. An alternative analysis was conducted to assess the impact of the use of the average water saturation and partition coefficient. For this analysis, only transport through the Blackwater Draw Formation was considered, and the VAF was calculated at a depth of 90 ft bgs. The results of this analysis, shown in Table 2Q-10, demonstrate that the use of average values in the application of the analytic model is acceptable.

Table 2Q-10. Alternative Analysis Comparison (Playa Recharge Scenario)

Scenario	Water Saturation	K_d (L/kg)	Width of Source Pulse (ft)	Advective Travel Time (years)	VAF ^a
Standard (Uranium)	Entire Column	0.50	7.96	9.8	29.2
Alternative (Uranium)	BWD Only	0.69	22	3.6	28.1

^aVAF calculated without consideration for radioactive decay.

2Q.3.2 Site-Specific SSLs

As stated above, the migration to groundwater pathway is not complete for Pantex Plant SRCs under upland recharge conditions. Therefore, no site-specific SSLs can be developed for this pathway. Radiological release sites in upland areas are evaluated for other pathways, such as worker or ecological exposure, but do not pose a potential threat to groundwater.

Site-specific SSLs for the playa recharge scenario were calculated using Equation 2Q-1 and the VAFs provided in Table 2Q-9. This calculation is presented in Table 2Q-11 for activity-based units.

Table 2Q-11. Calculation of Site-Specific SSLs (Playa Recharge Scenario)

SRC		MCL (pCi/L)	DAF _{EPA}	VAF	Soil Leachate Concentration (pCi/L)	Soil Concentration (SSL) (pCi/g)
Tritium		20,000	10	2.1	46.6	4.9×10^{-9}
²³⁹ Pu		15	10	∞	NA ^a	NA
²³² Th		15	10	∞	NA	NA
Natural Uranium	²³⁴ U	14.67 ^b	10	29.3	95.1	10.5
	²³⁵ U	0.66 ^b	10	29.2	4.26	1,380
	²³⁸ U	14.67 ^b	10	29.2	94.7	192,000
Depleted Uranium	²³⁴ U	4.26 ^c	10	29.3	27.6	1.75
	²³⁵ U	0.33 ^c	10	29.2	2.13	387
	²³⁸ U	25.41 ^c	10	29.2	164	193,000

^aNA indicates SRC did not reach the depth of perched groundwater within 1,000 years.

^bUranium MCL based on isotopic abundance of natural uranium and total uranium activity of 30 pCi/L.

^cUranium MCL based on isotopic abundance of depleted uranium and total uranium activity of 30 pCi/L.

In Table 2Q-11, the uranium MCL is represented as 30 pCi/L based on the recommendation found in the National Primary Drinking Water Standards. This MCL has been apportioned to the three uranium isotopes according to isotopic abundances of natural uranium. Because uranium releases at Pantex Plant include both natural and depleted uranium, a separate calculation was performed based on the isotopic composition of depleted uranium. The lowest SSL calculated for each type of uranium was selected as the SSL for that isotope. From the data presented in Table 2Q-11, the SSLs for depleted uranium were selected for ²³⁴U and ²³⁵U, and the SSL for natural uranium was selected for ²³⁸U.

Table 2Q-12 provides a summary of site-specific SSLs for the playa recharge scenario in both activity- and mass-based units.

**Table 2Q-12. SSLs for Migration to Groundwater
(Playa Recharge Scenario)**

SRC	MCL		SSL	
	(pCi/L)	(mg/L)	(pCi/g)	(mg/kg)
Tritium	20,000	2.1×10^{-9}	46.6	4.9×10^{-9}
²³⁹ Pu	15	2.4×10^{-7}	NA ^a	NA
²³² Th	15	0.14	NA	NA
²³⁴ U ^b	4.26	2.7×10^{-4}	27.6	1.75
²³⁵ U ^b	0.33	0.060	2.13	387
²³⁸ U ^c	14.7	29.8	94.7	192,000

^aNA indicates SRC did not reach the depth of perched groundwater within 1,000 years.

^b²³⁴U and ²³⁵U SSLs based on isotopic abundance of depleted uranium.

^c²³⁸U SSL based on isotopic abundance of natural uranium.

2Q.4 SUMMARY AND CONCLUSIONS

Site-specific SSLs were developed to be used as PRGs for evaluation of the soil to groundwater pathway.

EPA's Soil Screening Guidance for Radionuclides allows for the use of unsaturated zone fate and transport models to extend the applicability of SSLs to subsurface conditions that are not adequately addressed by the simple, standardized equations. Comparison of the SSLs calculated using EPA's PRG

Calculator illustrates how EPA's standardized equations may not adequately address the subsurface conditions at Pantex Plant and do not account for isotopic abundance of uranium. Therefore, generic SSLs and SSLs obtained using the PRG Calculator are not applicable for use at Pantex Plant, and unsaturated zone analytic fate and transport models were used to calculate site-specific SSLs for the migration to groundwater pathway in accordance with the methodology described in the Soil Screening Guidance for Radionuclides.

Results of unsaturated zone fate and transport models indicate no Pantex Plant SRCs have the potential to migrate to the depth of perched groundwater within several thousand years under upland recharge conditions. Under playa recharge conditions, tritium and uranium have the potential to migrate to the depth of perched groundwater. Therefore, site-specific tritium and uranium SSLs were developed for application to radiological release sites with focused recharge. Even under playa recharge conditions, plutonium and thorium do not have the potential to migrate to the depth of perched groundwater, and site-specific SSLs for were not developed for these SRCs.

**SUPPLEMENTAL EQUATIONS TO ATTACHMENT 2Q
ANALYTICAL SOLUTION TO THE ONE-DIMENSIONAL
ADVECTION DISPERSION EQUATION**

ANALYTICAL SOLUTION TO THE ONE-DIMENSIONAL ADVECTION DISPERSION EQUATION

This appendix presents an analytical solution for calculation of a vadose zone attenuation factor (VAF) using the one-dimensional advection-dispersion equation. This solution was contributed by Dr. Randall Charbeneau of the University of Texas.

The one-dimensional advection-dispersion equation with first-order decay is given by

Equation 2Q-1

$$R \frac{\partial c}{\partial t} + v \frac{\partial c}{\partial z} - D \frac{\partial^2 c}{\partial z^2} + \lambda c = 0$$

where:

- c = c(z,t) is the solute concentration
- D = longitudinal dispersion coefficient
- T = time
- z = depth
- v = flow velocity
- λ = decay constant
- R = retardation factor

Assume a constant flux (i_f) boundary condition for flow and a constant mass flux $J = i_f c_o$ over a finite duration Δt . Then the upper part of the soil profile has a uniform concentration c_o over a depth ΔL defined by

Equation 2Q-2

$$\Delta L = \frac{i_f \Delta t}{n S + \rho_b K_d}$$

where,

- i_f = constant water flux
- Δt = duration of solute release
- n = total soil porosity
- S = average water saturation in soil profile
- ρ_b = bulk density of soil matrix
- K_d = soil-water partitioning coefficient

For a “narrow” pulse ($\Delta L \ll L$, where L is the total length of the soil column) of solute at concentration equal to c_o , the analytical solution is given by

Equation 2Q-3

$$c(z, t) = \frac{c_o}{2} \left(\operatorname{erf} \left(\frac{z - vt/R}{\sqrt{4Dt/R}} \right) - \operatorname{erf} \left(\frac{z - \Delta L - vt/R}{\sqrt{4Dt/R}} \right) \right) \cdot e^{-\lambda t}$$

Further simplification can be made by substituting

Equations 2Q-4a and 4b

$$x = \frac{z - vt/R}{\sqrt{4Dt/R}}, \quad \Delta x = \frac{\Delta L}{\sqrt{4Dt/R}}$$

to yield (neglecting radioactive decay)

Equation 2Q-5

$$c(x, \Delta x, t) = \frac{c_o}{2} (\operatorname{erf}(x) - \operatorname{erf}(x - \Delta x))$$

The term $\operatorname{erf}(x - \Delta x)$ can be expressed as a Taylor Series expansion about Δx :

Equation 2Q-6

$$\operatorname{erf}(x - \Delta x) = \operatorname{erf}(x) + \sum_{n=1}^{\infty} (-1)^n \frac{d^n}{dx^n} \operatorname{erf}(x) \cdot \frac{\Delta x^n}{n!}$$

The definition of the error function and its derivatives can be used to express this expansion in terms of Hermite polynomials:

Equation 2Q-7

$$\operatorname{erf}(x - \Delta x) = \operatorname{erf}(x) - \sum_{n=1}^{\infty} H_{n-1}(x) \frac{\Delta x^n}{n!} \cdot \frac{2}{\sqrt{\pi}} e^{-x^2}$$

where $H_i(x)$ are

Equation 2Q-8

$$H_0(x) = 1, H_1(x) = 2x, H_2(x) = 4x^2 - 2, H_3(x) = 8x^3 - 12x, H_4(x) = 16x^4 - 48x^2 + 12, \dots$$

Evaluation of $H_0(x)$ yields the form

Equation 2Q-9

$$\operatorname{erf}(x - \Delta x) = \operatorname{erf}(x) - \frac{2\Delta x}{\sqrt{\pi}} e^{-x^2} \cdot \left[1 + \sum_{n=1}^{\infty} H_n(x) \frac{\Delta x^n}{(n+1)!} \right]$$

Equation 2Q-9 can be combined with Equation 2Q-5 to express the solute concentration $c(x, \Delta x, t)$ as

Equation 2Q-10

$$c(x, \Delta x, t) = \frac{c_o}{2} (\operatorname{erf}(x) - \operatorname{erf}(x - \Delta x)) = \frac{c_o}{2} \cdot \frac{2\Delta x}{\sqrt{\pi}} e^{-x^2} \cdot \left[1 + \sum_{n=1}^{\infty} H_n(x) \frac{\Delta x^n}{(n+1)!} \right]$$

More explicitly, this term is

Equation 2Q-11

$$c(x, \Delta x, t) = \frac{c_o \Delta x}{\sqrt{\pi}} e^{-x^2} \cdot \left[1 + H_1(x) \frac{\Delta x}{2} + H_2(x) \frac{\Delta x^2}{3!} + H_3(x) \frac{\Delta x^3}{4!} + H_4(x) \frac{\Delta x^4}{5!} \right]$$

By evaluating the first few Hermite polynomials (Equation 2Q-8),

Equation 2Q-12

$$c(x, \Delta x, t) = \frac{c_o \Delta x}{\sqrt{\pi}} e^{-x^2} \cdot \left[1 + x\Delta x + \frac{(2x^2 - 1)\Delta x^2}{3} + \frac{(2x^3 - 3x)\Delta x^3}{6} + \frac{(4x^4 - 12x^2 + 3)\Delta x^4}{30} + \dots \right]$$

The goal is to determine the peak concentration at a depth $z = L$. The concentration is largest at the midpoint of the pulse. Evaluating Equation 12 at the location $x = \Delta x/2$ yields

Equation 2Q-13

$$c(x, \Delta x, t)_{x=\Delta x/2} = c_o \frac{\Delta x}{\sqrt{\pi}} e^{-(\Delta x/2)^2} \cdot \left[1 + \frac{\Delta x^2}{6} + \frac{\Delta x^4}{60} + O(\Delta x^6) + \dots \right]$$

As long as the remainder term is negligible ($\Delta x^2/6 \ll 1$), the solution gives

Equation 2Q-14

$$c_{\text{bottom,max}} = c_o \frac{\Delta x}{\sqrt{\pi}} e^{-(\Delta x/2)^2}$$

Recall that Δx is $\Delta x = \frac{\Delta L}{\sqrt{4Dt/R}}$ (Equation 2Q-4b). Further, the evaluation is sought at $z = L$:

Equation 2Q-15

$$vt/R = L - \Delta L/2$$

The dispersion coefficient D can be expressed as

Equation 2Q-16

$$D = a_L v = (\beta L)v$$

Substitution of Equations 2Q-15 and 2Q-16 into the definition of Δx produces

Equation 2Q-17

$$\Delta x = \frac{\Delta L}{\sqrt{4\beta L(L - \Delta L/2)}} = \frac{(\Delta L/L)}{\sqrt{4\beta(1 - (\Delta L/L)/2)}}$$

Substitution of this expression into Equation 2Q-14 and insertion of the decay term then yields

Equation 2Q-18

$$c_{bottom,max} = c_o \frac{(\Delta L/L)}{\sqrt{4\pi\beta(1 - (\Delta L/L)/2)}} \exp\left(-\frac{(\Delta L/L)^2}{16\beta(1 - (\Delta L/L)/2)}\right) 2^{(-T/T_{0.5})}$$

The VAF is simply expressed as the ratio of initial solute concentration to the peak concentration of the arriving pulse, which yields the following form based on Equation 2Q-18:

Equation 2Q-19

$$VAF = \frac{c_o}{c_{bottom,max}} = (L/\Delta L) \sqrt{4\pi\beta(1 - (\Delta L/L)/2)} \exp\left(\frac{(\Delta L/L)^2}{16\beta(1 - (\Delta L/L)/2)}\right) \cdot 2^{(T/T_{0.5})}$$

Finally, consider an acceptable accuracy of 1% for $\Delta x/6$, which implies $\Delta x=0.25$ (since $\Delta x/6=0.01$). If $\beta=0.1$, then Equation 2Q-17 indicates $\Delta L/L=0.15$. At this limit the exponential term in Equation 2Q-19 is approximately unity, and for $\Delta L/L < 0.15$ the VAF (within 1% accuracy) is

Equation 2Q-20

$$VAF = \frac{c_o}{c_{bottom,max}} = (L/\Delta L) \sqrt{4\pi\beta(1 - (\Delta L/L)/2)} \cdot 2^{(T/T_{0.5})}$$

**SUPPLEMENTAL INFORMATION TO ATTACHMENT 2Q
SORPTION OF URANIUM ON BLACKWATER DRAW SEDIMENTS**

Sorption of Selected Metals on Blackwater Draw Sediments

By

Ken Rainwater, Matt Jones, Levi Hein,
Kartik Venkataraman, Yeontae Jeong, and John McEnery

Texas Tech University Water Resources Center
Box 41022
Lubbock, Texas 79409-1022

Submitted to

BWXT-Pantex
P.O. Box 30020
Amarillo, Texas 79120

Volume I. Report

2006

Table of Contents

List of Tables i
List of Figures ii

1. Problem Statement 1
2. Soil Characterization..... 2
3. Batch Equilibrium Tests 6
 3.1 Site 1 Isotherms..... 6
 3.2 Site 6 and 7 Isotherms..... 11
4. Soil Column Experiments 11
 4.1 Attempt at Soil Column Experiment with Silver and Site 1 Soil 11
 4.2 Experimental Design for Uranium Column Tests 13
 4.3 Uranium Column Operation 14
 4.4 Column Test Results 15
 4.4.1 Site 6 Columns 15
 4.4.2 Site 7 Columns 18
 4.4.3 Site 1 Columns 19
 4.4.4 Overview of Column Test Results 23
5. Equilibrium Chemistry Simulations 24
6. Summary and Conclusions 26
7. References 27

List of Tables

1. General Soil Characteristics..... 2
2. Water and Moisture Content Distributions 3
3. Grain-size Classifications for Sites 1, 6, and 7 5
4. Soil Mineral Content by Weigh 5
5. Selected Extractable Ions (as mg/ kg dry soil)..... 5
6. Metals Concentrations in Monitoring Well PTX06-1049 7
7. PTX06-1049 Water Quality 7
8. Site 1 Barium Isotherm pH Values 8
9. Site 1 Lead Isotherm pH Values 8
10. Site 1 Silver Isotherm pH Values..... 8
11. Site 1 Thorium Isotherm pH Values 9
12. Site 1 Uranium Isotherm pH Values 9
13. Site 1 Barium Isotherm Parameters 10
14. Site 1 Lead Isotherm Parameters 10
15. Site 1 Silver Isotherm Parameters..... 10
16. Site 1 Thorium Isotherm Parameters 10
17. Site 1 Uranium Isotherm Parameters 10
18. Initial U (C_i) and pH Values for Site 6 and 7 Uranium Isotherm Solutions 12
19. Site 6 and 7 Uranium Isotherm Parameters 12
20. Typical Pantex Soil and Pore Water Metal Levels (Stovall 2003) 12
21. Column Test K_d Values 23

List of Figures

1. Location of Geoprobe Sample Locations	1
2. Grain-size Analyses for Site 1	4
3. Grain-size Analyses for Site 6	4
4. Grain-size Analyses for Site 7	4
5. Bromide Breakthrough in Column 1, Site 1 Soil (Dispersivity = 0.63 cm)	13
6. Pressure and Flow Histories for Site 6 Columns	16
7. Bromide Tracer Fit for Column 6-1, $\alpha_x = 0.67$ cm.....	17
8. Bromide Tracer Fit for Column 6-2, $\alpha_x = 0.62$ cm.....	17
9. Bromide Tracer Fit for Column 6-3, $\alpha_x = 0.71$ cm.....	17
10. U Breakthrough Curves for Columns 6-1, 6-2, and 6-3	18
11. Pressure and Flow Histories for Site 7 Columns	19
12. Bromide Tracer Fit for Column 7-1, $\alpha_x = 0.96$ cm.....	20
13. Bromide Tracer Fit for Column 7-2, $\alpha_x = 1.1$ cm.....	20
14. Bromide Tracer Fit for Column 7-3, $\alpha_x = 0.84$ cm.....	20
15. U Breakthrough Curves for Columns 7-1, 7-2, and 7-3	21
16. Column 7-1 U Curve Fit, $R = 76$, $\alpha_x = 1.9$ cm	21
17. Column 7-2 U Curve Fit, $R = 74$, $\alpha_x = 1.9$ cm	21
18. Pressure and Flow Histories for Site 1 Column 1-2	22
19. Bromide Tracer Fit for Column 1-2, $\alpha_x = 0.56$ cm.....	22
20. U Breakthrough Curve for Column 1-2 (dashed line to smooth data).....	23
21. Speciation as Related to U^{+4}	25
22. Speciation as Related to UO_2^{+2}	25
23. Speciation as Related to CO_3^{-2}	25

1. Problem Statement

As part of the on-going environmental investigation, remediation, and risk assessment efforts at the Pantex Plant, BWXT-Pantex contracted the Texas Tech University Water Resources Center (TTUWRC) to perform laboratory experiments on the sorption of selected metals by Blackwater Draw sediments. The selected metals were barium, lead, silver, thorium, and uranium. It was originally planned that the sorption behavior would be observed in flow-through column experiments. As is discussed below, the significant sorptive capacity of the soil for several of the metals, in combination with the required sample sizes for chemical analyses, made column flow tests much too long to fit the project duration. The project then emphasized characterization of the soil and performance of batch equilibrium sorption tests. Special attention was given to uranium, which showed the least sorption in the batch tests, and column tests were performed to observe the sorption of uranium during flow.

The Blackwater Draw soils were taken from geoprobe samples at sites 1, 6, and 7, shown in Figure 1. In the first phase of the study, soil from Site 1 was characterized and exposed to all five metals in batch equilibrium sorption tests. Grain-size analyses showed that the soil from Site 1 had less clay fraction and cation exchange capacity than previously seen in Blackwater Draw samples (Laun, 1995; Givens, 1997). As will be shown later, barium, lead, silver, and thorium were all relatively highly sorbed, while uranium was least sorbed. Previous research

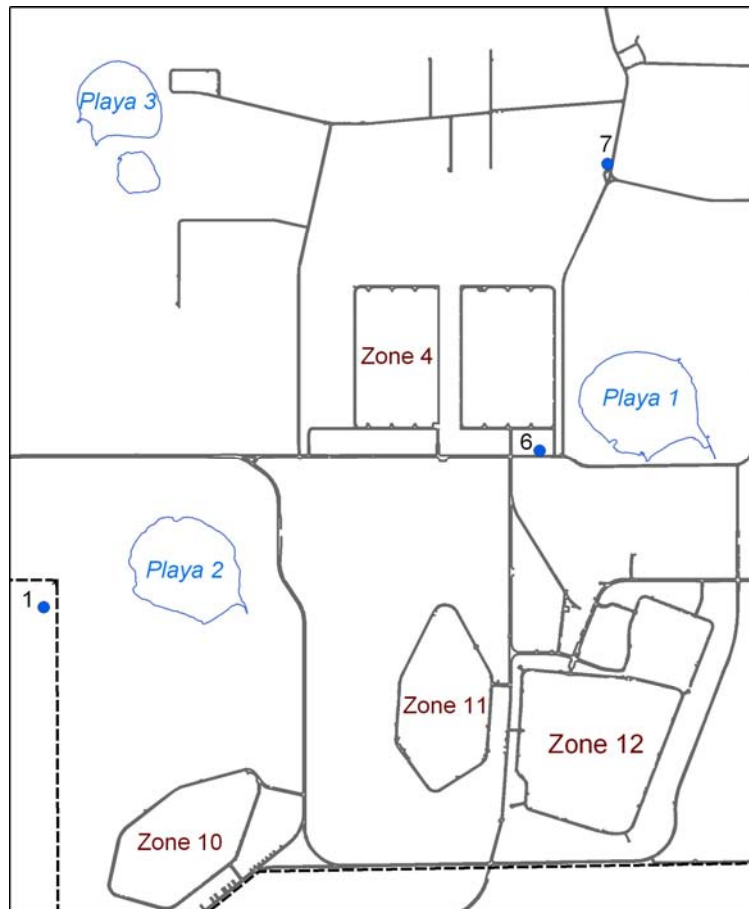


Figure 1. Location of Geoprobe Sample Locations

(Barnett et al. 2000) had found that column flow tests typically show more sorption of metals than batch equilibrium tests. Review of these results indicated that additional Blackwater Draw soil samples should be tested to examine the effects of variability in soil characteristics on the sorption of uranium. For the second phase of the work, additional soil samples were collected from Sites 6 and 7. These samples were used for batch equilibrium tests for uranium sorption, while soils from all three sites were employed in flow-through column tests. The results of both phases are presented in this report.

2. Soil Characterization

The soil samples were provided by BWXT-Pantex in the form of geoprobe samples taken from clean sites to total depths of 12 m (40 ft) or less. The moisture content analyses were done by collecting ten approximately 30-g samples for each site from the geoprobe sleeves prior to homogenization. After removal of those samples, the remaining soil was removed from the plastic sleeves and carefully homogenized by hand mixing. The general soil characteristics shown in Table 1 were found using typical standard methods (SD = standard deviation). Each test for pH, electrical conductivity (EC), cation exchange capacity (CEC), and organic carbon (OC) was performed on at least three replicates. MC and OC content were found gravimetrically (Wray 1986) using ovens set at 105° and 550°C, respectively. The MC values in Table 1 were estimated based on an assumed porosity of 0.40, which is similar to that found later in the packed columns. OC was also measured using the Walkley and Black (1934) chromic acid method, and the results were similar to the gravimetric approach. Soil pH and EC were found by the standard approaches set by the Soil Quality Institute (1999). CEC was found by the ammonium saturation method (Wray 1986). Table 2 shows the distribution of water and moisture contents at the three sites. Note that variability in pH, EC, and CEC is evident across the samples.

Table 1. General Soil Characteristics

Parameter	Units	Site 1		Site 6		Site 7	
		Mean	SD	Mean	SD	Mean	SD
pH	SU	8.06	0.09	7.66	0.03	7.76	0.02
EC	μS/cm	797	37	809	57	690	45
CEC	meq/100 g soil	8.1	0.8	14.9	0.2	14.5	0.5
OC	% (w/w, grav)	3.24	0.92	3.03	0.19	3.29	0.07
	% (w/w, W-B)	2.58	0.03	3.15	0.54	2.25	0.00
MC	% (v/v)	19.2	3.4	18.2	3.8	17.7	4.7

Grain-size distributions were found using three replicate mechanical sieve and hydrometer tests (Wray 1986) with soil masses of approximately 400 g. Figures 2, 3 and 4 display the results of the grain-size analyses for sites 1, 6, and 7, respectively. The similarity of the multiple curves for each site shows the homogenization procedure was effective. Table 3 shows the approximate fractions of gravel, coarse sand, fine sand, silt, and clay for the replicates for each site. These combinations lead to a classification of loamy sand for Site 1, sandy loam for Site 6, and sandy clay loam for Site 7. It should be noted that the clay content controls these differences in the USDA classifications

Table 2. Water and Moisture Content Distributions

Site	Depth (ft)	Depth (m)	Water Content (% w/w)	Moisture Content (% v/v)
1	6	1.8	12.2	19.6
	10	3.0	9.0	14.3
	14	4.3	11.2	18.0
	18	5.5	12.3	19.7
	26	7.9	13.6	21.7
	30	9.1	11.8	18.8
	32	9.8	11.3	18.1
	34	10.4	13.6	21.7
	36	11.0	8.9	14.3
	38	11.6	11.8	18.8
	40	12.2	15.7	25.2
6	6	1.8	9.6	15.4
	10	3.0	11.8	18.9
	14	4.3	10.5	16.8
	18	5.5	10.9	17.5
	22	6.6	10.1	16.2
	26	7.9	12.8	20.5
	29	9.0	14.4	23.1
	32	9.9	15.6	25.0
	36	11.0	10.0	16.0
	39	12.0	7.8	12.5
7	6	1.8	8.6	13.8
	10	23.0	9.3	14.9
	14	4.3	6.7	10.7
	18	5.5	13.1	21.0
	21	6.4	11.7	18.7
	24	7.5	9.7	15.5
	28	8.6	10.6	17.0
	32	9.9	11.4	18.3
	36	11.0	11.8	18.9
	38	11.7	17.5	28.0

The mineralogy of the soil was analyzed by Dr. Necip Guven of the TTU Geosciences department. X-ray diffraction and scanning electron microscopy were employed. The entire reports are provided in Appendix B. Table 4 shows the results of these analyses. Illite, smectite, and kaolinite are all clays that can contribute to high cation exchange capacity, sorption, and swelling. The electron microscopic analyses indicated that the smectites and illites were most likely produced by weathering of micas. The presence of iron and magnesium in the flakes indicated a biotite form of mica as the likely precursor. Smectites naturally include iron coating on their flakes as part of the clay mineral structure. The only iron noted was part of the clay

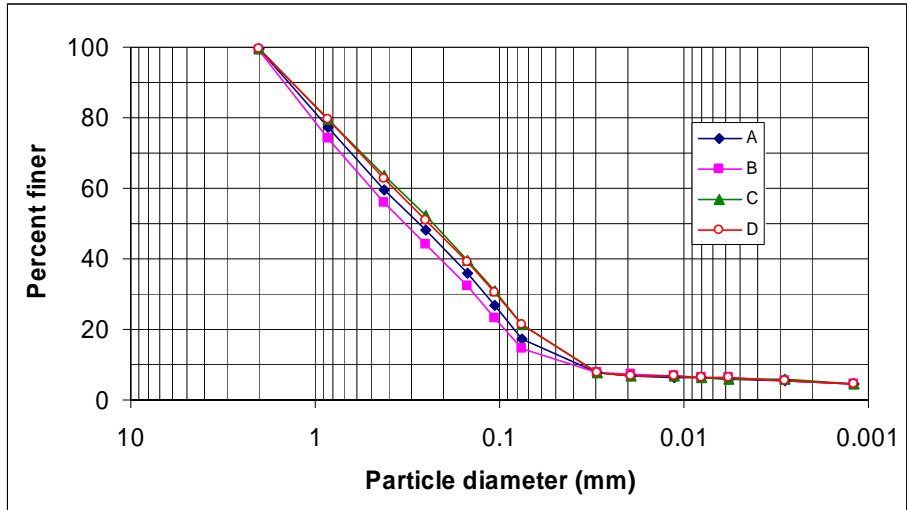


Figure 2. Grain-size Analyses for Site 1

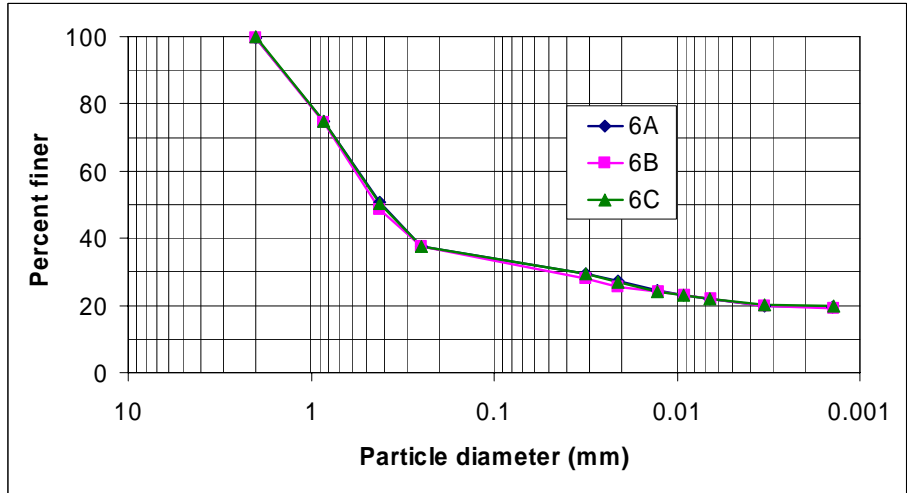


Figure 3. Grain-size Analyses for Site 6

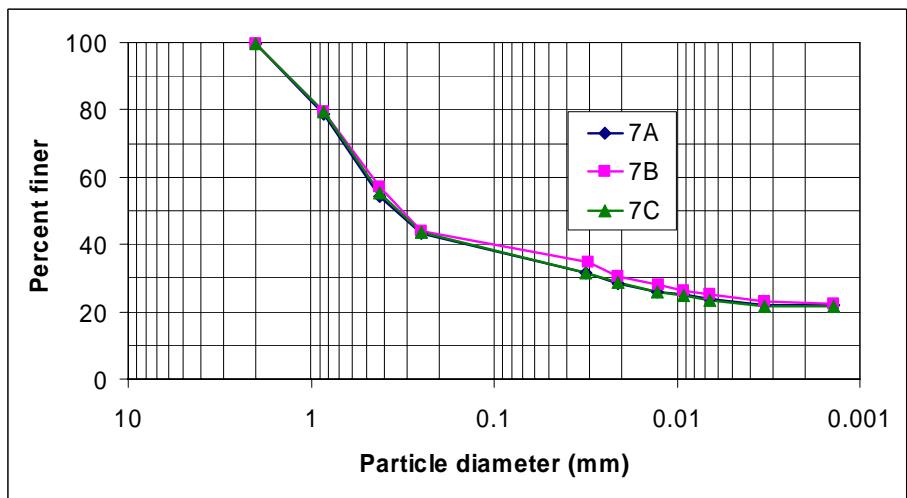


Figure 4. Grain-size Analyses for Site 7

Table 3. Grain-size Classifications for Sites 1, 6, and 7

Classification	Site 1 (% by weight)				Site 6 (% by weight)			Site 7 (% by weight)		
	A	B	C	D	A	B	C	A	B	C
Gravel (>2 mm)	0.9	0.9	0.3	0.4	0.3	0.3	0.1	0.3	0.3	0.4
Coarse sand (0.42-2 mm)	46.7	43.2	36.2	36.7	49.0	51.0	49.7	45.5	42.7	44.4
Fine sand (0.074-0.42 mm)	41.7	41.3	42.2	41.7	19.8	18.7	19.1	20.2	20.5	21.1
Silt (0.002-0.074 mm)	5.7	9.4	16.1	16.2	11.4	10.6	11.2	12.1	13.9	12.5
Clay (<0.002 mm)	5.0	5.2	5.2	5.0	19.5	19.4	19.9	22.0	22.6	21.6
Total	100	100	100	100	100	100	100	100	100	100

Table 4. Soil Mineral Content by Weight

Mineral	Weight %	
	Site 1	Sites 6, 7
Quartz	40	45
Calcite	15	15
Plagioclase	3	7
K-feldspar	2	3
Illite	10	15
Smectite	25	10
Kaolinite	5	5

structures, and as such that iron has little effect on the sorption of metals from solution.

The soil was also tested for selected extractable anions using distilled deionized (DDI) water extraction. The anions were analyzed by ion chromatography in the TTUWRC Environmental Science Laboratory (ESL), and the metals were analyzed by inductively-coupled plasma (ICP) spectrophotometry in the Geosciences Laboratory (Ca, Mg, Na, K) and at TraceAnalysis, Inc. (Fe, Sr). The liquid extract from Site 1 was not analyzed for iron. Table 5 summarizes those results. Nitrate, nitrite, bromide, and phosphate were <2 mg/kg at all the sites.

Table 5. Selected Extractable Ions (as mg/ kg dry soil)

Type	Specie	Site 1		Site 6		Site 7	
		Mean	SD	Mean	SD	Mean	SD
Metal	Calcium	21.3	0.96	81.1	9.30	73.0	4.03
	Sodium	17.3	0.20	42.4	0.83	43.6	0.76
	Magnesium	3.3	0.22	12.7	0.67	11.1	0.24
	Potassium	4.6	0.10	10.8	0.12	13.5	0.31
	Strontium	0.18	0.0	0.8	0.02	0.8	0.02
	Iron	nr ¹	nr ¹	5.8	1.20	5.3	2.68
Anion	Fluoride	2.42	0.03	7.0	0.05	8.2	0.08
	Chloride	15.0	0.49	27.0	0.28	26.9	0.34
	Sulfate	32.5	1.96	73.1	2.55	61.6	2.40

Note 1. nr = not run for this sample

3. Batch Equilibrium Tests

The batch tests contacted 10 g of soil with 200 mL of water. At least 100 mL of final water sample were required for the metals analyses. These analyses were performed at STL-St. Louis under a separate contract with BWXT-Pantex. Both perched aquifer water from PTX06-1049 (PW) and distilled deionized water (DW) were employed. Table 6 summarizes the metals concentrations for well PTX06-1049 provided by the BWXT-Pantex STR, Dr. Jeff Stovall (2003). Table 7 lists the major ionic components of the PTX06-1049 perched aquifer as analyzed during this project. The cations and bicarbonate as alkalinity were analyzed by TraceAnalysis, Inc., and the remaining anion concentrations were analyzed in the ESL.

3.1 Site 1 Isotherms

Both PW and DW were used as source solutions for the batch isotherm tests. The metal stock solutions were atomic absorption standards in acidic solvents. The ranges of initial solution concentrations were chosen based on the STL-St. Louis detection limits and the estimated sorption effects. For each metal isotherm test, three replicate sets of five or six different initial concentrations were employed. It was noted that even small additions of the acidic metal stock solutions could greatly depress the pH, so for each metal four isotherm sets were attempted: [1] PW, [2] DW, [3] PW with pH adjusted back to its initial level prior to the metal addition, and [4] DW with pH adjusted. The pH values of the PW and DW were checked each day of solution mixing, and some variation was noted. From day to day, the PW pH varied from 7.3 to 8.3, and the DW pH varied from 5.5 to 6.5. During set up of each test, sodium hydroxide was added to the 2-L volume of each initial metal concentration to return the pH level to that for the DW or PW for that day. Tables 8 to 12 show the pH effects on Ba, Pb, Ag, Th, and U solutions, respectively. It should also be noted that some problems were experienced with the Ba and Th solutions, as precipitation was seen at some combinations of source water, metal stock solution, and/or base. The 10 g of soil and 200 mL of solution were placed in 250-mL nalgene bottles and tumbled for 24 hr. After the test ended, 100 mL were extracted from each bottle and sent to STL-St. Louis for analysis.

The isotherms were plotted by comparing the final solution concentrations, C_f ($\mu\text{g/L}$ or ppb), to the calculated sorbed concentrations, S ($\mu\text{g/kg}$ soil or ppb). Occasionally the final metal concentrations were below detection in the bottles with lower initial concentrations, which limited the number of actual data pairs for plotting. All the data pairs from the three isotherm replicates for Site 1 soil and initial solution type (1, 2, 3, or 4) on one graph and then fit the isotherm equation. The fits are shown in Appendix A. The primary interest of this project was to define appropriate K_d (L/kg) values from the linear isotherm as

$$S = K_d C_f \quad [1]$$

The Freundlich isotherm as

$$S = K C_f^N \quad [2]$$

and the Langmuir isotherm as

Table 6. Metals Concentrations in Monitoring Well PTX06-1049

Metal	Value	Unit	Detection Limit
Silver	1.11	µg/L	5
Aluminum	138	µg/L	100
Arsenic	<5	µg/L	5
Boron	115	µg/L	30
Barium	181	µg/L	5
Beryllium	<0.20	µg/L	0.20
Cadmium	0.07	µg/L	1
Cobalt	<5	µg/L	5
Chromium	2.12	µg/L	5
Copper	<5	µg/L	5
Iron	181	µg/L	100
Magnesium	10,000	µg/L	10
Manganese	2.47	µg/L	5
Molybdenum	7.05	µg/L	10
Nickel	<5	µg/L	5
Lead	0.12	µg/L	2
Antimony	0.30	µg/L	2
Selenium	4.69	µg/L	5
Tin	<10	µg/L	10
Thallium	0.55	µg/L	0.50
Uranium	2.92	µg/L	0.20
Vanadium	11.80	µg/L	5
Zinc	3.37	µg/L	5
Thorium-228	0.02	pci/L	
Thorium-230	0.25	pci/L	
Thorium-232	0.07	pci/L	

Table 7. PTX06-1049 Water Quality

Cation	Concentration (mg/L)	Anion	Concentration (mg/L)
Calcium	40.9	Sulfate	10.5
Magnesium	10.4	Bicarbonate	149
Strontium	0.38	Chloride	23.1
Sodium	13.4	Fluoride	1.1
Potassium	5.24	Nitrate	0.89
		Bromide	0.26

Table 8. Site 1 Barium Isotherm pH Values

C _i (ppm)	1- PW	2-DW	3-PW/adj		4-DW/adj	
	w/Ba	w/Ba	w/Ba	w/Ba, NaOH	w/Ba	w/Ba,NaOH
20	7.8	2.3	7.8	nc ¹	2.3	5.8
40	7.8	2.1	7.8	nc ¹	2.1	5.9
100	7.7	1.7	7.7	nc ¹	1.7	5.8
200	7.7	1.4	7.7	nc ¹	1.4	5.8
300	7.5	1.2	7.5	7.8	1.2	5.8
400	7.5	p ²	7.5	7.7	p ²	p ²

Note 1. nc = no significant change in pH from raw water, too small to adjust.

Note 2. p = precipitation apparent in solution, not used.

Table 9. Site 1 Lead Isotherm pH Values

C _i (ppm)	1- PW	2-DW	3-PW/adj		4-DW/adj	
	w/Pb	w/Pb	w/Pb	w/Pb, NaOH	w/Pb	w/Pb,NaOH
250	7.6	4.0	7.6	7.8	4.0	6.2
500	7.5	3.8	7.5	8.3	3.8	6.0
750	6.9	3.6	6.9	8.4	3.6	6.0
1000	6.5	3.2	6.5	7.8	3.2	6.0
2000	6.4	3.2	6.4	7.8	3.2	6.0
4000	6.3	3.3	6.3	8.4	3.3	6.0

Table 10. Site 1 Silver Isotherm pH Values

C _i (ppm)	1- PW	2-DW	3-PW/adj		4-DW/adj	
	w/Ag	w/Ag	w/Ag	w/Ag, NaOH	w/Ag	w/Ag,NaOH
250	8.0	4.5	8.0	8.2	4.5	6.5
500	7.8	4.2	7.8	8.2	4.2	6.4
750	7.7	4.1	7.7	8.2	4.1	6.5
1000	7.5	4.0	7.5	8.2	4.0	6.4
2000	7.0	3.8	7.0	8.2	3.8	6.5
4000	6.7	3.6	6.7	8.2	3.6	6.6

Table 11. Site 1 Thorium Isotherm pH Values

C _i (ppm)	1- PW	2-DW	3-PW/adj		4-DW/adj	
	w/Th	w/Th	w/Th	w/Th, NaOH	w/Th	w/Th,NaOH
2	6.4	3.0	6.4	7.8	3.0	6.0
4	4.2	2.6	4.2	7.9	2.6	6.0
10	2.4	2.2	2.4	7.8	2.2	5.5
20	2.0	1.9	2.0	8.0	1.9	5.5
30	1.8	1.6	1.8	8.0	1.6	5.5
40	1.6	1.6	1.6	9.2	1.6	5.5

Table 12. Site 1 Uranium Isotherm pH Values

C _i (ppm)	1- PW	2-DW	3-PW/adj		4-DW/adj	
	w/U	w/U	w/U	w/U, NaOH	w/U	w/U,NaOH
1	7.1	4.0	7.1	7.3	4.0	6.0
2	6.9	3.9	6.9	7.3	3.9	6.0
3	6.7	3.7	6.7	7.3	3.7	6.0
4	6.5	3.6	6.5	7.3	3.6	6.0
7	6.1	3.4	6.1	7.3	3.4	6.0
10	5.8	3.3	5.8	7.3	3.3	6.0

$$S = \frac{\alpha\beta C_f}{1 + \alpha C_f} \quad [3]$$

were also considered to see if better fits were possible. All fits are reported graphically and with correlation coefficients in Appendix A. Tables 13 to 17 summarize the fitted parameters for all three isotherm equations for each of the five metals.

It is notable that both pH adjustment and ionic strength (PW vs. DW) significantly affected the calculated K_d values. The DW is likely much closer to the ionic strength of recharging rainfall that is normally seen as the solvent for metals transport in the shallow unsaturated zone. The pH-adjusted tests are likely more realistic, as the unadjusted pH values were sometimes more than 2 pH units lower than the initial DW or PW. The other isotherm fits are also of interest. The Freundlich fits are often quite good, with high correlation coefficients. The Ag and Th isotherms were problematic with all three isotherm equations.

The PW K_d values for Ba, Pb, Ag, and Th were all large enough (38, 4900, 45, and 8800 L/kg, respectively) to indicate that the duration of flow-through column tests would be much longer than the contract project period. As 100 mL of sample was necessary for the STL-St. Louis analytical protocol, any column apparatus would have to include a pore volume at least that large. Other studies, such as that of Barnett et al. (2000), that observed the passage of many hundreds to thousands of pore volumes did not have this sample volume requirement and

Table 13. Site 1 Barium Isotherm Parameters

Isotherm	K_d (L/kg)	K ([$\mu\text{g}/\text{kg}$][$\mu\text{g}/\text{L}$] ^{-N})	N	β (kg/ μg)	α (L/ μg)
1-1 (PW)	38.3	3210	0.626	6.25×10^6	2.23×10^{-5}
1-2 (DW)	43.8	19700	0.476	5.59×10^6	5.46×10^{-5}
1-3 (PW/adj)	57900	21700	1.103	2.30×10^{10}	2.75×10^{-6}
1-4 (DW/adj)	42400	1.69×10^6	0.662	3.92×10^9	2.80×10^{-5}

Table 14. Site 1 Lead Isotherm Parameters

Isotherm	K_d (L/kg)	K ([$\mu\text{g}/\text{kg}$][$\mu\text{g}/\text{L}$] ^{-N})	N	β (kg/ μg)	α (L/ μg)
1-1 (PW)	4900	16500	0.789	1.37×10^6	7.90×10^{-3}
1-2 (DW)	5910	27800	0.684	1.06×10^6	1.55×10^{-2}
1-3 (PW/adj)	9900	21100	0.721	2.99×10^5	4.66×10^{-2}
1-4 (DW/adj)	8600	4560	1.22	3.42×10^5	1.71×10^{-2}

Table 15. Site 1 Silver Isotherm Parameters

Isotherm	K_d (L/kg)	K ([$\mu\text{g}/\text{kg}$][$\mu\text{g}/\text{L}$] ^{-N})	N	β (kg/ μg)	α (L/ μg)
1-1 (PW)	45.4	1190	0.0023	1.04×10^3	4.16×10^{-1}
1-2 (DW)	395	3110	0.592	9.62×10^4	1.32×10^{-2}
1-3 (PW/adj)	58.7	601	0.539	2.25×10^3	3.90×10^{-2}
1-4 (DW/adj)	259	3410	0.552	6.10×10^4	2.81×10^{-2}

Table 16. Site 1 Thorium Isotherm Parameters

Isotherm	K_d (L/kg)	K ([$\mu\text{g}/\text{kg}$][$\mu\text{g}/\text{L}$] ^{-N})	N	β (kg/ μg)	α (L/ μg)
1-1 (PW)	8780	179000	0.307	8.20×10^5	6.10×10^{-2}
1-2 (DW)	7660	141000	0.364	1.05×10^6	2.61×10^{-2}

Note: There were not enough data above detection limits on the pH adjusted experiments to attempt to delineate an isotherm.

Table 17. Site 1 Uranium Isotherm Parameters

Isotherm	K_d (L/kg)	K ([$\mu\text{g}/\text{kg}$][$\mu\text{g}/\text{L}$] ^{-N})	N	β (kg/ μg)	α (L/ μg)
1-1 (PW)	9.39	63.7	0.753	5.18×10^4	3.14×10^{-4}
1-2 (DW)	30.3	1800	0.443	1.00×10^5	1.33×10^{-4}
1-3 (PW/adj)	7.61	94.4	0.703	9.35×10^4	1.42×10^{-3}
1-4 (DW/adj)	66.1	669	0.692	5.92×10^4	2.19×10^{-3}

employed much smaller columns. One column test was attempted with Ag and Site 1 soils, and that unsuccessful result is discussed in section 4. The PW K_d values for U, however, at less than 10 L/kg, were judged to be of sufficient concern to warrant additional study with soils from Sites 6 and 7.

3.2 Site 6 and 7 Isotherms

As discussed previously, the second phase of this study considered soil samples from two other sites, 6 and 7 in Figure 1, to determine the potential variability in Blackwater Draw soil characteristics on the sorption of U. Both batch equilibrium isotherm tests, reported in this section, and column flow tests, reported in section 4, were performed. The batch isotherm tests followed the same procedure presented for the Site 1 soil tests, except that U was the only metal tested, soil from both Sites 6 and 7 were exposed separately, and the BWXT-Pantex contract analytical laboratory had changed to the General Engineering Laboratory (GEL). GEL still required at least 100 mL of sample for the U analysis. The U stock solution was an atomic absorption standard in acidic solvent. The range of initial U solution concentrations was chosen based on the GEL reporting limit and the estimated sorption effects. GEL analyzed the U concentrations by ICP. For each U isotherm test, three replicate sets of eight different initial solution concentrations, C_i , were employed, ranging from 0 to 8 m/L (or ppm) of U. Table 18 shows the pH measurements for the four sets of initial isotherm solutions. The 10 g of soil and 200 mL of solution were placed in 250-mL nalgene bottles and tumbled for 24 hr. After the test ended, 100 mL were extracted from each bottle and sent to GEL for analysis.

The results of the isotherm tests are shown in Table 19. The plotted isotherm curves are provided in Appendix A. It is notable that the linear isotherm fits for K_d are relatively similar for isotherms pairs 6-1 and 7-1, 6-2 and 7-2, 6-3 and 7-3, and 6-4 and 7-4. While the fitted values are similar, the fits are especially poor for the unadjusted DW conditions in 6-2 and 7-2. When compared to the Site 1 K_d values of 9.4, 30, 7.6, and 66 L/kg for the PW, DW, PW adjusted, and DW adjusted conditions, respectively, it is notable that the PW and PW adjusted values are quite similar, while the DW and DW adjusted values are much larger for Sites 6 and 7. As seen with the Site 1 soil, both pH adjustment and ionic strength (PW vs. DW) significantly affected the calculated K_d values. The other isotherm fits are also of interest. The Freundlich and Langmuir fits were again often visually pleasing, sometimes with high correlation coefficients. The utility of these values, however, is limited as linear K_d values are more typically applied in fate and transport modeling and risk assessment applications.

4. Soil Column Experiments

4.1 Attempt at Soil Column Experiment with Silver and Site 1 Soil

One important constraint on the management of this project was the requirement that the metals analyses for the sorption tests be performed by STL-St. Louis, one of BWXT-Pantex's contract laboratories. This arrangement made good sense for budgetary reasons, but it did require that samples be sent off for analyses with a two- to four-week turnaround. This approach did not allow the TTUWRC team to monitor the potential changes in metal concentrations in a shorter time period. The data in Tables 6 and 20 were provided by the BWXT-Pantex STR

Table 18. Initial U (C_i) and pH Values for Site 6 and 7 Uranium Isotherm Solutions

C_i (mg/L)	pH (SU)					
	1- PW	2-DW	3-PW/adj		4-DW/adj	
	w/U	w/U	w/U	w/U, NaOH	w/U	w/U,NaOH
0.0	7.85	5.83	7.78	no adj	5.65	no adj
0.6	7.70	3.95	7.53	7.76	3.84	5.69
1.2	7.14	3.75	7.41	7.75	3.61	5.68
2.0	7.02	3.49	7.13	7.78	3.41	5.63
4.0	6.60	3.22	6.57	7.81	3.15	5.60
6.0	6.22	3.06	6.25	7.75	3.05	5.62
8.0	5.84	2.93	6.12	7.76	2.91	5.63

Table 19. Site 6 and 7 Uranium Isotherm Parameters

Isotherm	K_d (L/kg)	K ([$\mu\text{g}/\text{kg}$][$\mu\text{g}/\text{L}$] ^{-N})	N	β (kg/ μg)	α (L/ μg)
6-1 (PW)	10.7	14.9	0.79	74.6	0.35
6-2 (DW)	11.2	33.3	0.28	43.5	10.5
6-3 (PW/adj)	7.7	14.5	0.59	44.1	0.70
6-4 (DW/adj)	89.5	93.5	0.67	189	1.10
7-1 (PW)	10.0	16.3	0.72	75.2	0.30
7-2 (DW)	12.3	34.0	0.31	48.3	5.90
7-3 (PW/adj)	8.3	14.0	0.65	59.9	0.30
7-4 (DW/adj)	94.3	96.0	0.66	161	1.60

Table 20. Typical Pantex Soil and Pore Water Metal Levels (Stovall 2003)

Metal	K_d (L/kg)	Soil Concentration (mg/kg)	Pore Water Concentration ($\mu\text{g}/\text{L}$)
Barium (high)	2800	75400	26900
Barium (typical)	2800	500	178
Mercury (high)	580	1.2	2.07
Mercury (typical)	580	0.1	0.17
Lead (high)	597	380	637
Lead (typical)	597	20	33.5
Silver (high)	4	540	135000
Silver (typical)	4	3	750
Thorium	500	9.1	18.2
Uranium	50	75	1500
Antimony	6	20	3330

(Stovall 2003) to provide a starting point for estimating useful ranges of sorbed and solution concentrations for application in the column tests. The estimated K_d values were from EPA (1999). In addition, STL-St. Louis required 100-mL samples for their analytical protocols for the metals of interest. Silver was selected for the first column tests, which began before the batch isotherm tests were completed.

In order to get multiple 100-mL samples from a single pore volume, a column size of 30.5-cm (12-in) length by 7.5-cm (3-in) diameter was selected. At a target porosity of about 0.4, the pore volume would be about 540 mL. Three replicate stainless columns were assembled and plumbed to high pressure liquid chromatography (HPLC) pumps to provide the flow. The columns were carefully packed and tamped in 5-cm lifts. Perched aquifer water from PTX06-1049 was selected as the solvent.

The target flow rate for the column tests was initially 10 mL/min, but during the saturation of the columns it was found that only 2 mL/min was possible. The silver injection solution initially included 20 mg/L bromide and 200 ppb silver. The bromide broke through as expected, Figure 5, but after over 46 pore volumes, the silver had not broken through in any of the three columns. This result indicated much greater sorption than earlier anticipated based on the typical K_d values in Table 20, and the low flow rates would also require column test durations longer than the project duration. After discussion with the BWXT-Pantex STR, the decision was made to move forward with batch equilibrium tests rather than columns for all five metals in the first phase of the study.

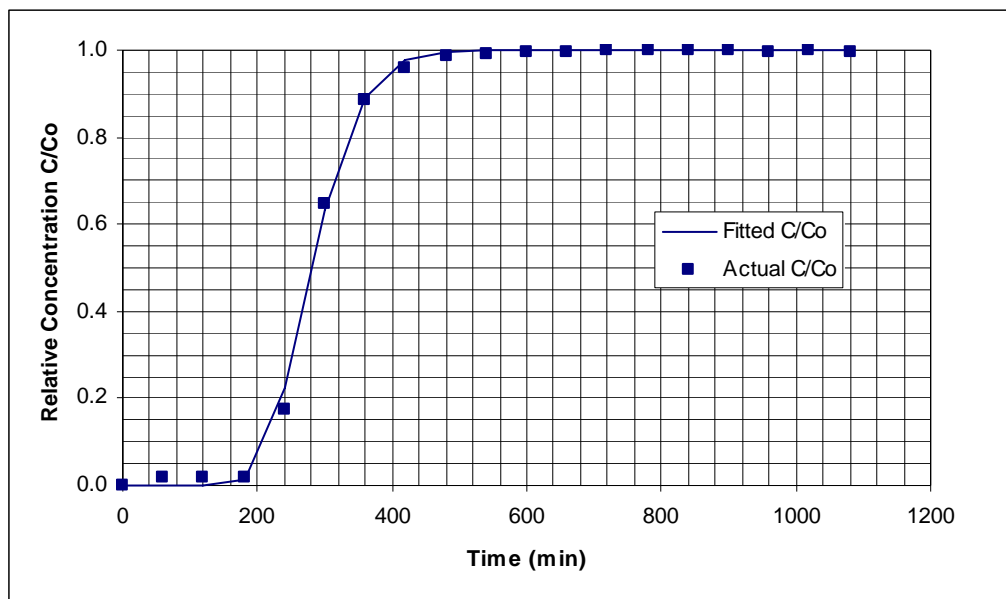


Figure 5. Bromide Breakthrough in Column 1, Site 1 Soil (Dispersivity = 0.63 cm)

4.2 Experimental Design for Uranium Column Tests

The conditions for the flow-through column tests for U sorption were considered carefully. One important constraint on the management of this project was the requirement that

the U analyses for the sorption tests be performed by GEL, one of BWXT-Pantex's contract laboratories. This arrangement made good sense for budgetary reasons, but it did require that samples be sent off for analyses with a minimum of 7-working-day turnaround. This approach did not allow the TTUWRC team to monitor the potential changes in U concentrations on a more immediate basis as might be possible if the U analyses were at the ESL. The GEL also required at least 100 mL for a U analysis. The limited duration of the second phase of the sorption project led to the conclusion that the soil columns must be made as small as practicable to control the duration of the tests. It was estimated that as many as 200 pore volumes would have to pass through each column to demonstrate the complete breakthrough of U. The decision was made to size the columns for pore volume sizes of 100 mL, so each pore volume could comprise a sample for U analysis. This approach was also attractive as the timing of the sample volumes could be used to carefully monitor the flow rate in each column. The HPLC pumps used to drive the flow in the columns were known to give somewhat imprecise flow rate readings, and experience has shown that often flow rates drop as injection pressure builds over long test durations.

The soil columns were constructed in 3.58-cm (1.41-in) diameter stainless steel pipes, with a target soil length in the column of 25.4 cm (10 in). At a target porosity of 0.40, these dimensions for the soil gave a pore volume of 100 mL. Three replicate stainless steel columns were assembled for each soil site. The columns were carefully packed and tamped in 5-cm lifts. At both the upstream and downstream ends of the pipes, geotextile fabric and small diameter gravel were used to distribute flow across the soil cross-section and keep the fines from finding their way into the tubing. The pipes were carefully capped with threaded stainless steel caps, and the caps were also drilled and threaded to allow connection to the injection and discharge tubing. The HPLC pumps had nominal pressure limits of 1600 psi, and it was possible for clogs to cause the pumps to over-pressurize and shut down. The column tests were planned in triplicate to observe replicated behavior, but also as a precaution in case one or more columns was not able to sustain flow for the entire test duration.

After assembly, the columns were placed in a support structure for vertical upward flow. The columns were slowly saturated from the bottoms upward over several days with perched aquifer water from PTX06-1049. This process encouraged removal of all air pockets and allowed for some small amount of swelling of the clay particles. The procedure was repeated using soil from all three sample sites, so nine columns were constructed and operated. Six HPLC pumps were available, which meant only six columns could be operated simultaneously. The first six columns contained soil from Sites 6 and 7. The soil from Site 1 was packed into the last three columns.

4.3 Uranium Column Operation

The target flow rate for the column tests was intended to be 1.0 mL/min, but, during the saturation of the columns, it was found that only 0.8 mL/min was actually possible without over-pressurizing. As is shown later, that 0.8 mL/min could not be maintained in some of the columns. The uranium injection solution was made from the PTX06-1049 water with approximately 360 ppb of added U (no pH adjustment), and it also included 20 mg/L Br for the first 300 mL. The pH of the injection solution was typically 7.65, while the PW was typically 7.8. The Br tracer tests were performed in the first few pore volumes of flow in each column to

demonstrate that short circuiting was not occurring. Ten-mL samples were collected sequentially during the Br phase and analyzed by ion chromatography in the ESL. After the end of the Br phase, 100-mL samples were collected sequentially, each representing approximately one pore volume. While all samples were retained, only every tenth sample was sent to GEL for U analysis. If the U front was very sharp, the U concentrations would jump significantly between two of the decadal samples, and the retained samples between those two could then be forwarded to GEL.

As the U samples were collected, the start and end time for each 100-mL sample was recorded, as well as the pressure reading. The samples were collected in 150-mL nalgene bottles that had been previously marked with a line to show the 100-mL level. This approach allowed a volumetric check on the column flow rates. The tests were planned to push 200 pore volumes through each column. If the U did not break through within 200 pore volumes, that result would imply a K_d of at least 50, assuming a porosity of 0.40.

4.4 Column Test Results

4.4.1 Site 6 Columns

The flow and pressure readings for the three columns packed with homogenized soil from Site 6 are shown in Figure 6. The flow rates in all three columns were lowered from the initial 0.8 mL/min to manage the injection pressures. Columns 6-1 and 6-3 were able to stabilize at 0.6 mL/min and injection pressures of approximately 400 psi. Column 6-2 was more problematic, as its injection pressure rose quickly to almost 800 psi, so its flow rate was lowered to approximately 0.4 mL/min about halfway through its test duration. As the x-axis in Figure 6 has units of time, not pore volumes, the different columns have different endpoints when 200 pore volumes were reached.

The Br breakthrough curves for all three columns are shown in Figures 7, 8, and 9, respectively. Based on the arrival of the relative concentration, C/C_o , of 0.5, which represents the passing of one pore volume of injected water with the conservative tracer, it was possible to estimate the porosity of the soil in the columns. The porosities, n , of columns 6-1, 6-2, and 6-3 were 0.41, 0.41, and 0.43, respectively. These values were similar to those observed in previous column studies with Blackwater Draw soils performed at the TTUWRC by Laun (1995) and Givens (1997). The packed pore volumes were quite close to the target 100-mL value. The shapes of the Br breakthrough curves did not show indications of short-circuit flow. The fitted dispersivities, α_x , as shown in the figure captions, were reasonable for this column size. The dispersivities were found by fitting the one-dimensional advection-dispersion equation to the data as

$$C(L,t) = \frac{C_o}{2} \left(\operatorname{erfc} \left[\frac{L - v_x t}{2\sqrt{D_x t}} \right] + \exp \left(\frac{v_x L}{D_x} \right) \operatorname{erfc} \left[\frac{L + v_x t}{2\sqrt{D_x t}} \right] \right) \quad [4]$$

and

$$D_x = \alpha_x v_s \quad [5]$$

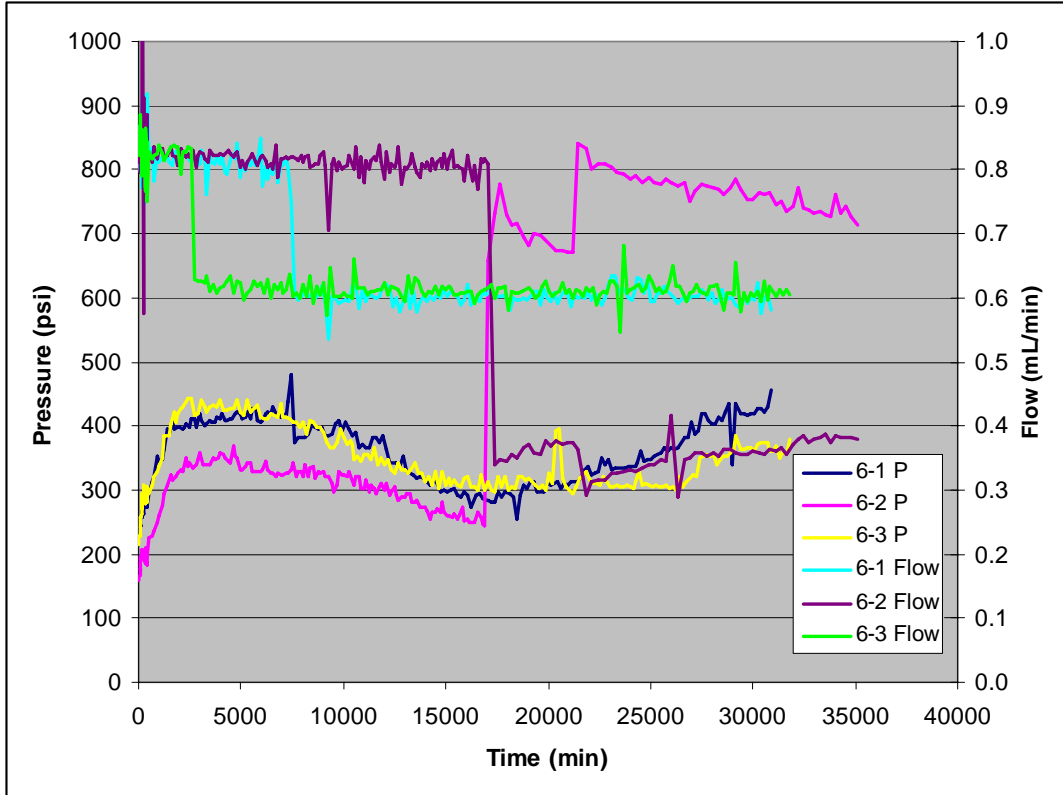


Figure 6. Pressure and Flow Histories for Site 6 Columns

where $C(L,t)$ = effluent U concentrations over time as ppb, C_o = injected U concentration in ppb, L = column length at 25.4 cm, v_x = pore water velocity in cm/min, and D_x = dispersion coefficient in cm^2/min .

Figure 10 displays the U breakthrough curves for columns 6-1, 6-2, and 6-3. The relative concentrations of U are shown, based on the average concentration of the last several samples after the effluent U concentration had stabilized. These curves were based on the analysis of every tenth sample, and based on the shape of the U breakthrough curves, it was not necessary to analyze any additional intermediate samples. The retardation factor, R , could be found by identifying the number of pore volumes required to reach a relative concentration C/C_o of 0.5. These R values were 87, 78, and 83, respectively, for columns 6-1, 6-2, and 6-3. Because of the changing flow rates in all three columns, it was not possible to directly use Equations 4 and 5 with a retarded U velocity to fit the U breakthrough curves. The K_d values were calculated as

$$K_d = (R - 1) \frac{n}{\rho_b} \quad [6]$$

with

$$\rho_b = (n - 1) \rho_s \quad [7]$$

where ρ_b = bulk density in g/cc, and ρ_s = density of soil solid particles at 2.67 g/cc. These

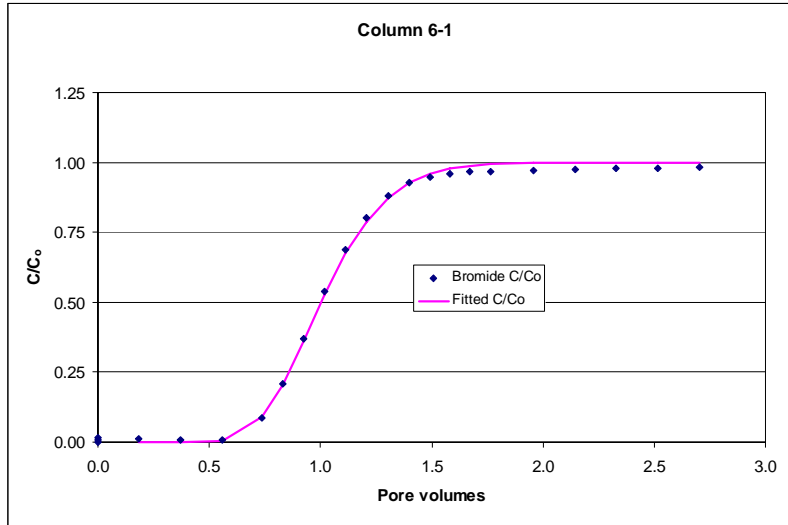


Figure 7. Bromide Tracer Fit for Column 6-1, $\alpha_x = 0.67$ cm

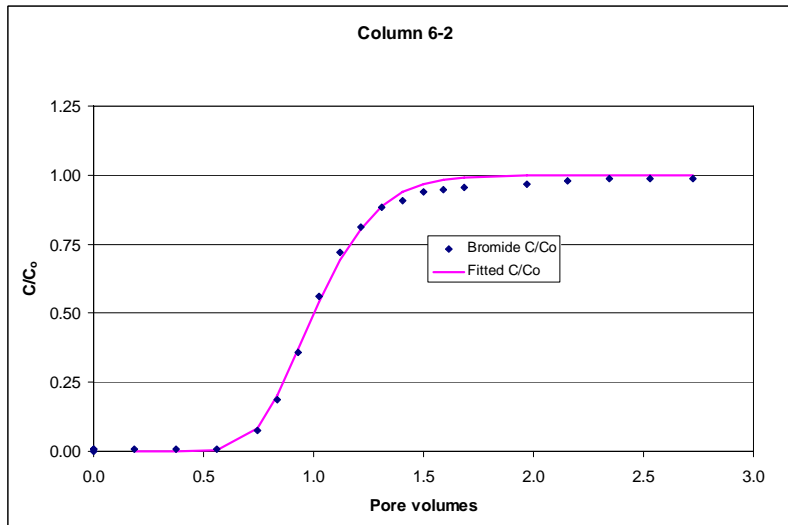


Figure 8. Bromide Tracer Fit for Column 6-2, $\alpha_x = 0.62$ cm

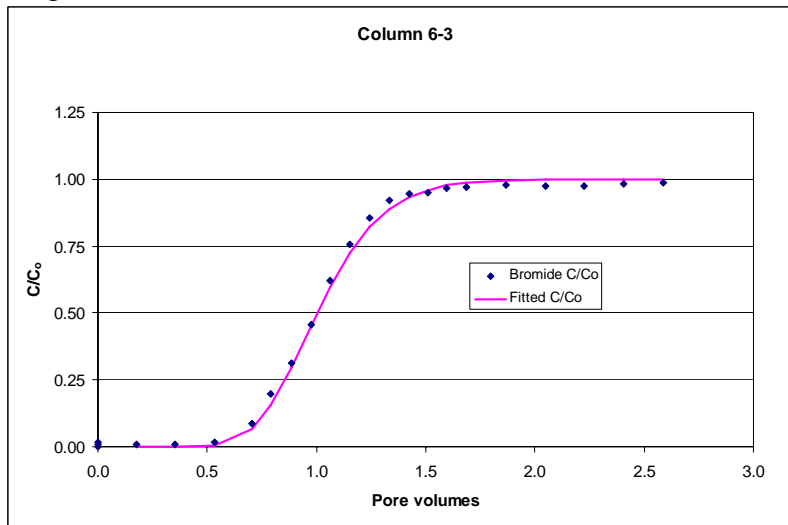


Figure 9. Bromide Tracer Fit for Column 6-3, $\alpha_x = 0.71$ cm

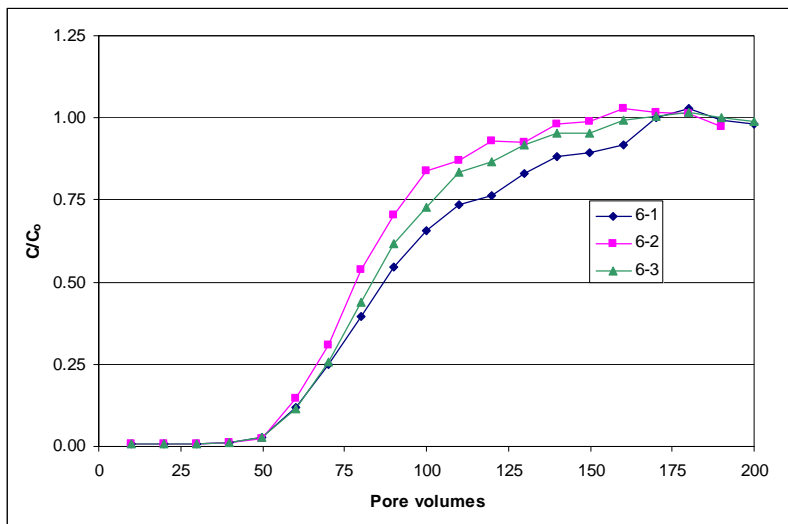


Figure 10. U Breakthrough Curves for Columns 6-1, 6-2, and 6-3

calculations returned K_d values of 22, 20, and 23 for the three columns, respectively, with an average value of 22.

4.4.2 Site 7 Columns

The pressure and flow variations observed with the three columns packed with soil from Site 7 are shown in Figure 11. The flow rates for columns 7-1 and 7-2 stayed close to the target 0.8 mL/min for most of the test duration, while their pressure readings stayed below 400 psi. The pressure readings for column 7-3 were significantly higher than those for the other two columns, and the flow rate was adjusted downward to 0.6 and then 0.4 mL/min to complete the test.

The Br breakthrough curves for columns 7-1, 7-2, and 7-3 are shown in Figures 12, 13, and 14, respectively. As with the Br curves for Site 6, all three displayed the typical S-shape and did not indicate the presence of short-circuit flow. Based on the arrival of the relative concentration, C/C_0 of 0.5, the porosities were estimated at 0.38, 0.41, and 0.45 for columns 7-1, 7-2, and 7-3, respectively. The dispersivity values fitted from Equations 4 and 5 are shown in the figure titles, and were similar in magnitude to those for the Site 6 soils.

The U breakthrough curves are shown for all three columns in Figure 15. The relative concentrations of U were calculated based on the average of the later samples after stabilization of the U effluent. The R values were again found by finding the number of pore volumes required for C/C_0 of 0.5. The associated R values were 76, 74, and 76 for columns 7-1, 7-2, and 7-3, respectively. The K_d values were then calculated using Equations 6 and 7. The resulting K_d values were 17, 19, and 23, respectively, with an average value of 20.

The stable flow rates for columns 7-1 and 7-2 allowed fitting of the advection-dispersion Equation 4 to the data, using the retarded U velocities. Figures 16 and 17 display the two fitted curves, which both resulted in fitted dispersivities of 1.9 cm, about twice as large as the values in

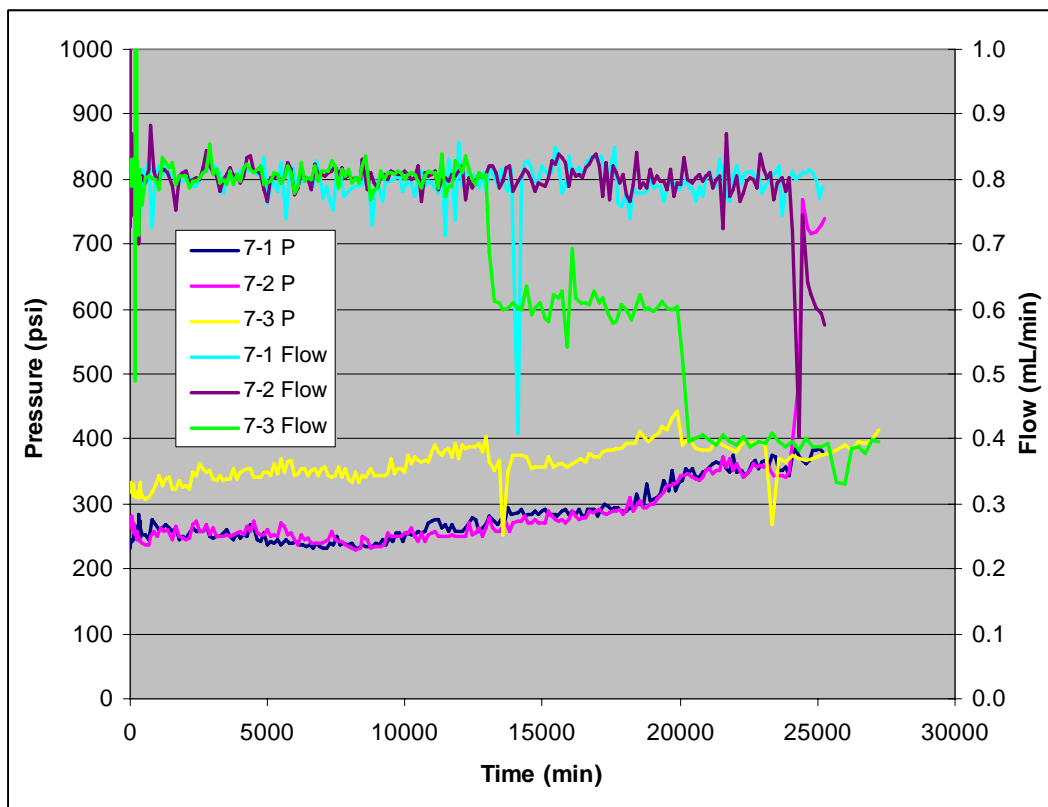


Figure 11. Pressure and Flow Histories for Site 7 Columns

the Br breakthrough curve fits. This result indicates the reproducibility of these flow-through experiments, as the movement of U through both columns was quite similar.

4.4.3 Site 1 Columns

During the operation of the three columns with soil from Site 1, two of the columns, 1-1 and 1-3, failed as high pressure caused leakage from the plumbing connecting the HPLC pumps to the columns. The project schedule did not allow time for reconstruction of these columns, so only column 1-2 was able to complete the 200-pore volume target. Figure 18 shows the pressure and flow variations observed during the operation of column 1-2. The pressure slowly rose to above 1000 psi, so great care was taken to keep the flow rate low enough to complete the test. The flow rate was slowed from 0.6 mL/min at the commencement of the test eventually to 0.4 mL/min after about one week of operation. As stated in the experimental design, the purpose of replicate columns was meant to insure that at least one would successfully make it through the entire test successfully.

The Br breakthrough curve for column 1-2 is shown in Figure 19. The shape of the breakthrough curve is similar to those seen in the other columns. The fitted dispersivity of 0.56 cm is similar to those seen for the Site 6 soil columns. As with the other columns, there were no indications of short-circuit flow. The calculated porosity was 0.42.

The U breakthrough curve is shown in Figure 20. The data show some fluctuation after

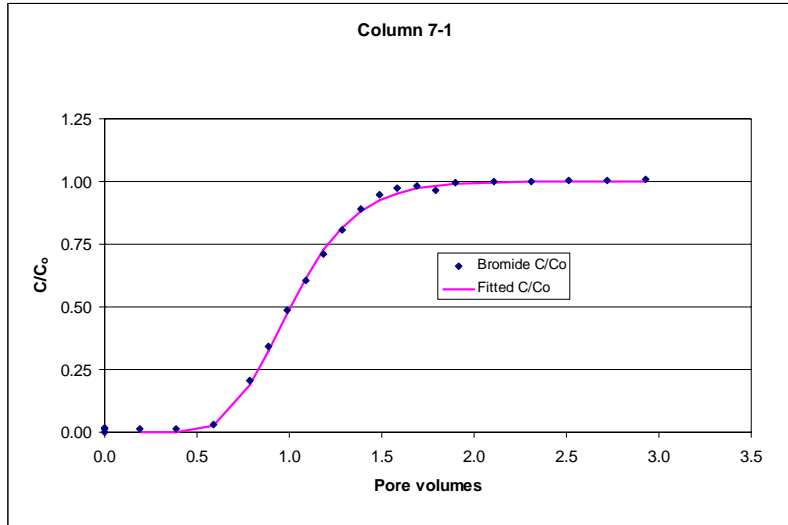


Figure 12. Bromide Tracer Fit for Column 7-1, $\alpha_x = 0.96$ cm

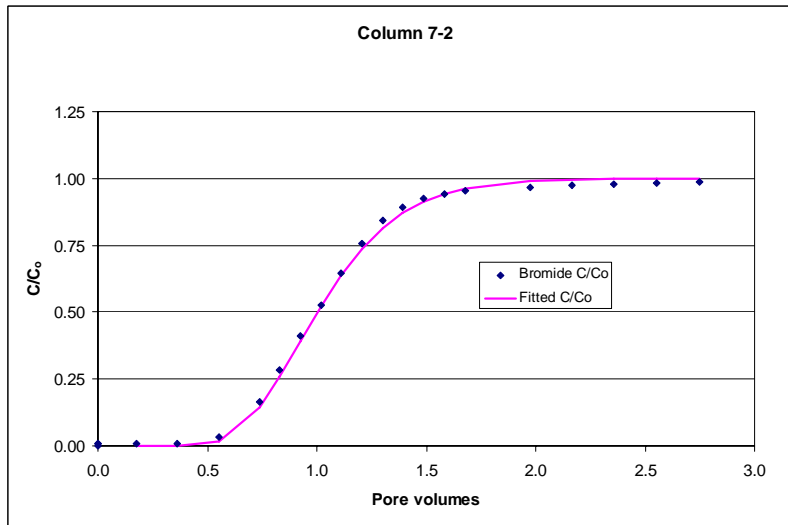


Figure 13. Bromide Tracer Fit for Column 7-2, $\alpha_x = 1.1$ cm

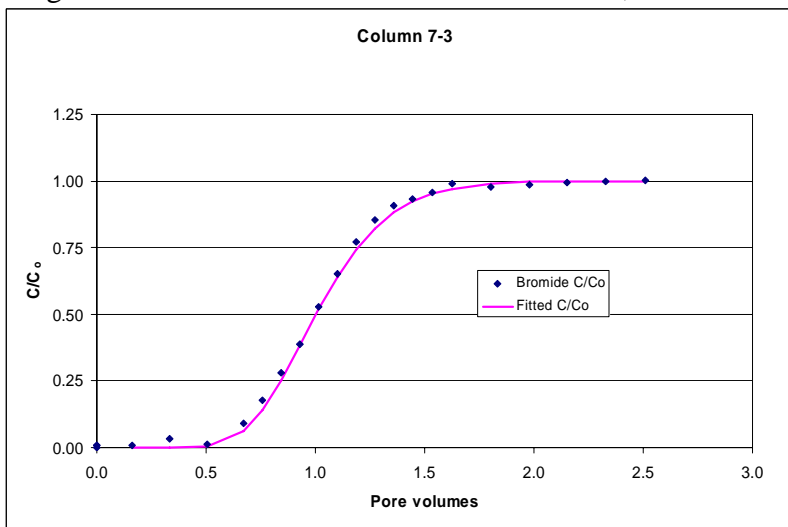


Figure 14. Bromide Tracer Fit for Column 7-3, $\alpha_x = 0.84$ cm

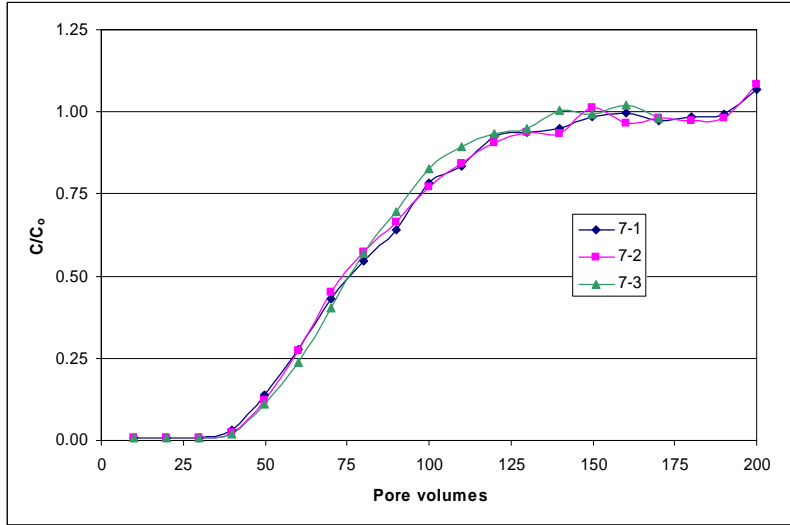


Figure 15. U Breakthrough Curves for Columns 7-1, 7-2, and 7-3

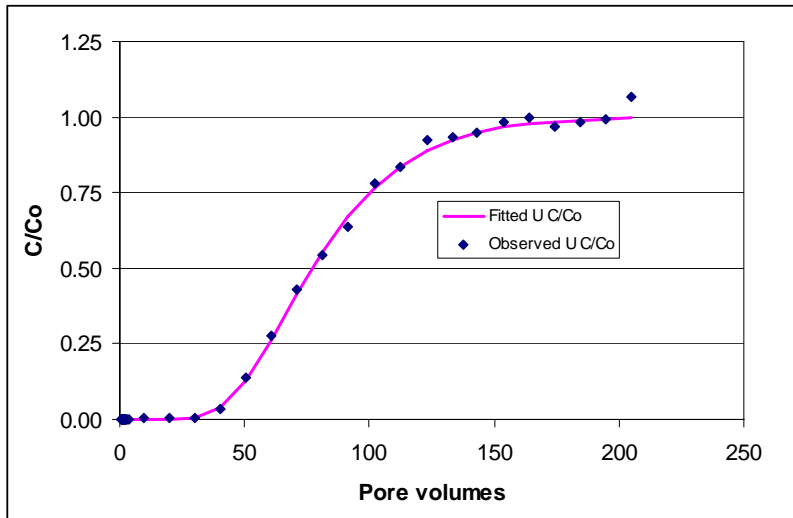


Figure 16. Column 7-1 U Curve Fit, $R = 76$, $\alpha_x = 1.9$ cm

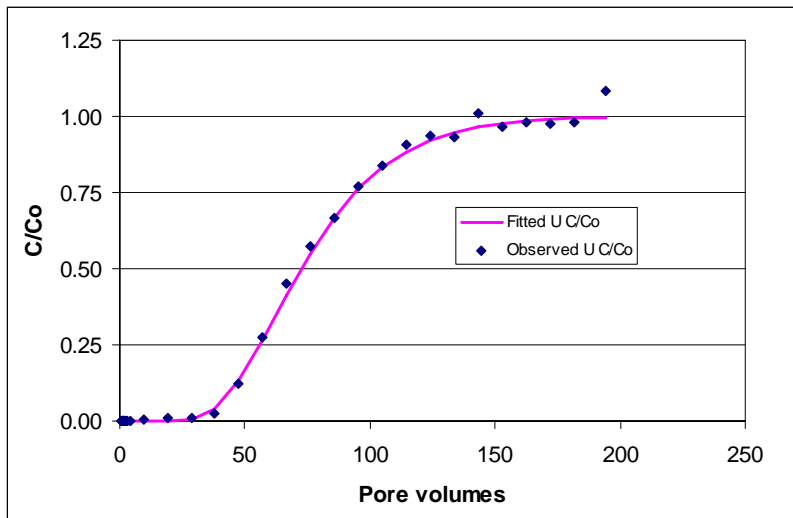


Figure 17. Column 7-2 U Curve Fit, $R = 74$, $\alpha_x = 1.9$ cm

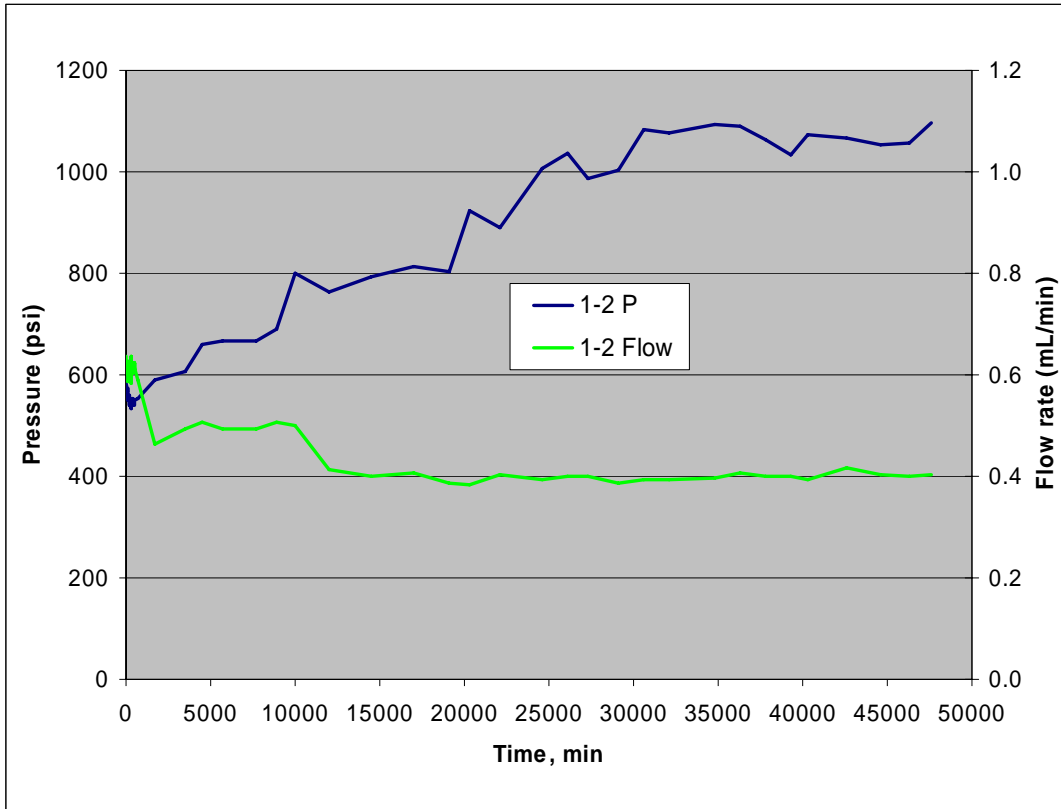


Figure 18. Pressure and Flow Histories for Site 1 Column 1-2

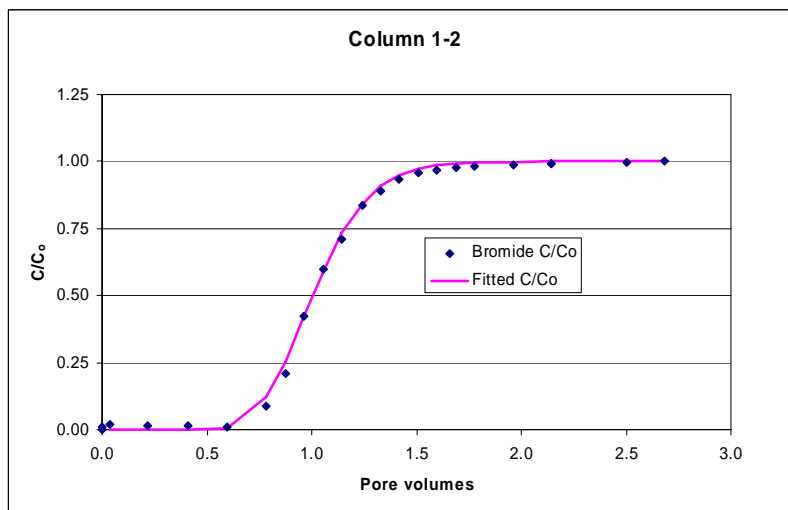


Figure 19. Bromide Tracer Fit for Column 1-2, $\alpha_x = 0.56$ cm

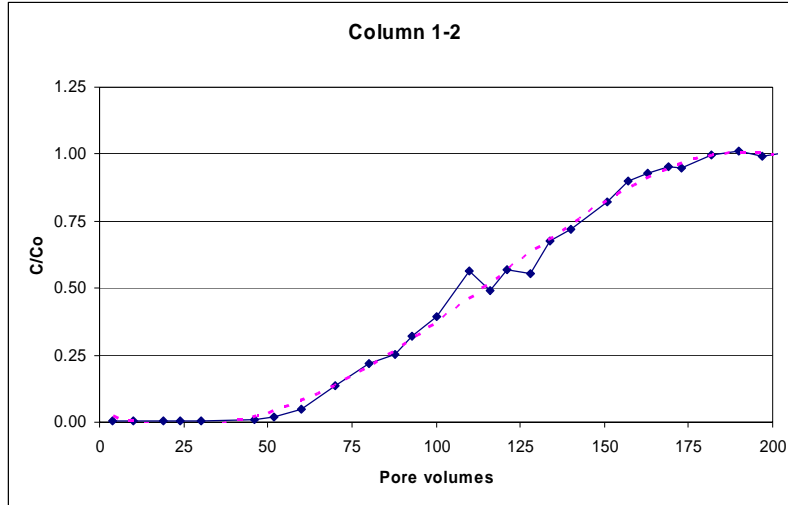


Figure 20. U Breakthrough Curve for Column1-2 (dashed line to smooth data)

about 100 pore volumes, but then settled down toward the end of the test. A simple polynomial trendline, shown as a dashed line in Figure 20 was used to place a smooth line through the U data. The relative concentrations of U were again calculated based on the average of the later samples after stabilization of the U effluent. The R value, 114, was determined from the number of pore volumes required for C/C_0 of 0.5 on the smoothed dashed line. Applying Equations 6 and 7, this R value corresponds to a K_d of 31. The changing flow rate did not allow direct fitting of Equation 4.

4.4.4 Overview of Column Test Results

The three sets of column tests showed very similar behavior for the reactive transport of U through the three samples of Blackwater Draw soils. The most direct way of combining these results is to simply average the seven K_d values, as shown in Table 21. The average K_d value for the seven tests is 22 L/kg, with a standard deviation of 4.5 L/kg. The flow test results are more representative of the sorption effects in the natural soil conditions than the batch equilibrium test results. Barnett et al. (2000) demonstrated that observed sorption of U was greater in column

Table 21. Column Test K_d Values

Soil Column	K_d (L/kg)
1-2	31
6-1	22
6-2	20
6-3	23
7-1	17
7-2	19
7-3	23
Average	22
SD	4.5

tests than in batch equilibrium tests with soils from the Department of Energy's Oak Ridge facility in Tennessee (silt loam), Savannah River facility in South Carolina (sandy clay loam), and Hanford site in Washington (sand). Barnett et al. (2000) identified several shortcomings of batch tests. These weaknesses include [1] low solid to solution ratio relative to the actual porous medium, [2] possible accumulation of reaction products and intermediates in the pore space, [3] mass transport limitations in the porous medium, and [4] particle abrasion that can change surface reactivity. They found that the observed U sorption in their column tests was about twice the amount that would be predicted by their batch tests. Rancon (1973) reported a range of U K_d values of 16 L/kg for a clay/calcite sand to 39 L/kg for a river sediment. These values bracket those observed in these column tests.

5. Equilibrium Chemistry Simulation

The chemistry model Visual Minteq version 2.4 based on MINTEQA2 (Allison et al. 1991) was used to define the uranium speciation and total dissolved carbonate distribution as a function of pH for the perched aquifer water. The model used a mass balance approach to solve for the final equilibrium concentrations of various species. The measured cations, anions, and alkalinity of the perched aquifer water were used to define their constituent values in the model. The alkalinity measured in the perched aquifer water was in the form of bicarbonate. The water quality values employed in the simulations were presented in Table 7 with the U value in Table 6. The uranium component of the model was defined into the model in two forms: U^{+4} and UO_2^{+2} . The concentrations of these components and their related species were determined by running the model at a specific pH and observing the equilibrium concentrations. All simulations considered the temperature to be 25°C. All thermodynamic coefficients were available in the Minteq database, and none were adjusted by the user. The model only considers the chemical equilibrium between species and does not take into account the sorptive capacity of the surrounding soil matrix.

The model was run using the "Multi-problem/Sweep" option of the program. This option allowed the model to vary the pH in 0.5 pH-unit increments and solve for equilibrium concentrations at those intervals. Several outputs are available after a successful run of the model where convergence occurs. The first output of interest is the concentrations (mol/L) and activities of all aqueous species. The second is the species distribution of every component present in the model in molar percentages. The species distribution for U^{+4} and UO_2^{+2} and total dissolved carbonate were plotted in Excel as functions of pH to identify dominant species over the pH range.

The purpose of these simulations was to identify which uranium species were most likely to be present in the perched aquifer water and infiltrating water moving through the Blackwater Draw soils. As shown in Figure 21, for pH > 5, the dominant specie related to U^{+4} is $U(OH)_4$ (aq), with UF_3^+ and UF_4 (aq) becoming significant at pH between 5 and 6. Speciation relative to UO_2^{+2} is much more complicated, as displayed in Figure 22. Above pH 8, the major specie is $Ca_2UO_2(CO_3)_3$ (aq), with $UO_2(CO_3)_2^{-2}$ as the next but much less prevalent specie. Between pH 6.5 and 8, the three main species are $Ca_2UO_2(CO_3)_3$ (aq), $UO_2(CO_3)_2^{-2}$, and UO_2CO_3 (aq). Below pH 6.5, virtually all of the different species can be present. Figure 23 shows the familiar distribution of H_2CO_3 , HCO_3^- , and CO_3^{2-} typical to natural fresh waters. At pH > 8.3, other

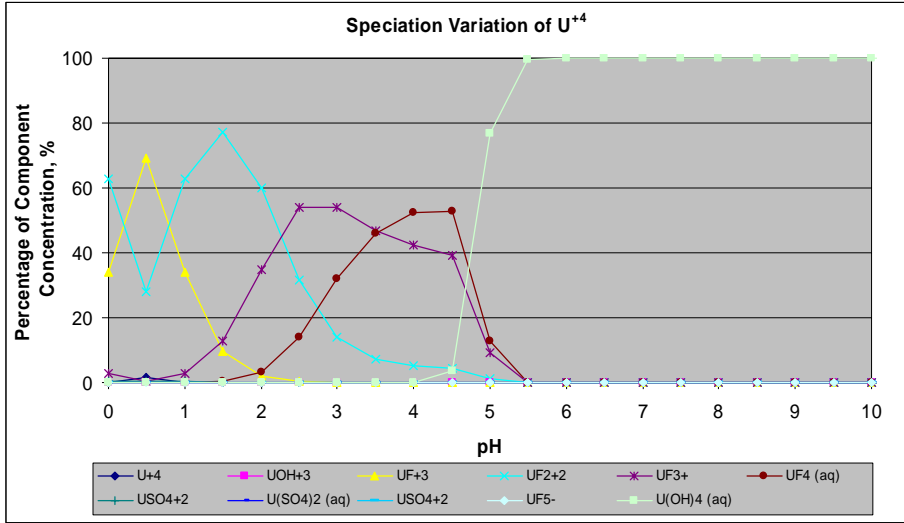


Figure 21. Speciation as Related to U^{+4}

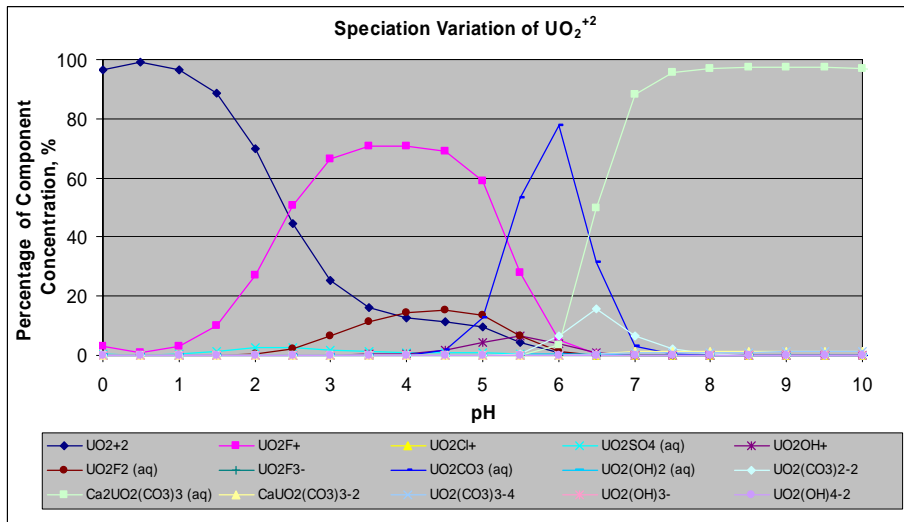


Figure 22. Speciation as Related to UO_2^{+2}

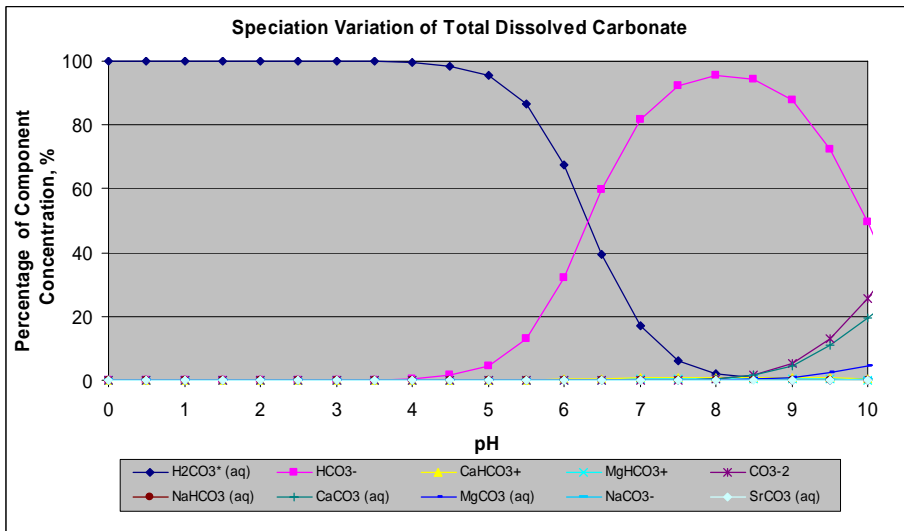


Figure 23. Speciation as Related to CO_3^{-2}

mineral carbonates start to form. As these results are considered, it is important to remember that any specie followed by “(aq)” represents a neutral mineral that has the potential to precipitate on its own or as an impurity with other solids. Anions are typically more mobile in subsurface waters, which means $\text{UO}_2(\text{CO}_3)_2^{-2}$ could be mobile. It should be noted that these figures present the percentage by mass of each component in solution, not molar or mg/L concentrations. The total U concentration for the PTX06-1049 water sample shown in Table 6 was only 3 ppb, which would lead to very low concentrations of other U species in that water.

6. Summary and Conclusions

BWXT-Pantex contracted with the TTUWRC to study the sorption of Ba, Pb, Ag, Th, and U on Blackwater Draw soils, typical of the shallow subsurface at the Pantex Plant site. The general scope of work was to use batch equilibrium and column flow experiments to estimate the distribution coefficients, K_d , for each metal with this soil matrix. These values were needed for fate and transport modeling in support of remediation and risk assessment efforts at the Plant.

The soil samples to be tested were collected with a geoprobe by BWXT-Pantex staff at three clean locations, referred to as Sites 1, 6, and 7, in the Pantex vicinity. The soils were characterized for grain-size distribution, initial moisture and organic carbon content, cation exchange capacity, electrical conductivity, pH, extractable ions, and mineralogy. The USDA soil classifications ranged from loamy sand to sandy clay loam, and the other characteristics were somewhat variable across the three sites.

In the first phase of the study, batch equilibrium isotherm tests were performed to observe sorption of the metals over a reasonable range of solution concentrations when exposed to soil from Site 1. The metals were spiked from acidic stock solutions into water solutions based on local perched aquifer water from well PTX06-1049 and distilled deionized water, both with and without pH adjustment. Linear, Freundlich, and Langmuir isotherms were fitted to the observed data. Both ionic strength (perched water vs. DDI water) and pH (adjusted vs. non-adjusted) affected the isotherm parameters significantly. The batch K_d values for Ba, Pb, Ag, and Th were approximately 40, 5000, 45, and 9000 L/kg, while the batch K_d value for U was less than 10 L/kg. Column flow experiments had been planned for all five metals, but the results of the batch tests, and one unsuccessful Ag column test, indicated that column tests would not be feasible within the time and analytical constraints of the project for Ba, Pb, Ag, and Th. The batch values showed that mobility of these four metals in Blackwater Draw soil is limited, and the batch K_d values can be used in other fate and transport applications. Further study of U sorption was planned in the next phase.

In the second phase of the study, soil from Sites 6 and 7 were subjected to batch equilibrium tests similar to those in the first phase, and to column flow tests with solutions spiked with U. The batch tests resulted in K_d and other fitted isotherm parameters similar to those seen for the soil from Site 1. All three soils were used in soil column tests with U spiked into the perched aquifer water. A total of seven soil column tests were completed, and the average K_d value was 22 L/kg, with a standard deviation of 4.5 L/kg. Observation of higher sorption of U in column tests than in batch equilibrium tests has been observed previously by

Barnett et al. (2000). The U K_d value of 22 L/kg is recommended for other fate and transport applications, instead of the batch U K_d value.

The ionic composition of the PTX06-1049 water with its known U concentration was simulated with Minteq, an equilibrium chemistry speciation model. This simulation was presented to identify the relative concentrations of U that might exist under different pH conditions. This effort was of interest as a demonstration of which dissolved ionic or neutral species could contain the U in solution. Other applications of this information could include fate of U in the perched aquifer, or approximation of U fate during infiltration through the unsaturated zone.

7. References

Allison, J.D., Brown, D.S., and Novo-Gradac, 1991. MINTEQA2/PRODEFA2, A Geochemical Assessment Model for Environmental Systems: Version 3.0 User's Manual, EPA/600/3-91/021, U.S. Environmental Protection Agency, Washington, D.C., 115 p.

Barnett, M.O., Jardine, P.M., Brooks, S.C., and Selim, H.M., 2000. Adsorption and Transport of Uranium (VI) in Subsurface Media, *Soil Sciences Society of America Journal*, 4:980-917.

Environmental Protection Agency, 1999. Understanding Variation in Partition Coefficient, K_d , Values, Vols. I and II, Report EPA 402-R-99-004B, Washington, D.C.

Givens, D.R., 1997. Sorption Studies of Pantex Soils, master's thesis, Texas Tech University, Lubbock, Texas, 79 p.

Laun, S.G., 1995. Chromium Contaminant Mobility in the Subsurface Soils at the Pantex Plant, master's thesis, Texas Tech University, Lubbock, Texas, 120 p.

Rancon, D., 1973. The Behavior in Underground Environments of Uranium and Thorium Discharge by the Nuclear Industry, in *Environmental Behavior of Radionuclides Released in the Nuclear Industry*, IAEA-SM-172/55, International Atomic Energy Agency Proceedings, Vienna, Austria, pp. 333-346.

Sheppard, M. I. and Thibault, D. H., 1990. Default Soil Solid/Liquid Partition Coefficients, K_{ds} , for Four Major Soil Types: A Compendium, *Health Physics*, 59: (4)471-482.

Soil Quality Institute, 1999. Soil Quality Test Kit Guide, U.S. Department of Agriculture, Washington, D.C., 88 p.

Stovall, J.N., 2003. Personal communication.

Walkley, A. and Black, I. A., 1934. An Examination of Degtjareff Method for Determining Soil Organic Matter and a Proposed Modification of the Chromic Acid Titration Method, *Soil Science*, 37: 29-37.

Wray, W.K., 1986. Measuring Engineering Properties of Soil, Prentice-Hall, Inc., Newark, New Jersey.

Sorption of Selected Metals on Blackwater Draw Sediments

By

Ken Rainwater, Matt Jones, Levi Hein,
Kartik Venkataraman, Yeontae Jeong, and John McEnery

Texas Tech University Water Resources Center
Box 41022
Lubbock, Texas 79409-1022

Submitted to

BWXT-Pantex
P.O. Box 30020
Amarillo, Texas 79120

Volume II. Appendices

2006

Table of Contents

Appendix A. Isotherm Results.....	1
A-1. Isotherm Results for Barium, Lead, Silver, Thorium, Uranium on Site 1 Soils.....	2
Barium.....	2
Lead.....	15
Silver.....	28
Thorium.....	41
Uranium.....	48
A-2. Isotherm Results for Uranium on Site 6 and 7 Soils.....	61
Appendix B. Clay Mineralogical Analyses.....	68
B-1. Site 1 Soil.....	69
B-2. Combination of Site 6 and 7 Soils.....	73
Appendix C. Raw Sorption Data Summaries.....	77
C-1. Isotherm Results for Barium, Lead, Silver, Thorium, and Uranium on Site 1 Soils.....	78
C-2. Isotherm Results for Uranium on Site 6 and 7 Soils.....	83
C-3. Soil Column Bromide and Uranium Effluent Concentrations.....	85

Appendix A

Isotherm Results

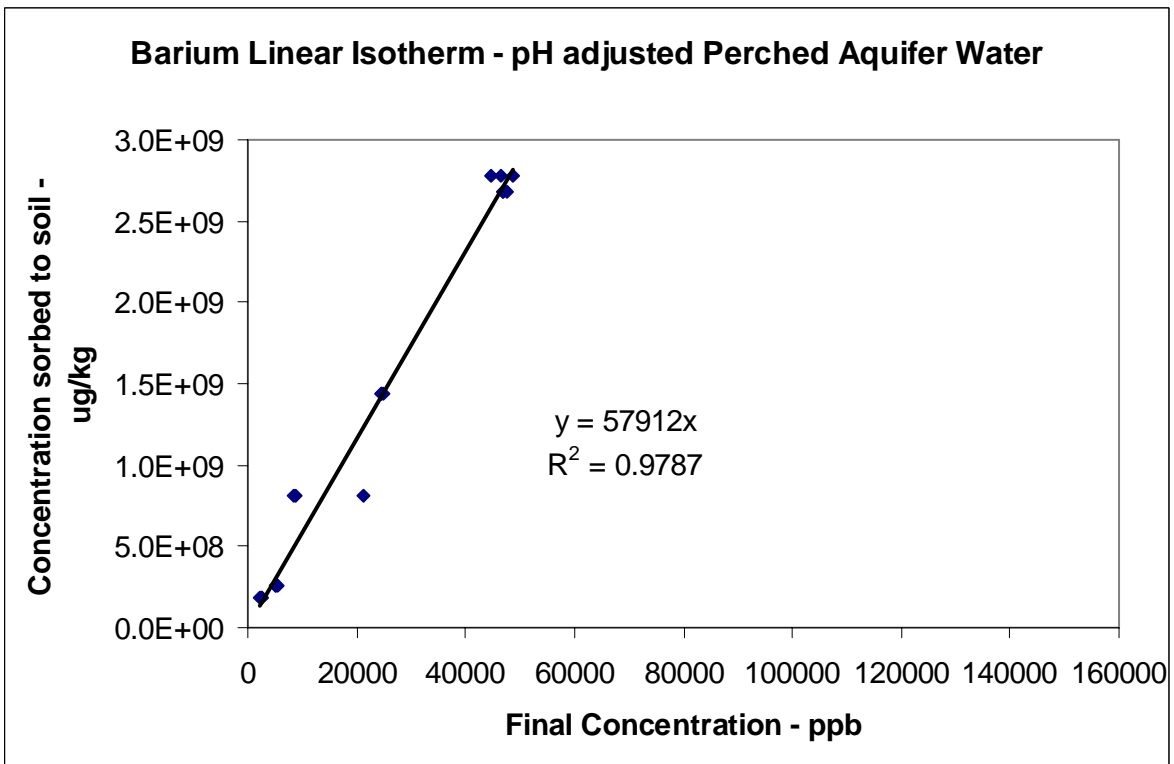
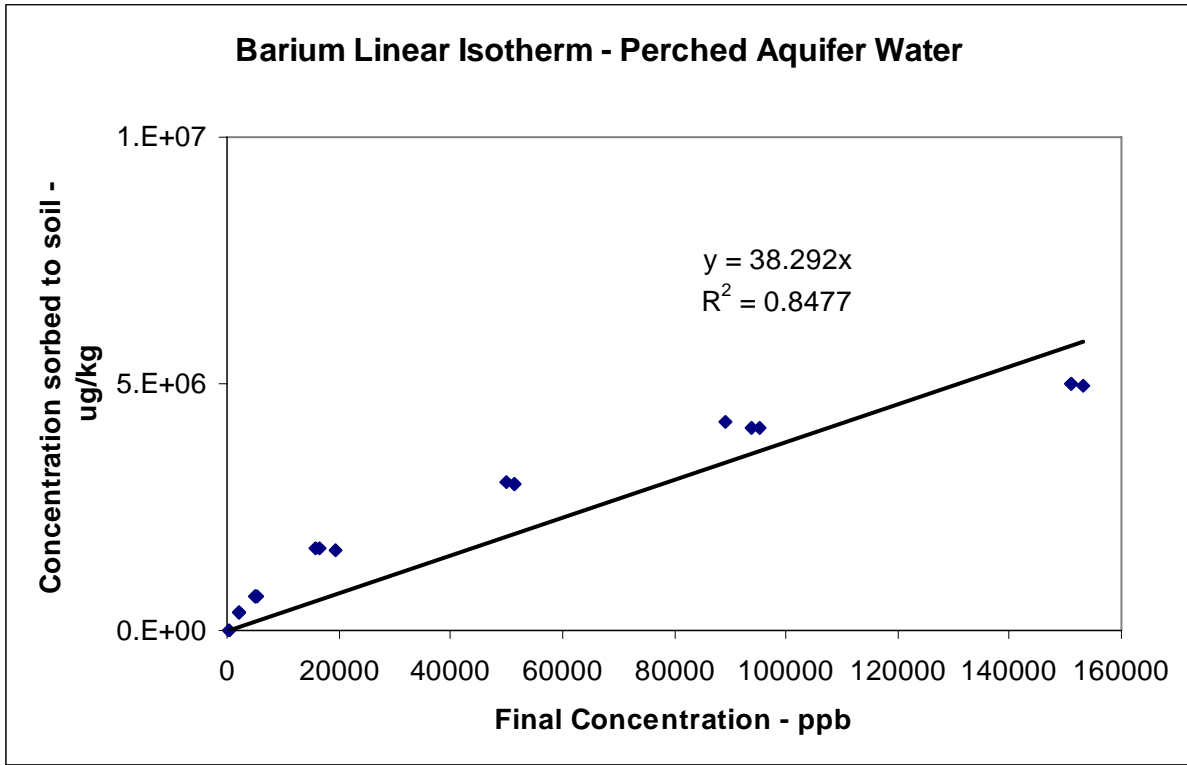
A-1. Isotherm Results for Barium, Lead, Silver, Thorium, and Uranium on Site 1 Soils

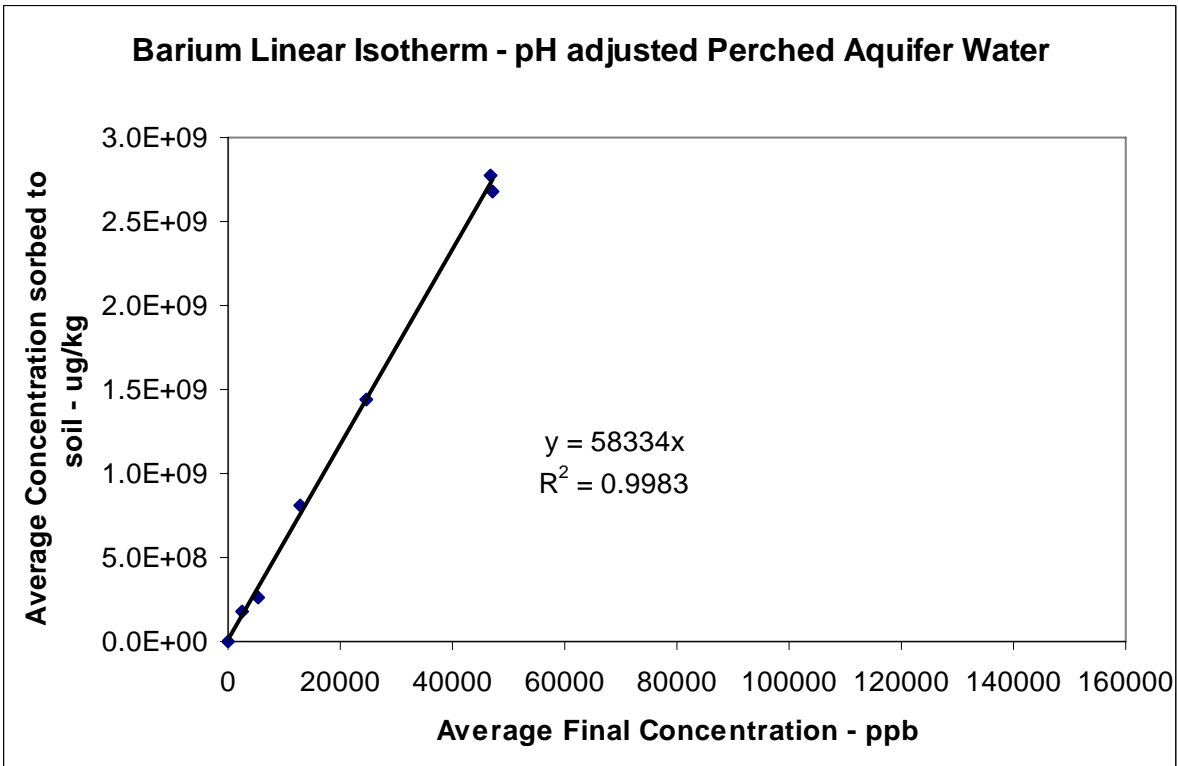
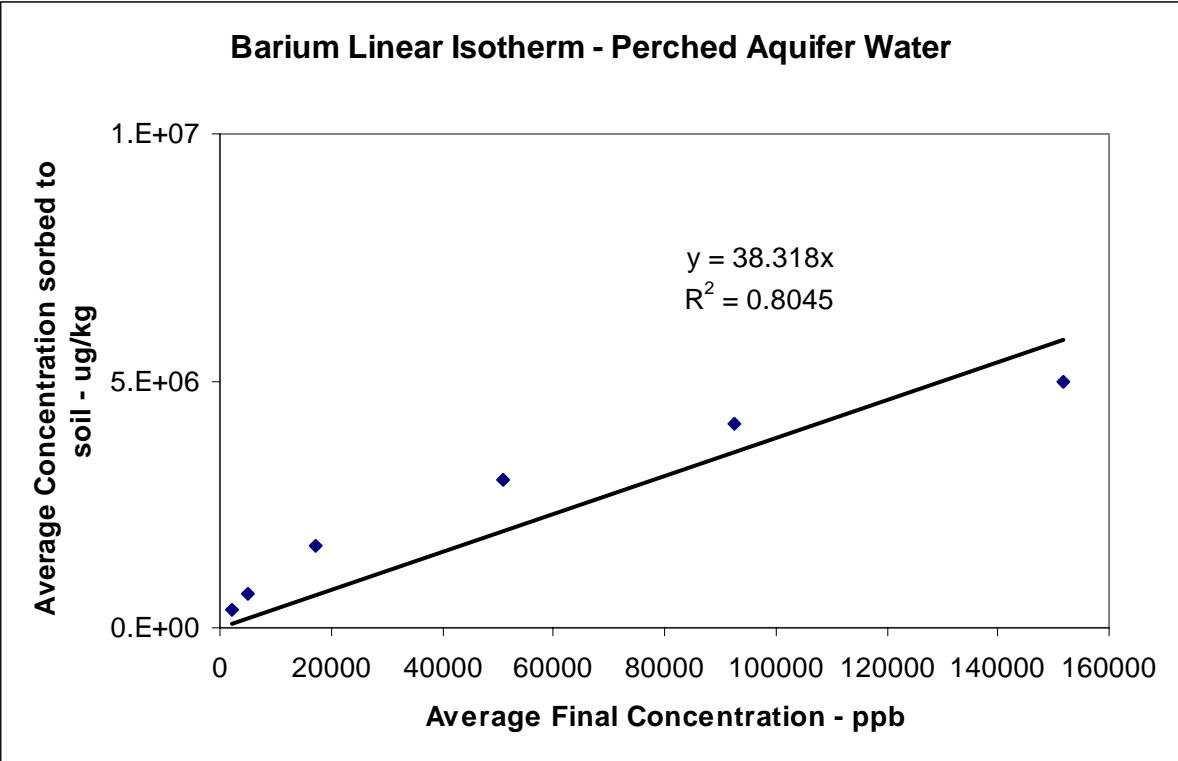
A-2. Isotherm Results for Uranium on Site 6 and 7 Soils

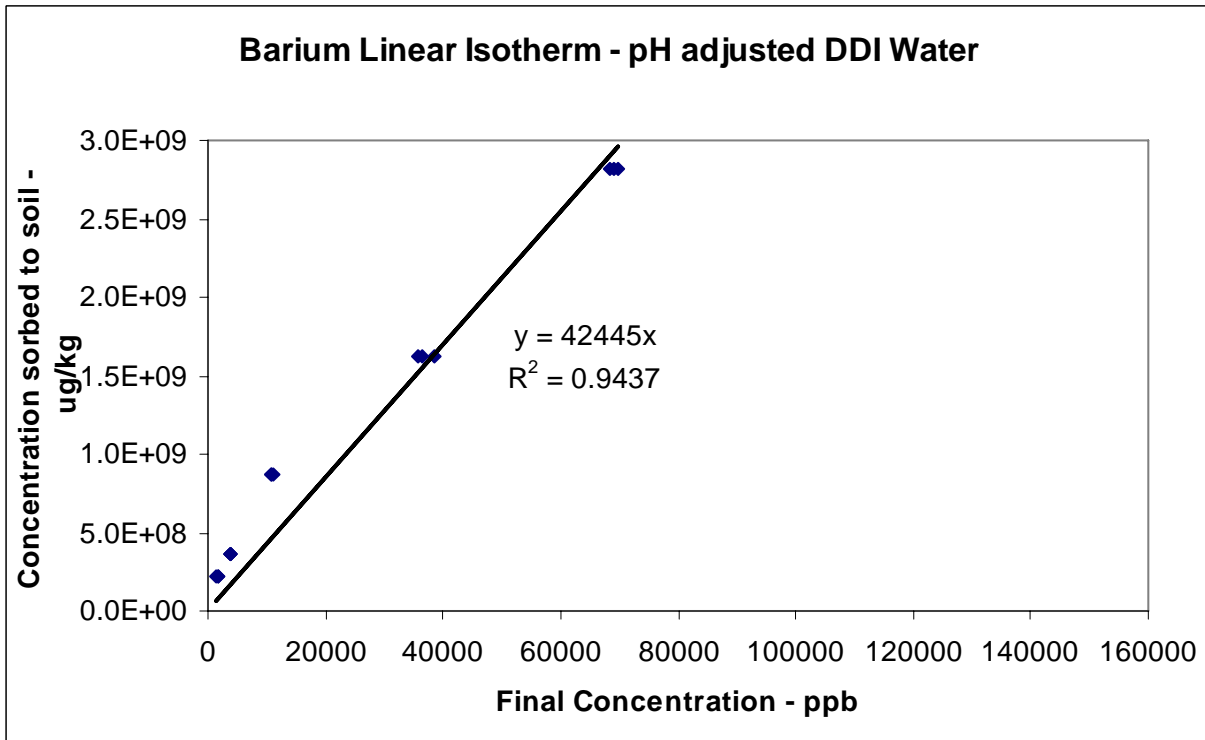
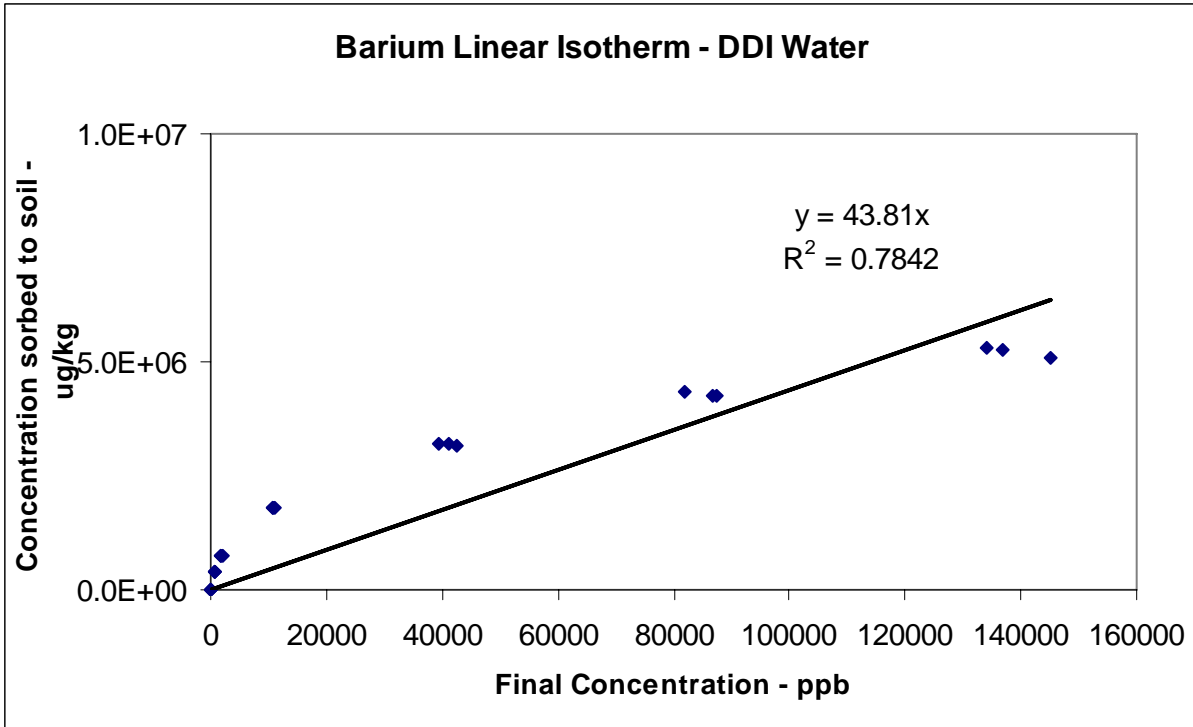
Appendix A-1. Isotherm Results for Barium, Lead,
Silver, Thorium, and Uranium on Site 1 Soils

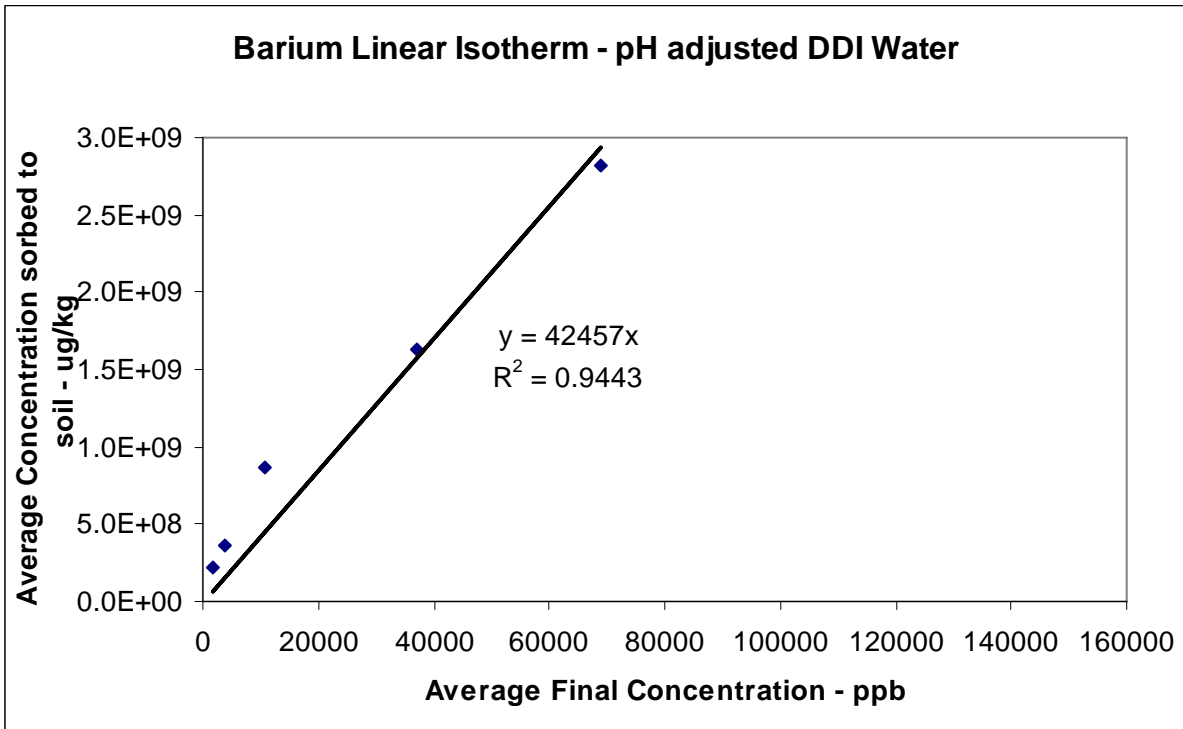
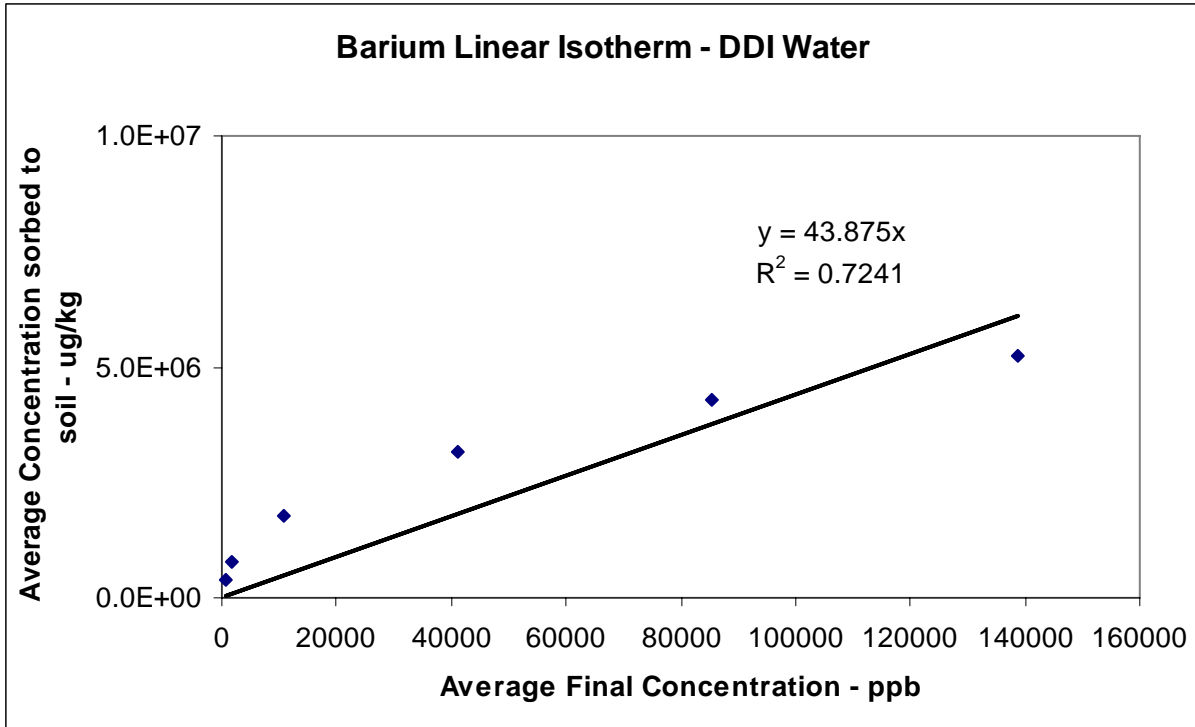
Pantex Barium Isotherm Data

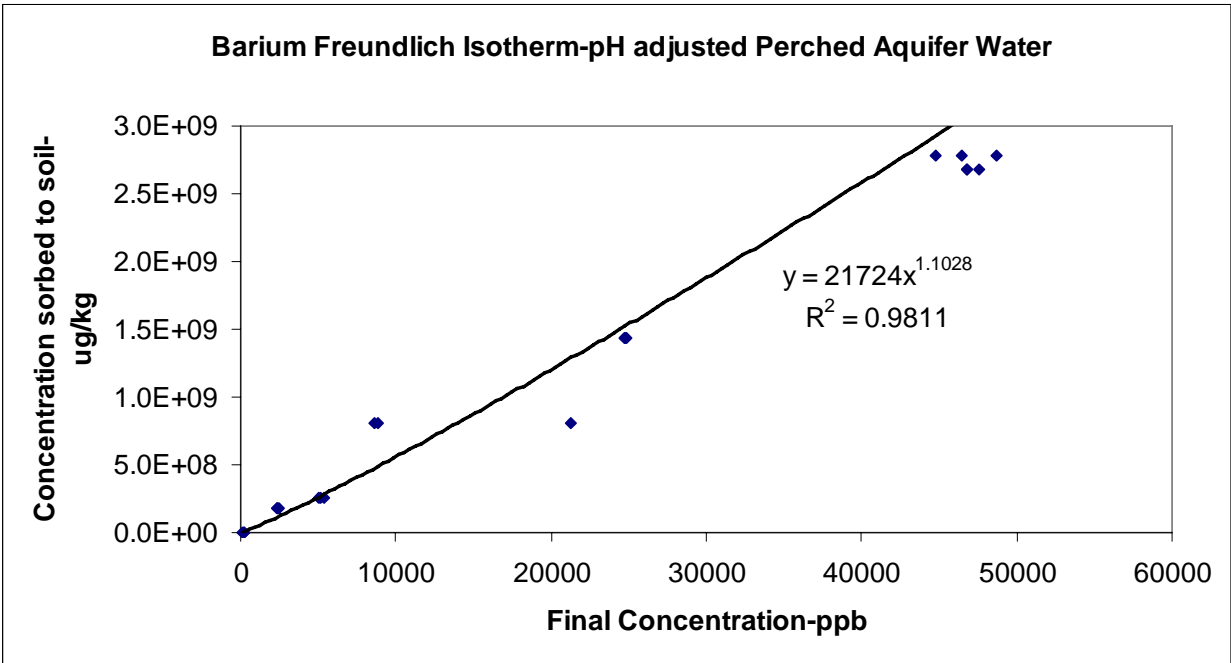
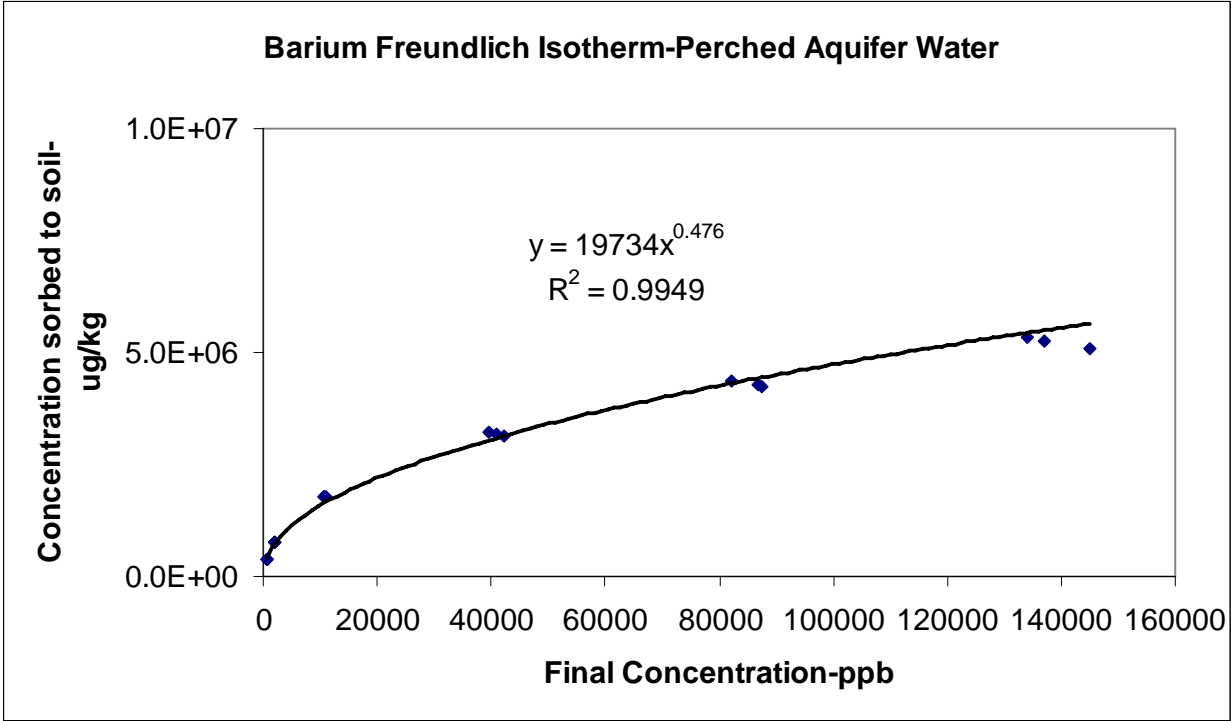
Source Water	K_d (L/kg)	K ([$\mu\text{g}/\text{kg}$][$\mu\text{g}/\text{L}$] ^{-N})	N	β (kg/ μg)	α (L/ μg)
Perched Aquifer	38.3	3210	0.626	6.25E6	2.23E-5
pH adjusted Perched Aquifer	57900	21700	1.103	2.30E10	2.75E-6
DDI	43.8	19700	0.476	5.59E6	5.46E-5
pH adjusted DDI	42400	1.69E6	0.662	3.92E9	2.80E-5

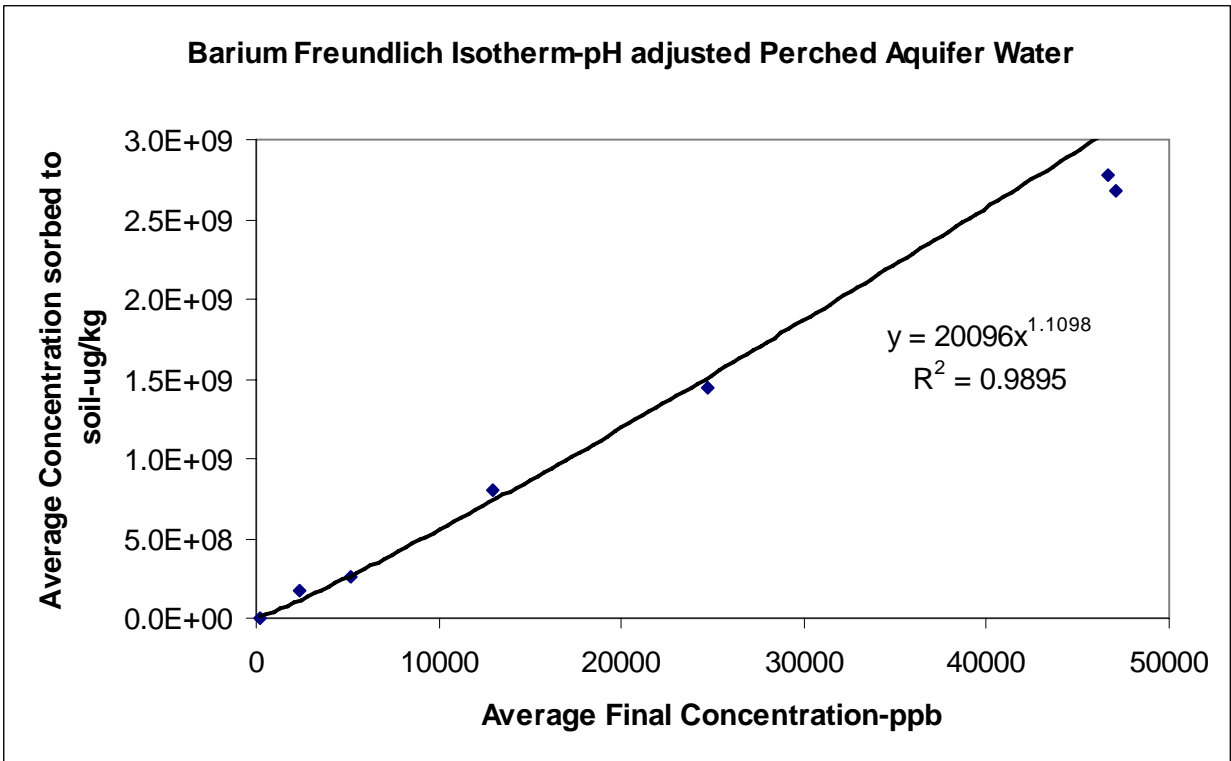
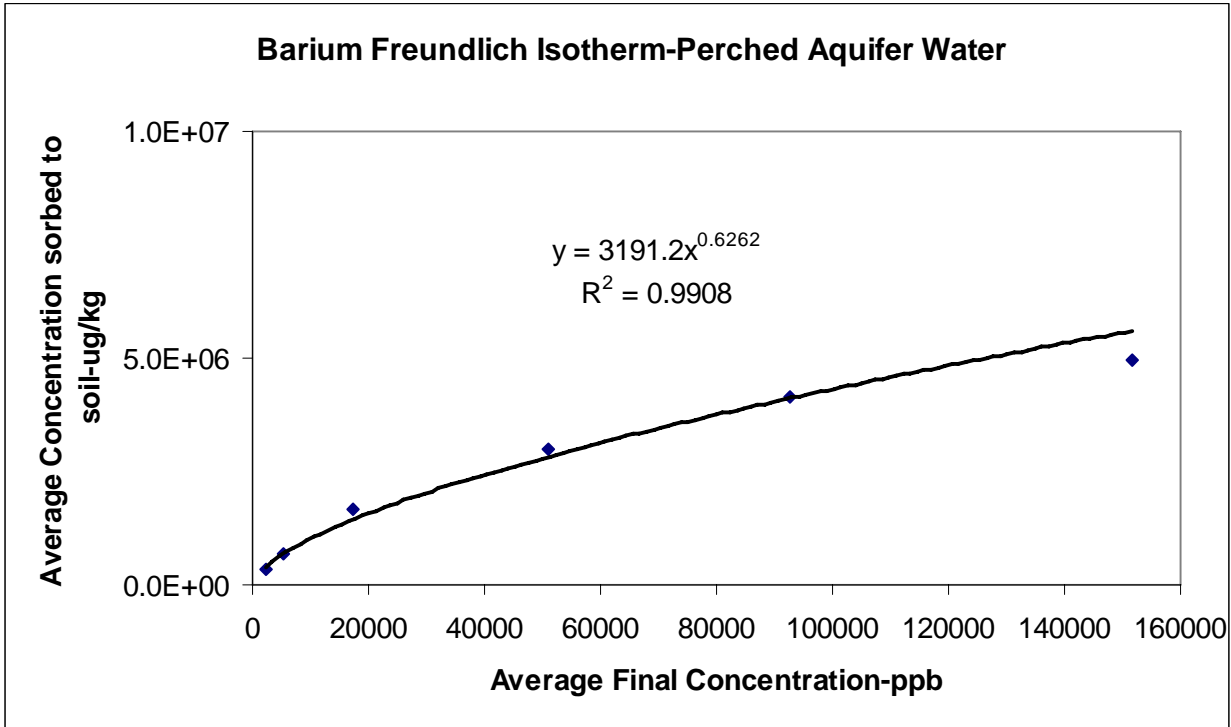


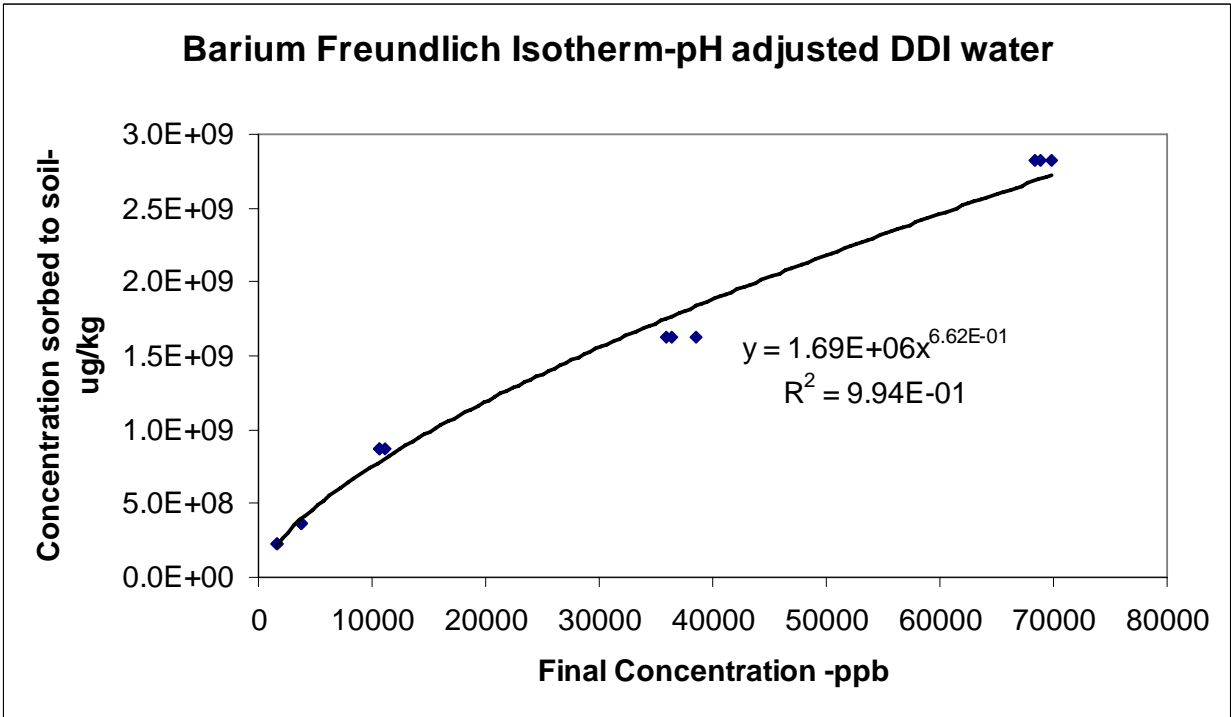
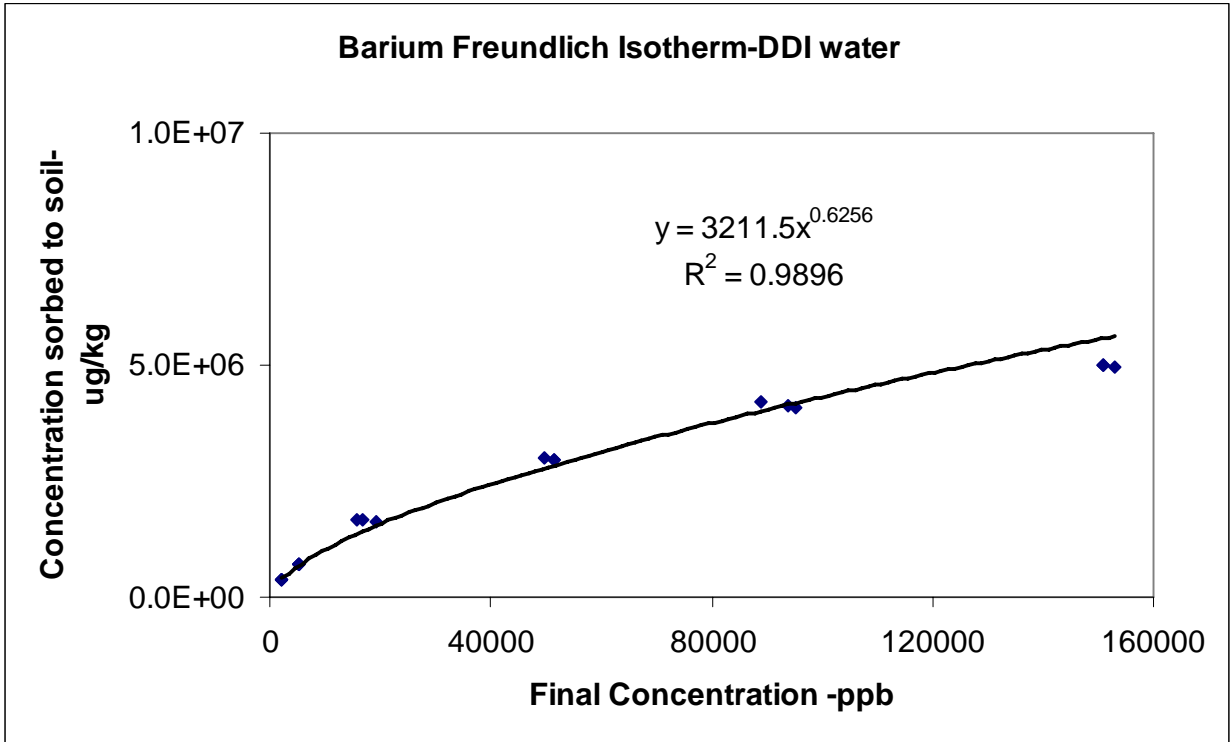


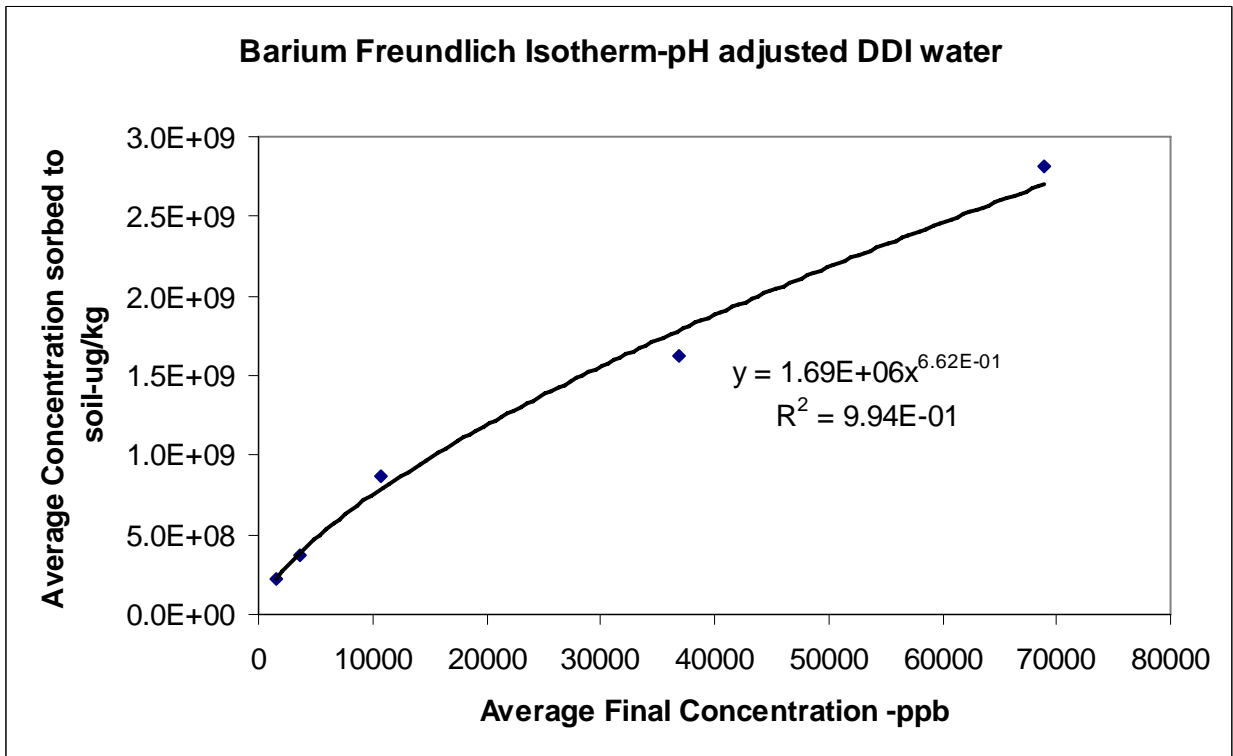
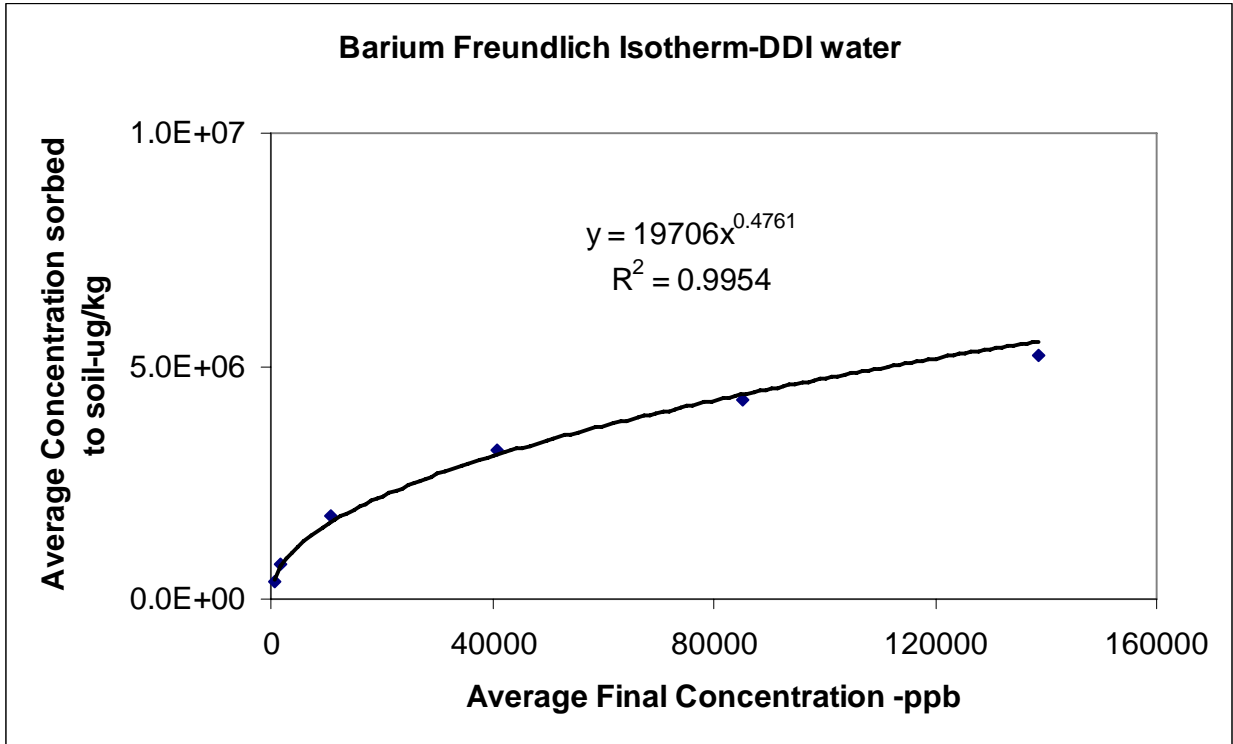




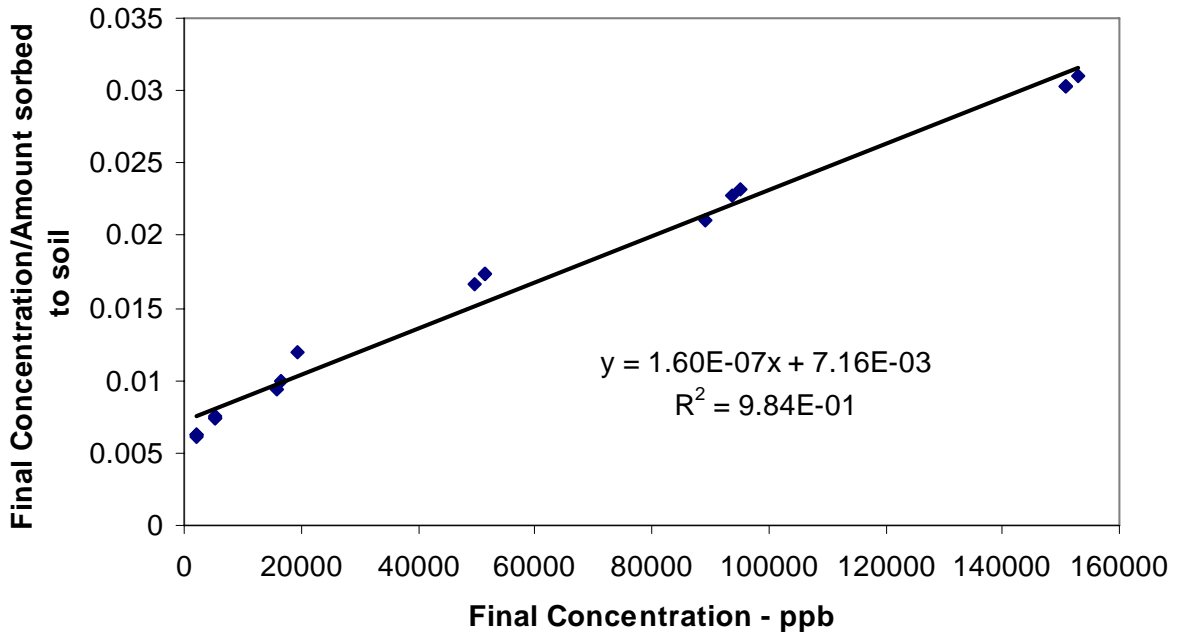




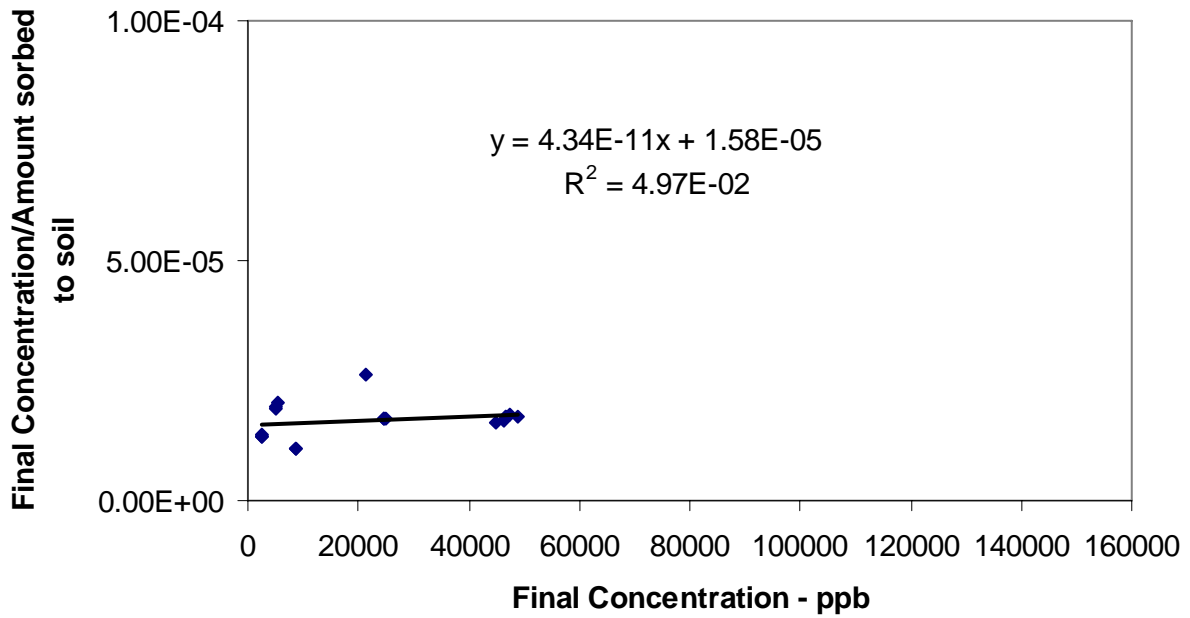


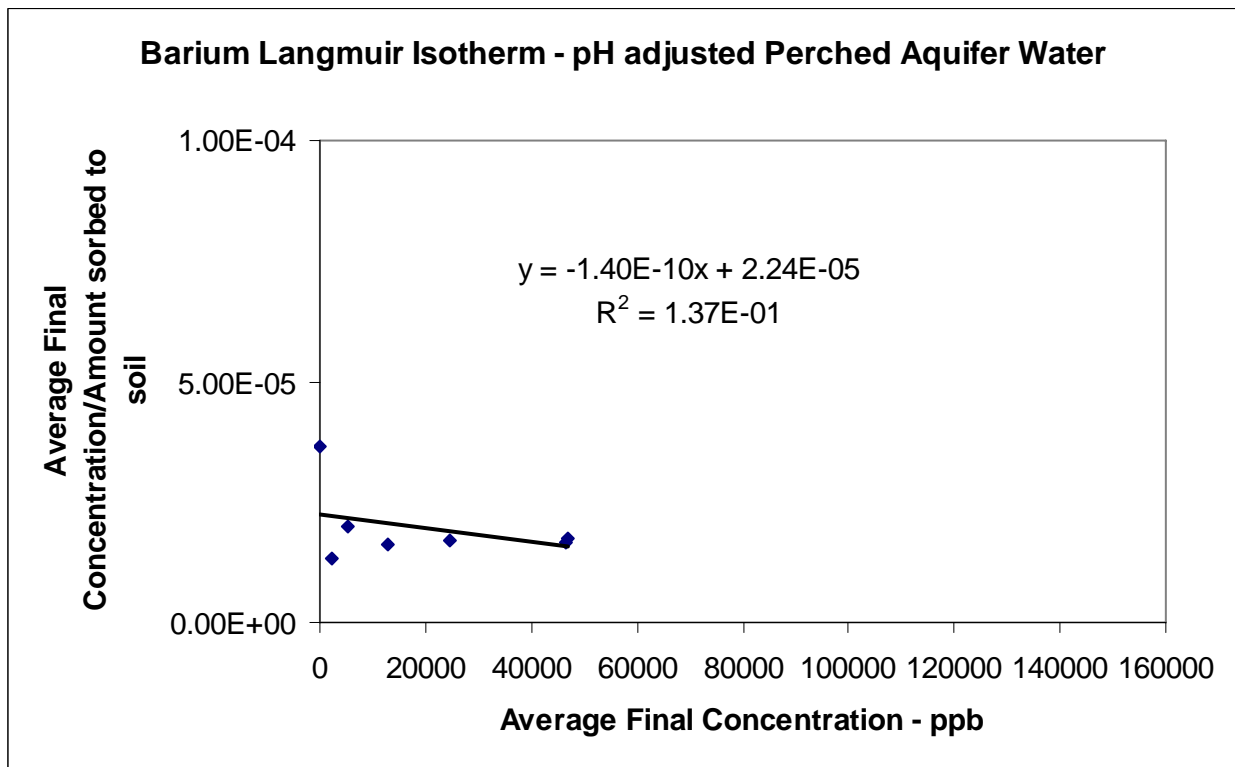
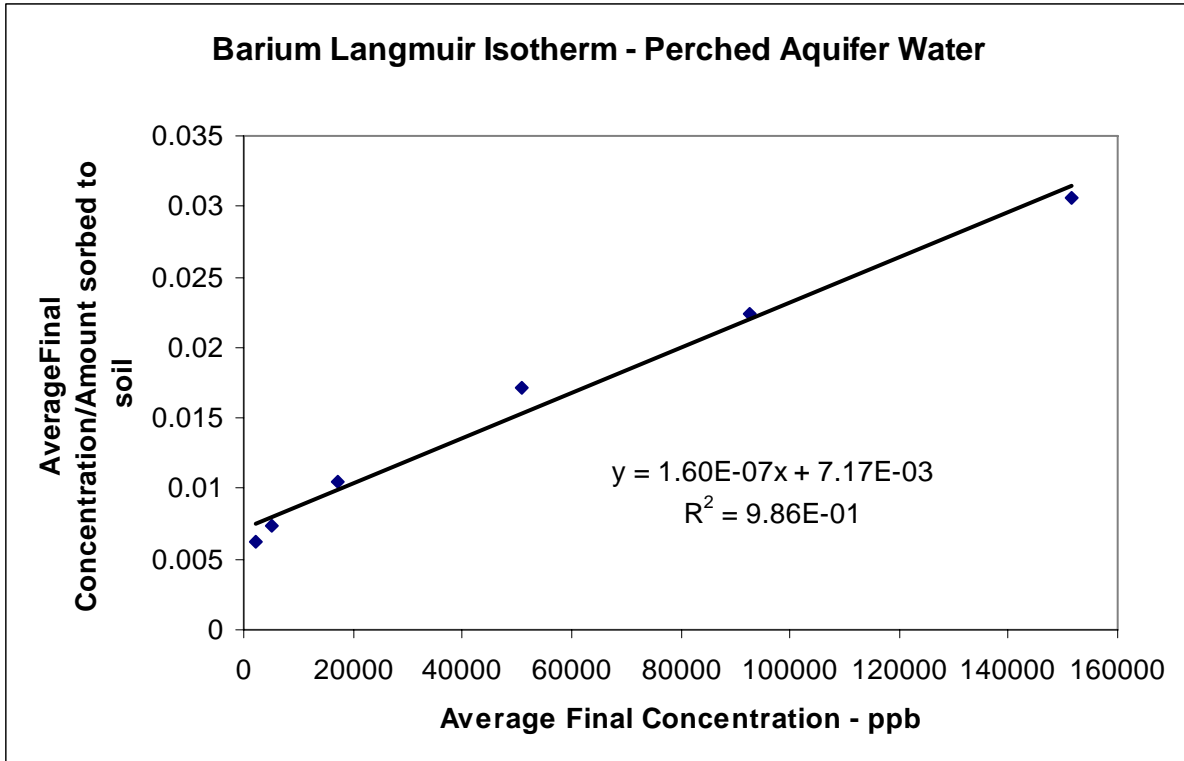


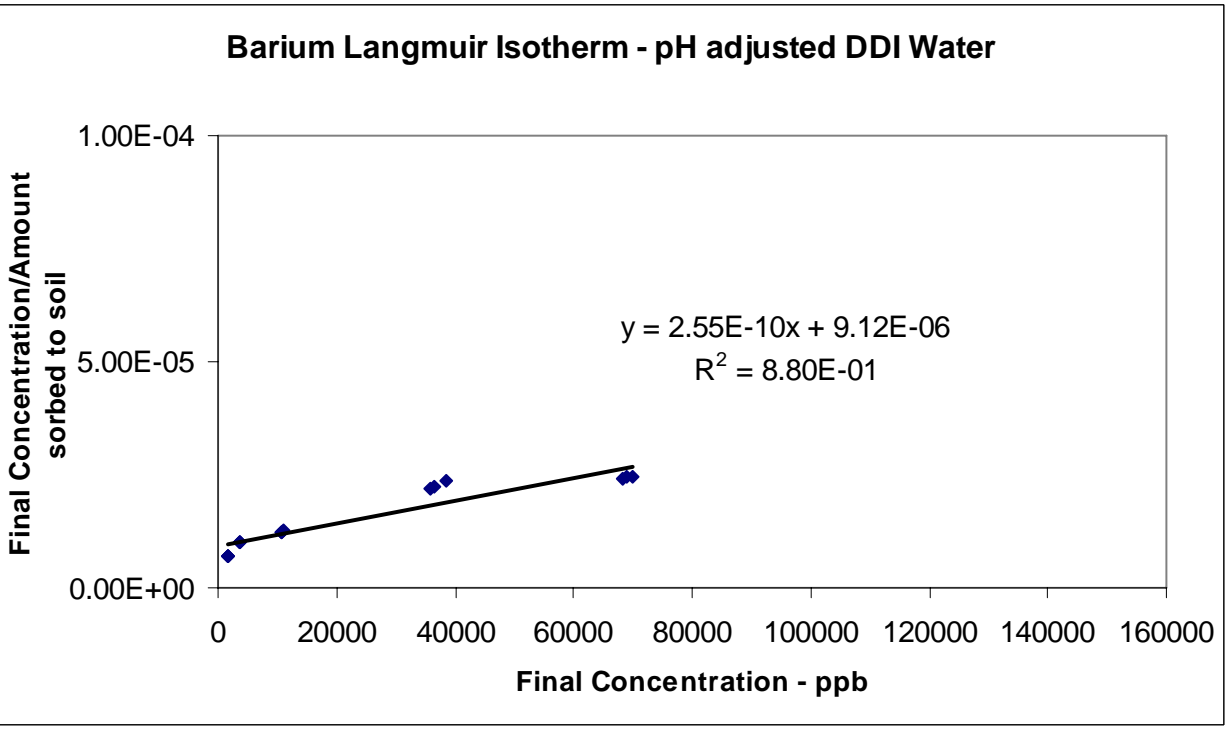
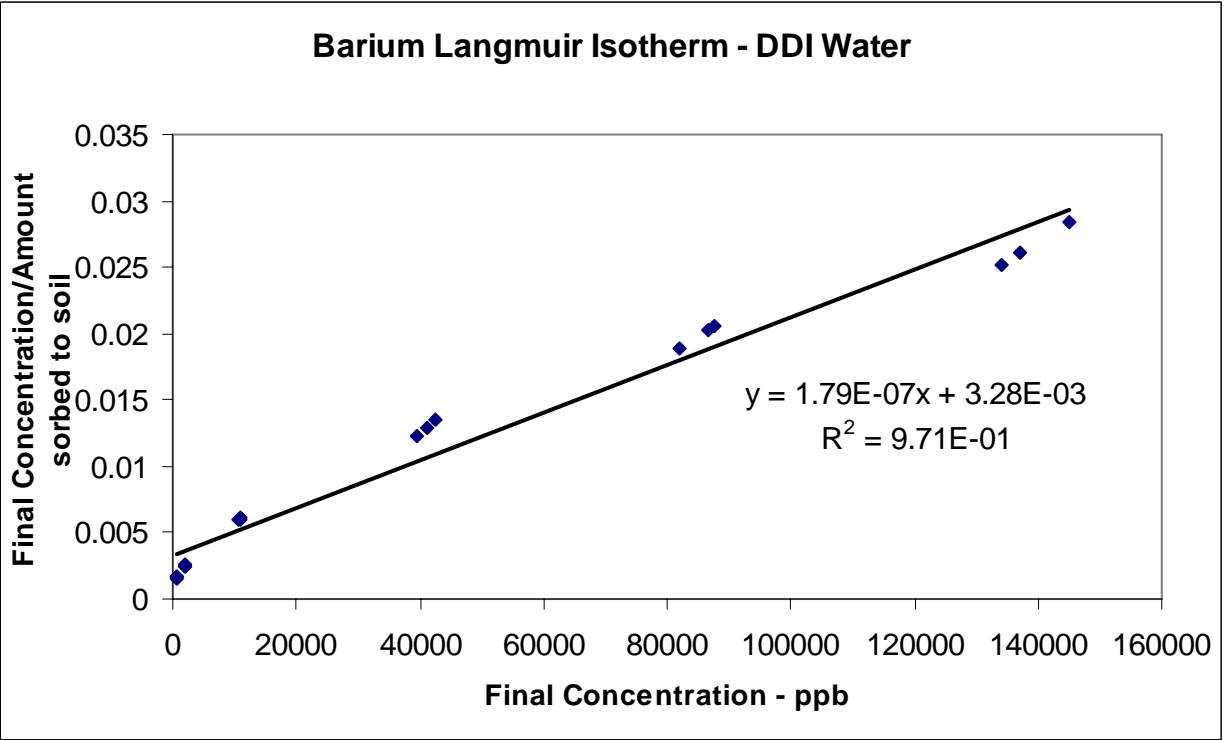
Barium Langmuir Isotherm - Perched Aquifer Water

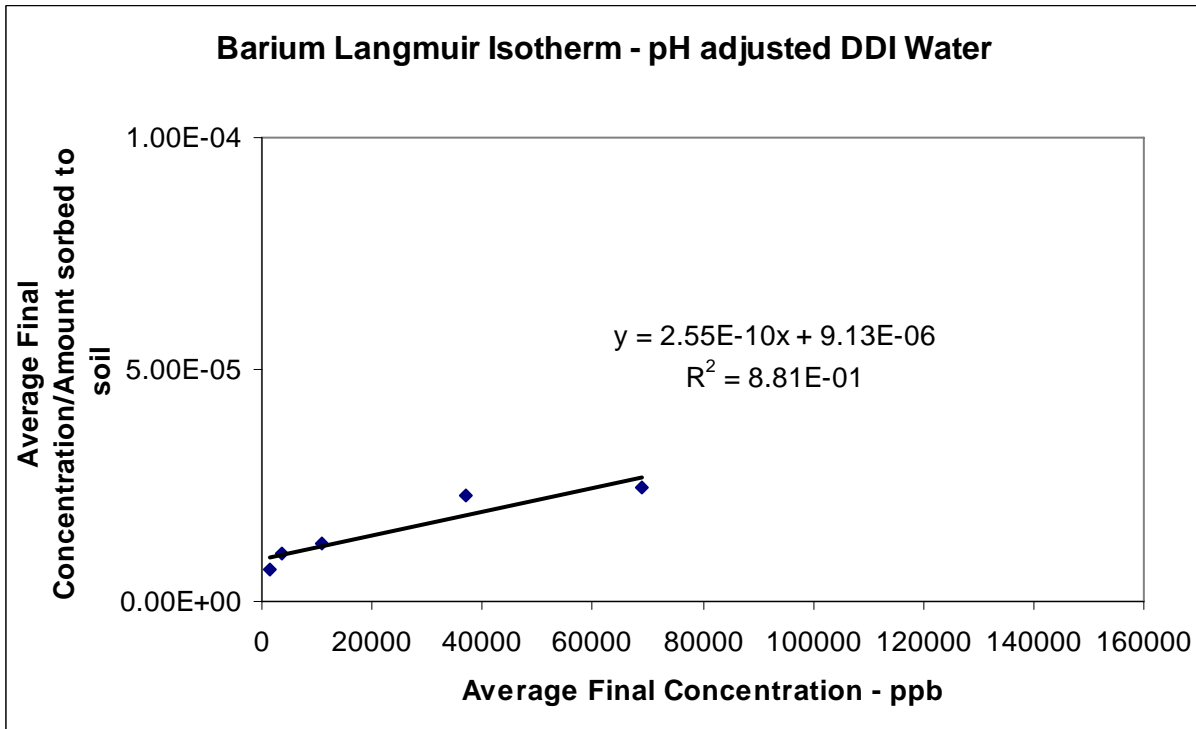
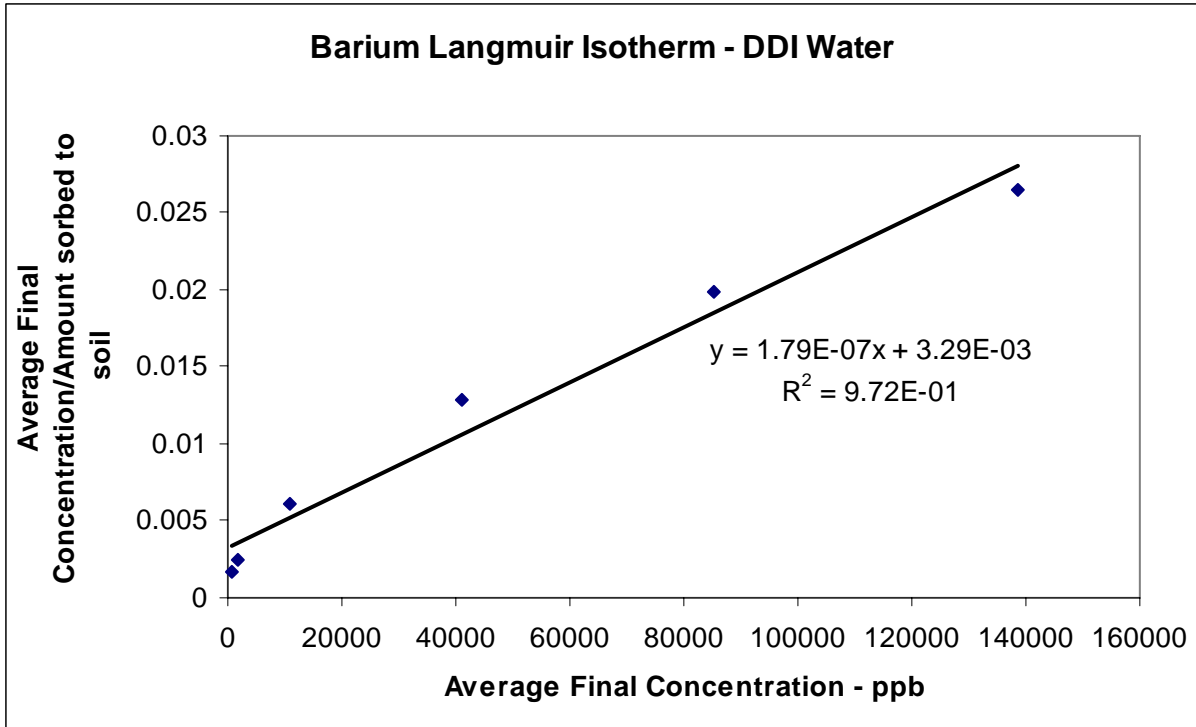


Barium Langmuir Isotherm - pH adjusted Perched Aquifer Water



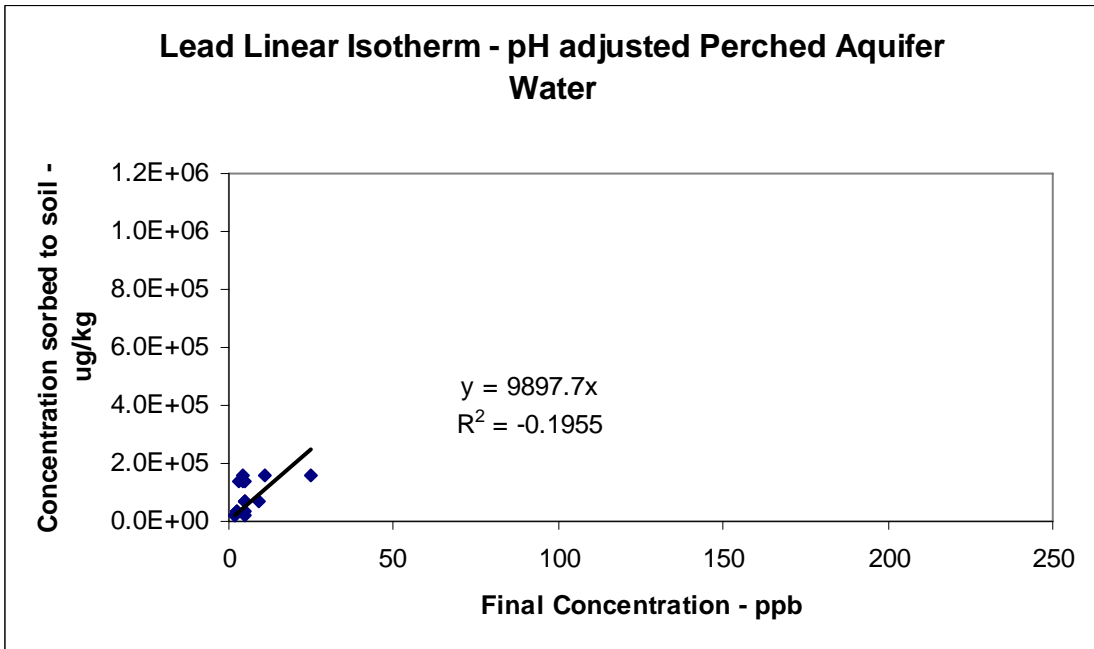
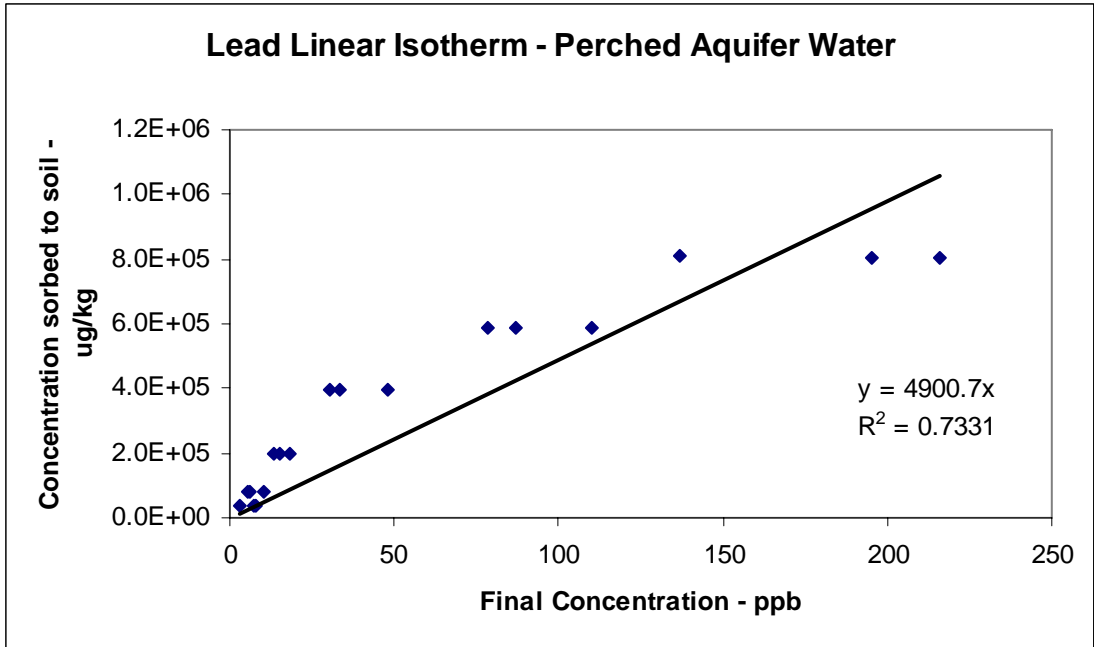


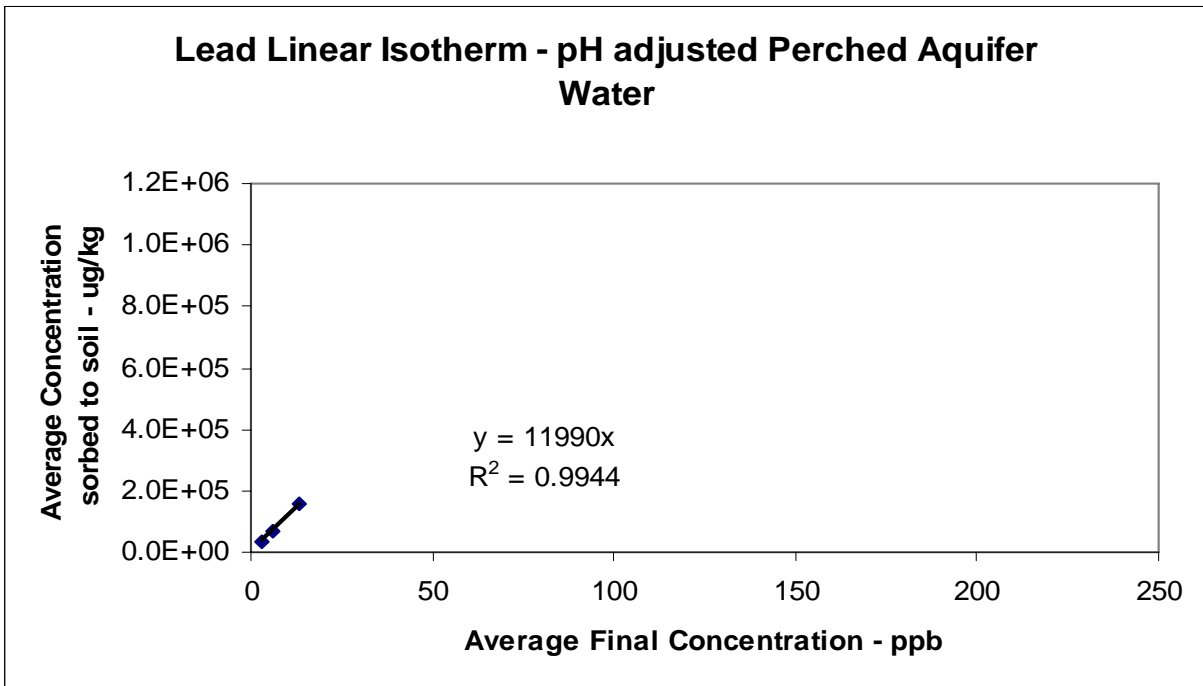
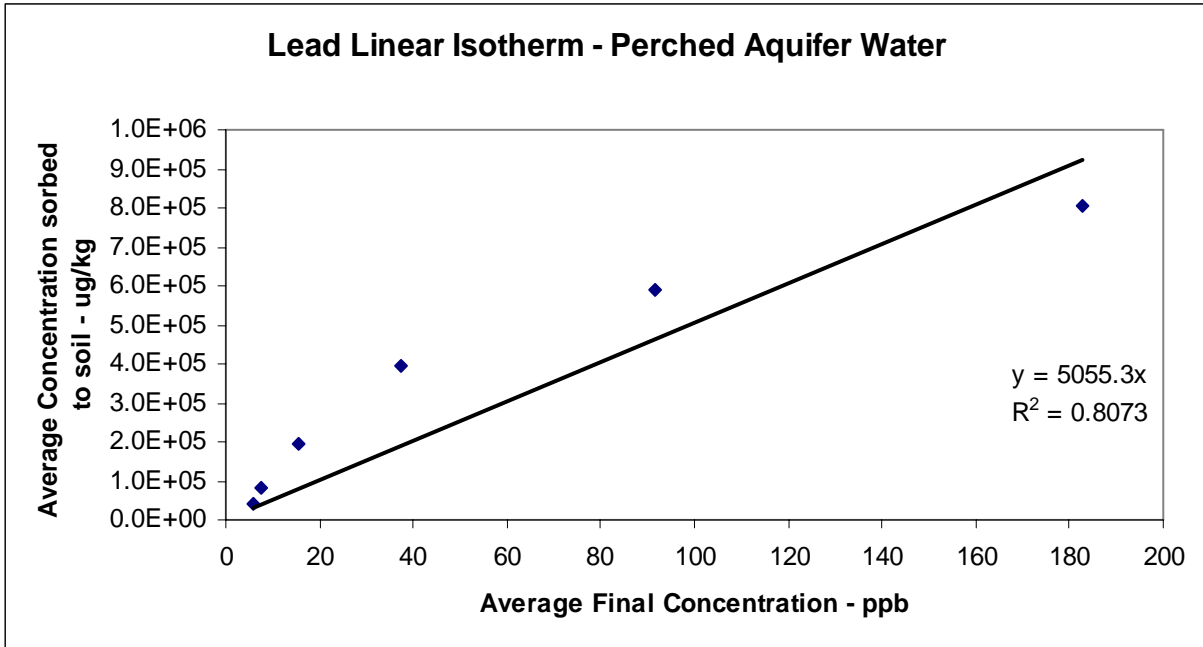


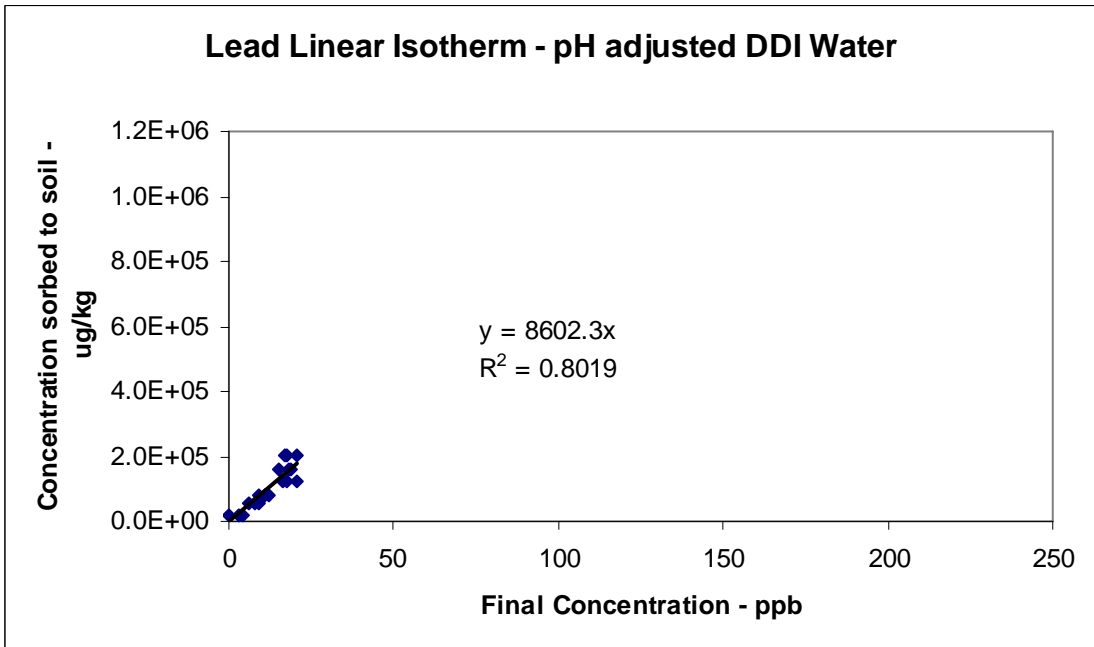
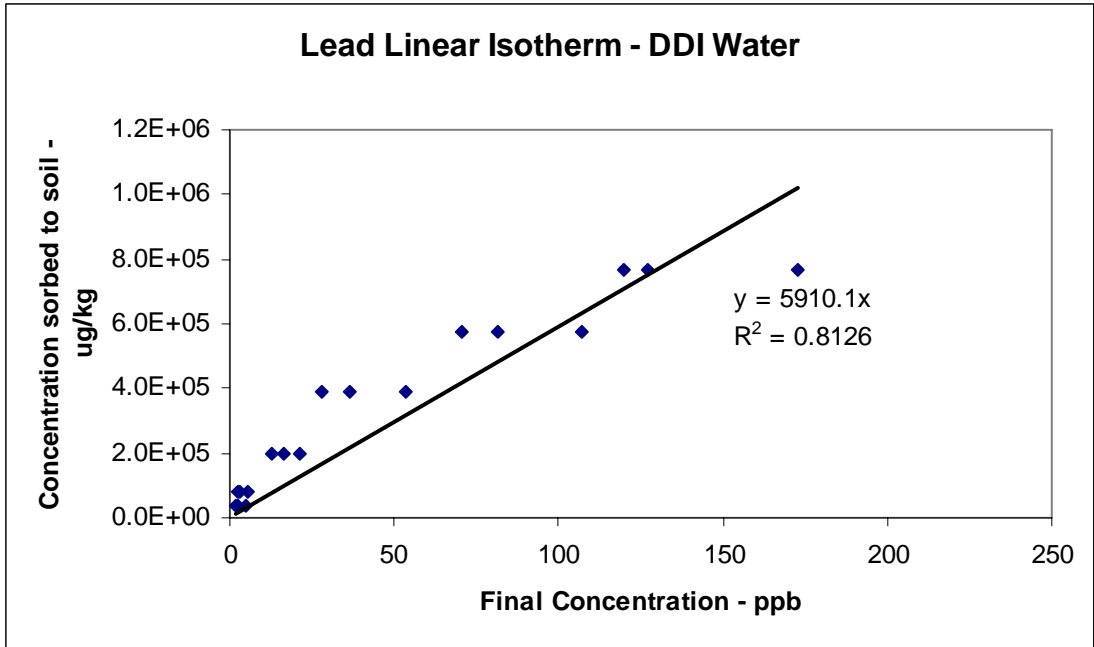


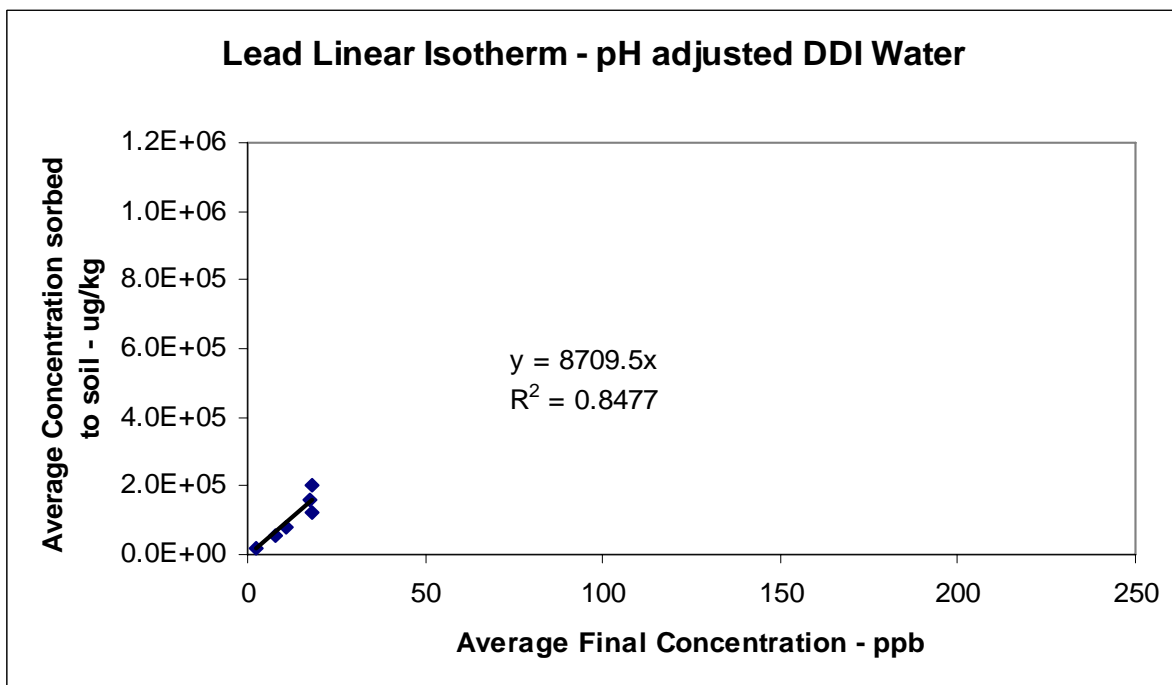
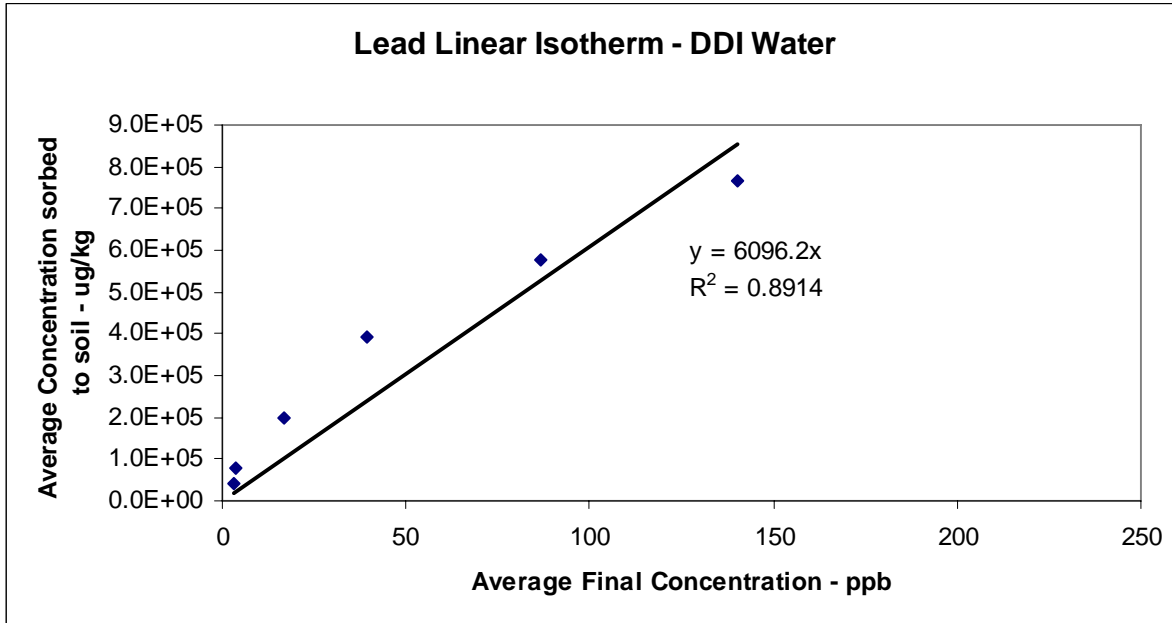
Pantex Lead Isotherm Data

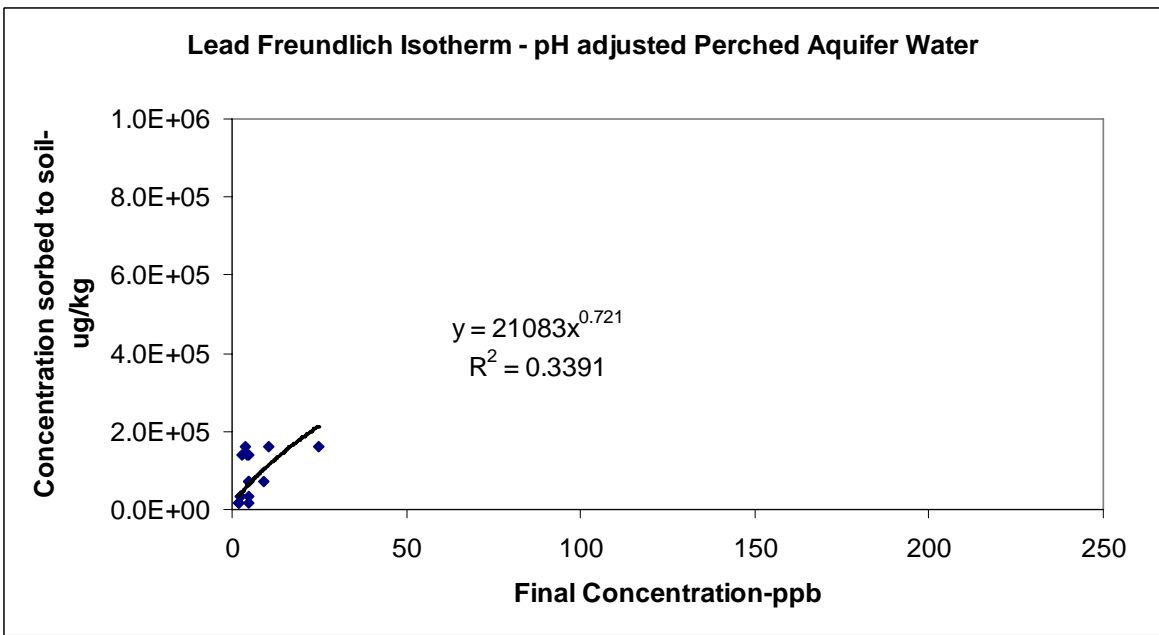
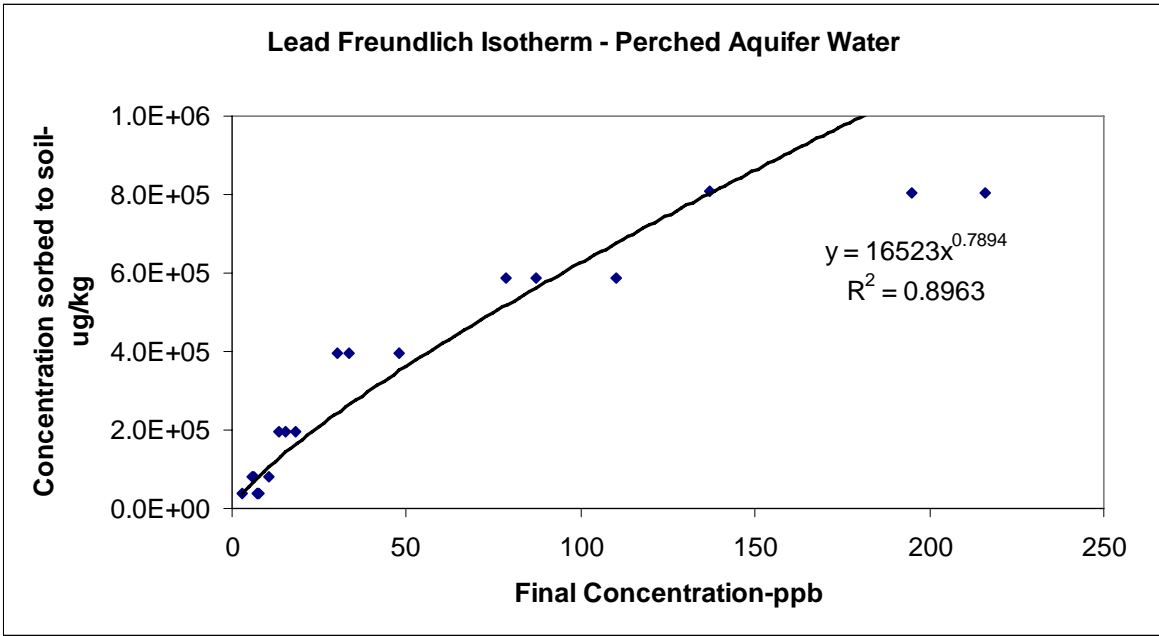
Source Water	K_d (L/kg)	K ([$\mu\text{g}/\text{kg}$][$\mu\text{g}/\text{L}$] ^{-N})	N	β (kg/ μg)	α (L/ μg)
Perched Aquifer	4900	16500	0.789	1.37E6	7.90E-3
pH adjusted Perched Aquifer	9900	21100	0.721	2.99E5	4.66E-2
DDI	5910	27800	0.684	1.06E6	1.55E-2
pH adjusted DDI	8600	4560	1.22	3.42E5	1.71E-2

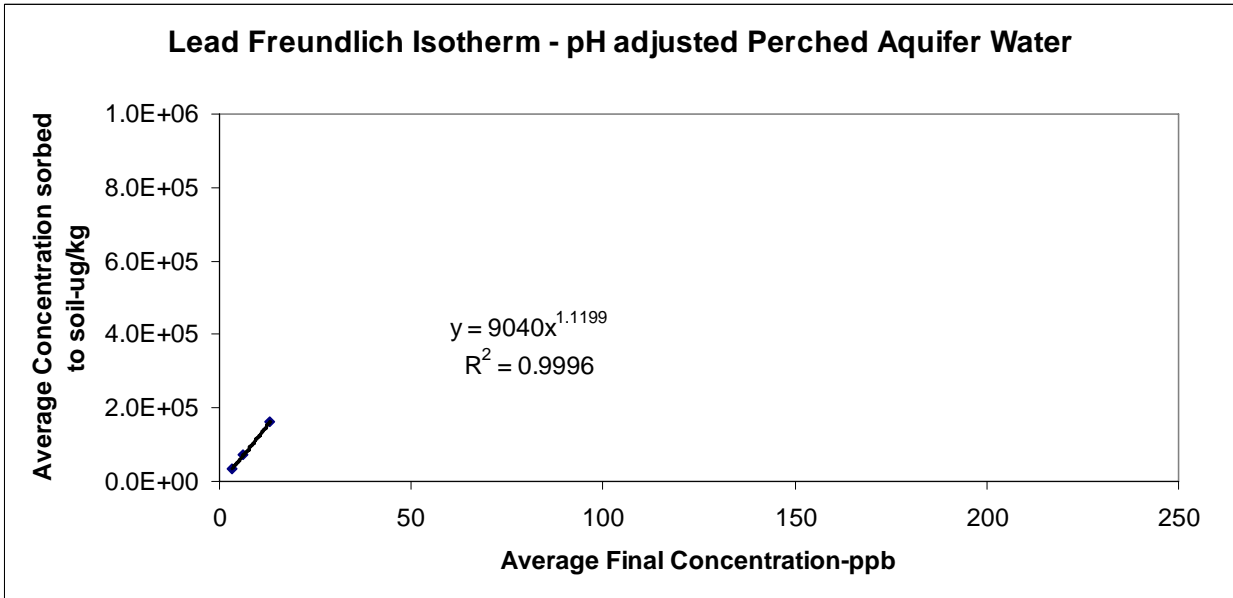
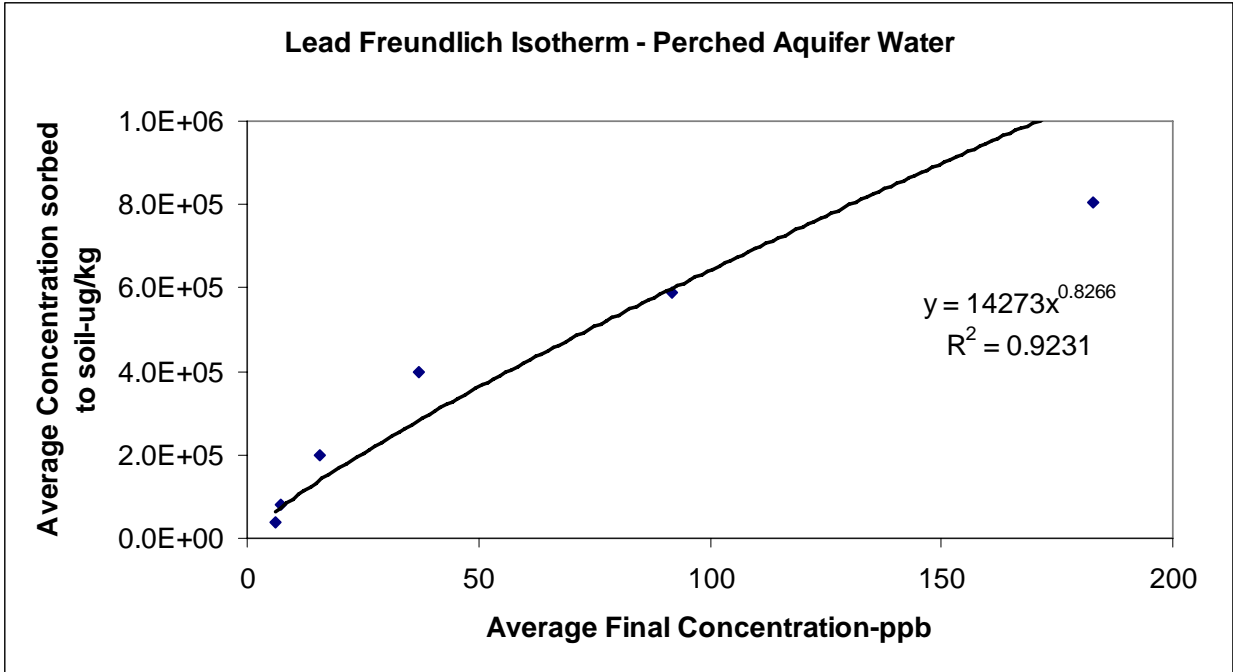


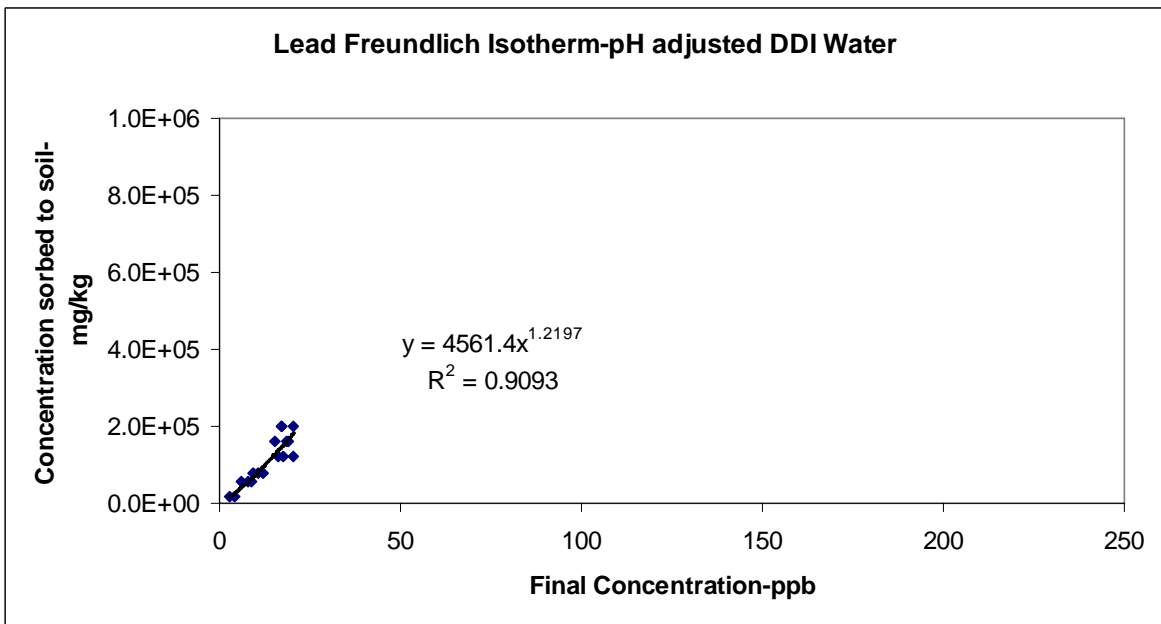
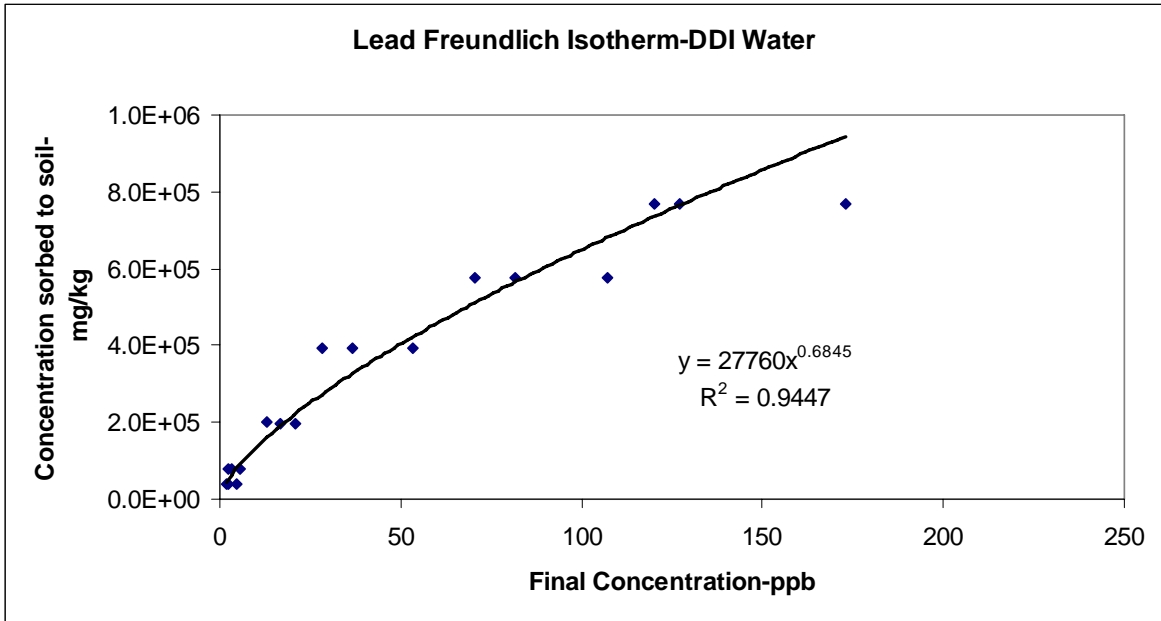


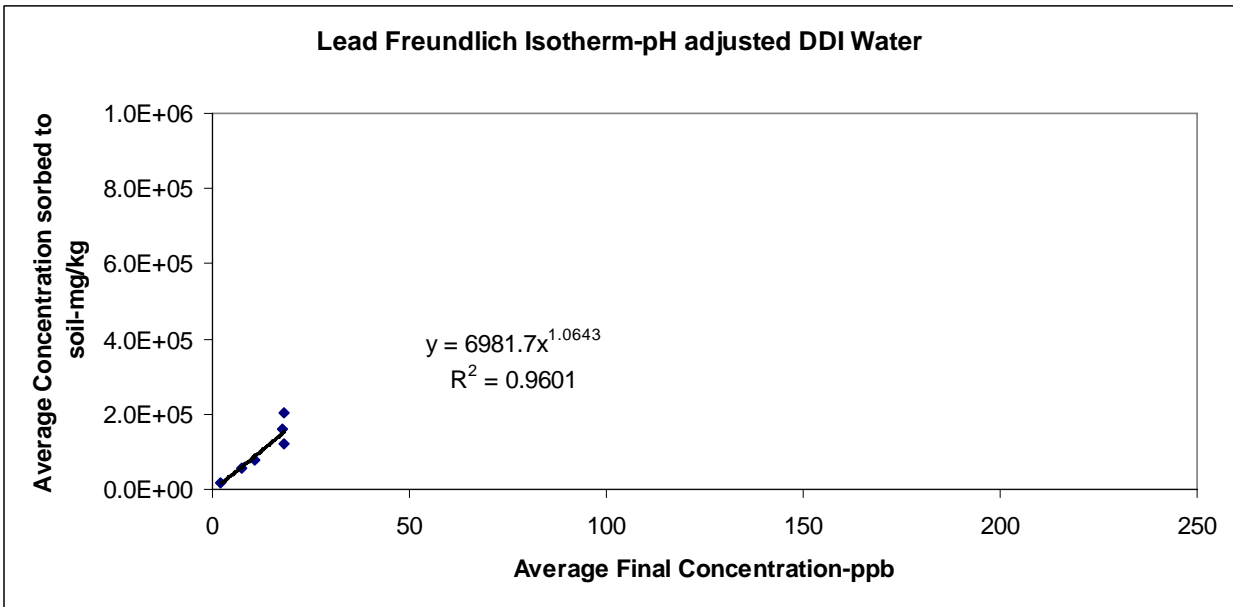
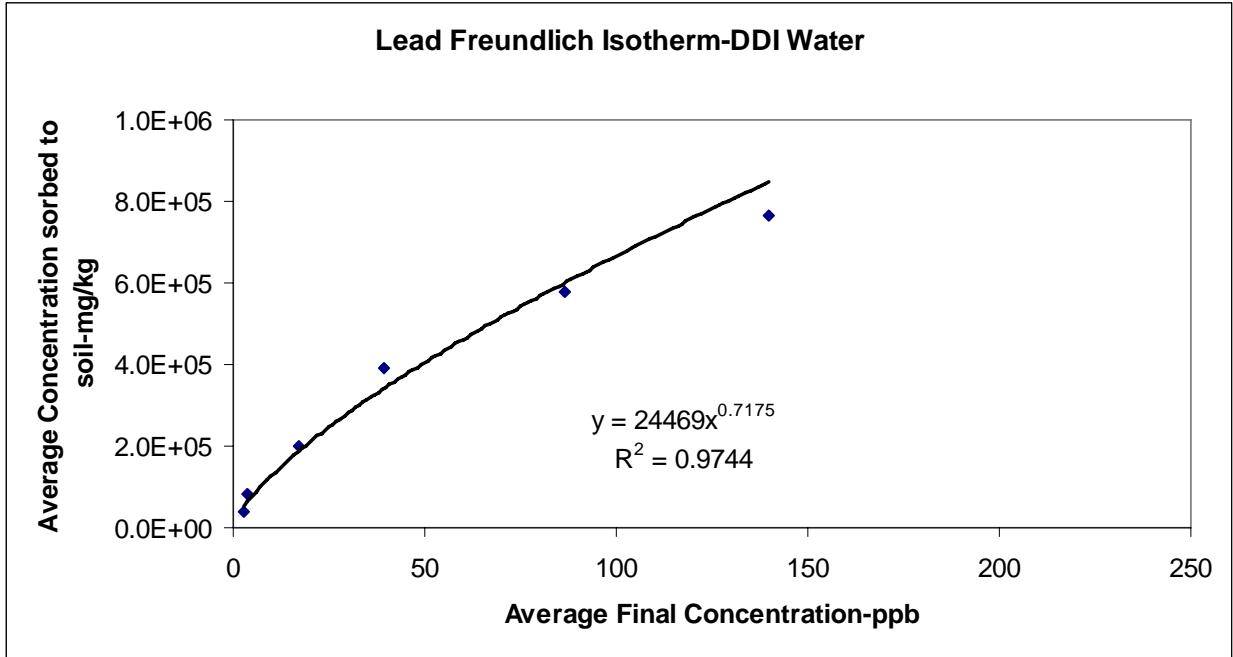


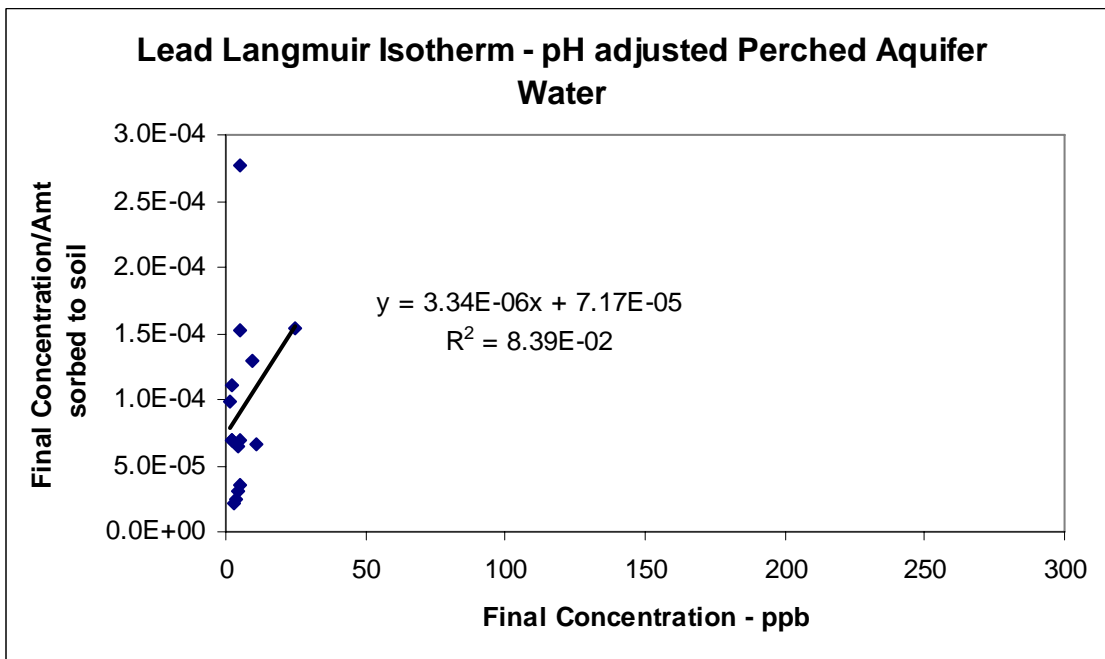
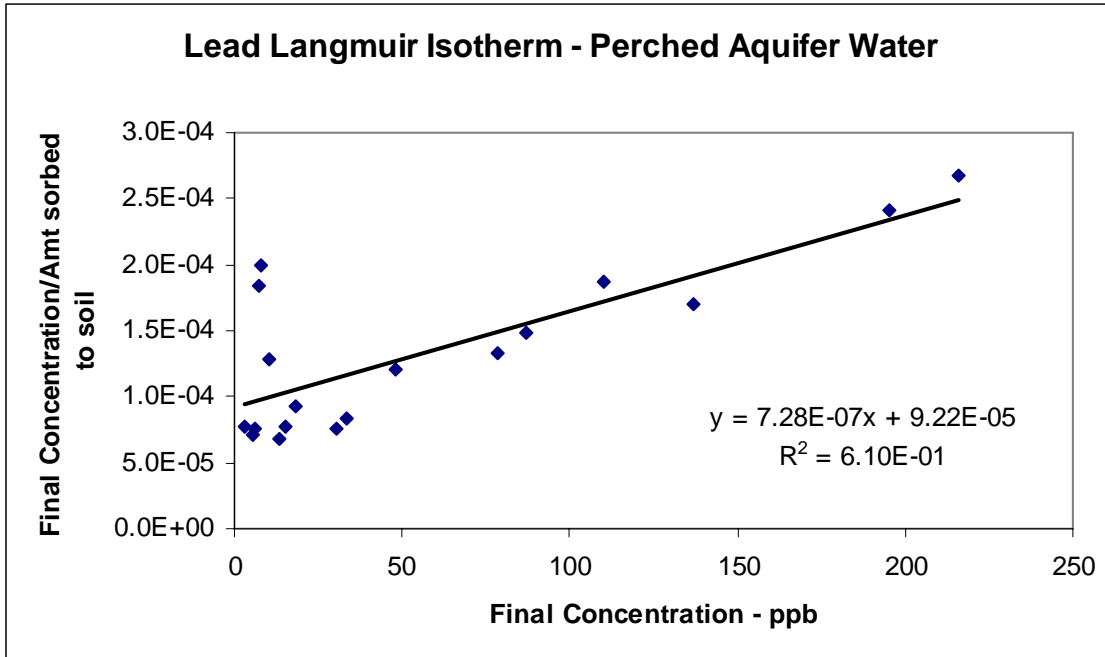


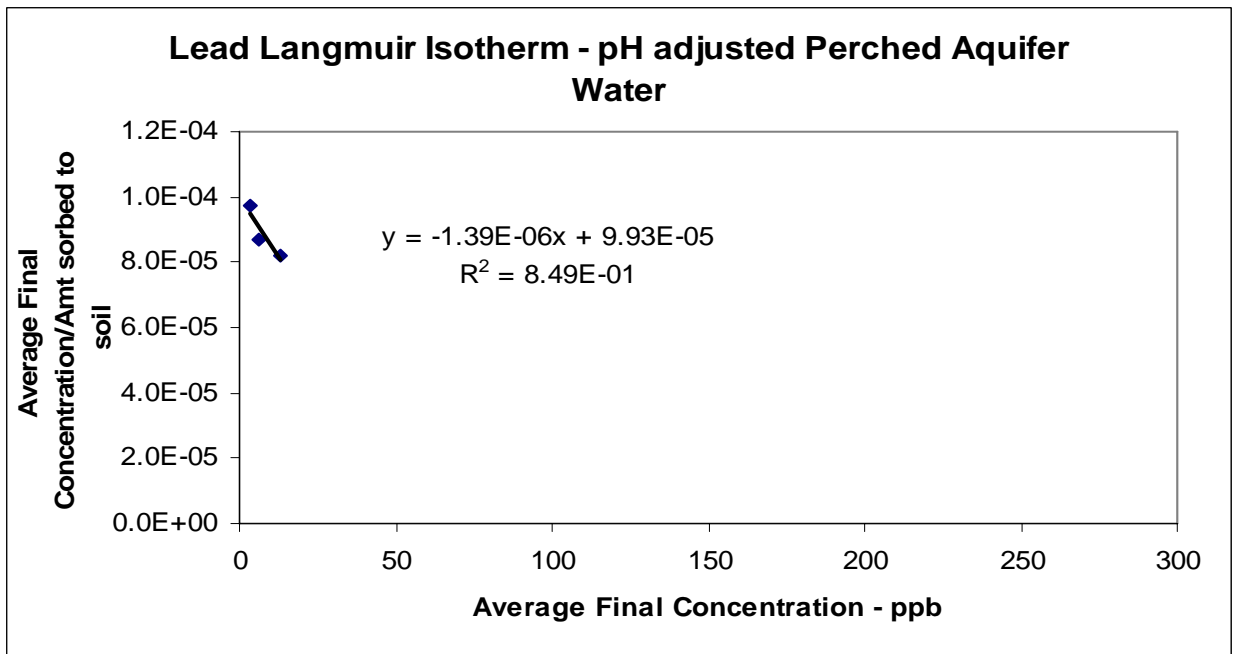
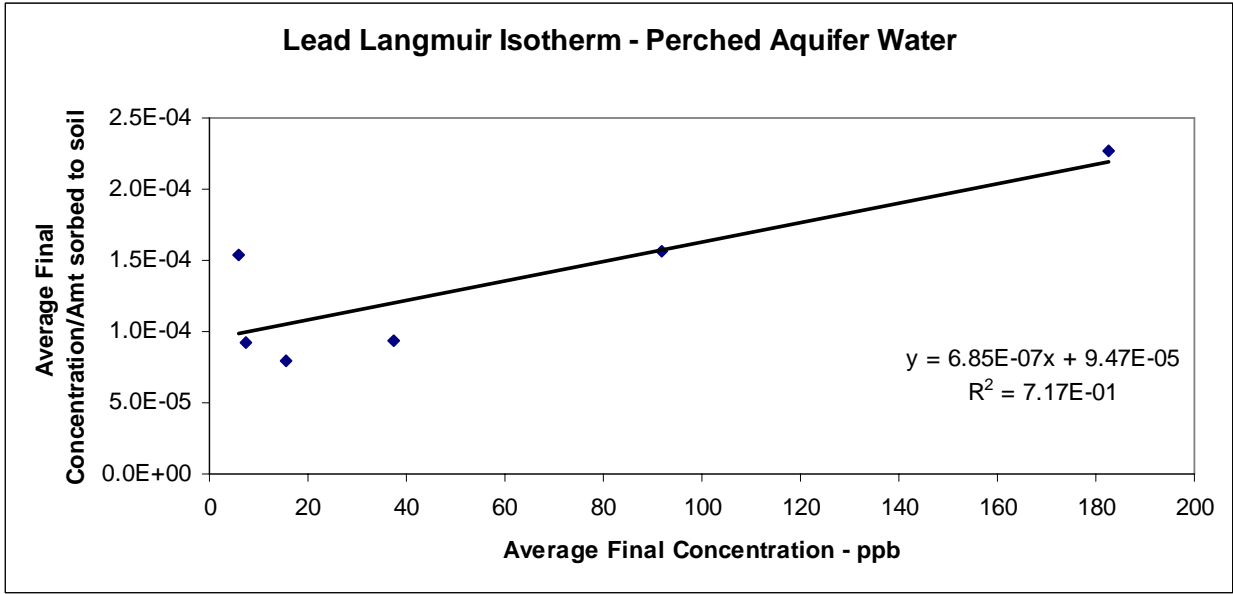


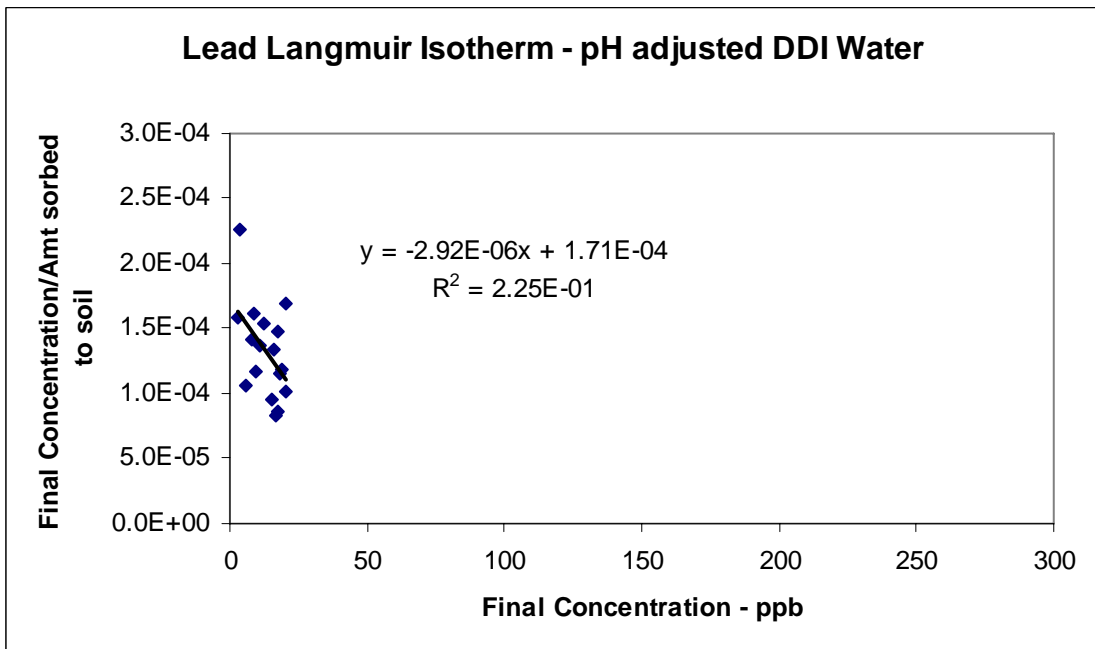
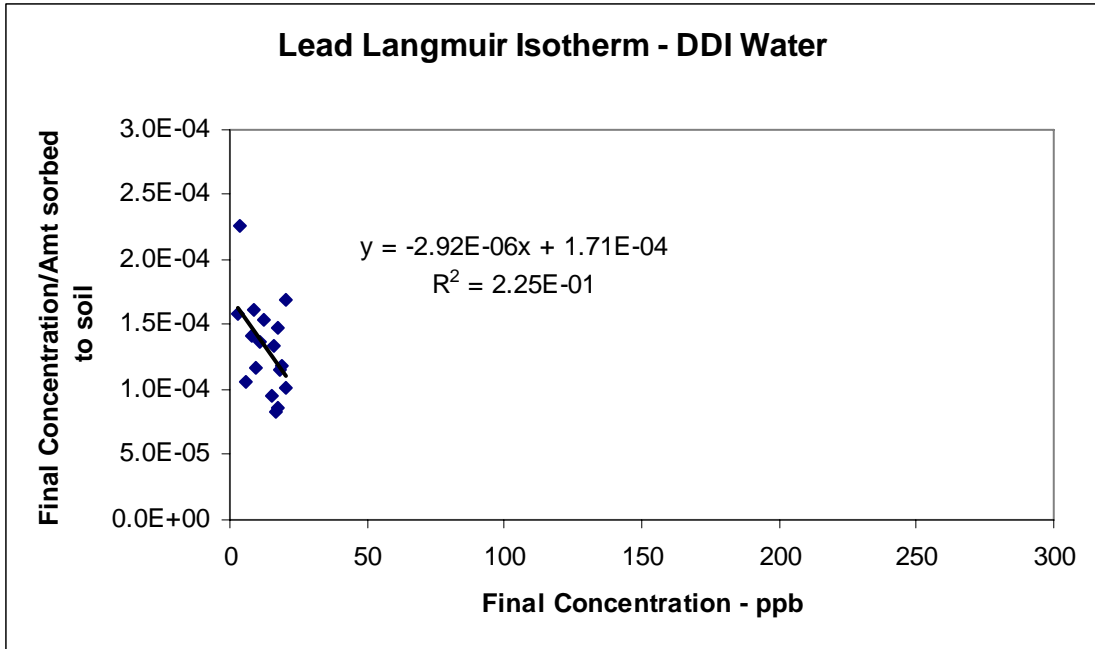


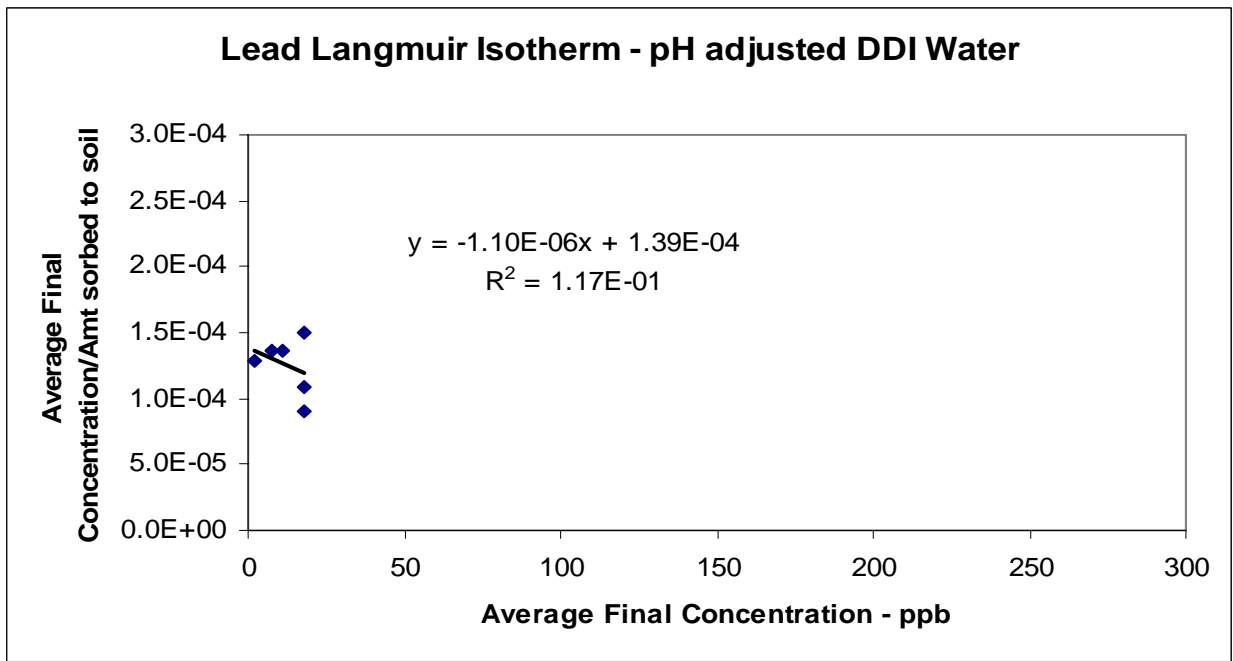
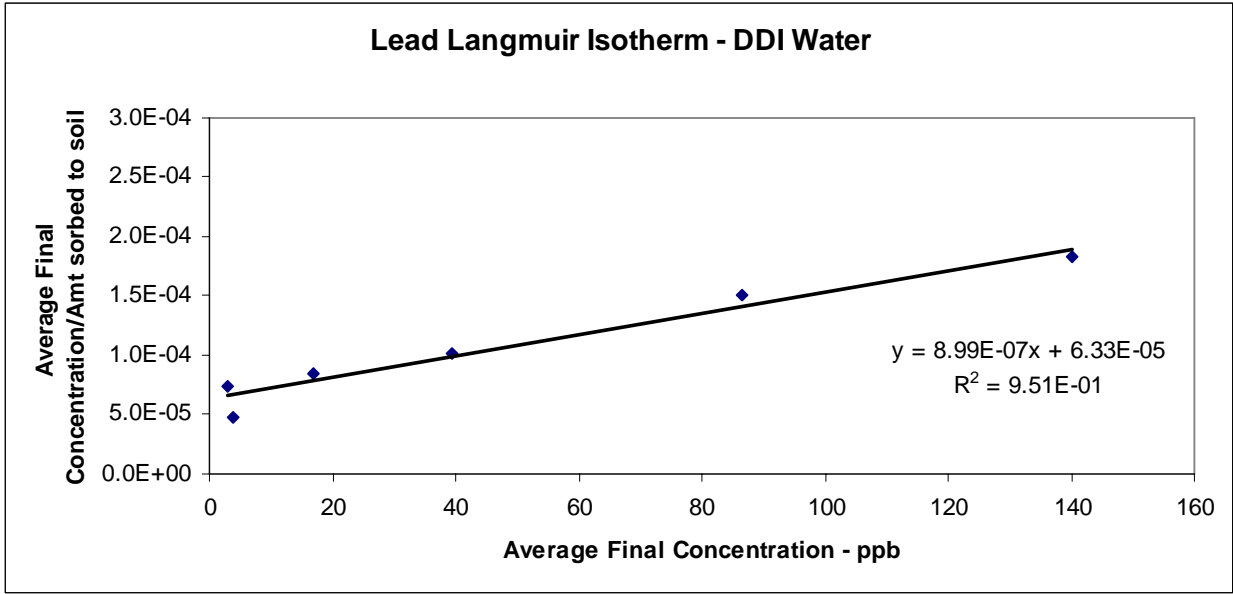






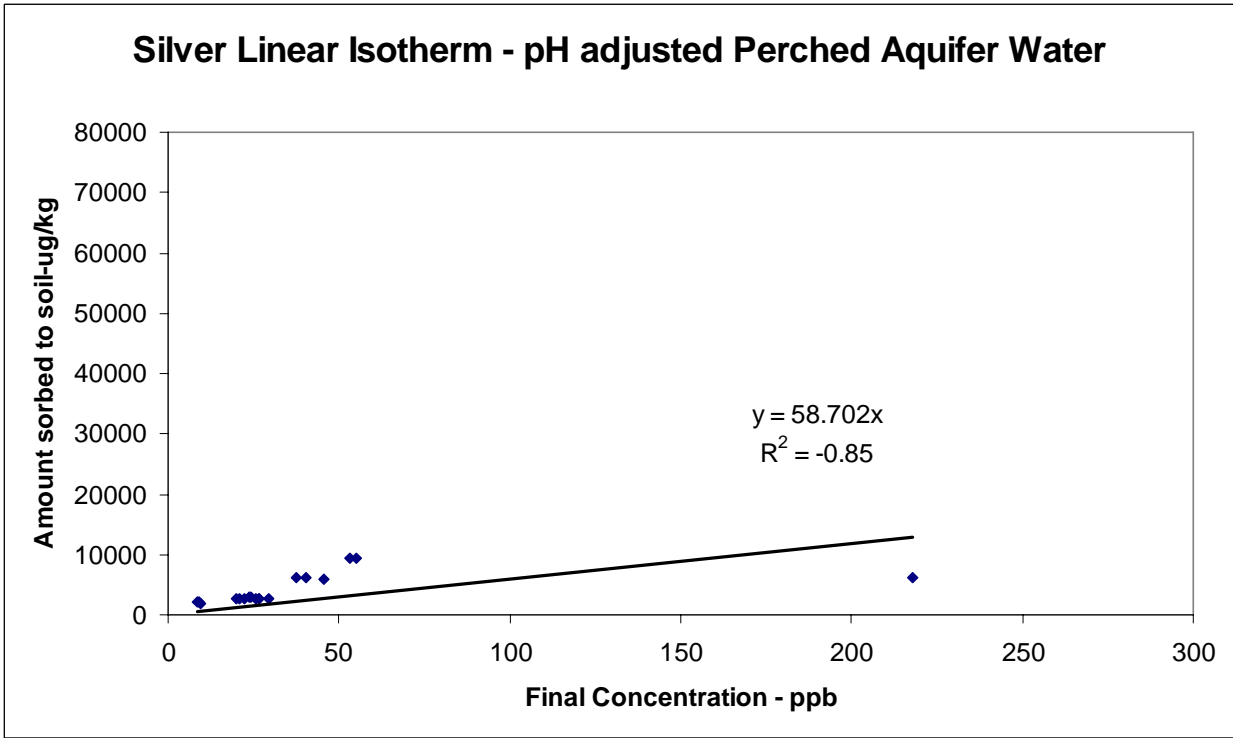
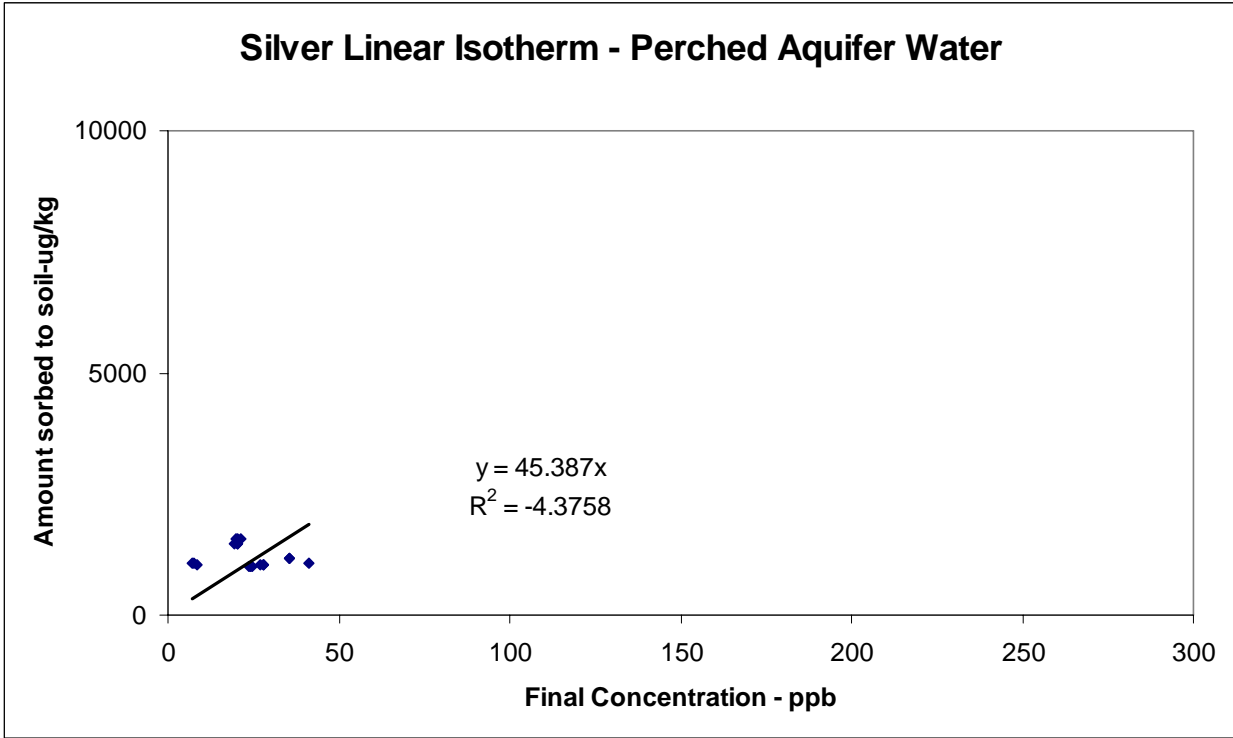




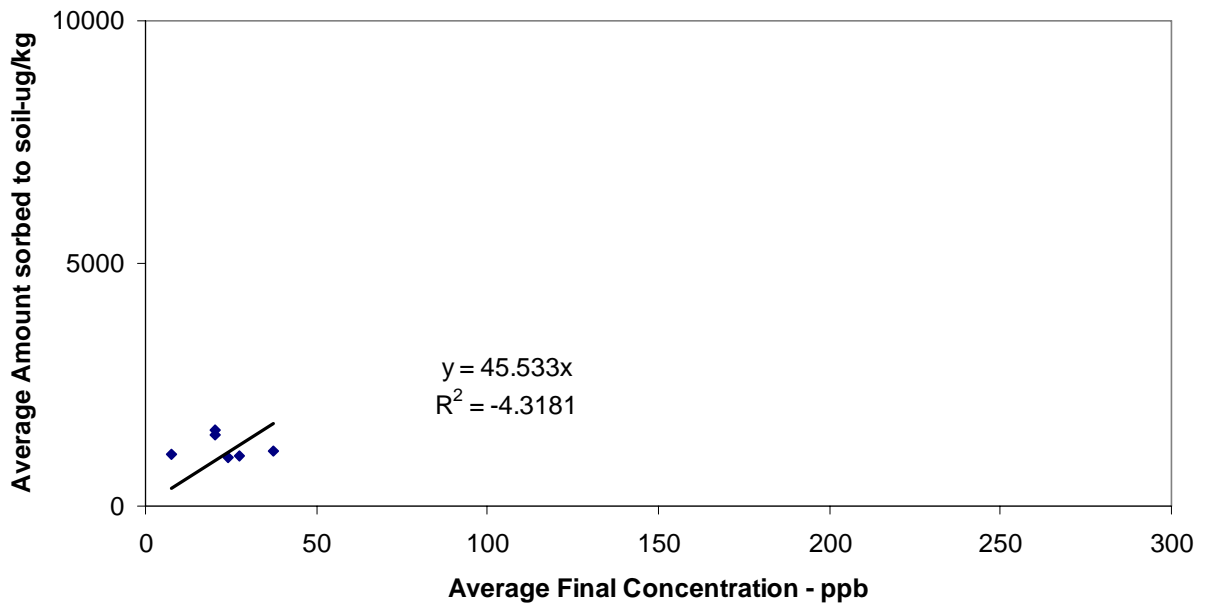


Pantex Silver Isotherm Data

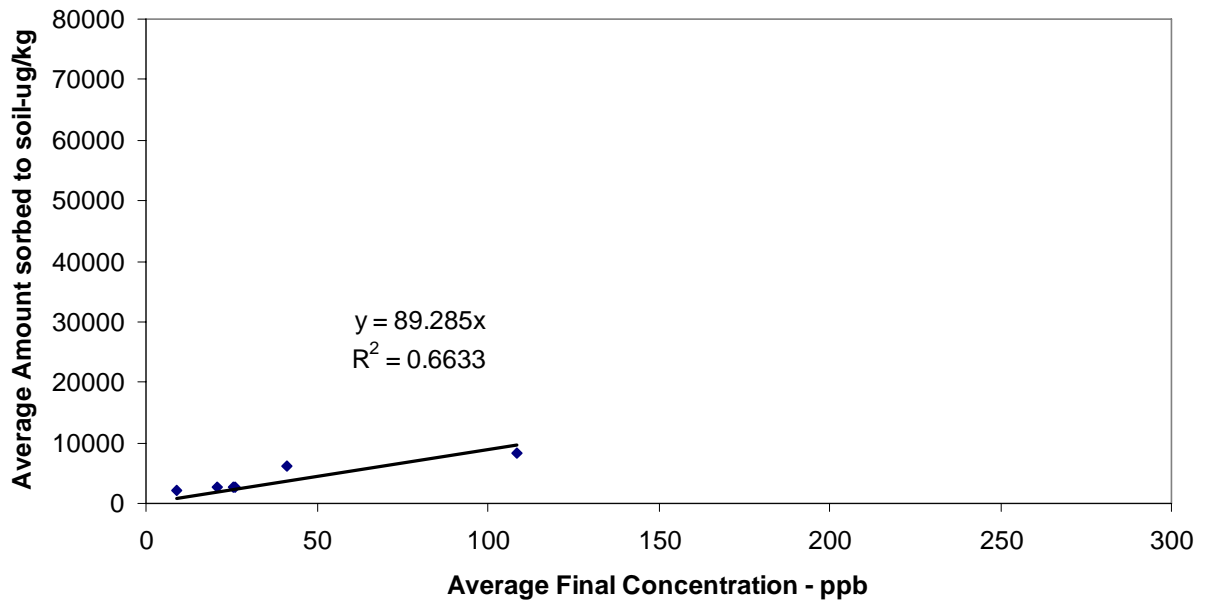
Source Water	K_d (L/kg)	K ([$\mu\text{g}/\text{kg}$][$\mu\text{g}/\text{L}$] ^{-N})	N	β (kg/ μg)	α (L/ μg)
Perched Aquifer	45.4	1190	0.0023	1.04E3	4.16E-1
pH adjusted Perched Aquifer	58.7	601	0.539	2.25E3	3.90E-2
DDI	395	3110	0.592	9.62E4	1.32E-2
pH adjusted DDI	259	3410	0.552	6.10E4	2.81E-2

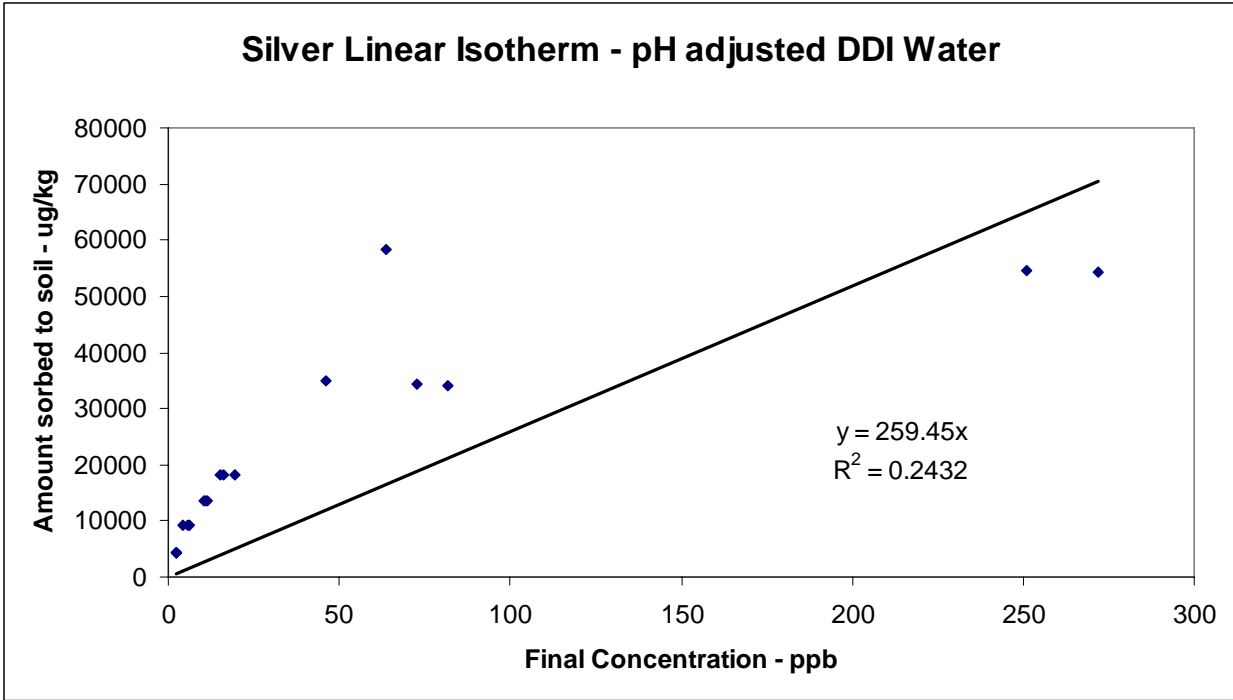
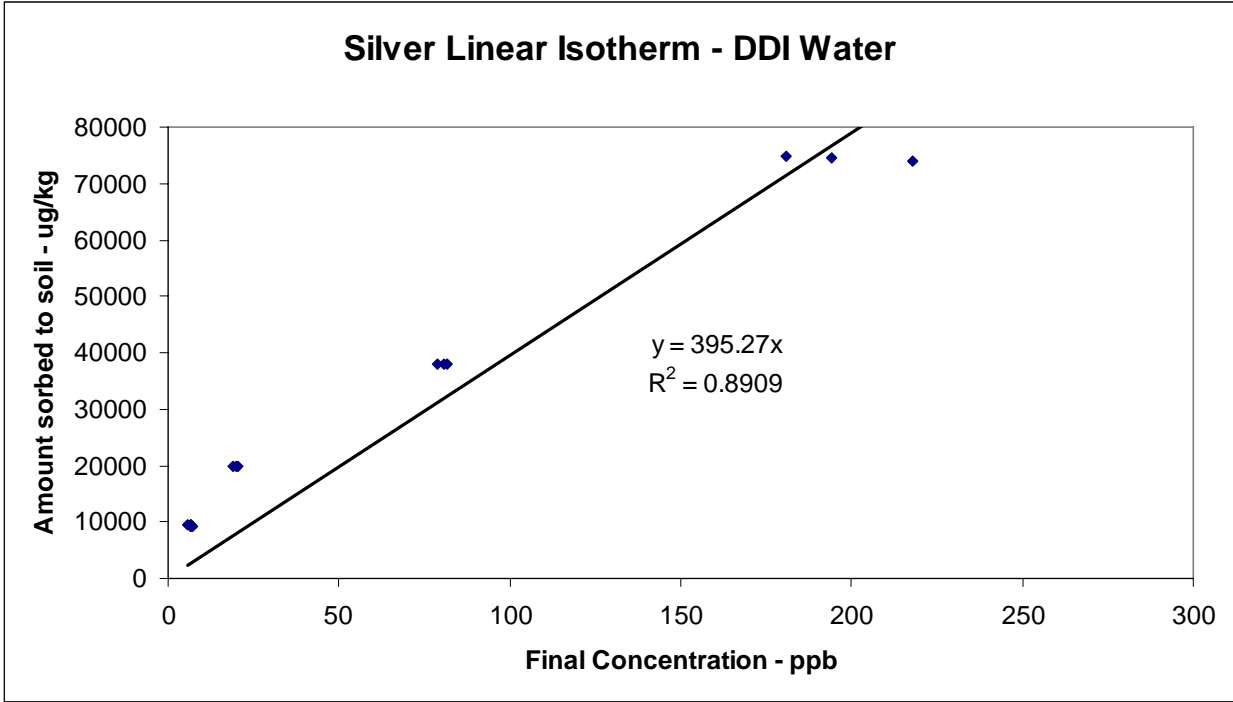


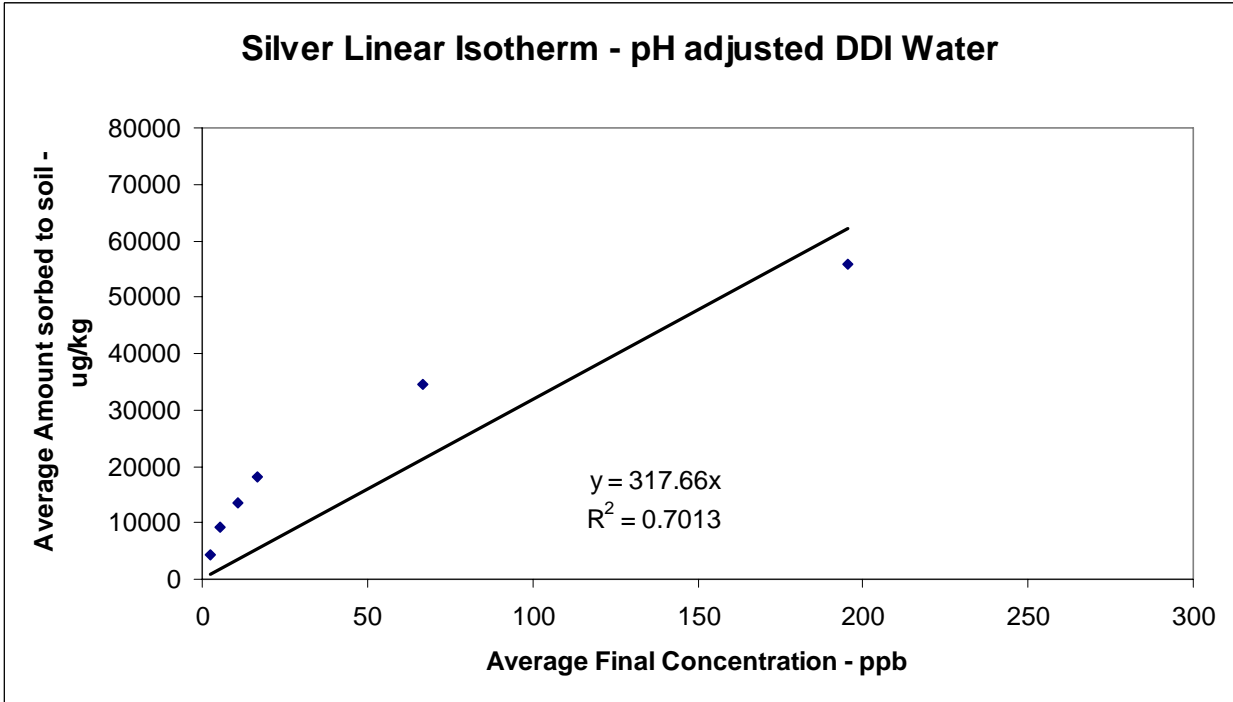
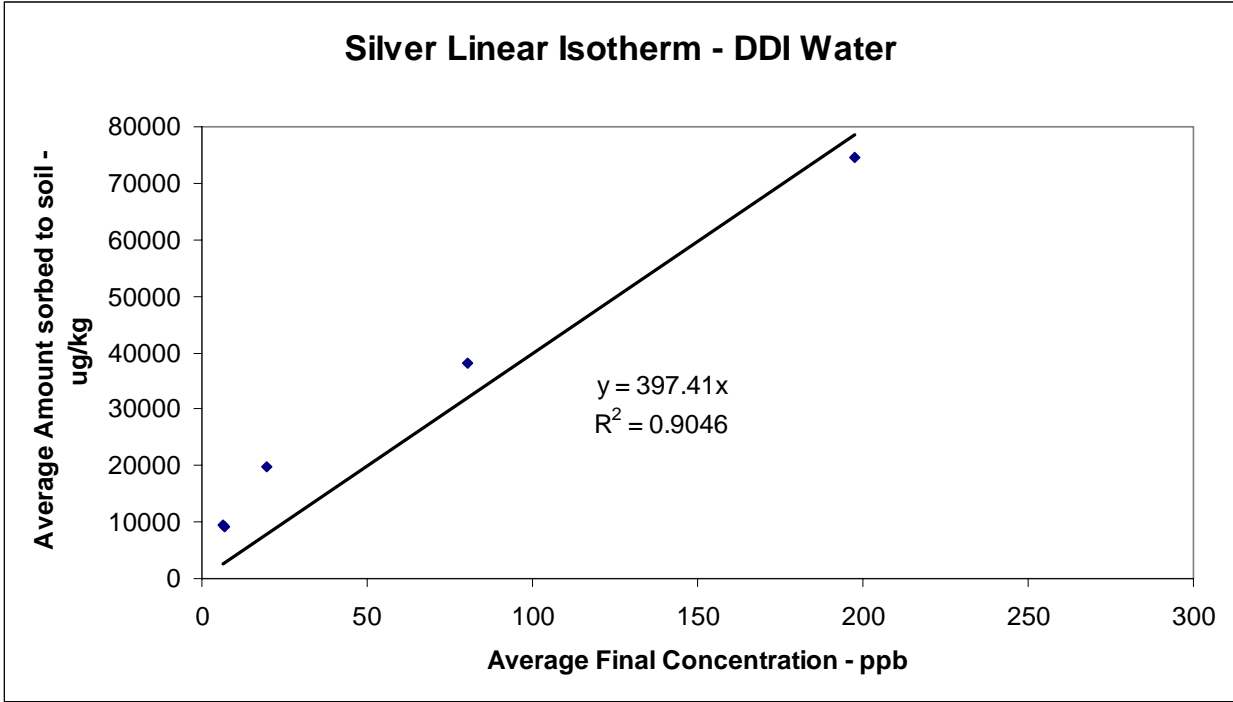
Silver Linear Isotherm - Perched Aquifer Water

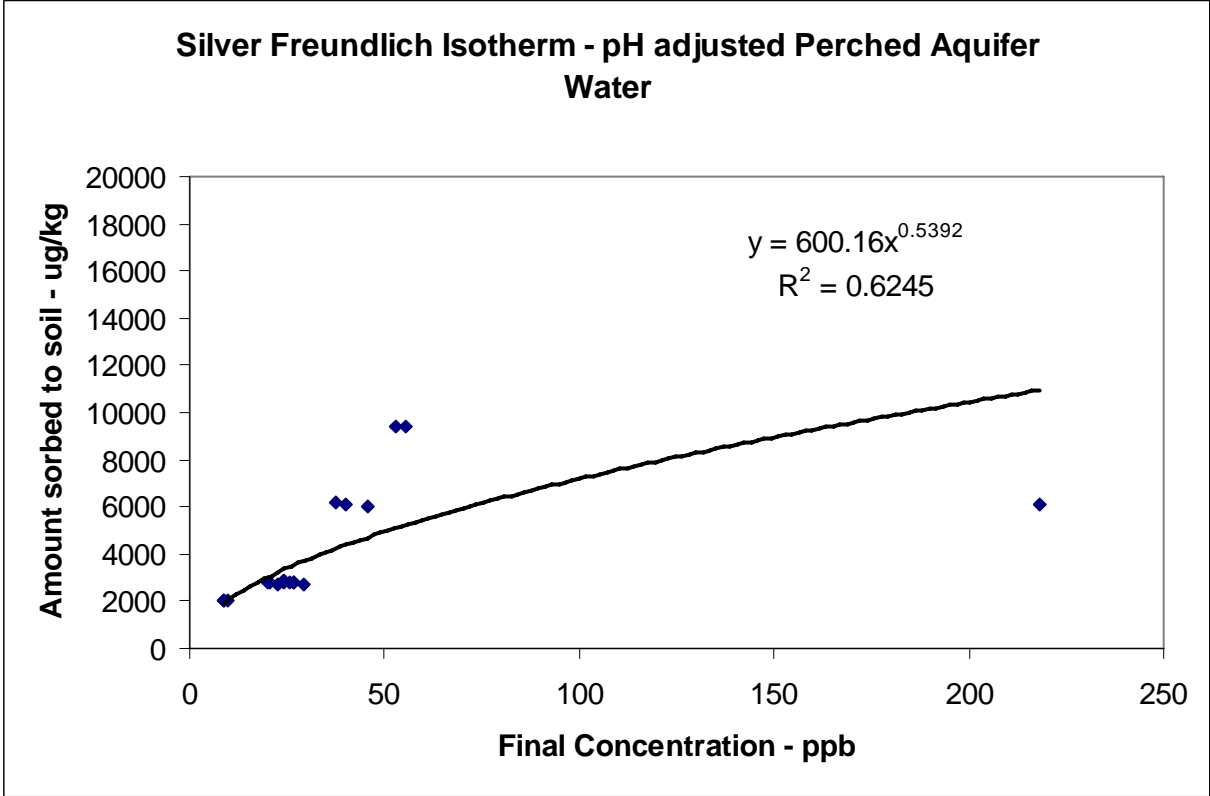
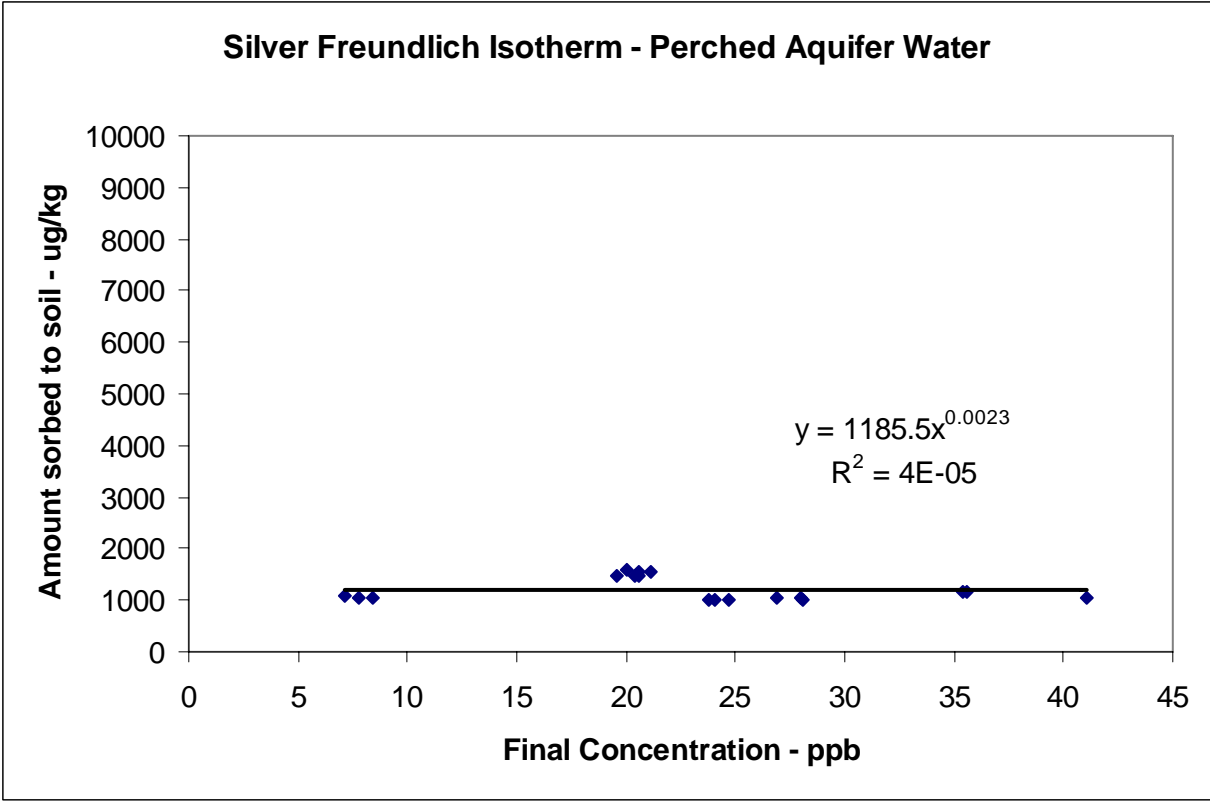


Silver Linear Isotherm - pH adjusted Perched Aquifer Water

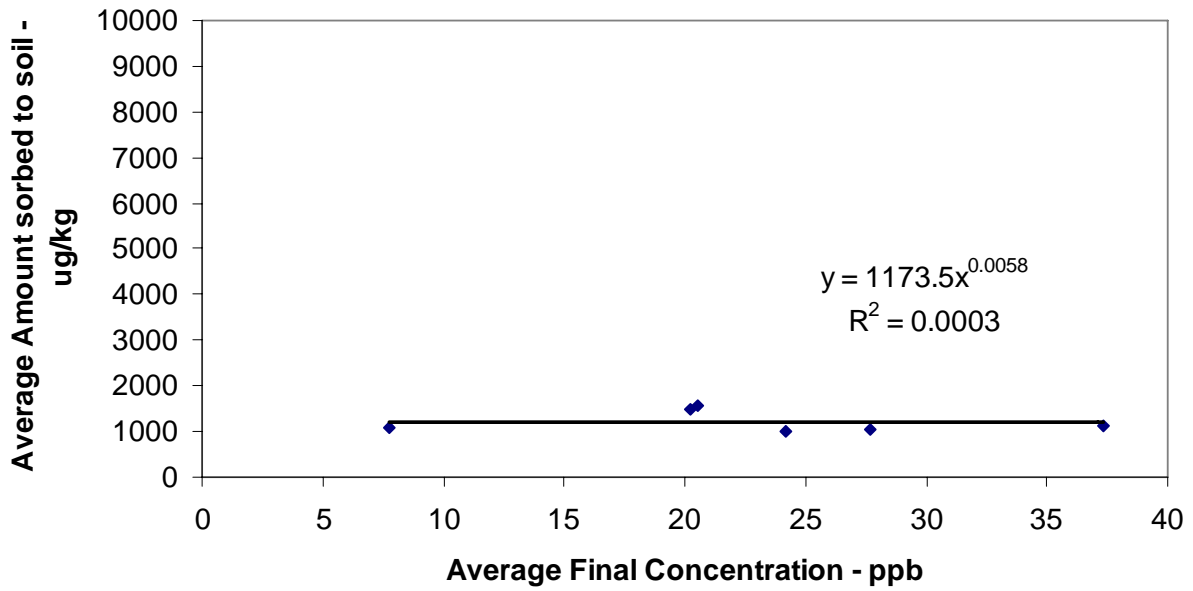




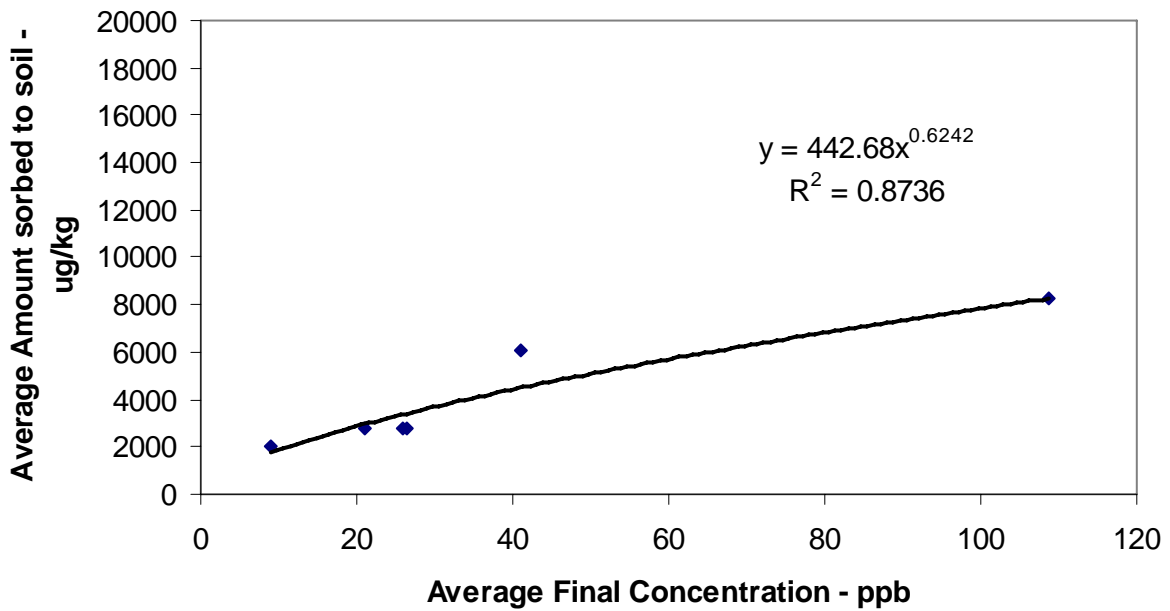


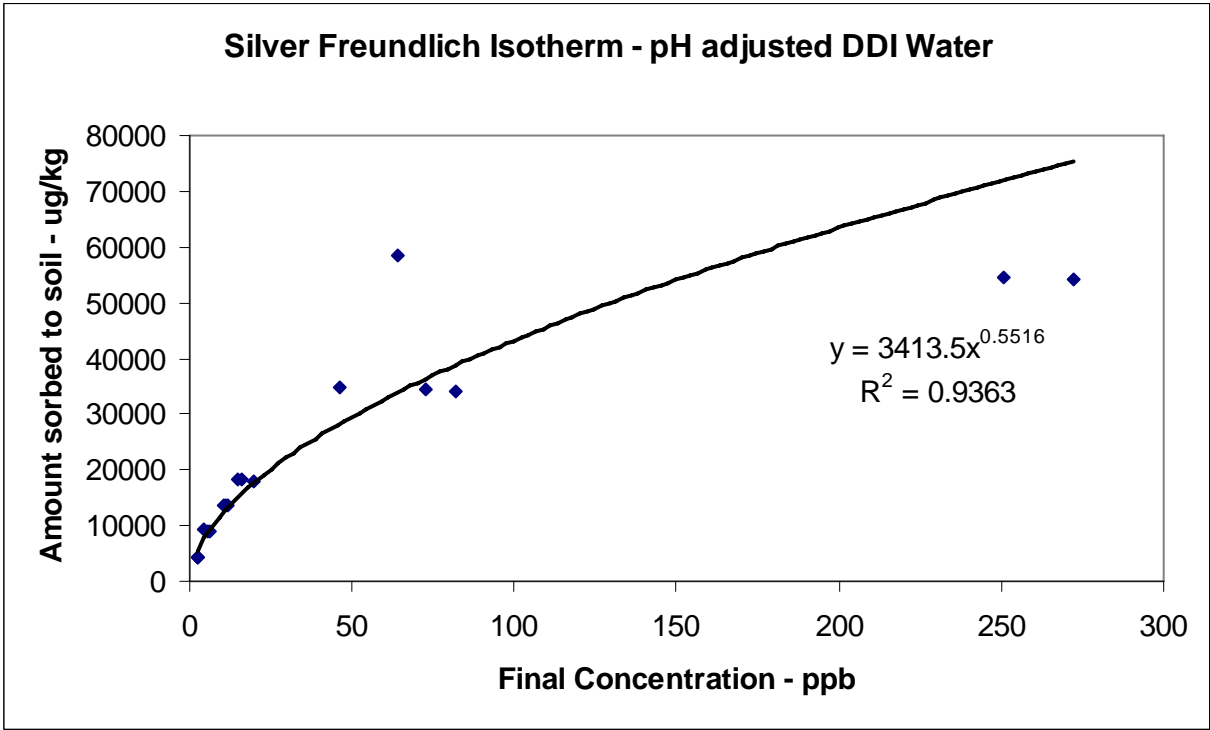
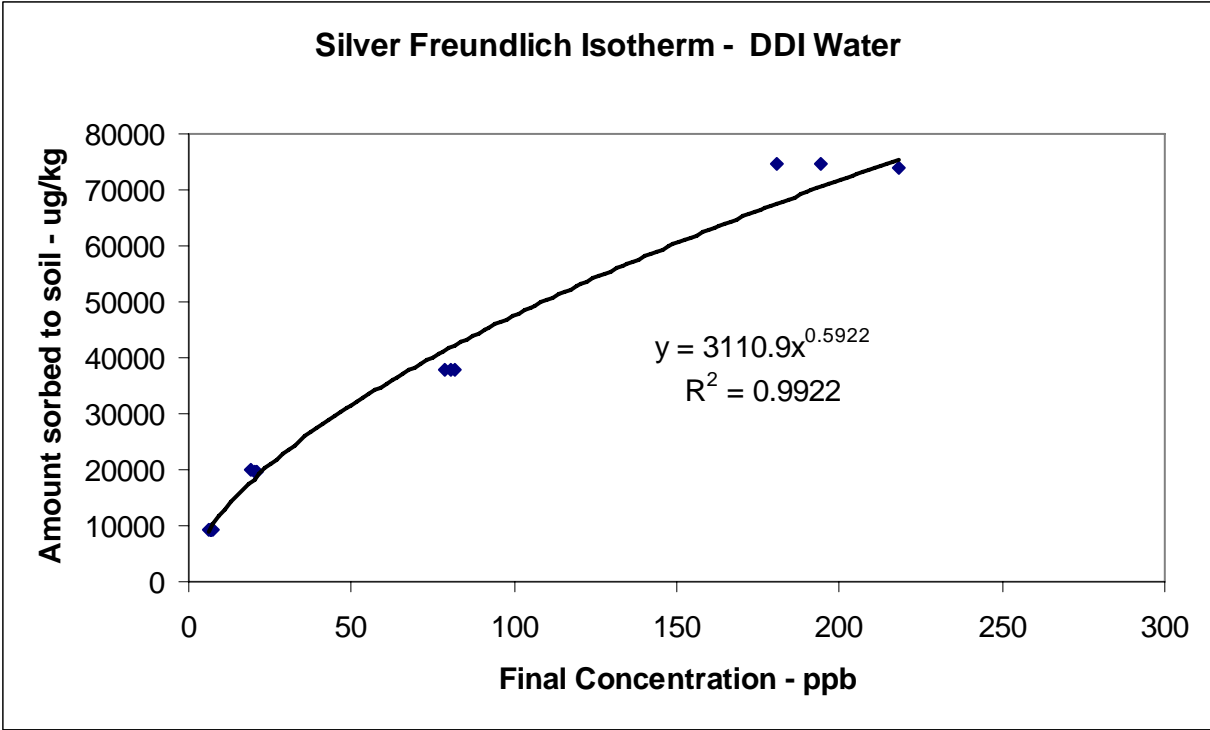


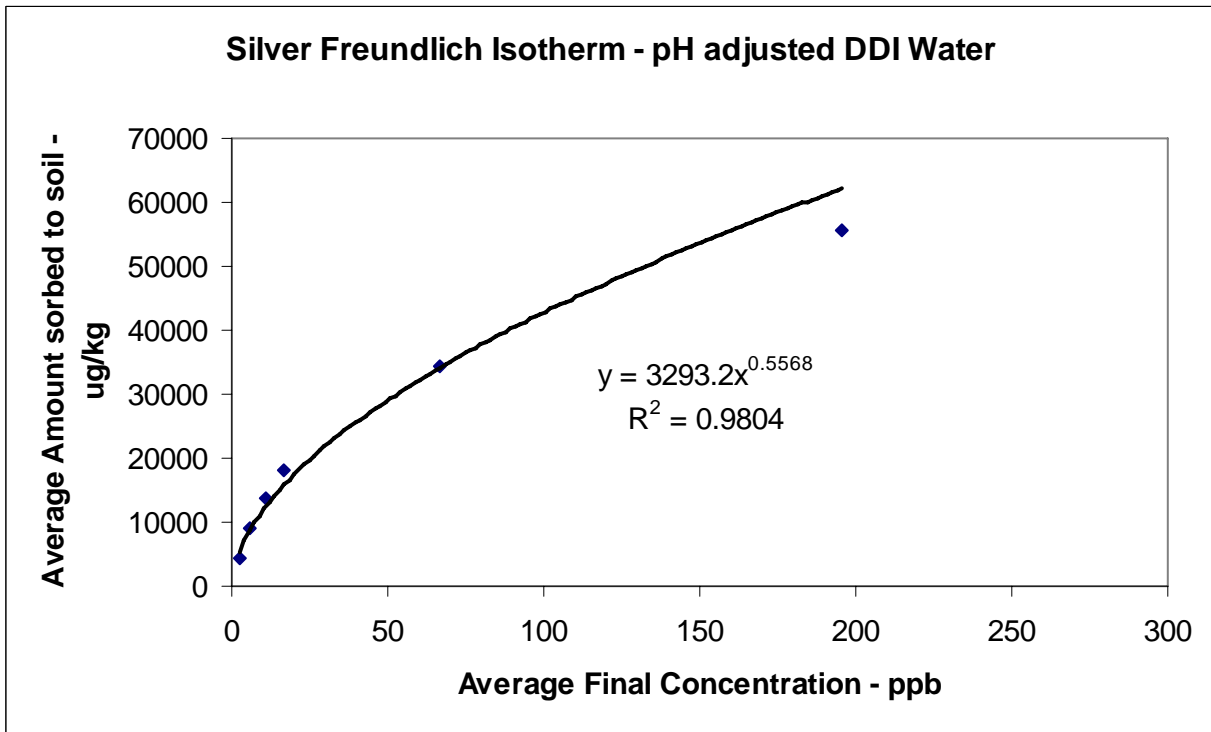
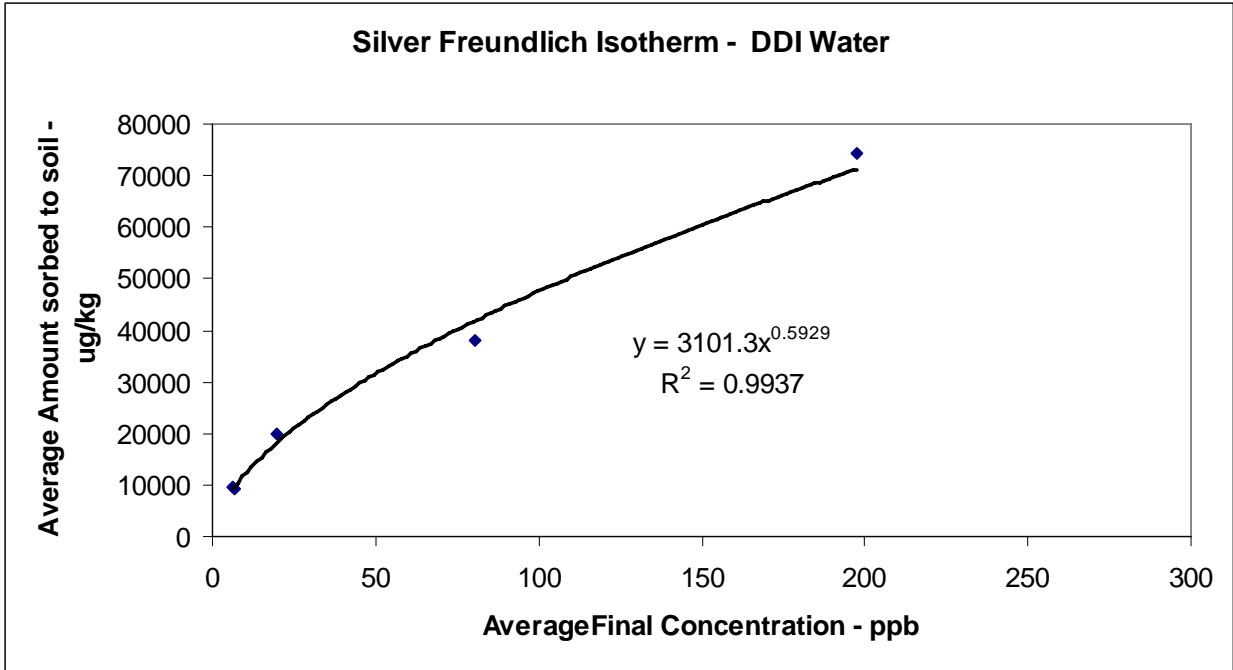
Silver Freundlich Isotherm - Perched Aquifer Water

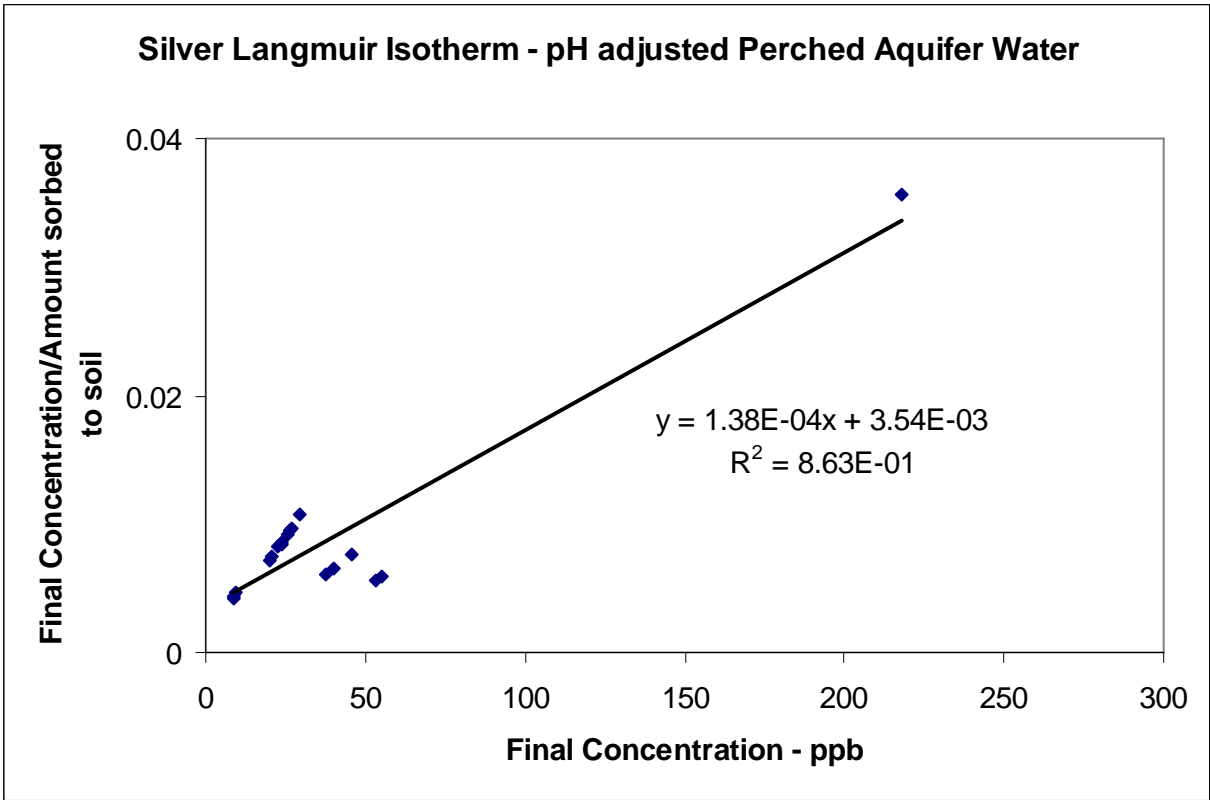
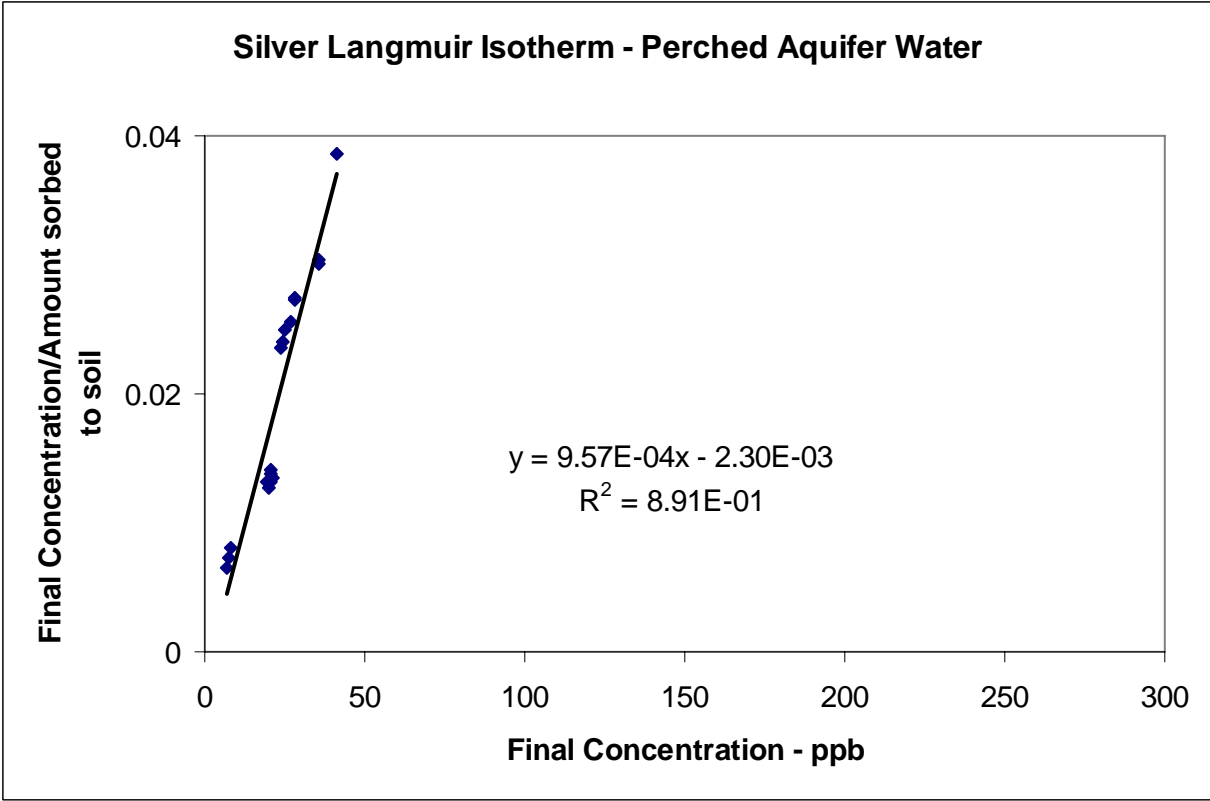


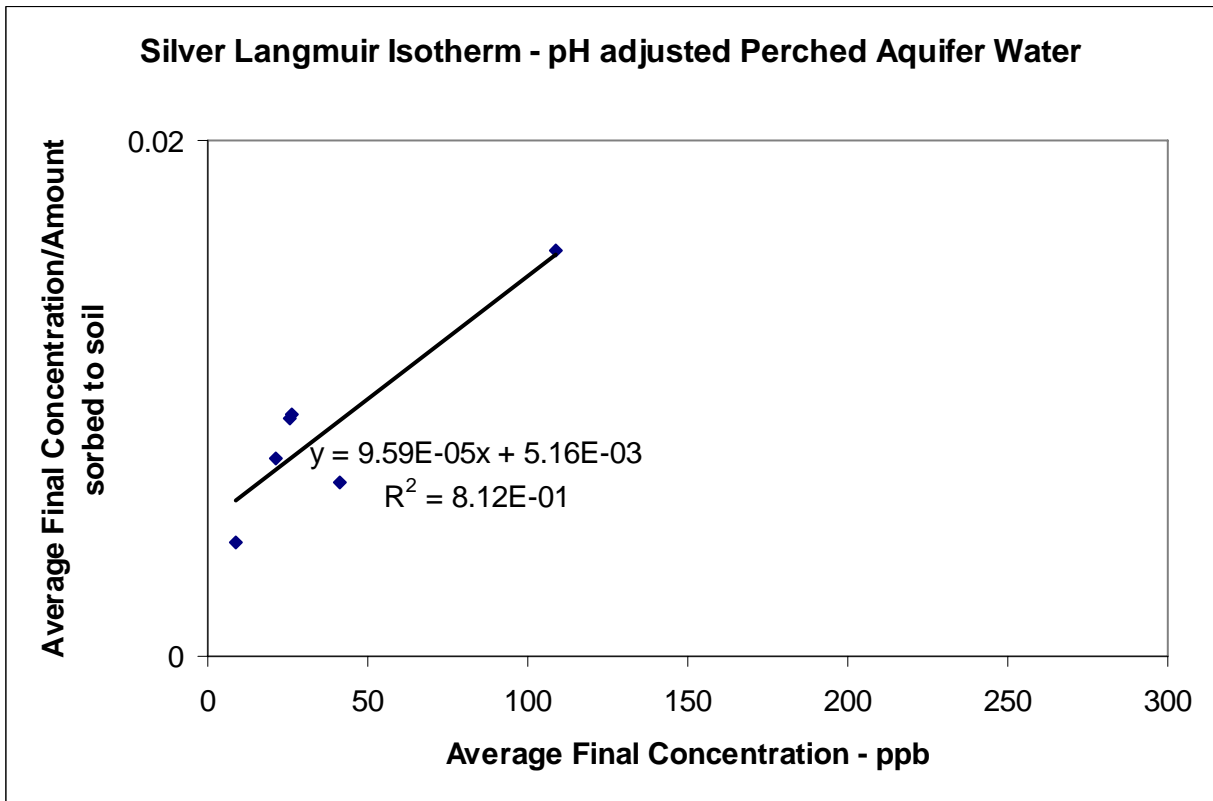
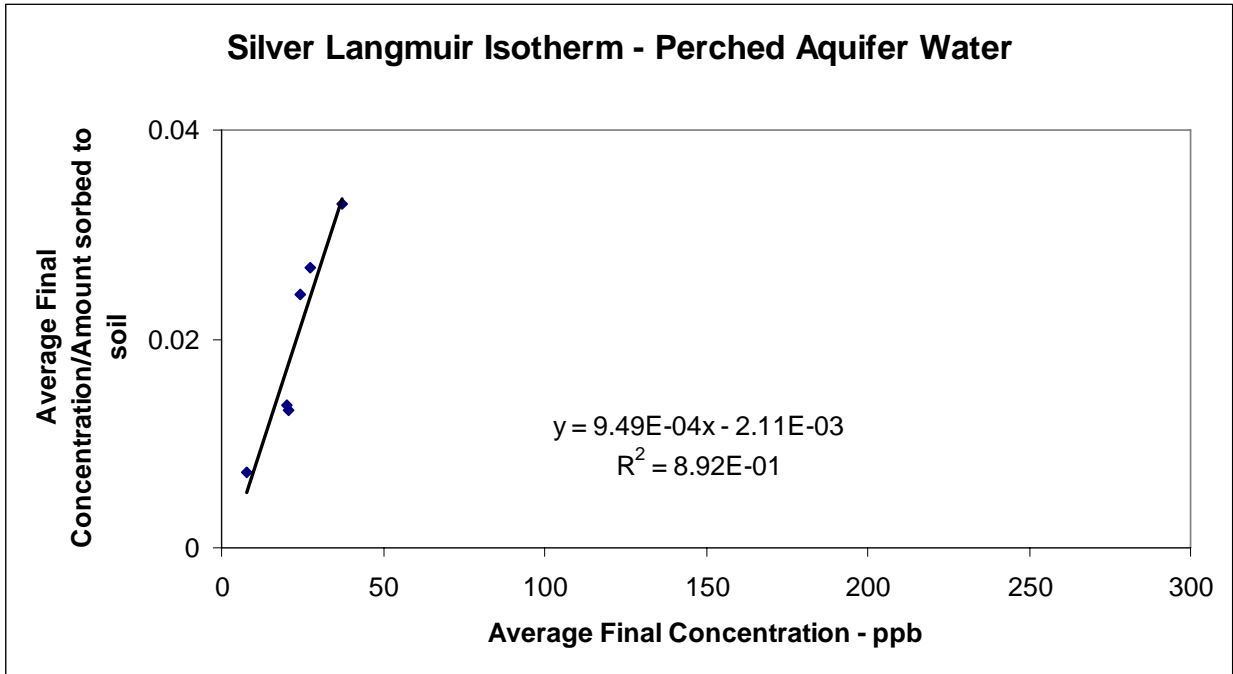
Silver Freundlich Isotherm - pH adjusted Perched Aquifer Water

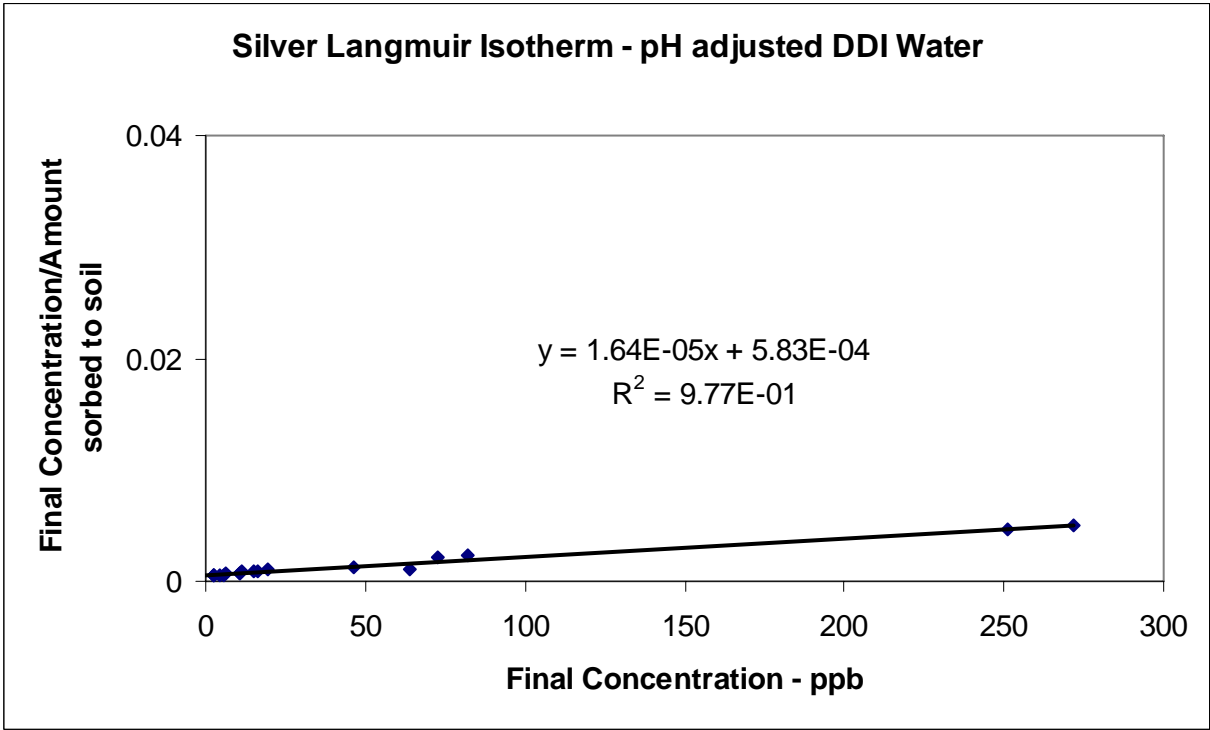
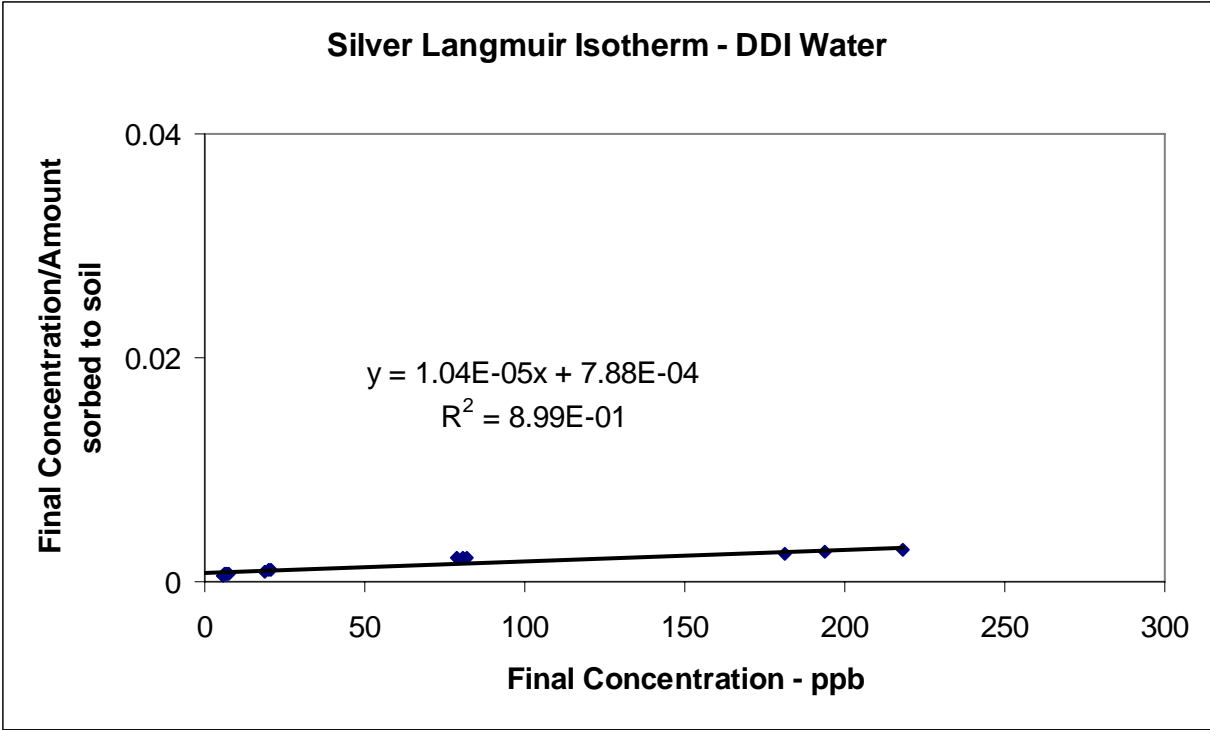


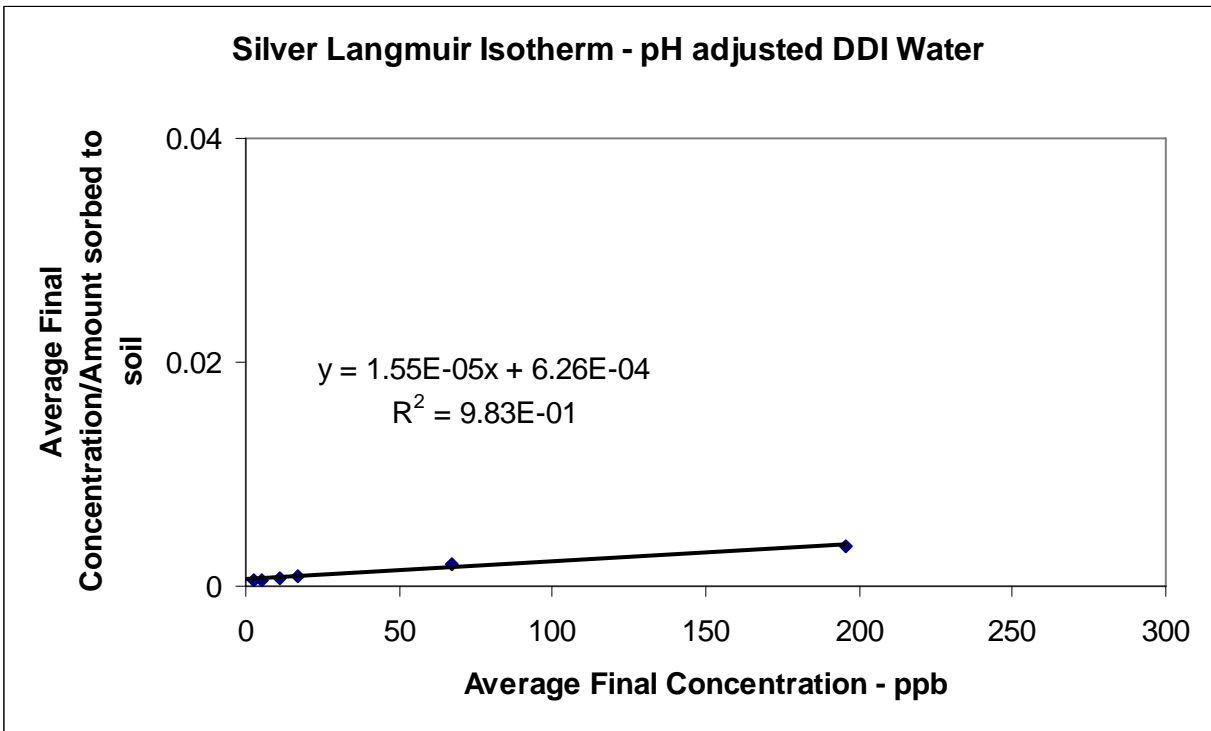
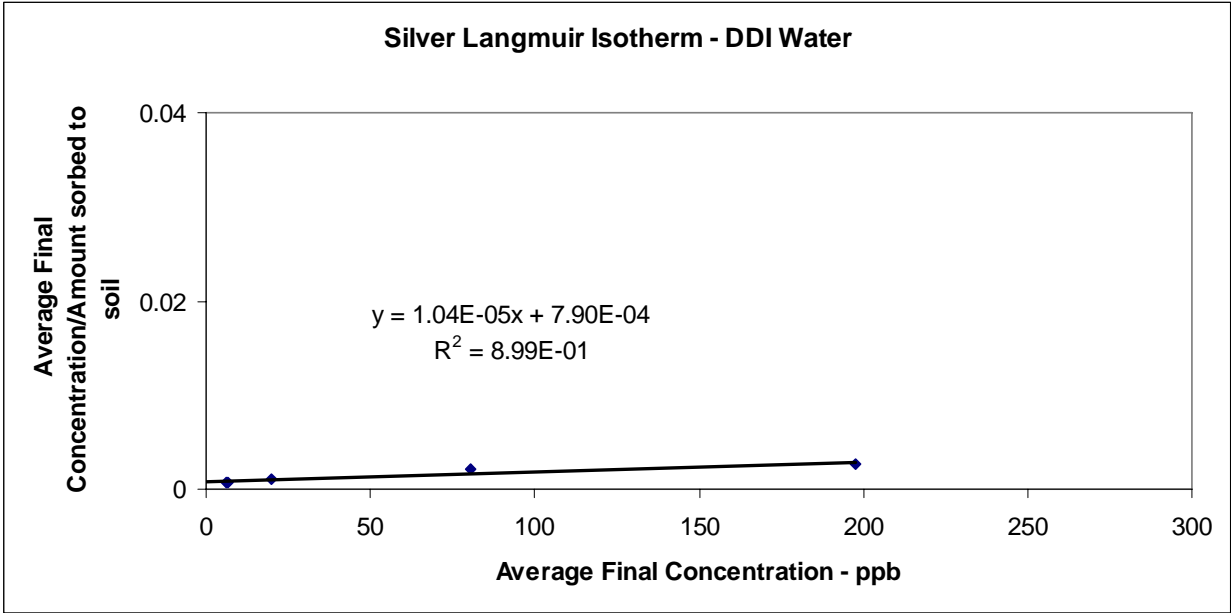








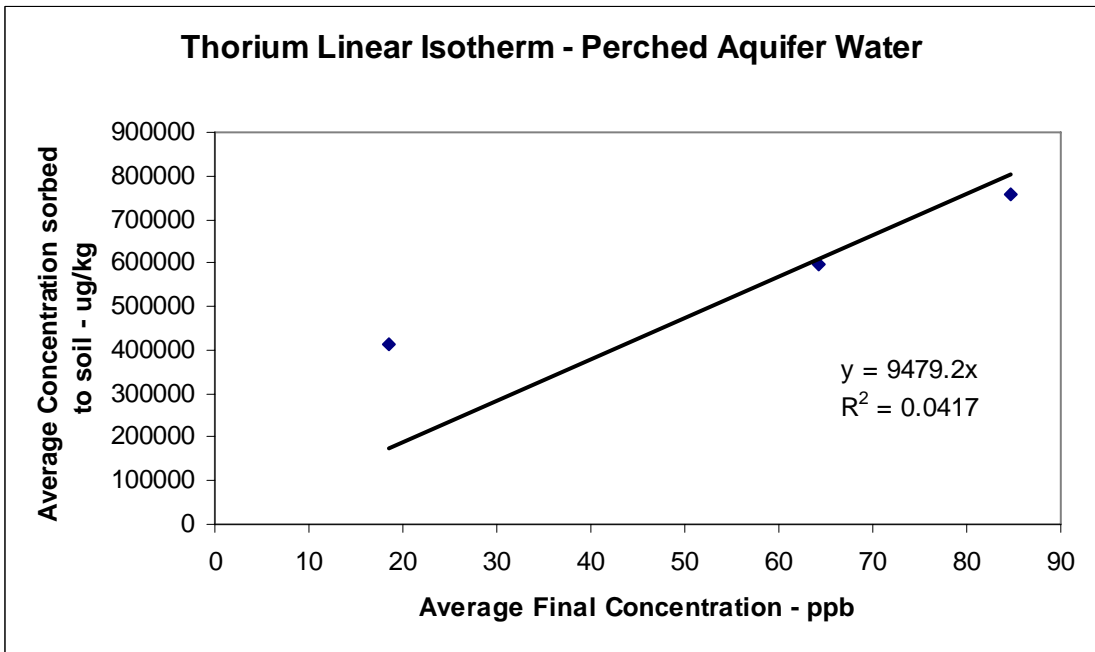
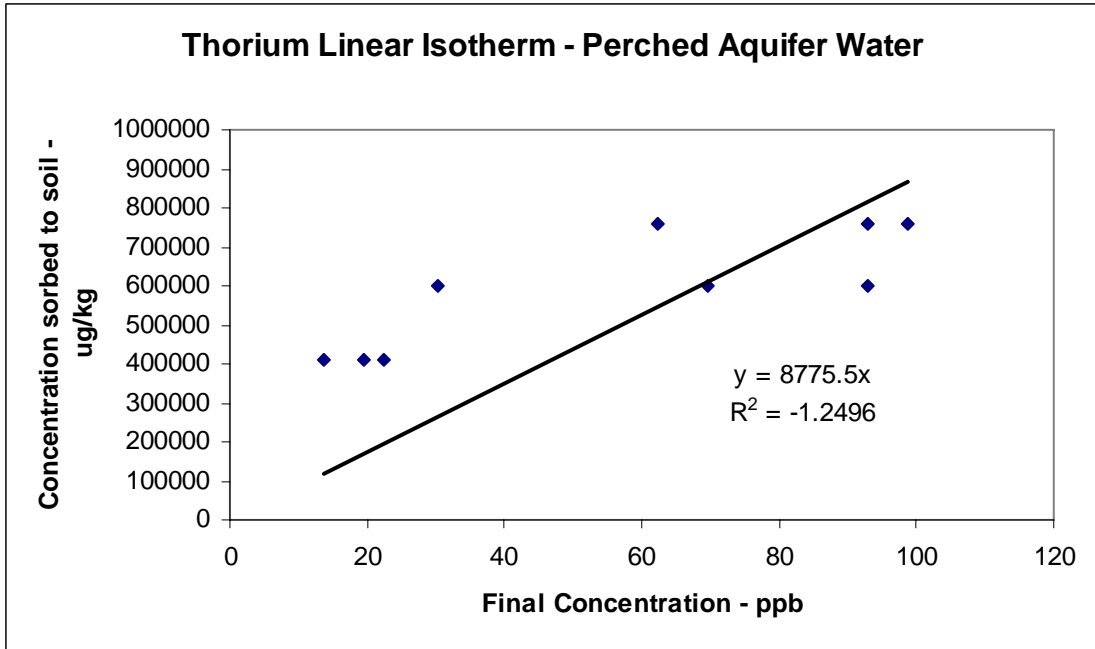


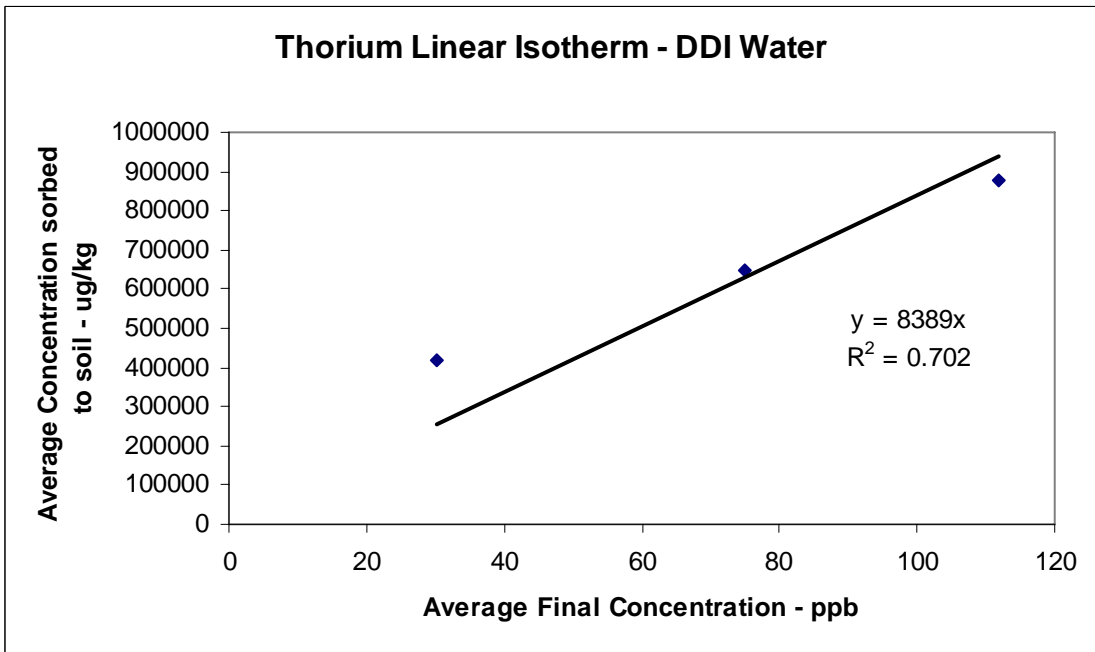
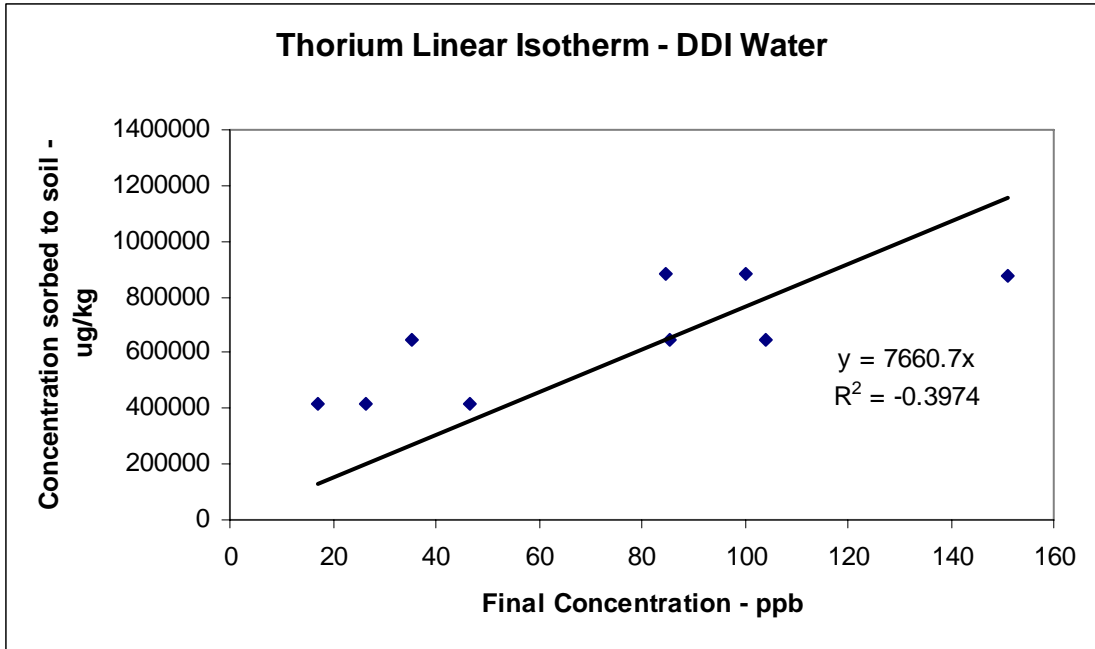


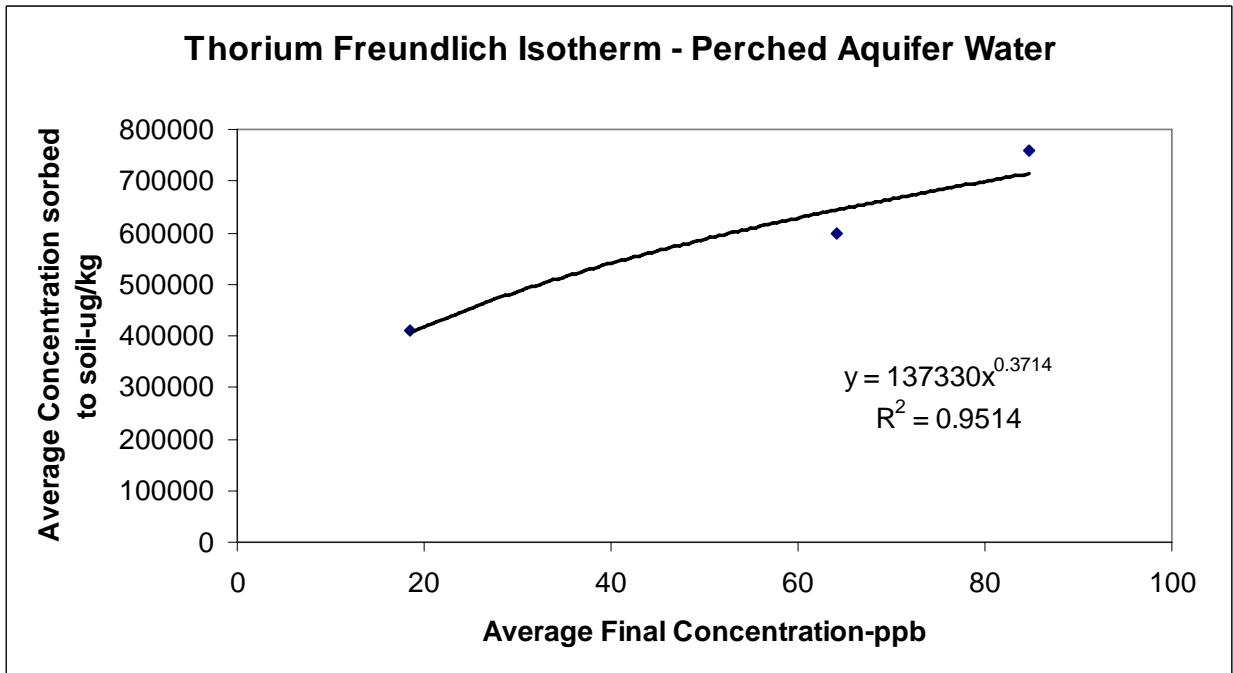
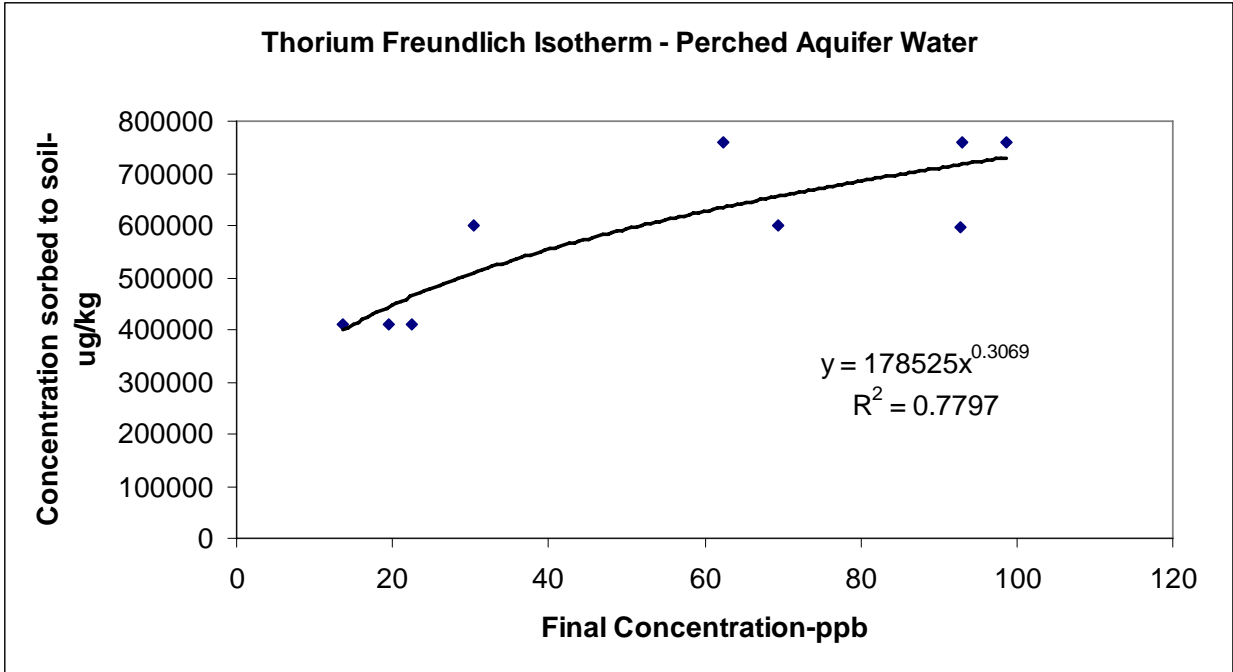
Pantex Thorium Isotherm Data

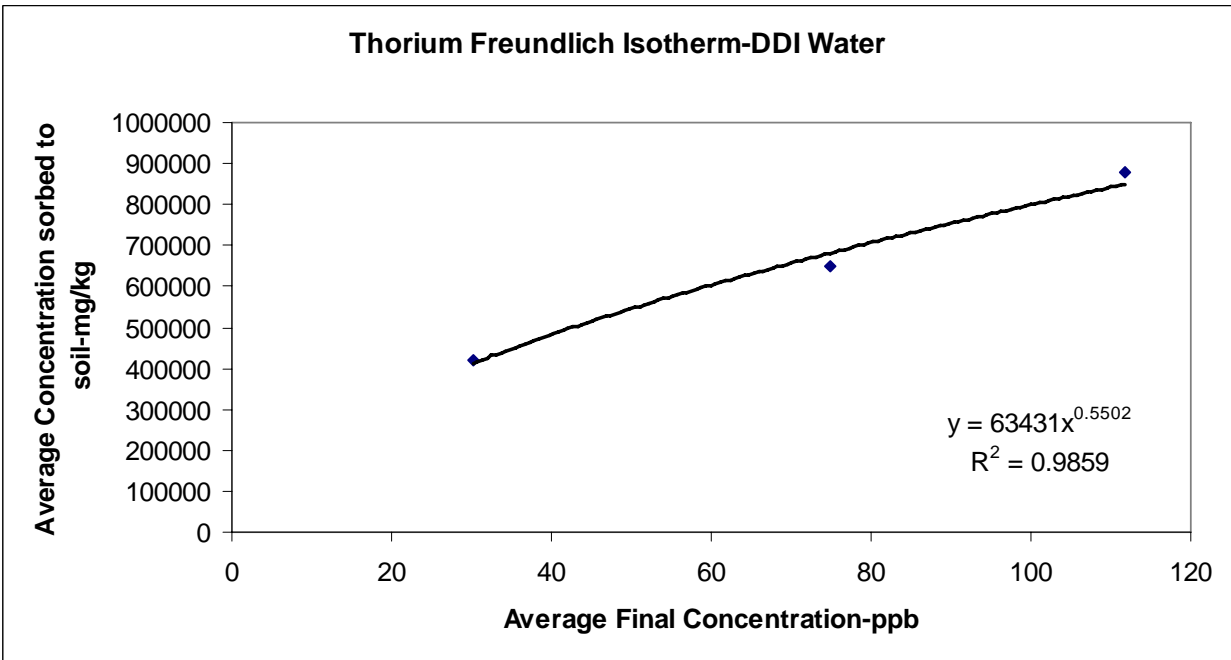
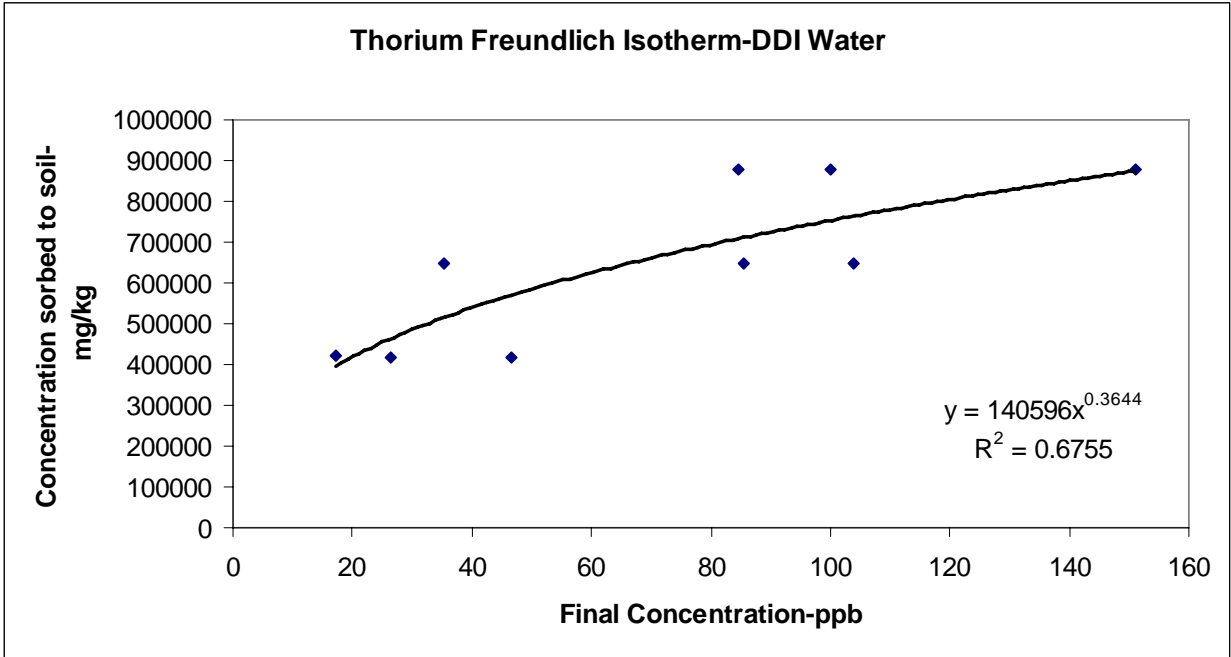
Source Water	K_d (L/kg)	K ([$\mu\text{g}/\text{kg}$][$\mu\text{g}/\text{L}$] ^{-N})	N	β (kg/ μg)	α (L/ μg)
Perched Aquifer	8780	179000	0.307	8.20E5	6.10E-2
DDI	7660	141000	0.364	1.05E6	2.61E-2

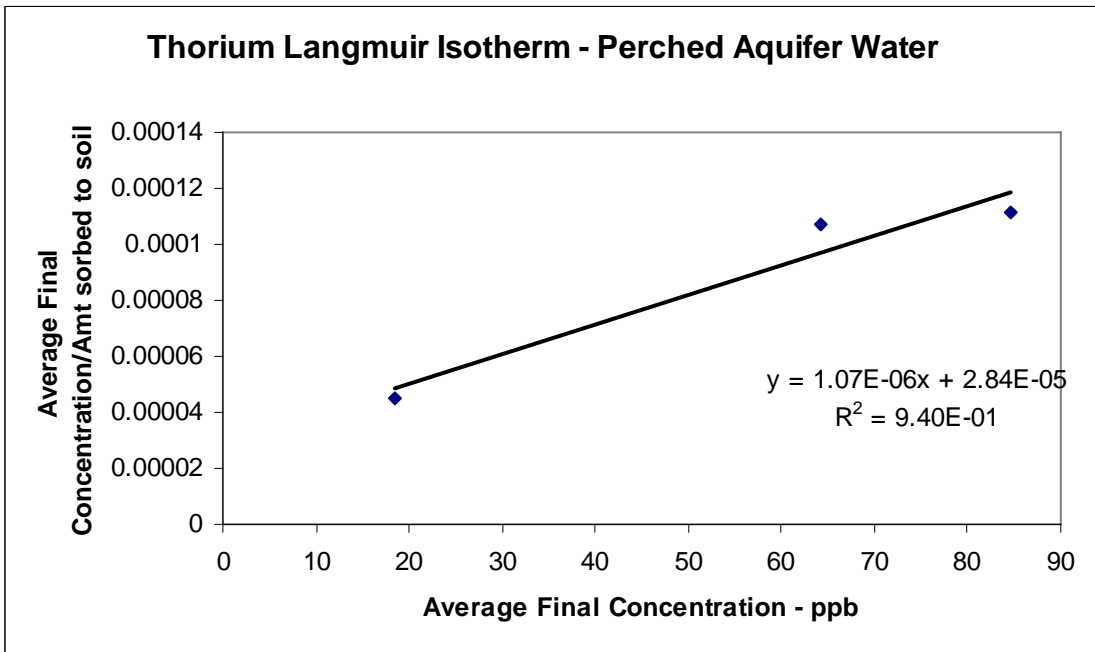
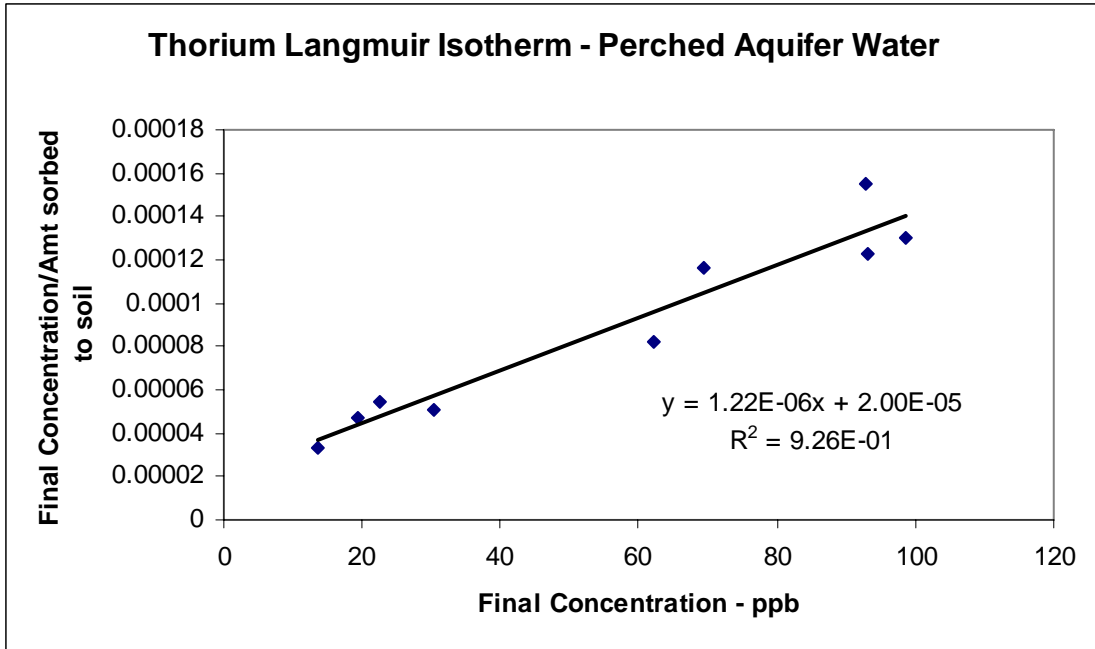
Note: There was not enough data above detection limits on the pH adjusted experiments to attempt to delineate an isotherm.

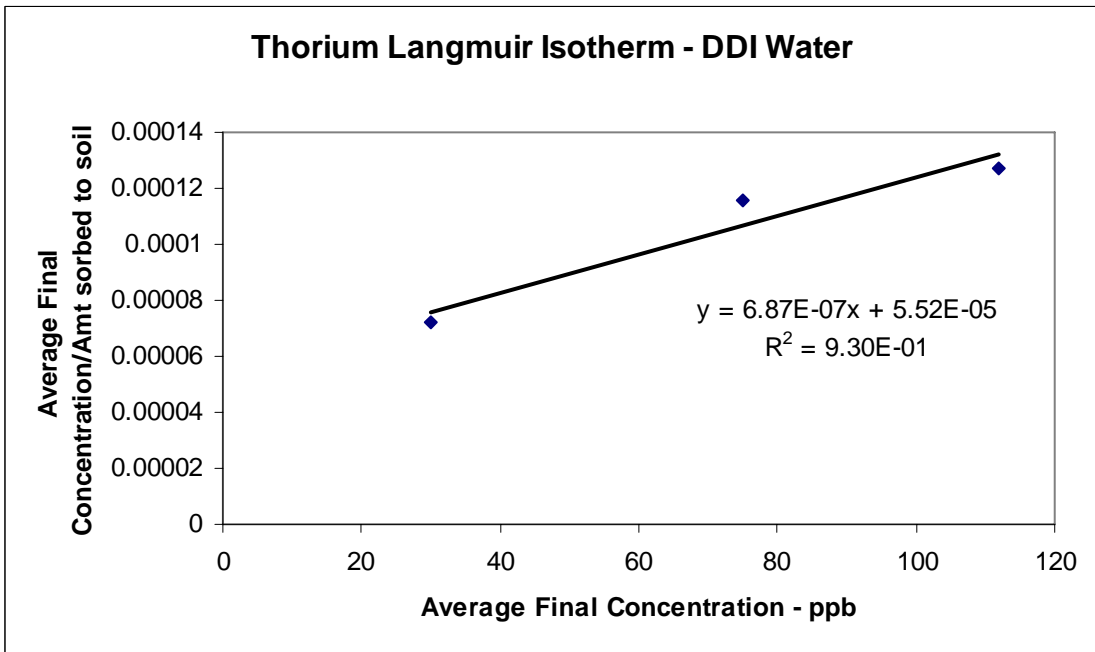
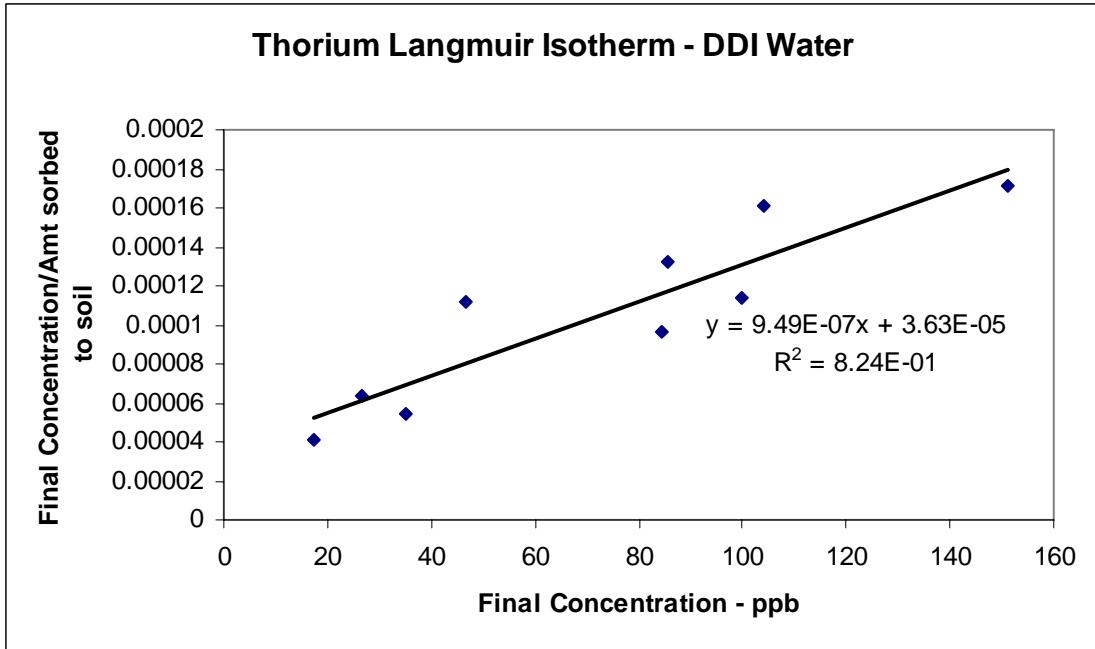








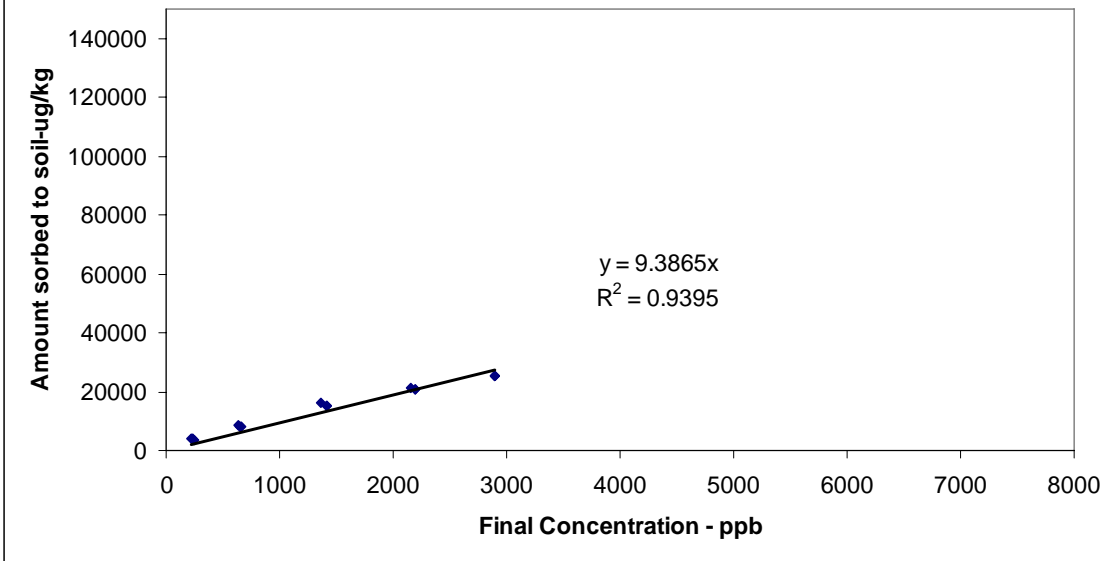




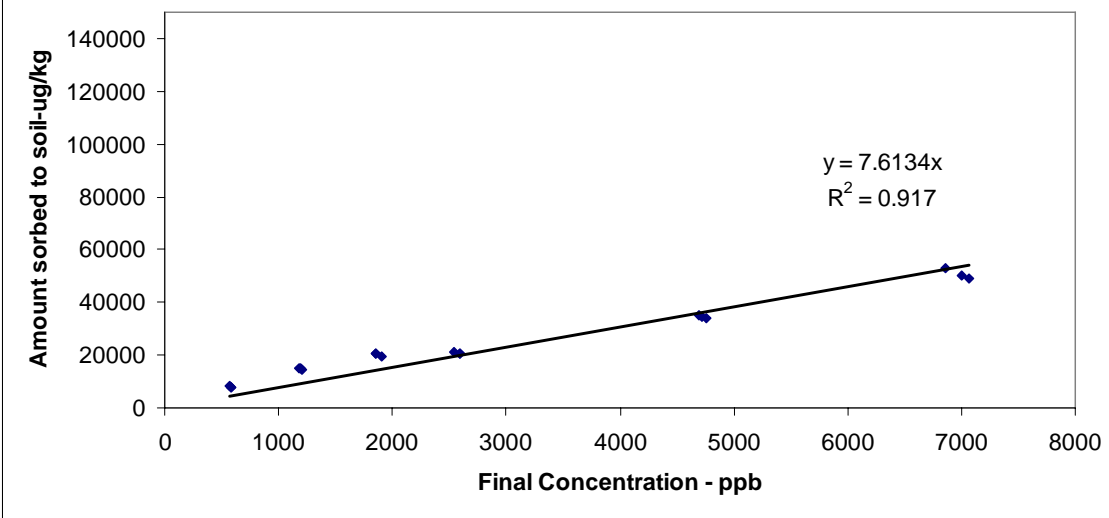
Pantex Uranium Isotherm Data

Source Water	K_d (L/kg)	K ([$\mu\text{g}/\text{kg}$][$\mu\text{g}/\text{L}$] ^{-N})	N	β (kg/ μg)	α (L/ μg)
Perched Aquifer	9.39	63.7	0.753	5.18E4	3.14E-4
pH adjusted Perched Aquifer	7.61	94.4	0.703	9.35E4	1.42E-3
DDI	30.3	1800	0.443	1.00E5	1.33E-4
pH adjusted DDI	66.1	669	0.692	5.92E4	2.19E-3

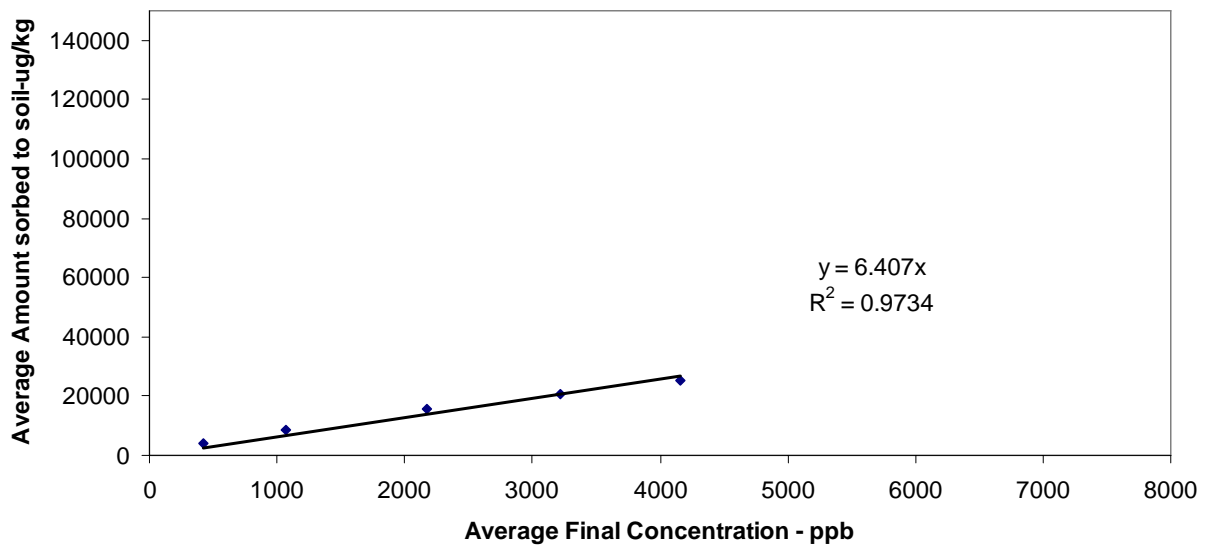
Uranium Linear Isotherm - Perched Aquifer Water



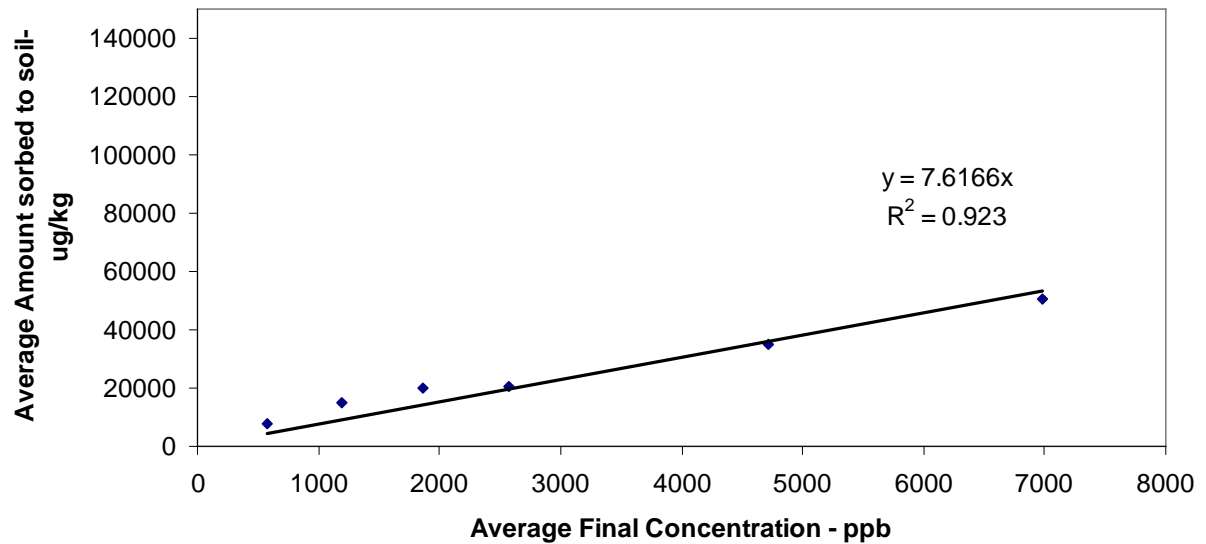
Uranium Linear Isotherm - pH adjusted Perched Aquifer Water



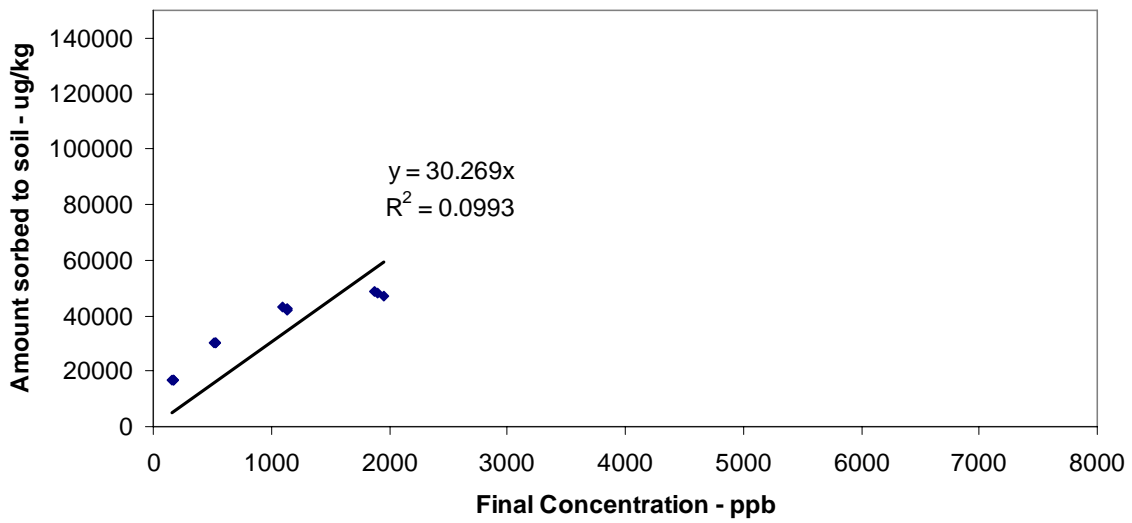
Uranium Linear Isotherm - Perched Aquifer Water



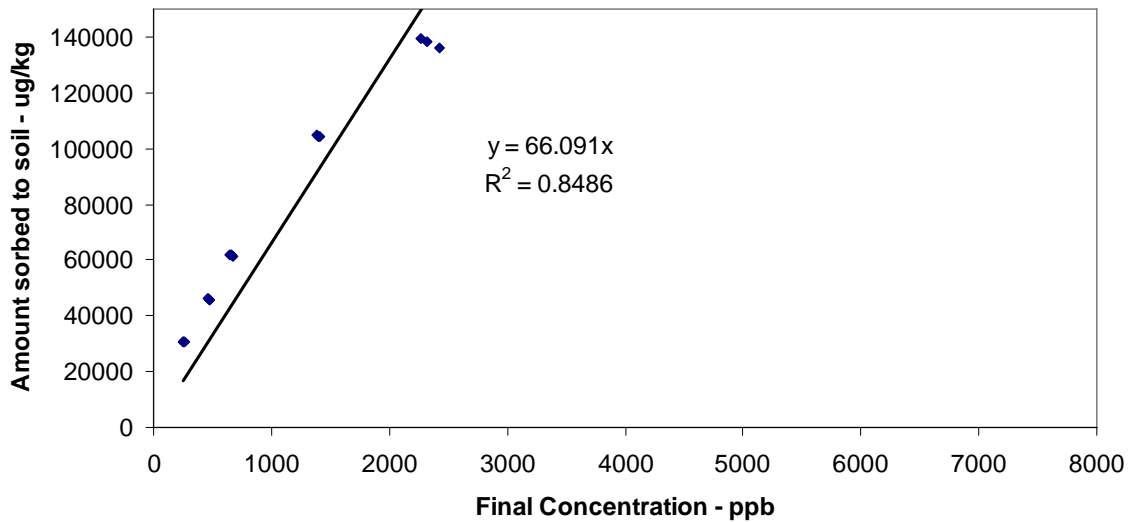
Uranium Linear Isotherm - pH adjusted Perched Aquifer Water



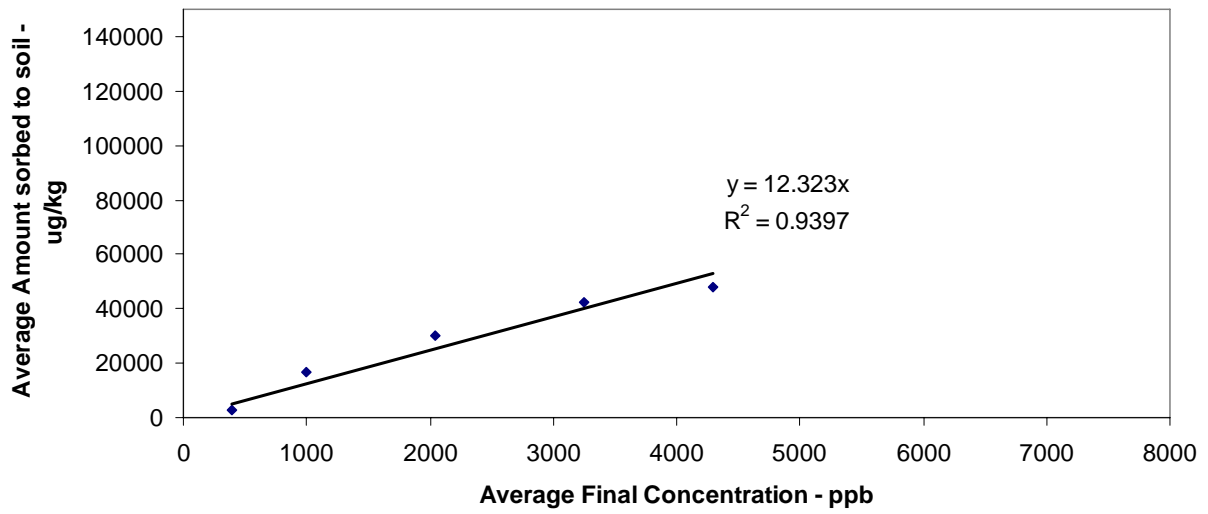
Uranium Linear Isotherm - DDI Water



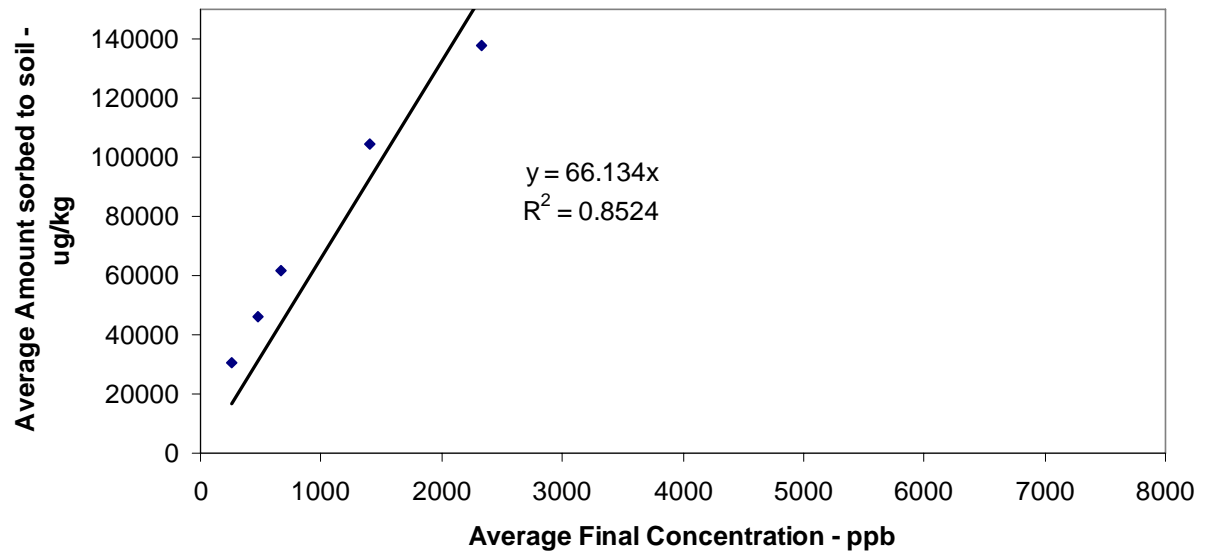
Uranium Linear Isotherm - pH adjusted DDI Water



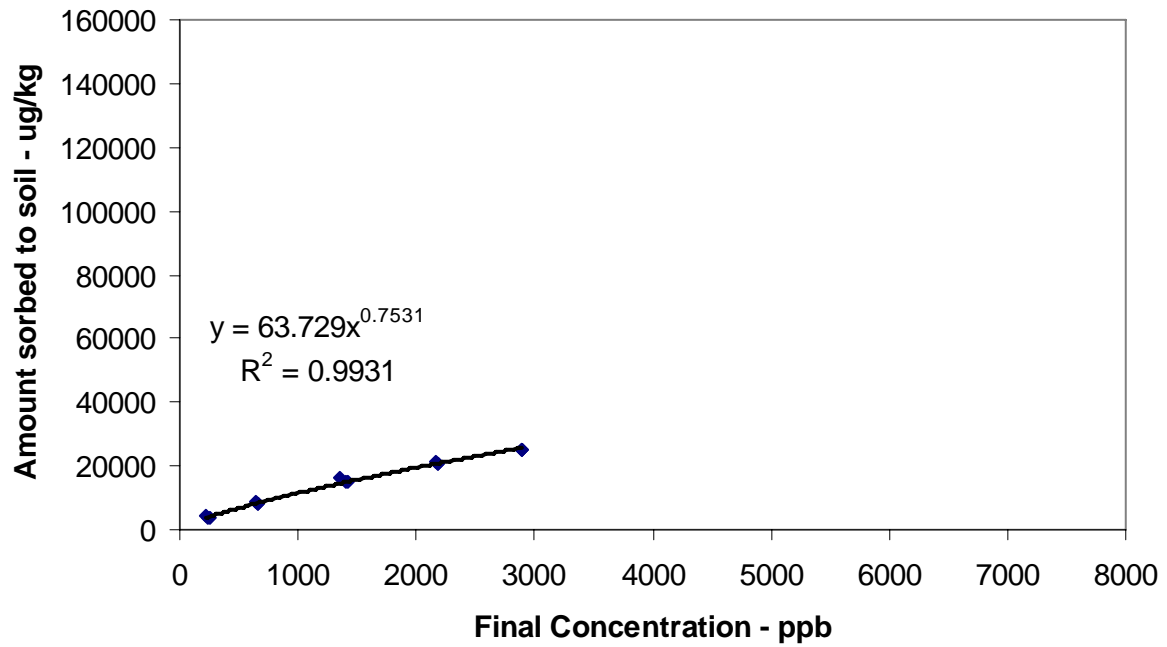
Uranium Linear Isotherm - DDI Water



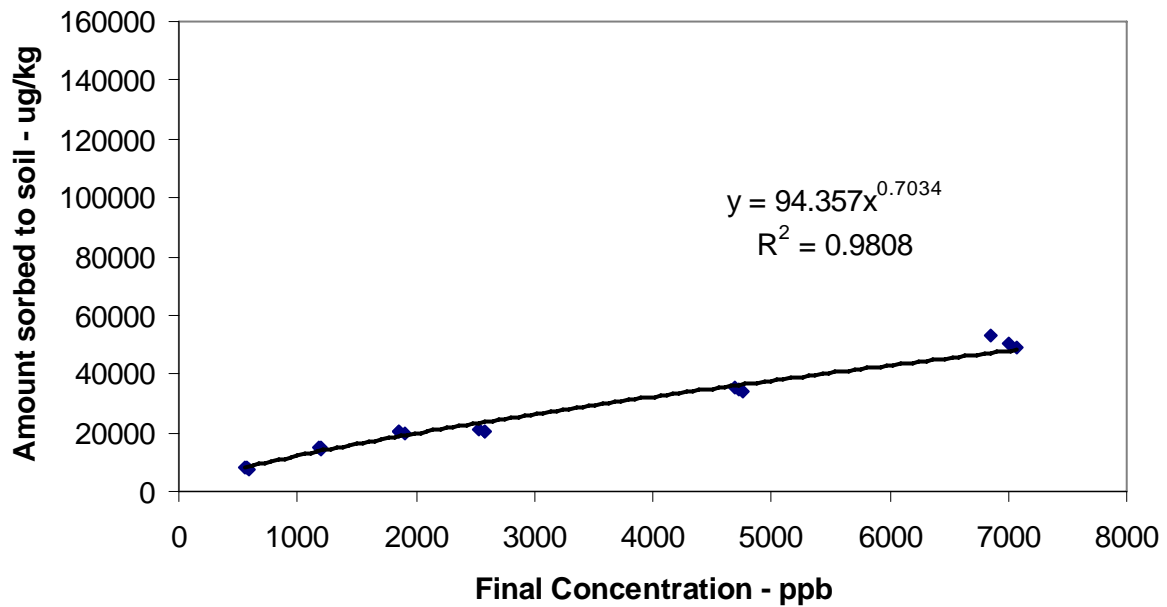
Uranium Linear Isotherm - pH adjusted DDI Water



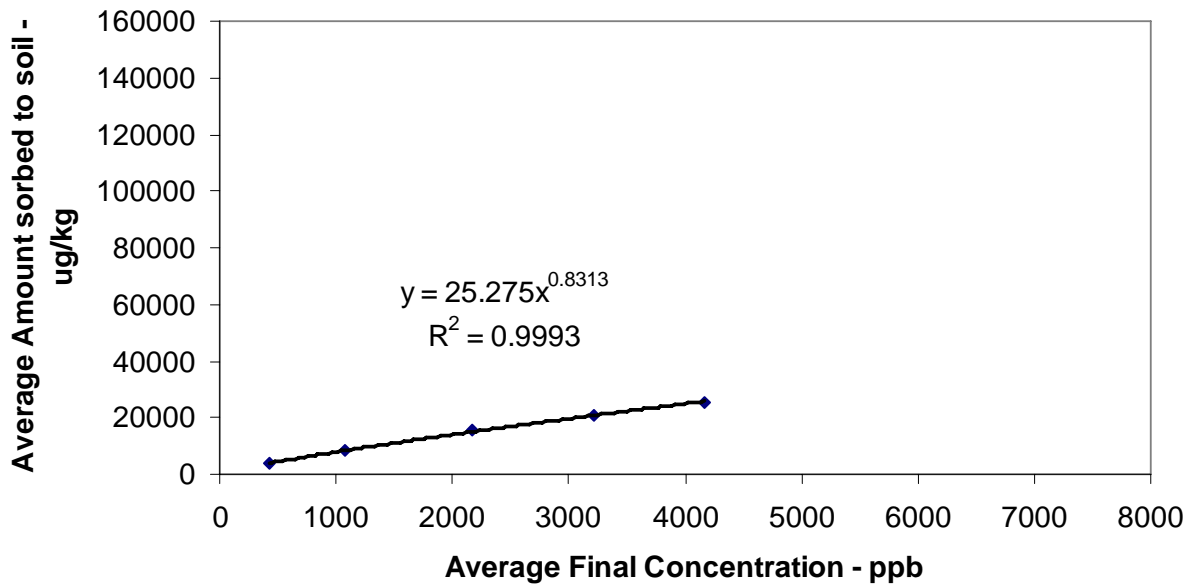
Uranium Freundlich Isotherm - Perched Aquifer Water



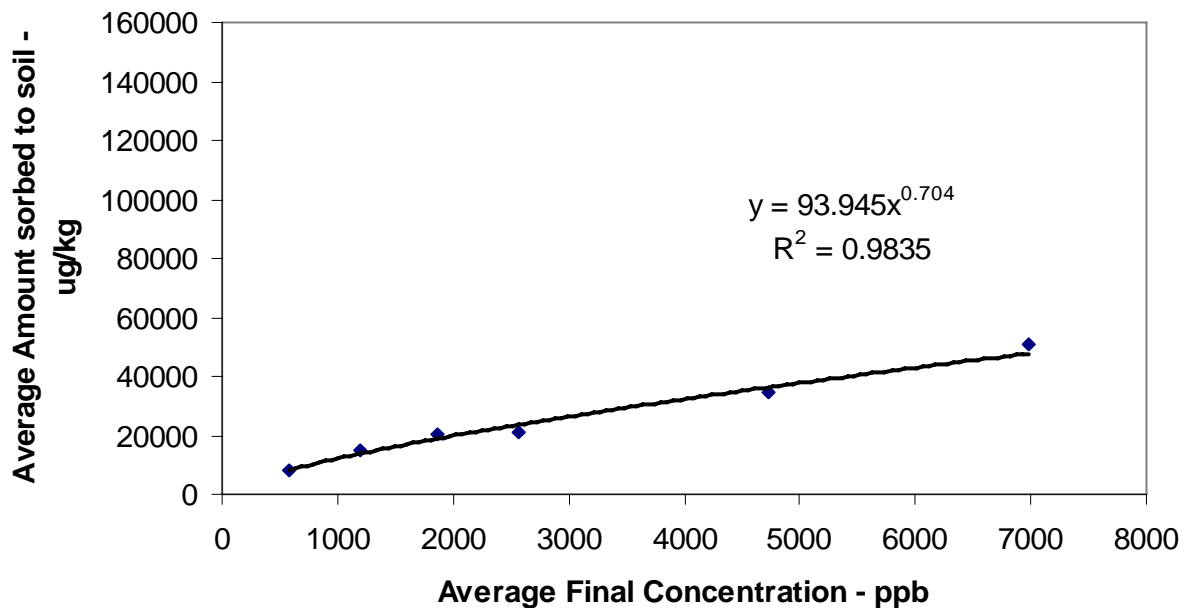
Uranium Freundlich Isotherm - pH adjusted Perched Aquifer Water



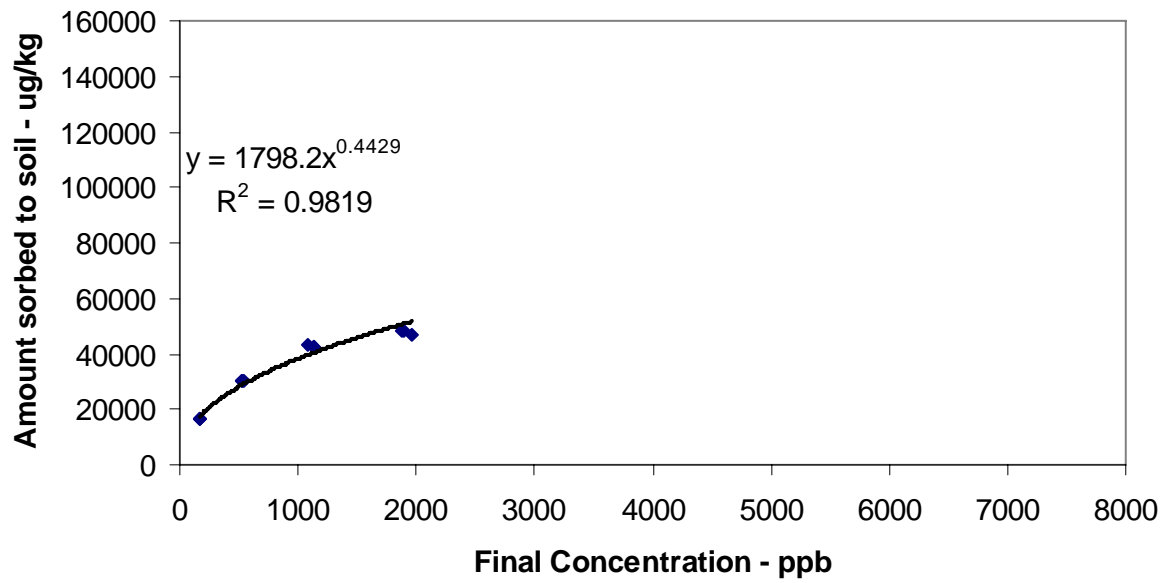
Uranium Freundlich Isotherm - Perched Aquifer Water



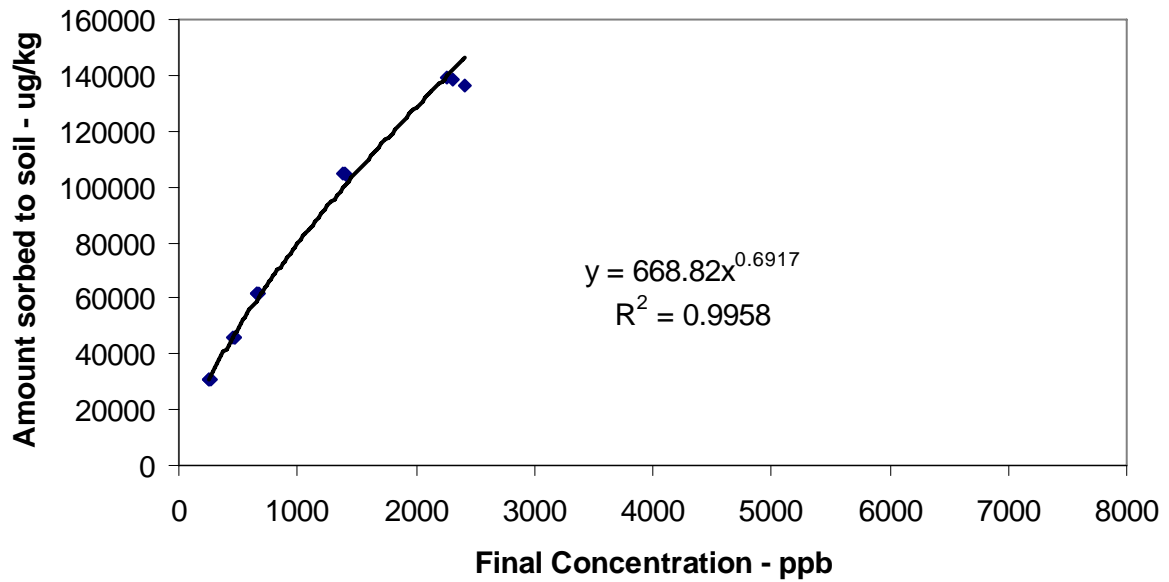
Uranium Freundlich Isotherm - pH adjusted Perched Aquifer Water

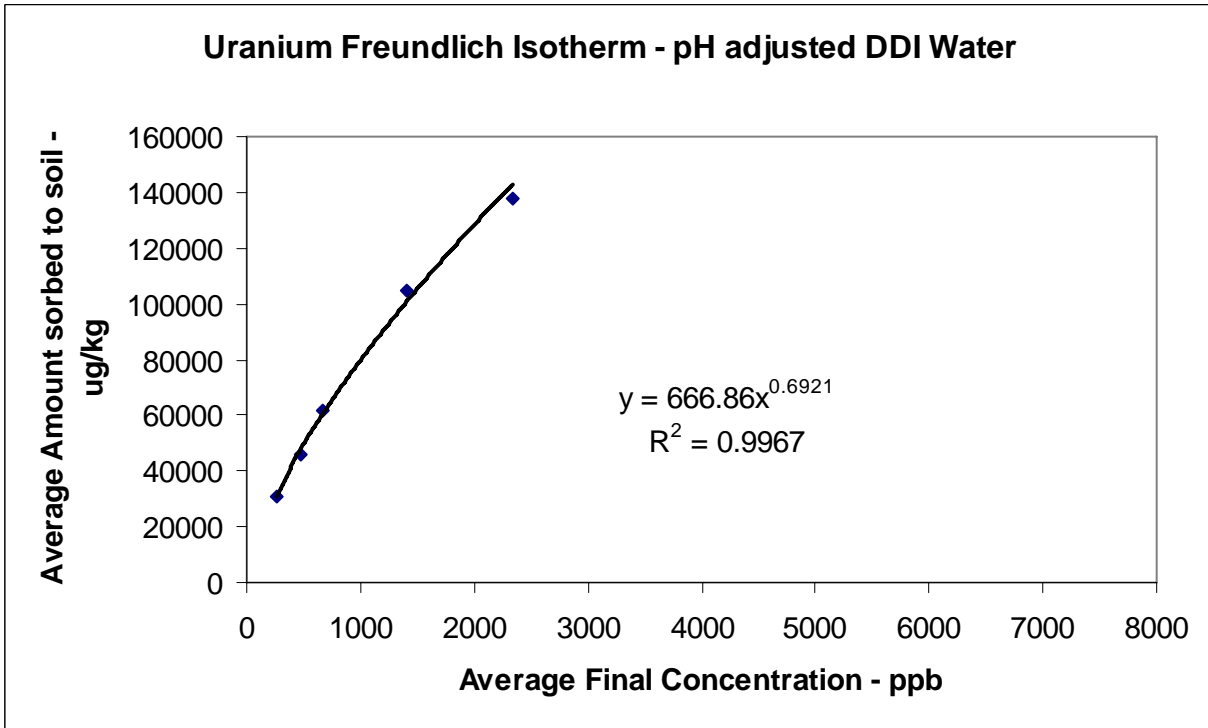
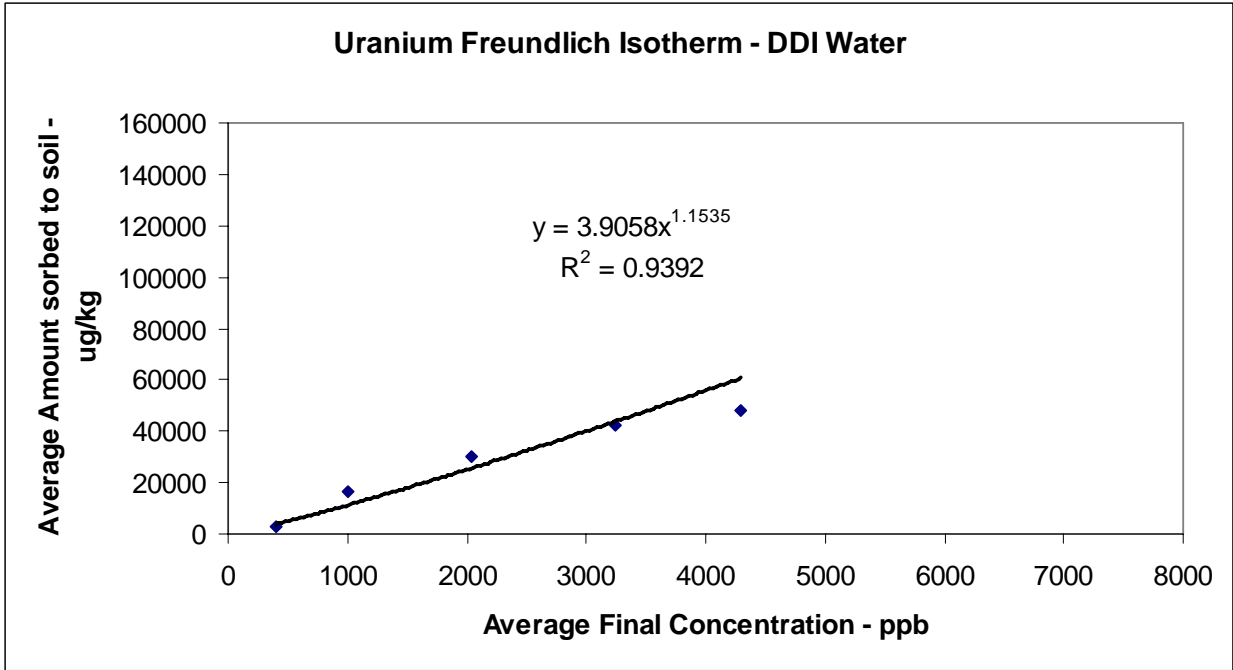


Uranium Freundlich Isotherm - DDI Water

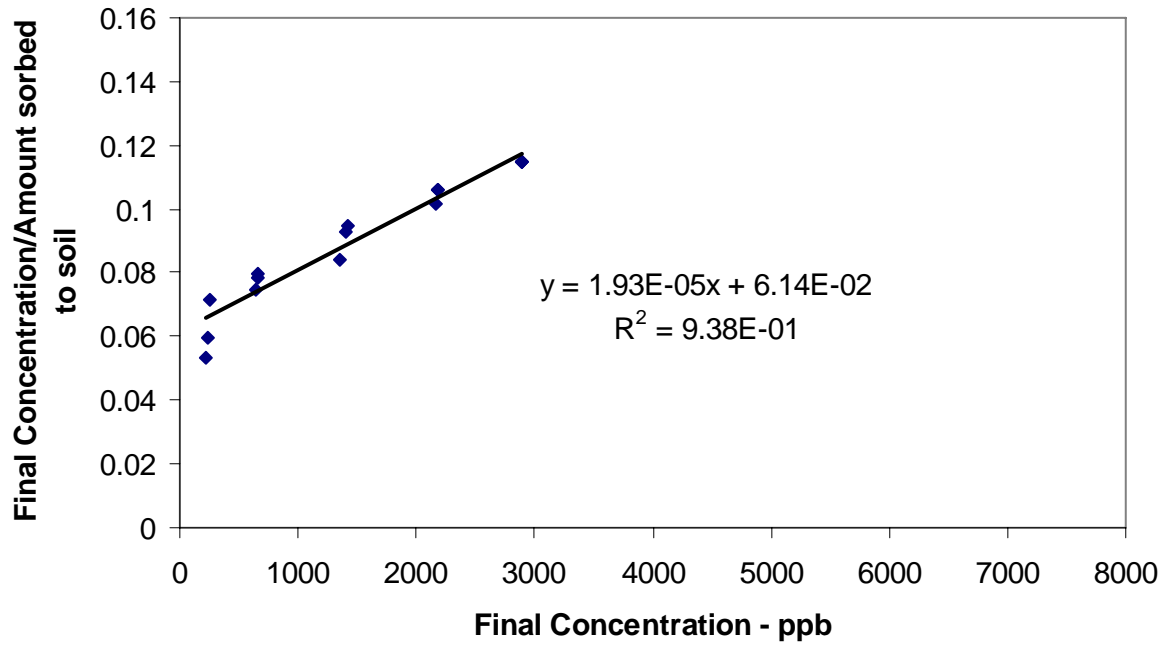


Uranium Freundlich Isotherm - pH adjusted DDI Water

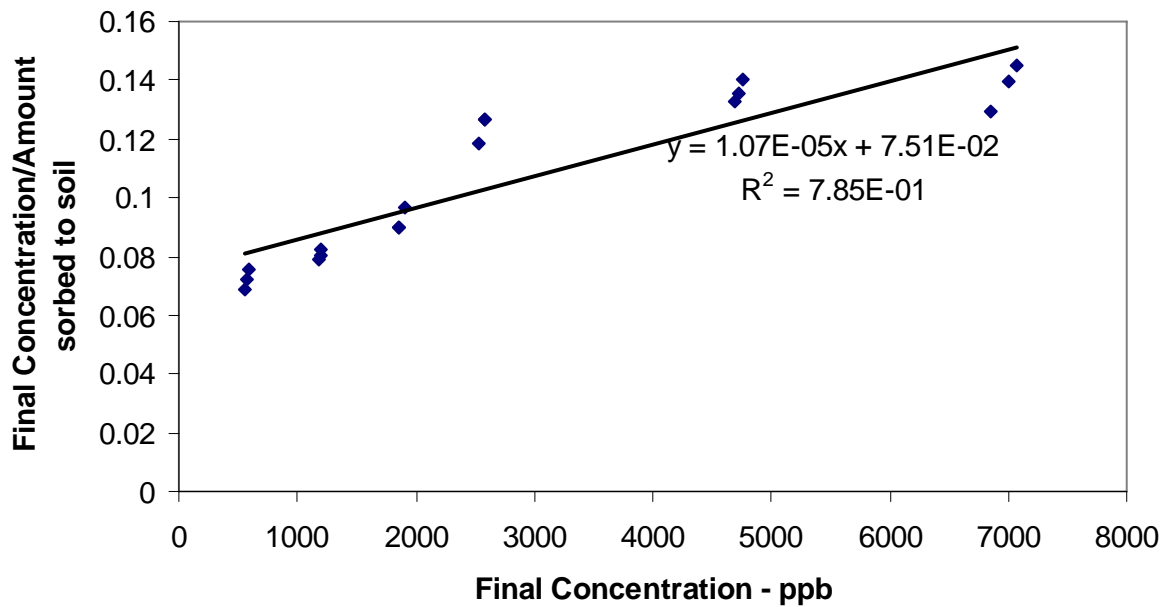




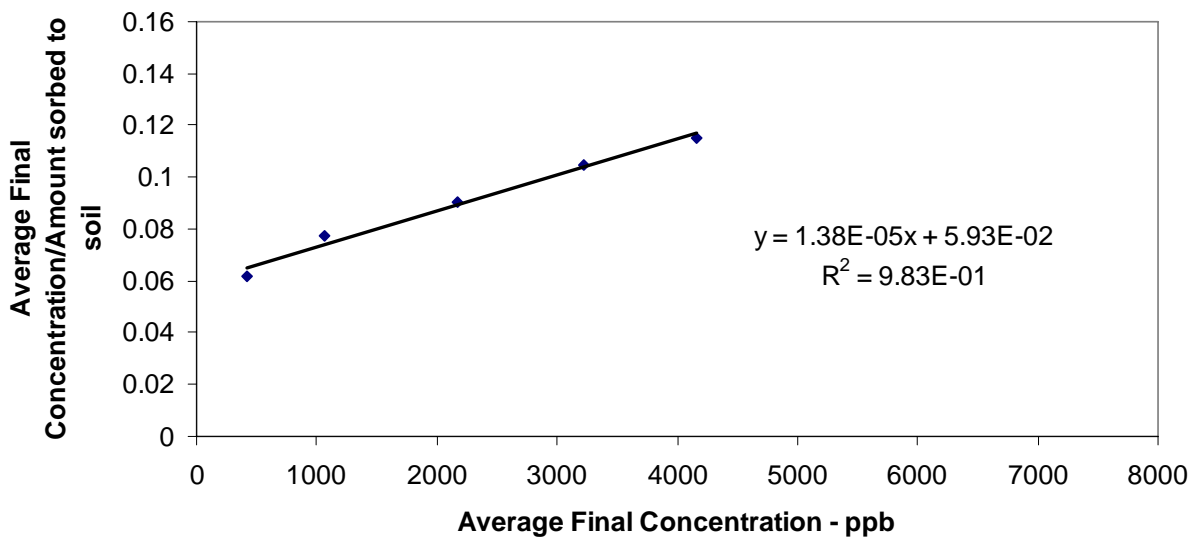
Uranium Langmuir Isotherm - Perched Aquifer Water



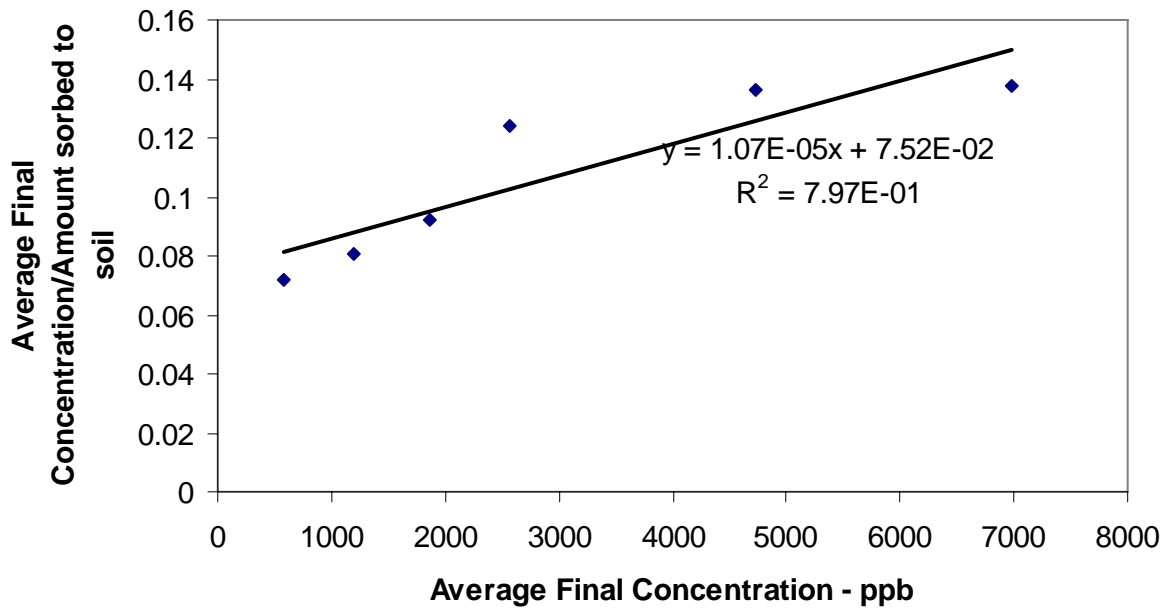
Uranium Langmuir Isotherm - pH adjusted Perched Aquifer Water

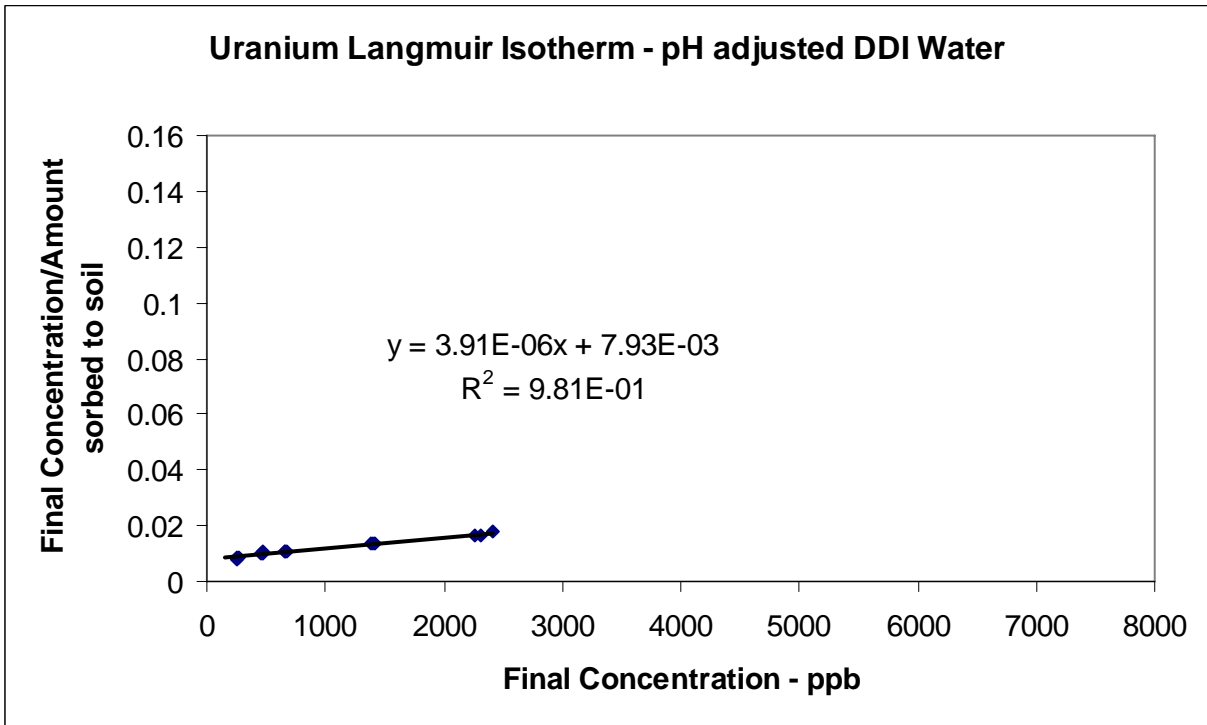
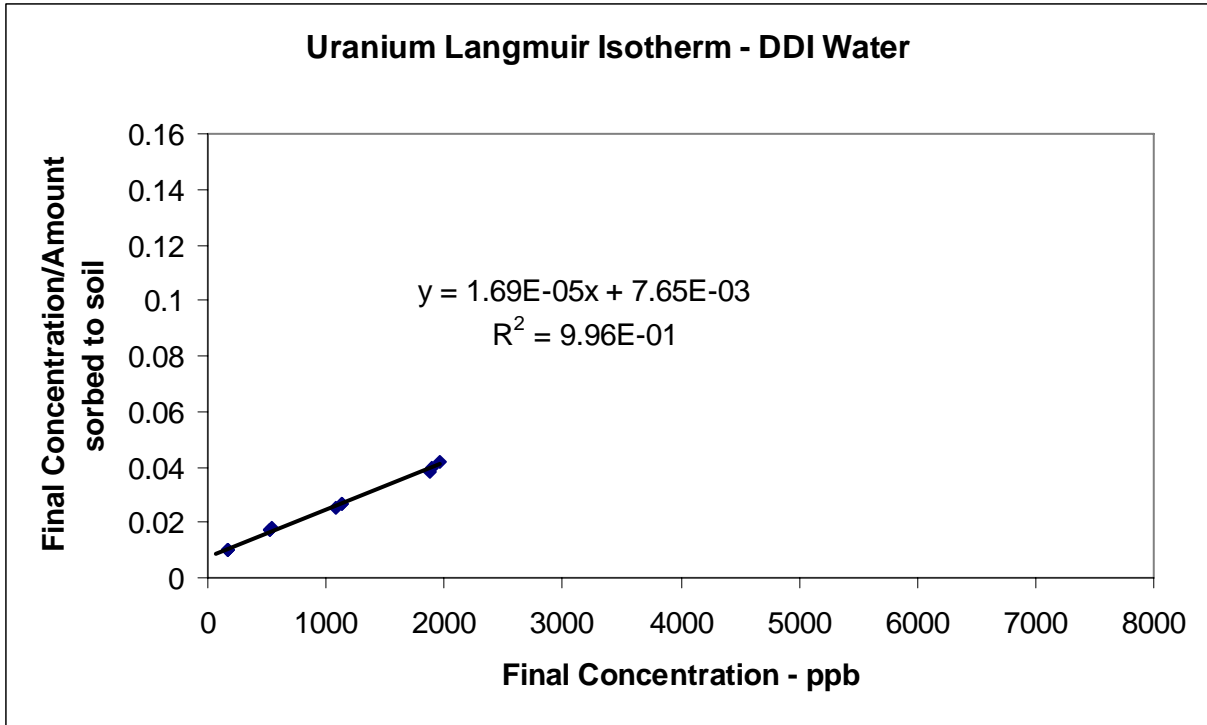


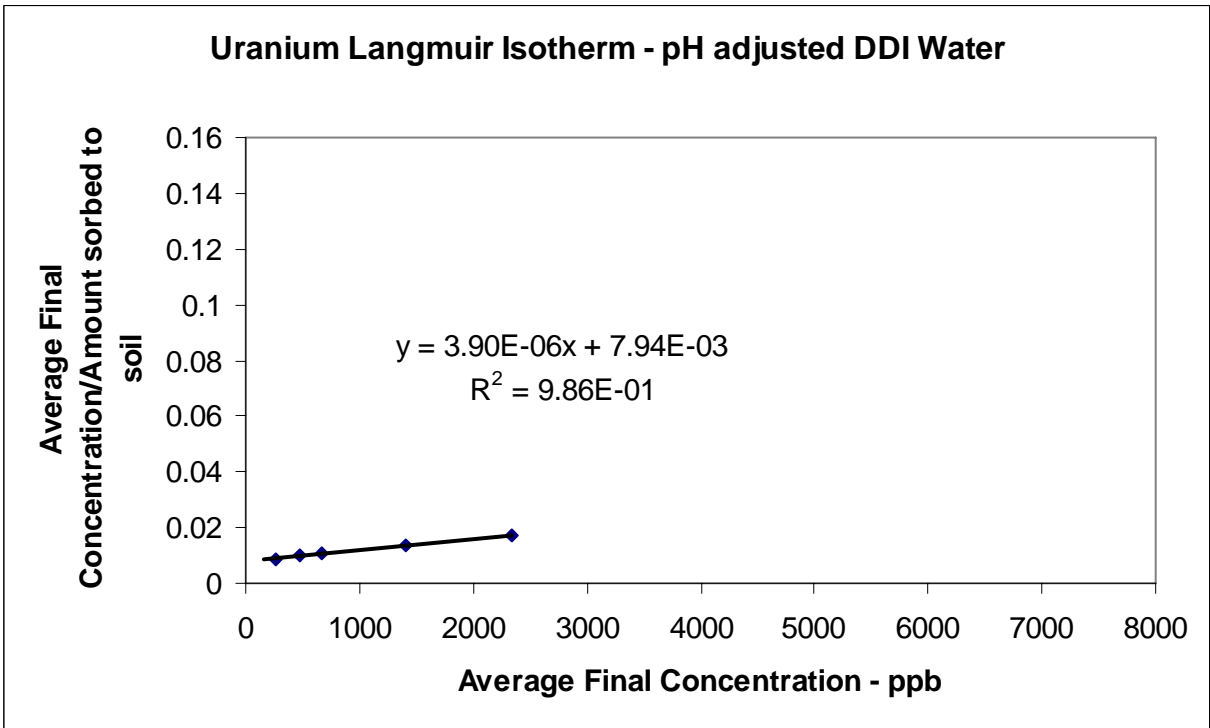
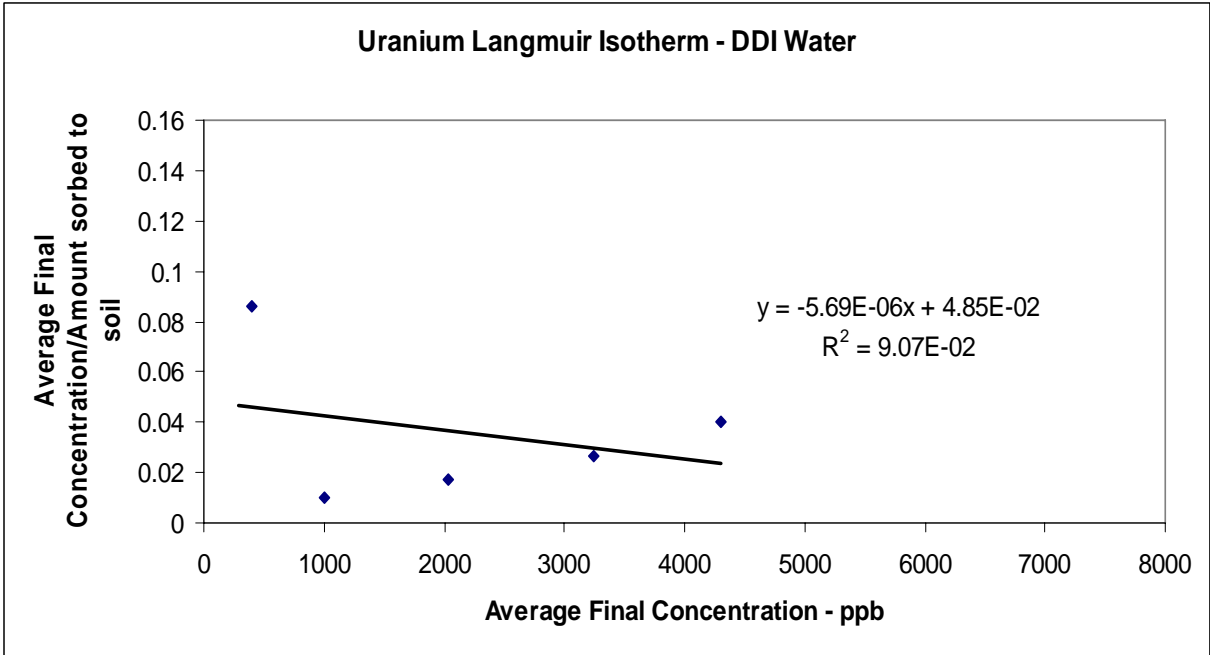
Uranium Langmuir Isotherm - Perched Aquifer Water



Uranium Langmuir Isotherm - pH adjusted Perched Aquifer Water



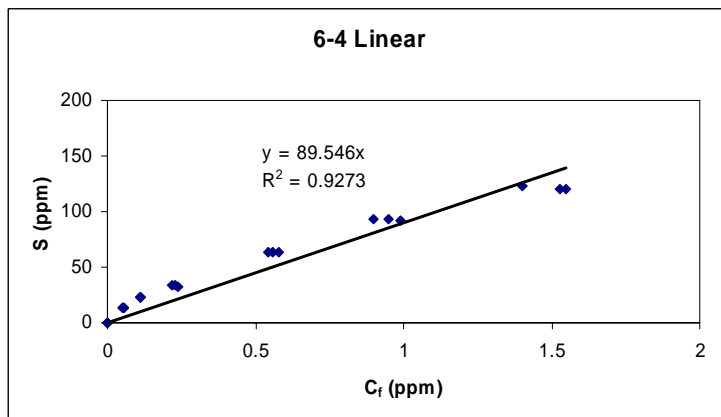
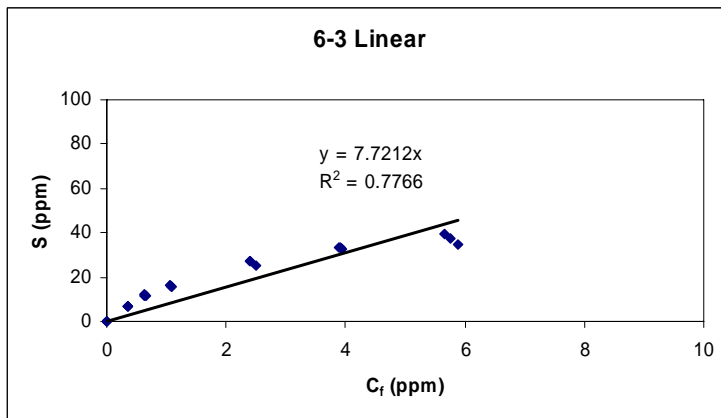
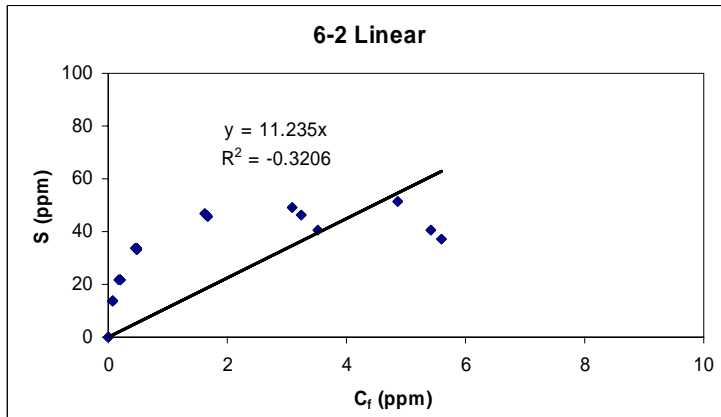
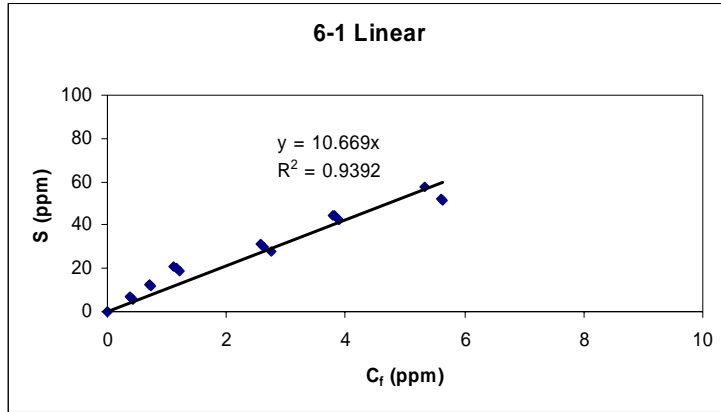


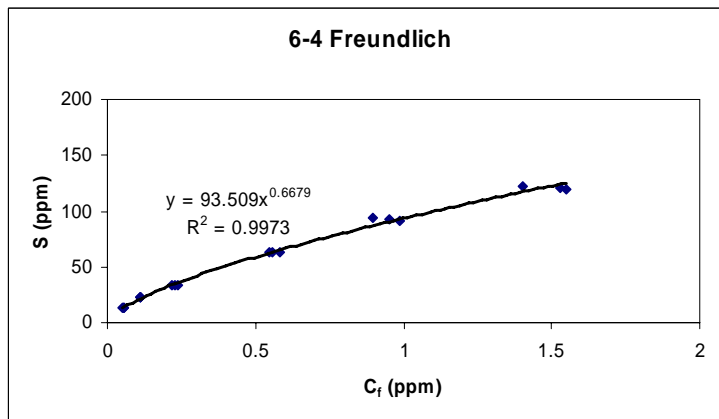
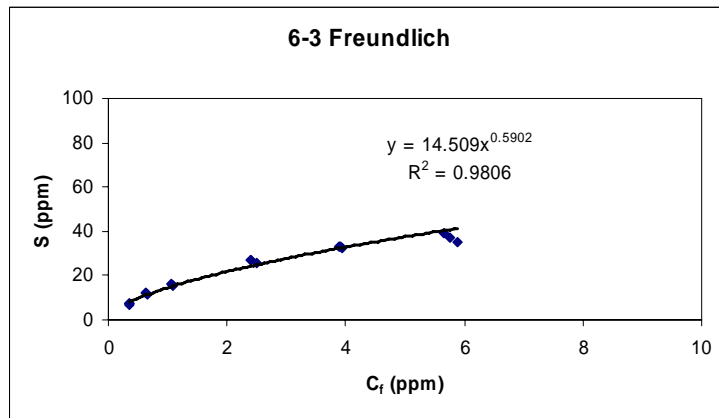
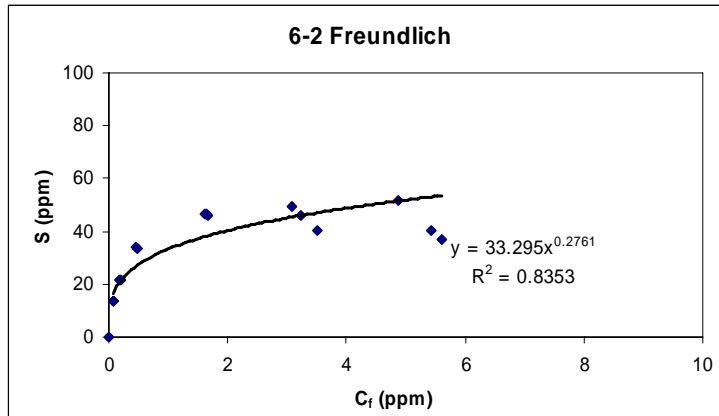
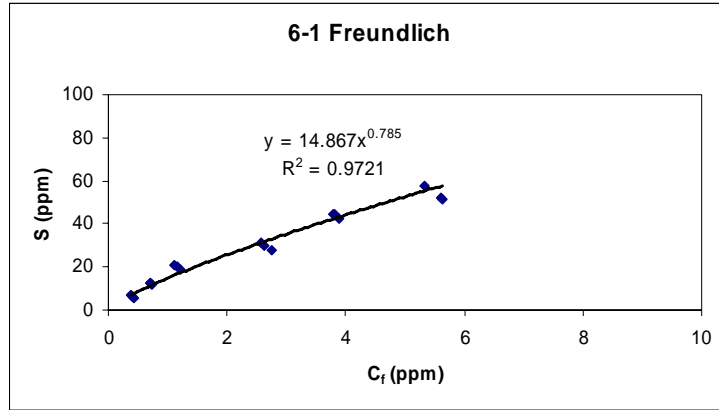


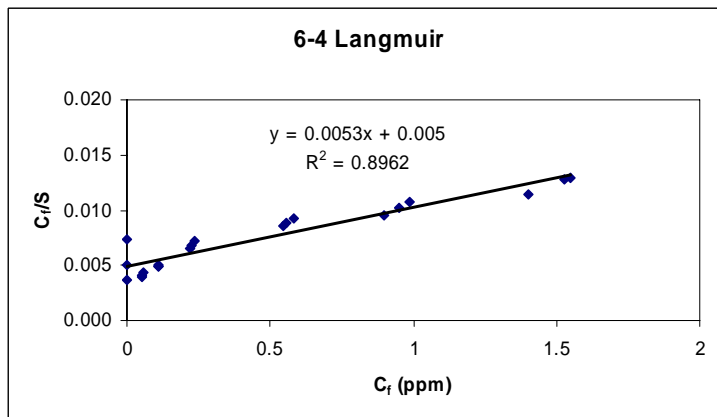
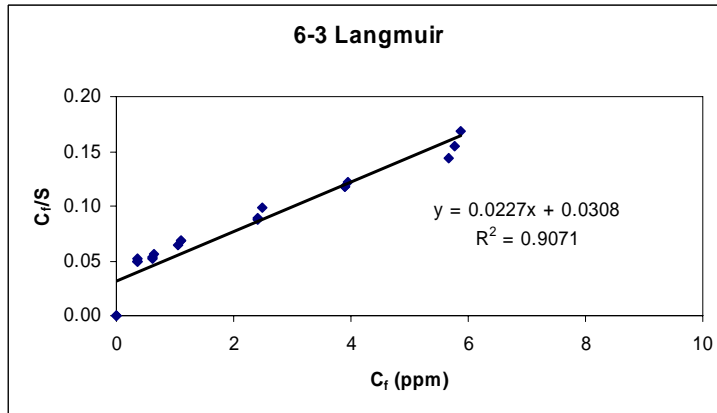
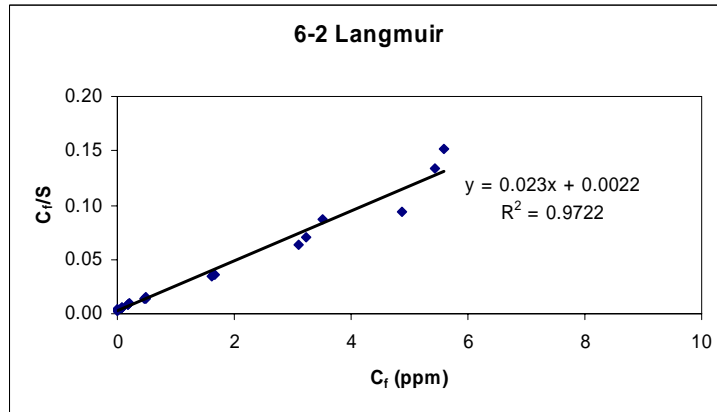
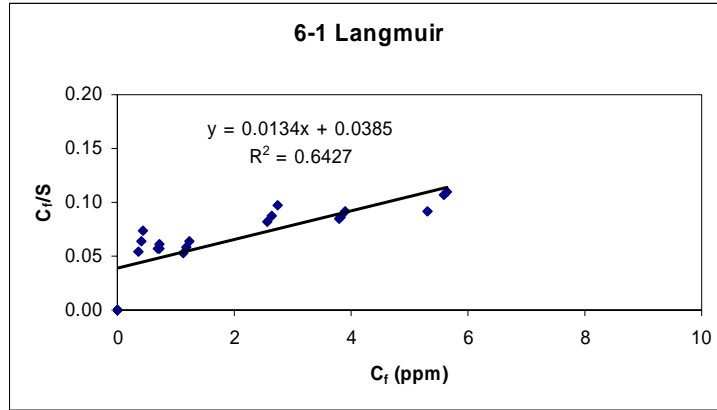
A-2. Isotherm Results for Uranium on Site 6 and 7 Soils

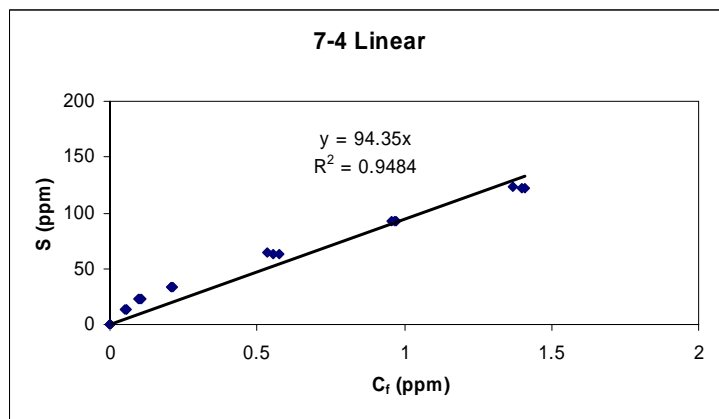
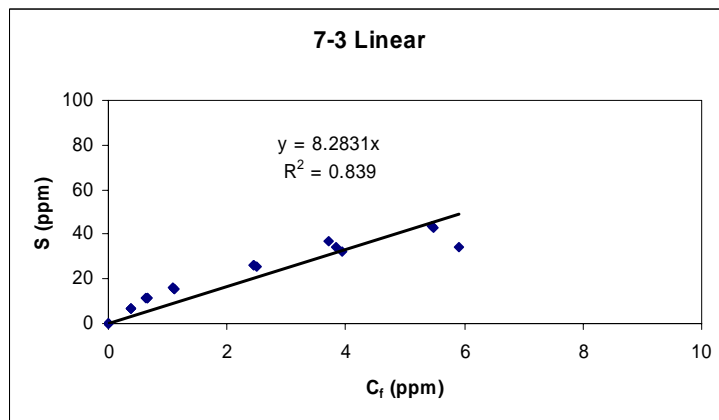
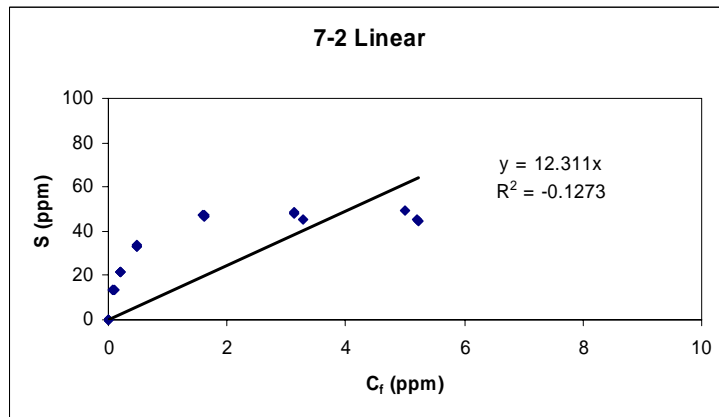
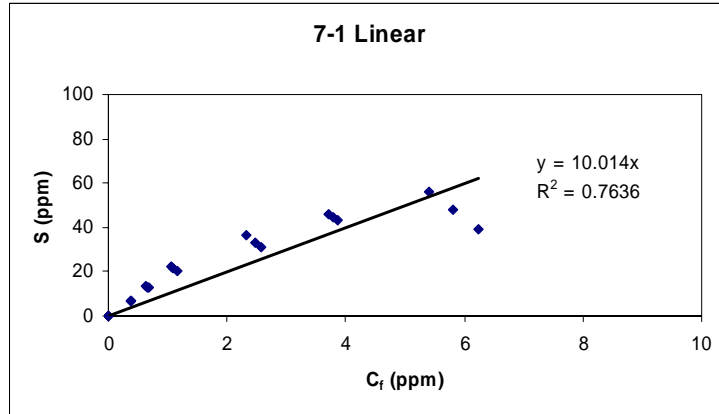
Pantex Uranium Isotherm Data

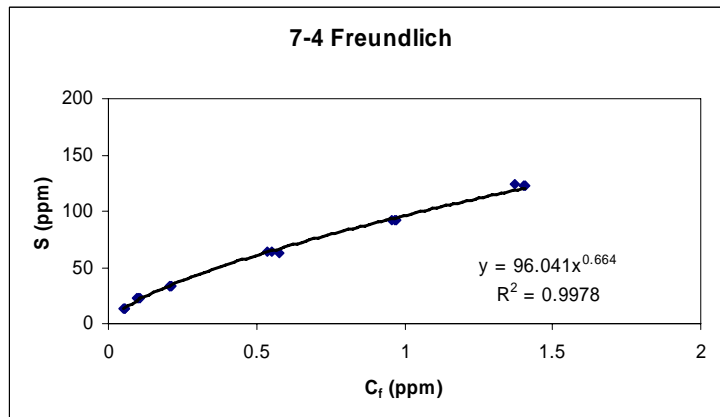
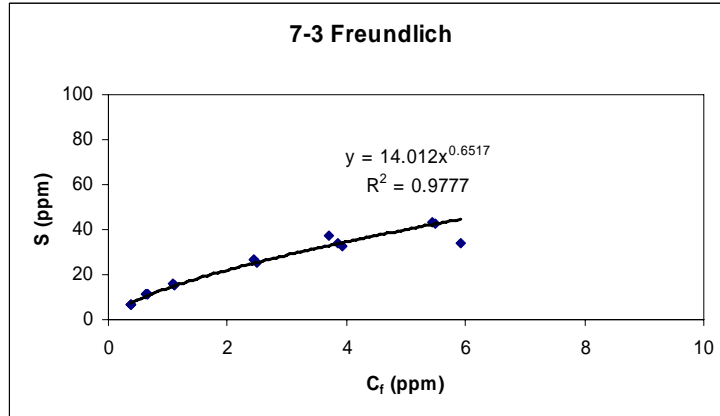
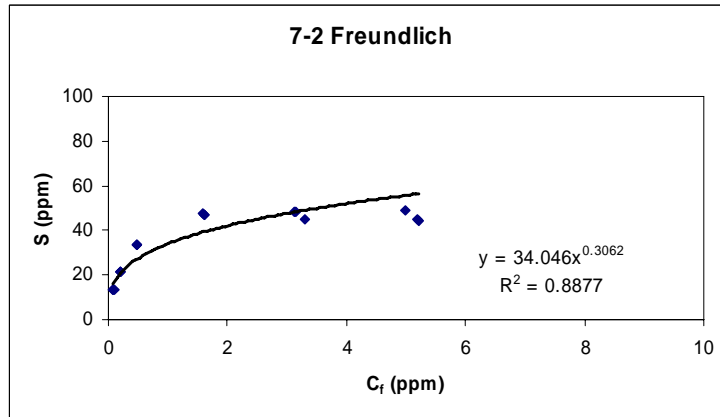
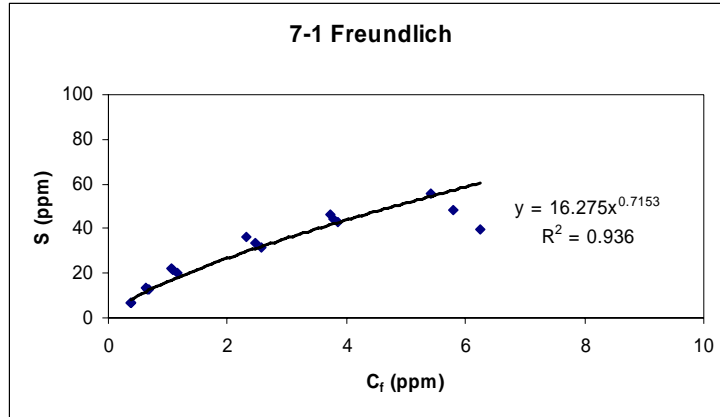
Source Water	K_d (L/kg)	K (($\mu\text{g}/\text{kg}$)[$\mu\text{g}/\text{L}$] ^{-N})	N	β (kg/ μg)	α (L/ μg)
6-1 (PW)	10.7	14.9	0.79	74.6	0.35
6-2 (DW)	11.2	33.3	0.28	43.5	10.5
6-3 (PW/adj)	7.7	14.5	0.59	44.1	0.70
6-4 (DW/adj)	89.5	93.5	0.67	189	1.10
7-1 (PW)	10.0	16.3	0.72	75.2	0.30
7-2 (DW)	12.3	34.0	0.31	48.3	5.90
7-3 (PW/adj)	8.3	14.0	0.65	59.9	0.30
7-4 (DW/adj)	94.3	96.0	0.66	161	1.60

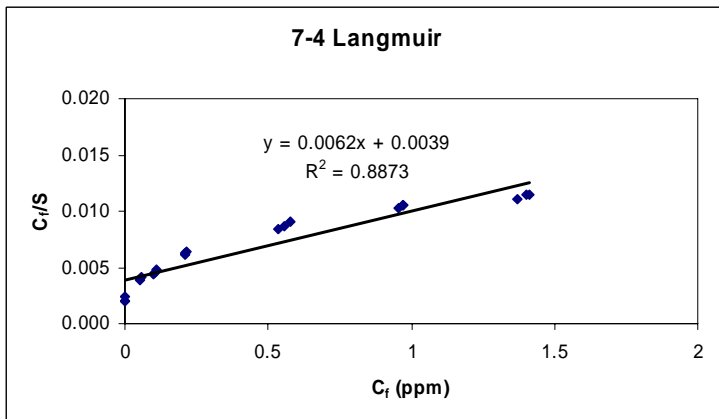
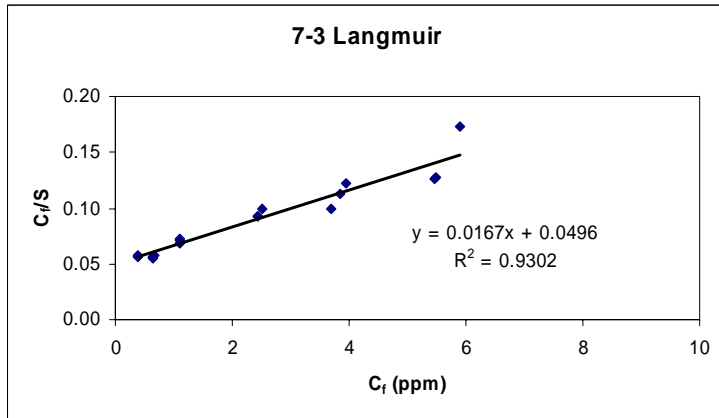
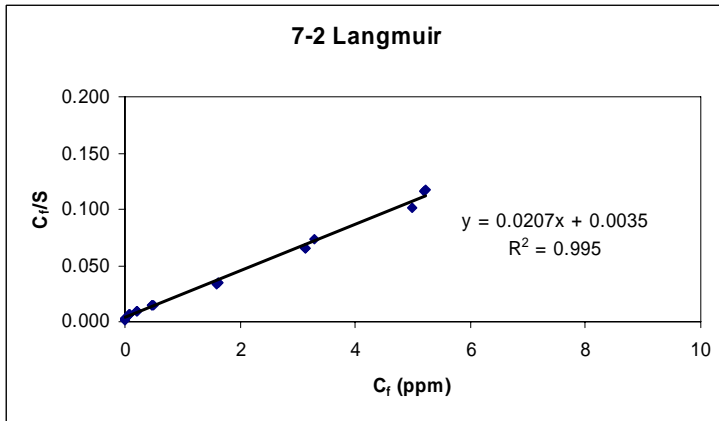
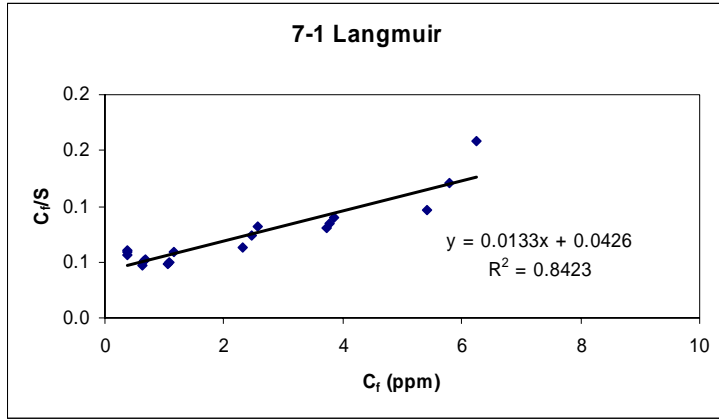












Appendix B

Clay Mineralogical Analyses

B-1. Site 1 Soil

B-2. Combination of Site 6 and 7 Soils

**X-RAY DIFFRACTION AND ELECTRON MICROSCOPIC ANALYSES
OF
PANTEX SHALLOW WATER SOIL**

X-ray diffraction analysis shows that the soil is composed of the minerals listed below:

Quartz	40%
Calcite	15
Plagioclase	3
K-feldspar	2
Illite	10
Smectite	25
Kaolinite	5

Smectite is a swelling clay and electron images suggest a genetic relationship between illite and smectite. Typical illite flakes are shown in Figures 1a and 2a. Illite flakes range in size from 0.2 to 4.0 microns. Typical X-ray spectra obtained from illite flakes is displayed in Figure 2b. The latter shows K, Si, Al, Na, and O as the main spectral lines with a rather weak Fe-line. Smectite flakes seem to be weathering product of illites and other micas (Figure 3a). Its X-ray spectra in Figure 3b clearly show the loss of Na and K from the illite structure. Calcites appear as precipitates of calcium carbonate in the lake. Calcite grains display well-developed crystal forms (Figure 3a).

Some of the fine calcite rhombs (about 0.4 microns in size) in Figure 1a (very top) contain significant amounts of iron in their structures.

In summary, smectite and illite are the main clay minerals. These minerals are surface active and have high ion exchange, adsorption and swelling capacities.

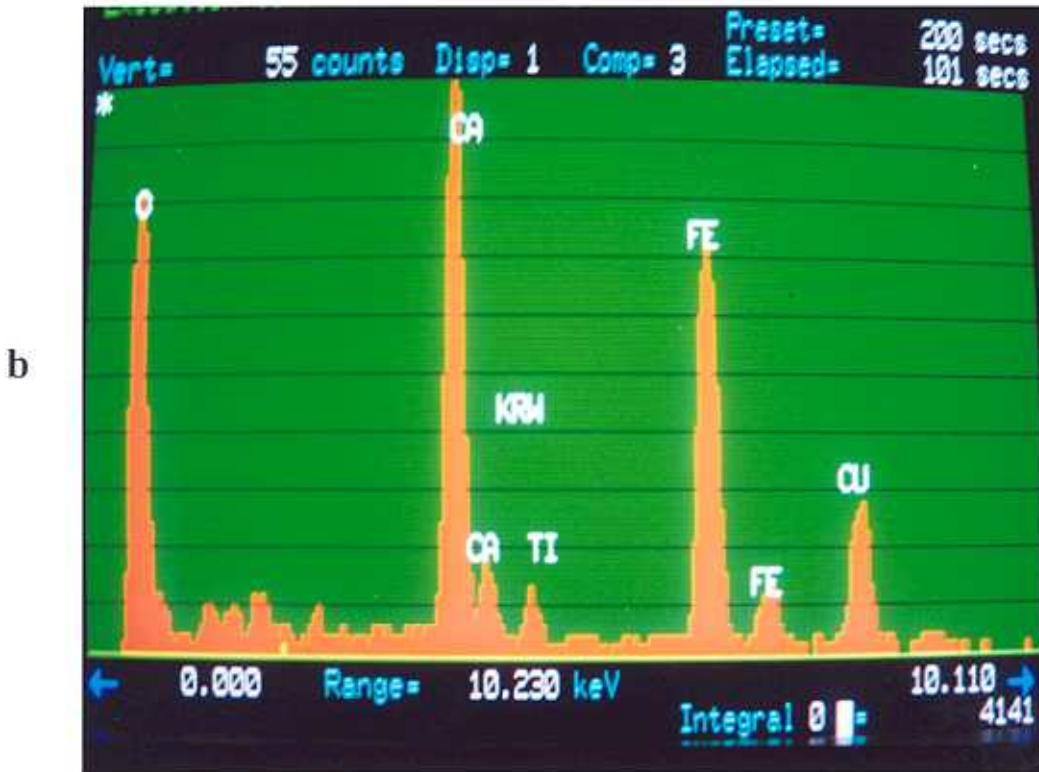
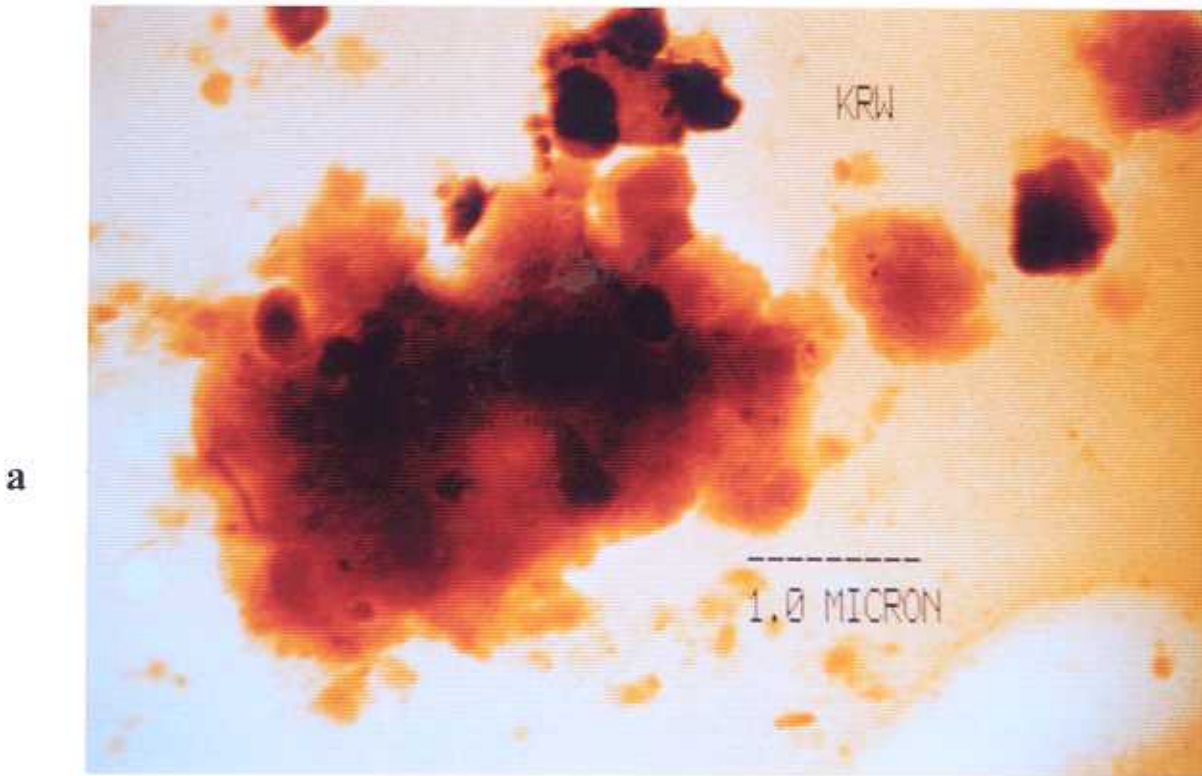
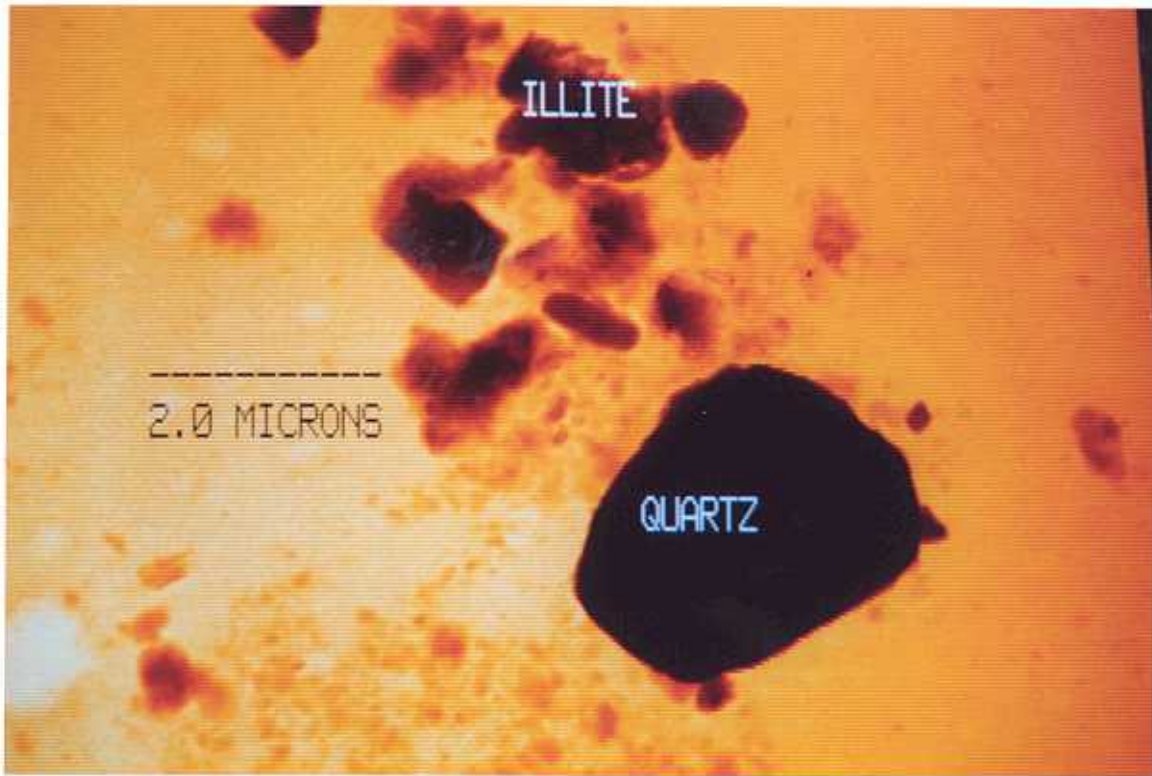


Figure 1a) Clay flakes (illite) ranging in size from 0.2 to 4.0 microns and dense precipitates of a ferrous carbonate (at the top); and b) X-ray spectrum obtained from the rhomb-shaped, dense carbonate crystal.

a



b

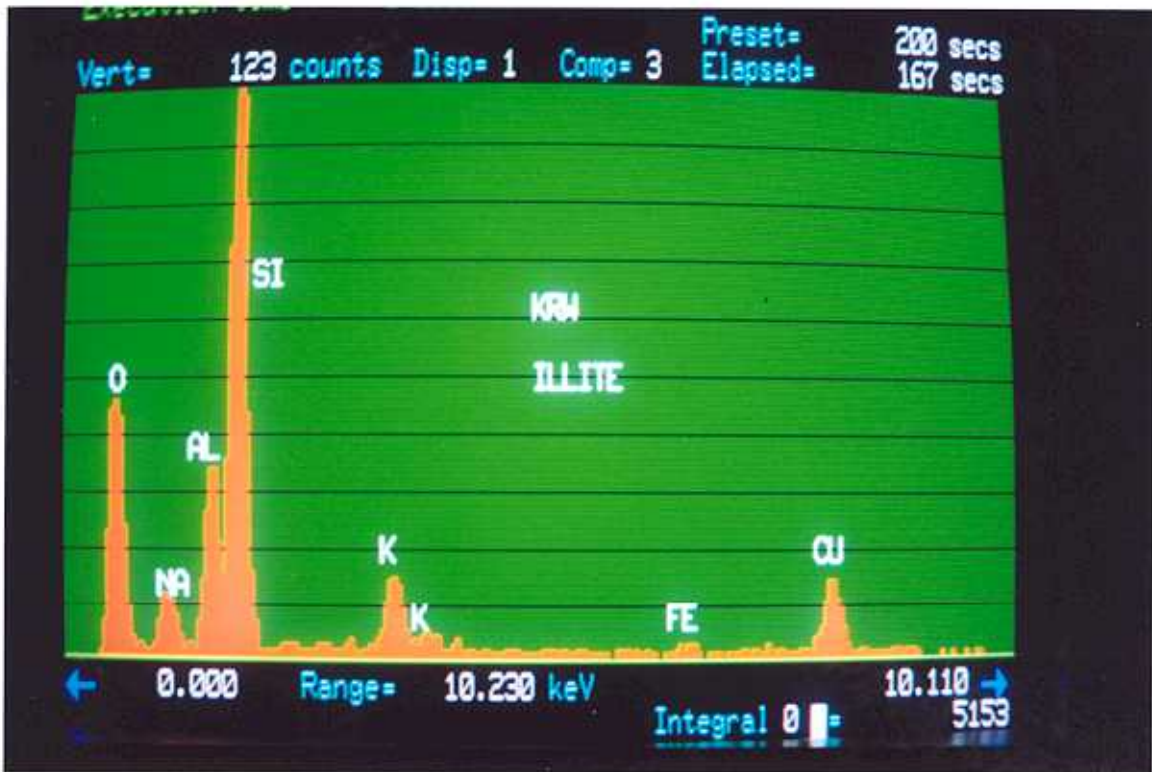


Figure 2a) A typical quartz grain and various flakes of clay (illite);
b) X-ray spectrum obtained from illite.

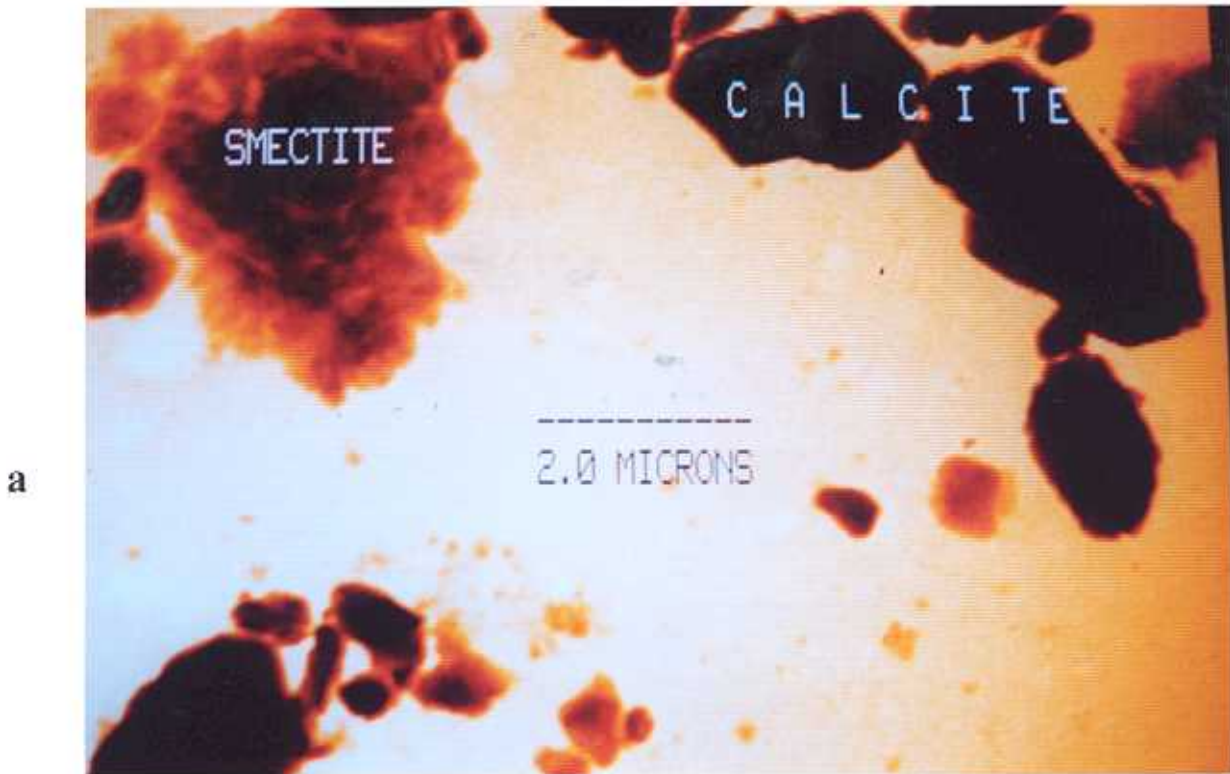


Figure 3a) Common authigenic calcite crystallites up to 5.0 microns in size; and a large smectite flake; and
b) X-ray spectrum obtained from the smectite.

**X-RAY DIFFRACTION AND ELECTRON MICROSCOPIC ANALYSES
OF
A SOIL SAMPLE FROM SITE 7, ESL 13961**

X-ray diffraction analysis shows the presence of the following minerals as the crystalline components of the soil excluding the organic matter:

Quartz	45%
Plagioclase	7
K-feldspar	3
Calcite	15
Illite	15
Smectite	10
Kaolinite	5

Electron microscopic images of the clay particles in Figure 1a indicate that the smectites and illites are probably the weathering products of micas. Their X-ray spectra of the partially altered flakes (Figure 1b) show high concentrations of Fe and Mg which suggest a biotite-type mica precursor. Smectites appear as aggregates of curled thin foils and flakes (Figure 2a). Their typical X-ray spectra in Figure 2b show significant amounts of iron coating on them.

Calcite occurs at about 15% in the soil in the form of well-developed rhombohedral crystallites as shown in Figure 3a with its X-ray spectrum in Figure 3b. The latter illustrates strong Ca- and O-lines as expected from a calcite.

LEGENDS – Descriptions of the images

STEM Images **Site #7/ESL 13961**

Figure 1a) Common clay particles and weathered mica flakes in the soil; and
b) X-ray spectrum obtained from an altered biotite flakes above. (Note that 'Mg'-line next to 'Al' was mislabeled as 'Fe' in the image)

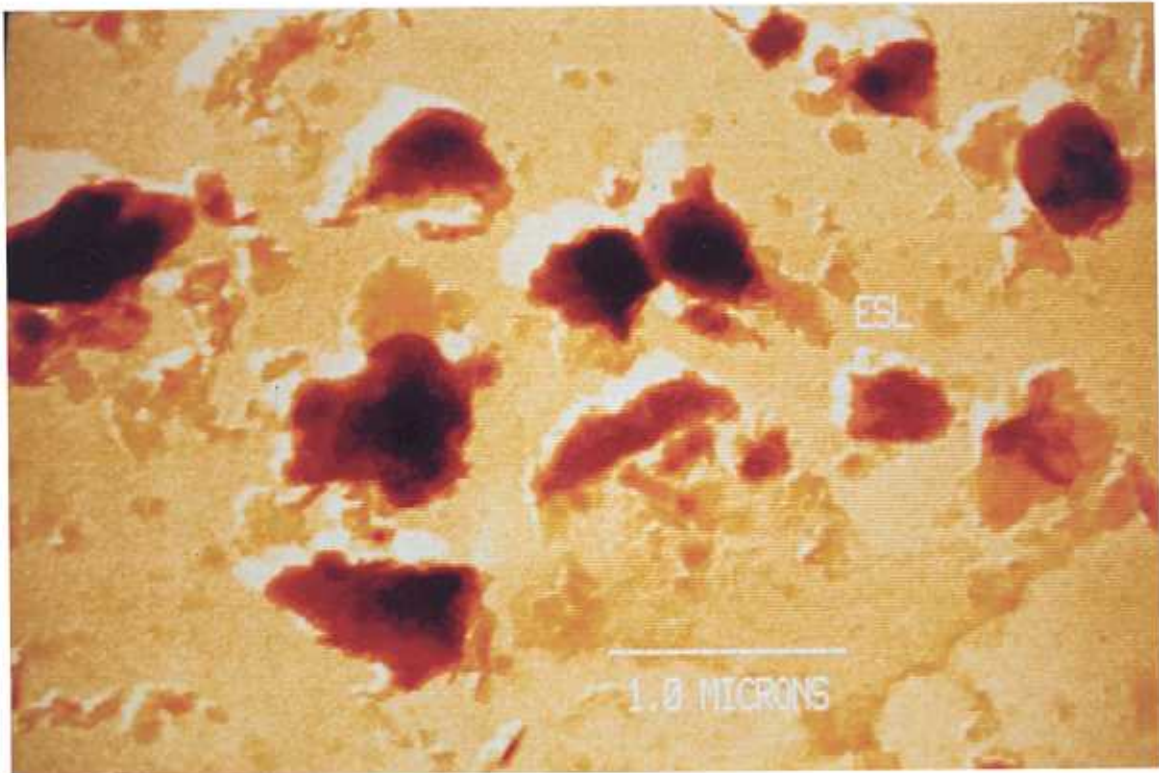
STEM Images **Site #7/ESL 13961**

Figure 2a) A typical aggregate of smectite flakes in the sample; and
b) its X-ray spectrum.

STEM Images **Site #7/ESL 13961**

Figure 3a) Denser crystals of calcite and feldspar; and
b) X-ray spectrum of calcite.

a



b

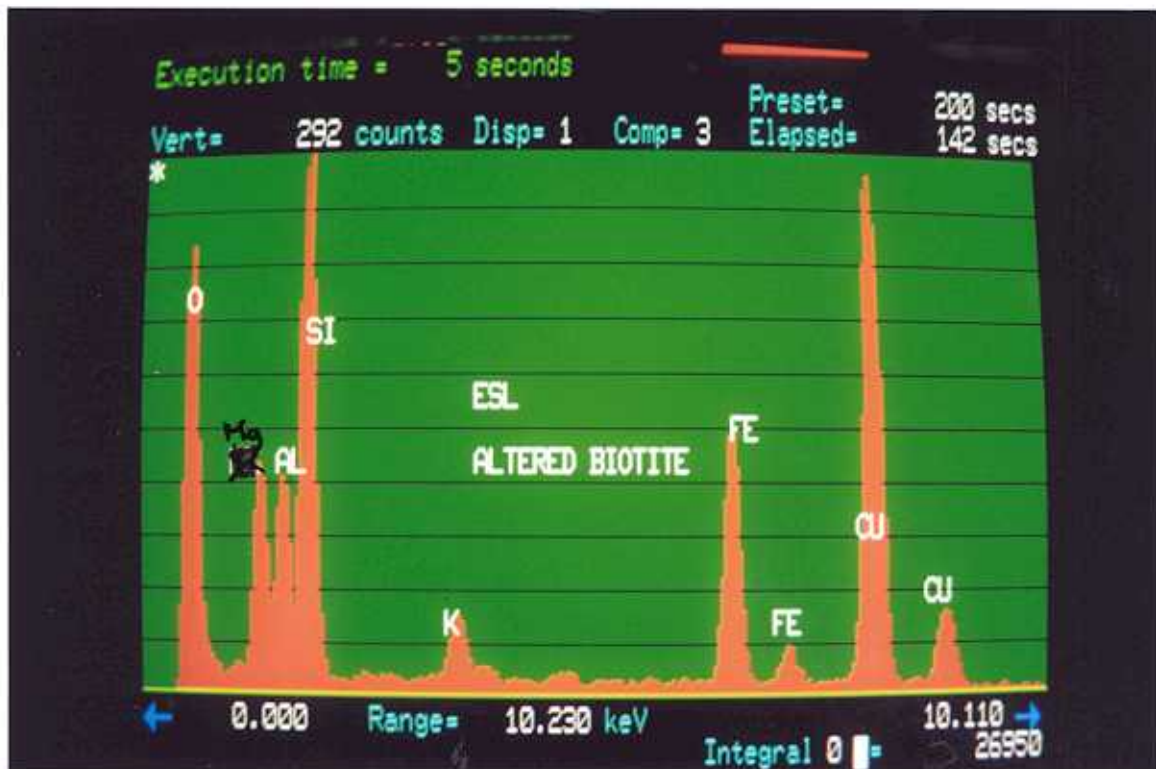


Figure 1a) Common clay particles and weathered mica flakes in the soil; and
 b) X-ray spectrum obtained from an altered biotite flake above. (Note that 'Mg'-line next to 'Al' was mislabeled as 'Fe' in the image)

a



b



Figure 2a) A typical aggregate of smectite flakes in the sample; and
b) its X-ray spectrum.

a



b

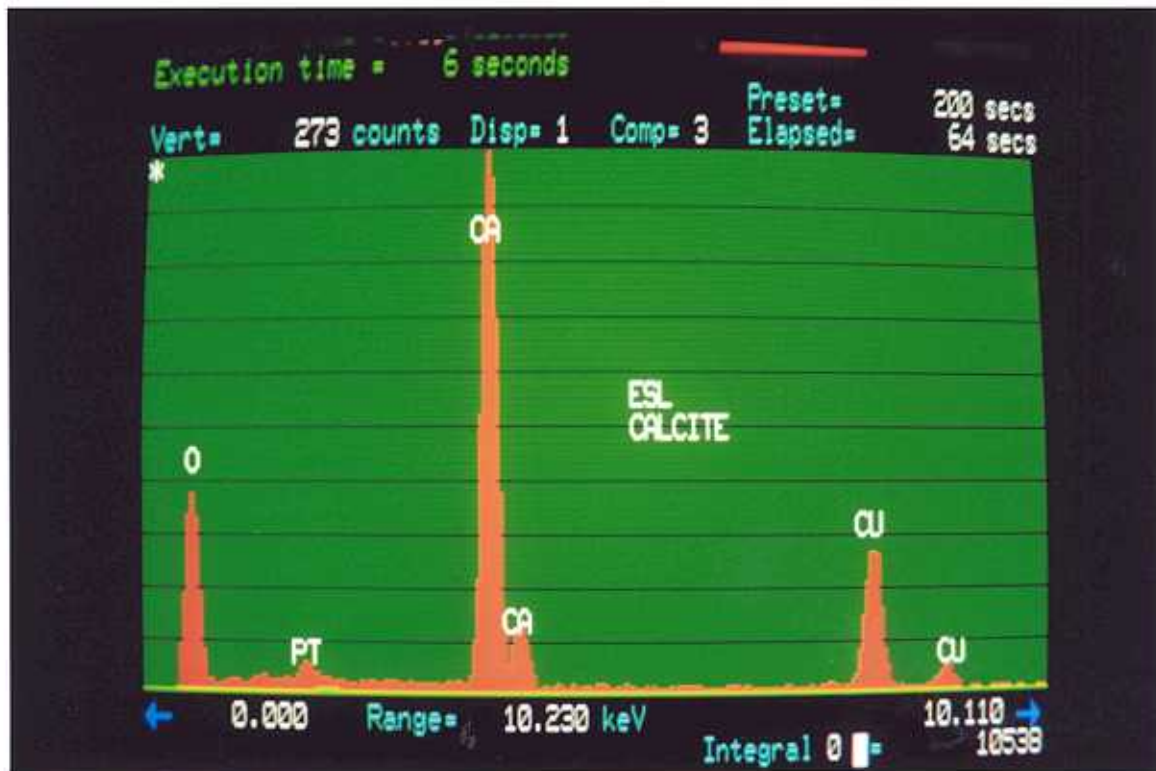


Figure 3a) Denser crystals of calcite and feldspar; and
b) X-ray spectrum of calcite.

Appendix C

Raw Sorption Data Summaries

- C-1. Isotherm Results for Barium, Lead, Silver, Thorium, and Uranium on Site 1 Soils
- C-2. Isotherm Results for Uranium on Site 6 and 7 Soils
- C-3. Soil Column Bromide and Uranium Effluent Concentrations

C-1. Isotherm Results for Barium, Lead, Silver, Thorium, and Uranium on Site 1 Soils

Table C-1.1. Barium Isotherm Data for Site 1 Soil

Set	C _i mg/L	C _f μg/L	S μg/kg	Set	C _i μg/L	C _f μg/L	S μg/kg
PW-1	blank	374	-	PW Adj-1	243	166	4.86E+06
	blank	188	-		243	187	4.86E+06
	blank	205	-		243	176	4.86E+06
PW-2	20	2240	3.55E+05	PW Adj-2	8950	2390	1.79E+08
	20	2210	3.56E+05		8950	2450	1.79E+08
	20	2200	3.56E+05		8950	2360	1.79E+08
PW-3	40	5280	6.94E+05	PW Adj-3	13100	5050	2.62E+08
	40	5130	6.97E+05		13100	5330	2.62E+08
	40	5130	6.97E+05		13100	5180	2.62E+08
PW-4	100	19300	1.61E+06	PW Adj-4	40300	8590	8.06E+08
	100	16700	1.67E+06		40300	8840	8.06E+08
	100	15800	1.68E+06		40300	21300	8.06E+08
PW-5	200	49800	3.00E+06	PW Adj-5	72000	24700	1.44E+09
	200	51500	2.97E+06		72000	24700	1.44E+09
	200	51500	2.97E+06		72000	24800	1.44E+09
PW-6	300	89000	4.22E+06	PW Adj-6	139000	44800	2.78E+09
	300	93700	4.13E+06		139000	48700	2.78E+09
	300	95200	4.10E+06		139000	46500	2.78E+09
PW-7	400	151000	4.98E+06				
	400	151000	4.98E+06				
	400	153000	4.94E+06				
DW-1	blank	123	-	DW Adj-1	0	168	-
	blank	170	-		0	164	-
	blank	123	-		0	191	-
DW-2	20	636	3.87E+05	DW Adj-2	11300	1580	2.26E+08
	20	656	3.87E+05		11300	1560	2.26E+08
	20	611	3.88E+05		11300	1620	2.26E+08
DW-3	40	1930	7.61E+05	DW Adj-3	18300	3720	3.66E+08
	40	1880	7.62E+05		18300	3730	3.66E+08
	40	1860	7.63E+05		18300	3690	3.66E+08
DW-4	100	10800	1.78E+06	DW Adj-4	43500	11100	8.70E+08
	100	11000	1.78E+06		43500	10600	8.70E+08
	100	10600	1.79E+06		43500	10700	8.70E+08
DW-5	200	41000	3.18E+06	DW Adj-5	81400	36400	1.63E+09
	200	42400	3.15E+06		81400	38500	1.63E+09
	200	39500	3.21E+06		81400	35900	1.63E+09
DW-6	300	86700	4.27E+06	DW Adj-6	141000	68300	2.82E+09
	300	82000	4.36E+06		141000	69800	2.82E+09
	300	87500	4.25E+06		141000	68900	2.82E+09
DW-7	400	134000	5.32E+06				
	400	137000	5.26E+06				
	400	145000	5.10E+06				

Table C-1.2 Lead Isotherm Data for Site 1 Soil

Set	C _i μg/L	C _f μg/L	S μg/kg	Set	C _i μg/L	C _f μg/L	S μg/kg
PW-1	1940	7.7	3.86E+04	PW Adj-1	bdl	bdl	-
	1940	7.1	3.87E+04		bdl	bdl	-
	1940	3.0	3.87E+04		bdl	bdl	-
PW-2	4010	5.7	8.01E+04	PW Adj-2	910	1.8	1.82E+04
	4010	10.3	8.00E+04		910	5.0	1.81E+04
	4010	6.1	8.01E+04		910	2.0	1.82E+04
PW-3	9880	18.3	1.97E+05	PW Adj-3	1650	5.0	3.29E+04
	9880	13.3	1.97E+05		1650	2.3	3.30E+04
	9880	15.3	1.97E+05		1650	2.3	3.30E+04
PW-4	19900	33.3	3.97E+05	PW Adj-4	3580	9.2	7.14E+04
	19900	30.3	3.97E+05		3580	4.6	7.15E+04
	19900	48.1	3.97E+05		3580	4.9	7.15E+04
PW-5	29500	110.0	5.88E+05	PW Adj-5	6940	2.9	1.39E+05
	29500	78.4	5.88E+05		6940	4.3	1.39E+05
	29500	87.0	5.88E+05		6940	5.0	1.39E+05
PW-6	40500	216.0	8.06E+05	PW Adj-6	8050	4.0	1.61E+05
	40500	195.0	8.06E+05		8050	24.8	1.61E+05
	40500	137.0	8.07E+05		8050	10.7	1.61E+05
DW-1	1980	4.7	3.95E+04	DW Adj-1	bdl	bdl	-
	1980	2.2	3.96E+04		bdl	bdl	-
	1980	1.9	3.96E+04		bdl	bdl	-
DW-2	4030	5.6	8.05E+04	DW Adj-2	888	0.0	1.78E+04
	4030	2.5	8.06E+04		888	4.0	1.77E+04
	4030	3.3	8.05E+04		888	2.8	1.77E+04
DW-3	9950	21.1	1.99E+05	DW Adj-3	2790	5.9	5.57E+04
	9950	16.7	1.99E+05		2790	7.9	5.56E+04
	9950	13.0	1.99E+05		2790	9.0	5.56E+04
DW-4	19600	36.7	3.91E+05	DW Adj-4	3940	12.1	7.86E+04
	19600	53.5	3.91E+05		3940	9.2	7.86E+04
	19600	28.1	3.91E+05		3940	10.8	7.86E+04
DW-5	28900	107.0	5.76E+05	DW Adj-5	6060	16.2	1.21E+05
	28900	81.8	5.76E+05		6060	20.4	1.21E+05
	28900	70.7	5.77E+05		6060	17.8	1.21E+05
DW-6	38500	120.0	7.68E+05	DW Adj-6	8070	19.0	1.61E+05
	38500	127.0	7.67E+05		8070	18.5	1.61E+05
	38500	173.0	7.67E+05		8070	15.3	1.61E+05

bdl = below detection limit for this matrix

Table C-1.3 Silver Isotherm Data for Site 1 Soil

Set	C _i μg/L	C _f μg/L	S μg/kg	Set	C _i μg/L	C _f μg/L	S μg/kg
PW-1	7.7	bdl	-	PW Adj-1	9.6	bdl	-
	7.7	bdl	-		9.6	bdl	-
	7.7	bdl	-		9.6	bdl	-
PW-2	61.0	7.8	1064	PW Adj-2	110.0	9.5	2010
	61.0	7.1	1078		110.0	8.9	2022
	61.0	8.4	1052		110.0	8.5	2030
PW-3	74.2	23.8	1008	PW Adj-3	159.0	20.7	2766
	74.2	24.7	990		159.0	20.0	2780
	74.2	24.1	1002		159.0	22.5	2730
PW-4	79.4	26.9	1050	PW Adj-4	166.0	23.9	2842
	79.4	28.0	1028		166.0	29.4	2732
	79.4	28.1	1026		166.0	24.1	2838
PW-5	94.0	20.4	1472	PW Adj-5	166.0	26.6	2788
	94.0	20.6	1468		166.0	26.7	2786
	94.0	19.6	1488		166.0	25.6	2808
PW-6	94.3	41.1	1064	PW Adj-6	345.0	45.6	5988
	94.3	35.4	1178		345.0	40.2	6096
	94.3	35.6	1174		345.0	37.6	6148
PW-7	98.9	20.0	1578	PW Adj-7	524.0	55.2	9376
	98.9	20.6	1566		524.0	218.0	6120
	98.9	21.1	1556		524.0	53.1	9418
DW-1	0.0	bdl	-	DW Adj-1	bdl	bdl	-
	0.0	bdl	-		bdl	bdl	-
	0.0	bdl	-		bdl	bdl	-
DW-2	242.0	bdl	4740	DW Adj-2	223.0	bdl	4410
	242.0	bdl	4740		223.0	bdl	4414
	242.0	bdl	4796		223.0	bdl	4412
DW-3	468.0	6.5	9230	DW Adj-3	463.0	6.3	9134
	468.0	6.7	9226		463.0	5.7	9146
	468.0	7.3	9214		463.0	bdl	-
DW-4	478.0	6.5	9430	DW Adj-4	694.0	10.4	13672
	478.0	6.6	9428		694.0	10.8	13664
	478.0	5.9	9442		694.0	11.5	13650
DW-5	1010.0	20.6	19788	DW Adj-5	925.0	16.3	18174
	1010.0	18.8	19824		925.0	19.5	18110
	1010.0	20.1	19798		925.0	15.0	18200
DW-6	1980.0	78.9	38022	DW Adj-6	1790.0	82.0	34160
	1980.0	80.5	37990		1790.0	46.1	34878
	1980.0	81.6	37968		1790.0	72.6	34348
DW-7	3920.0	181.0	74780	DW Adj-7	2980.0	272.0	54160
	3920.0	218.0	74040		2980.0	251.0	54580
	3920.0	194.0	74520		2980.0	63.8	58324

bdl = below detection limit for this matrix

Table C-1.4 Thorium Isotherm Data for Site 1 Soil

Set	C _i μg/L	C _f μg/L	S μg/kg
PW-1	500	bdl	-
	500	bdl	-
	500	bdl	-
PW-2	2060	bdl	-
	2060	bdl	-
	2060	bdl	-
PW-3	4110	bdl	-
	4110	bdl	-
	4110	bdl	-
PW-4	4110	bdl	-
	4110	bdl	-
	4110	bdl	-
PW-5	20600	22.5	4.12E+05
	20600	13.7	4.12E+05
	20600	19.4	4.12E+05
PW-6	30000	30.4	5.99E+05
	30000	92.8	5.98E+05
	30000	69.5	5.99E+05
PW-7	38000	93	7.58E+05
	38000	62.3	7.59E+05
	38000	98.6	7.58E+05
DW-1	500	bdl	-
	500	bdl	-
	500	bdl	-
DW-2	2160	bdl	-
	2160	bdl	-
	2160	bdl	-
DW-3	4290	bdl	-
	4290	bdl	-
	4290	bdl	-
DW-4	10900	15.9	2.18E+05
	10900	bdl	-
	10900	bdl	-
DW-5	21000	46.7	4.19E+05
	21000	26.5	4.19E+05
	21000	17.2	4.20E+05
DW-6	32500	85.5	6.48E+05
	32500	35.2	6.49E+05
	32500	104	6.48E+05
DW-7	44100	100	8.80E+05
	44100	151	8.79E+05
	44100	84.5	8.80E+05

bdl = below detection limit for this matrix

Table C-1.5 Uranium Isotherm Data for Site 1 Soil

Set	C _i μg/L	C _f μg/L	S μg/kg	Set	C _i μg/L	C _f μg/L	S μg/kg
PW-1	223	bdl	-	PW Adj-1	bdl	bdl	-
	223	bdl	-		bdl	bdl	-
	223	bdl	-		bdl	bdl	-
PW-2	422	230	3840	PW Adj-2	977	588	7780
	422	248	3480		977	565	8240
	422	218	4080		977	578	7980
PW-3	1070	657	8260	PW Adj-3	1930	1200	14600
	1070	641	8580		1930	1190	14800
	1070	653	8340		1930	1180	15000
PW-4	2170	1420	15000	PW Adj-4	2880	1850	20600
	2170	1410	15200		2880	1850	20600
	2170	1360	16200		2880	1900	19600
PW-5	3220	2160	21200	PW Adj-5	3610	2540	21400
	3220	2190	20600		3610	2590	20400
	3220	2190	20600		3610	2590	20400
PW-6	4160	2900	25200	PW Adj-6	6460	4690	35400
	4160	2900	25200		6460	4720	34800
	4160	2900	25200		6460	4760	34000
PW-7				PW Adj-7	9510	7000	50200
					9510	6860	53000
					9510	7070	48800
DW-1	186	bdl	-	DW Adj-1	bdl	bdl	-
	186	bdl	-		bdl	bdl	-
	186	bdl	-		bdl	bdl	-
DW-2	395	bdl	-	DW Adj-2	804	bdl	11080
	395	bdl	-		804	bdl	11080
	395	bdl	-		804	bdl	11080
DW-3	1000	166	16680	DW Adj-3	1790	254	30720
	1000	168	16640		1790	251	30780
	1000	165	16700		1790	262	30560
DW-4	2040	533	30140	DW Adj-4	2770	463	46140
	2040	520	30400		2770	473	45940
	2040	527	30260		2770	479	45820
DW-5	3250	1090	43200	DW Adj-5	3750	650	62000
	3250	1140	42200		3750	673	61540
	3250	1130	42400		3750	662	61760
DW-6	4300	1900	48000	DW Adj-6	6620	1400	104400
	4300	1960	46800		6620	1410	104200
	4300	1870	48600		6620	1390	104600
DW-7				DW Adj-7	9230	2320	138200
					9230	2270	139200
					9230	2420	136200

bdl = below detection limit for this matrix

C-2. Isotherm Results for Uranium on Site 6 and 7 Soils

Table C-2.1 Uranium Isotherm Data for Site 6 Soil

Set	C _i μg/L	C _f μg/L	S μg/kg	Set	C _i μg/L	C _f μg/L	S μg/kg
PW-1	2.8	3.2	-	PW Adj-1	2.8	3.3	-
	2.8	3.2	-		2.8	3.5	-
	2.8	3.1	-		2.8	3.3	-
PW-2	711	425	5720	PW Adj-2	709	360	6980
	711	400	6220		709	352	7140
	711	369	6840		709	354	7100
PW-3	1320	706	12280	PW Adj-3	1220	644	11520
	1320	726	11880		1220	623	11940
	1320	704	12320		1220	627	11860
PW-4	2170	1120	21000	PW Adj-4	1880	1090	15800
	2170	1170	20000		1880	1060	16400
	2170	1220	19000		1880	1090	15800
PW-5	4140	2630	30200	PW Adj-5	3760	2400	27200
	4140	2740	28000		3760	2410	27000
	4140	2570	31400		3760	2490	25400
PW-6	6020	3790	44600	PW Adj-6	5560	3910	33000
	6020	3890	42600		5560	3940	32400
	6020	3810	44200		5560	3900	33200
PW-7	8210	5600	52200	PW Adj-7	7620	5760	37200
	8210	5320	57800		7620	5880	34800
	8210	5630	51600		7620	5660	39200
DW-1	6.3	0.36	119	DW Adj-1	6.3	0.81	110
	6.3	0.41	118		6.3	0.43	117
	6.3	0.36	119		6.3	0.58	114
DW-2	756	80.2	13516	DW Adj-2	720	54.6	13308
	756	80.3	13514		720	52.3	13354
	756	78.6	13548		720	57.3	13254
DW-3	1280	192	21760	DW Adj-3	1230	112	22360
	1280	189	21820		1230	110	22400
	1280	195	21700		1230	111	22380
DW-4	2150	475	33500	DW Adj-4	1890	238	33040
	2150	488	33240		1890	218	33440
	2150	458	33840		1890	228	33240
DW-5	3960	1620	46800	DW Adj-5	3730	581	62980
	3960	1640	46400		3730	557	63460
	3960	1660	46000		3730	545	63700
DW-6	5550	3240	46200	DW Adj-6	5580	989	91820
	5550	3090	49200		5580	950	92600
	5550	3520	40600		5580	896	93680
DW-7	7450	4870	51600	DW Adj-7	7540	1550	119800
	7450	5600	37000		7540	1400	122800
	7450	5430	40400		7540	1530	120200

Table C-2.2 Uranium Isotherm Data for Site 7 Soil

Set	C _i μg/L	C _f μg/L	S μg/kg	Set	C _i μg/L	C _f μg/L	S μg/kg
PW-1	2.8	2.5	6	PW Adj-1	2.8	3.1	0
	2.8	2.5	6		2.8	4.6	0
	2.8	2.5	6		2.8	4.9	0
PW-2	711	386	6500	PW Adj-2	709	374	6700
	711	389	6440		709	376	6660
	711	377	6680		709	381	6560
PW-3	1320	679	12820	PW Adj-3	1220	639	11620
	1320	642	13560		1220	646	11480
	1320	666	13080		1220	654	11320
PW-4	2170	1170	20000	PW Adj-4	1880	1090	15800
	2170	1080	21800		1880	1100	15600
	2170	1070	22000		1880	1110	15400
PW-5	4140	2470	33400	PW Adj-5	3760	2440	26400
	4140	2570	31400		3760	2440	26400
	4140	2320	36400		3760	2500	25200
PW-6	6020	3860	43200	PW Adj-6	5560	3850	34200
	6020	3720	46000		5560	3940	32400
	6020	3790	44600		5560	3700	37200
PW-7	8210	5410	56000	PW Adj-7	7620	5480	42800
	8210	6240	39400		7620	5450	43400
	8210	5800	48200		7620	5910	34200
DW-1	6.3	0.28	120	DW Adj-1	6.3	0.24	121
	6.3	0.28	120		6.3	0.29	120
	6.3	0.24	121		6.3	0.24	121
DW-2	756	84.7	13426	DW Adj-2	720	55.5	13290
	756	84.8	13424		720	53.6	13328
	756	90.8	13304		720	51.5	13370
DW-3	1280	204	21520	DW Adj-3	1230	108	22440
	1280	209	21420		1230	103	22540
	1280	207	21460		1230	98.6	22628
DW-4	2150	485	33300	DW Adj-4	1890	210	33600
	2150	473	33540		1890	213	33540
	2150	483	33340		1890	208	33640
DW-5	3960	1610	47000	DW Adj-5	3730	536	63880
	3960	1620	46800		3730	576	63080
	3960	1580	47600		3730	554	63520
DW-6	5550	3130	48400	DW Adj-6	5580	969	92220
	5550	3290	45200		5580	973	92140
	5550	3140	48200		5580	955	92500
DW-7	7450	4990	49200	DW Adj-7	7540	1370	123400
	7450	5220	44600		7540	1410	122600
	7450	5200	45000		7540	1400	122800

C-3. Soil Column Bromide and Uranium Effluent Concentrations

Table C-3.1 Bromide Breakthrough for Site 6 Columns

Sample	Column 6-1			Column 6-2			Column 6-3		
	Time (min)	Flow (mL/min)	Br (ppm)	Time (min)	Flow (mL/min)	Br (ppm)	Time (min)	Flow (mL/min)	Br (ppm)
2	24.7	0.82	0.3	24.6	0.81	0.1	24.0	0.82	0.3
4	49.6	0.79	0.1	48.7	0.83	0.2	47.2	0.86	0.2
6	74.3	0.80	0.3	73.1	0.79	0.2	70.6	0.85	0.2
8	98.7	0.82	0.1	97.3	0.86	0.2	93.6	0.88	0.2
10	123.2	0.81	0.2	121.6	0.82	0.2	117.1	0.84	0.3
12	146.3	0.91	1.7	145.5	0.85	1.5	141.7	0.79	1.6
13	159.3	0.77	4.0	157.5	0.83	3.6	154.1	0.80	3.8
14	171.7	0.81	7.0	170.1	0.79	6.9	165.7	0.86	6.0
15	184.0	0.81	10.3	182.3	0.82	10.7	178.2	0.80	8.7
16	196.2	0.82	13.2	194.6	0.81	13.8	190.6	0.81	11.9
17	208.2	0.83	15.3	202.1	1.34	15.5	202.4	0.84	14.5
18	221.6	0.75	16.9	219.4	0.58	16.9	214.8	0.81	16.4
19	233.1	0.87	17.7	232.1	0.79	17.4	227.4	0.79	17.6
20	245.9	0.78	18.2	244.8	0.79	18.0	239.4	0.83	18.1
21	257.1	0.90	18.4	257.9	0.77	18.1	251.7	0.81	18.2
22	269.6	0.80	18.5	268.8	0.91	18.3	264.0	0.81	18.5
23	281.9	0.81	18.5	281.3	0.80	ns	276.0	0.83	18.5
25	306.7	0.81	18.6	306.7	0.76	18.5	300.1	0.85	18.7
27	331.3	0.82	18.7	330.1	0.84	18.7	325.1	0.83	18.7
29	355.7	0.83	18.7	354.4	0.82	18.9	350.3	0.82	18.7
31	380.3	0.80	18.7	378.9	0.82	18.9	374.2	0.82	18.8
33	404.4	0.92	18.8	402.6	0.80	18.9	399.3	0.75	18.9

ns = not sampled

Table C-3.2 Uranium Breakthrough for Site 6 Columns

Pore Volumes	Column 6-1			Column 6-2			Column 6-3		
	Time (d)	Flow (mL/min)	U (µg/L)	Time (d)	Flow (mL/min)	U (µg/L)	Time (d)	Flow (mL/min)	U (µg/L)
10	0.9	0.82	2.9	0.9	0.82	2.9	0.9	0.81	3
20	1.7	0.81	3.3	1.8	0.82	3.4	1.8	0.83	2.9
30	2.6	0.81	3.2	2.6	0.82	3.3	2.9	0.62	2.9
40	3.4	0.79	3.4	3.4	0.80	3.7	4.0	0.62	3.6
50	4.3	0.80	9.2	4.3	0.81	8.1	5.1	0.64	9.8
60	5.2	0.75	40.6	5.2	0.82	50.7	6.3	0.62	38.1
70	6.3	0.60	84.9	6.0	0.81	107	7.3	0.66	86.2
80	7.5	0.58	134	6.9	0.80	186	8.5	0.60	146
90	8.6	0.59	185	7.8	0.80	244	9.6	0.61	205
100	9.8	0.59	222	8.7	0.80	290	10.7	0.60	243
110	11.0	0.59	249	9.5	0.79	301	11.9	0.62	278
120	12.1	0.60	259	10.4	0.82	322	13.0	0.61	289
130	13.3	0.60	282	11.2	0.81	320	14.1	0.61	306
140	14.4	0.61	299	12.5	0.34	339	15.3	0.61	317
150	15.6	0.60	303	14.4	0.37	342	16.4	0.68	318
160	16.7	0.60	311	16.5	0.33	355	17.6	0.61	330
170	17.8	0.62	339	18.5	0.35	352	18.7	0.61	335
180	19.0	0.60	348	20.4	0.36	355	19.8	0.58	338
190	20.2	0.60	336	22.4	0.38	336	21.0	0.61	333
200	21.3	0.60	333	24.2	0.38	ns	22.1	0.60	329

ns = not sampled

Table C-3.3 Bromide Breakthrough for Site 7 Columns

Sample	Column 7-1			Column 7-2			Column 7-3		
	Time (min)	Flow (mL/min)	Br (ppm)	Time (min)	Flow (mL/min)	Br (ppm)	Time (min)	Flow (mL/min)	Br (ppm)
2	24.3	0.83	0.2	21.2	0.73	0.2	24.7	0.83	0.2
4	48.7	0.81	0.3	44.8	0.85	0.2	49.4	0.82	0.2
6	73.1	0.83	0.2	69.7	0.75	0.2	74.3	0.79	0.2
8	97.2	0.83	0.3	93.5	0.83	0.2	98.5	0.83	0.7
10	121.7	0.83	0.6	118.0	0.82	0.6	123.1	0.81	0.3
12	146.1	0.82	3.9	142.6	0.82	3.2	147.5	0.81	1.8
13	158.0	0.84	6.5	154.8	0.82	5.5	159.7	0.82	3.4
14	170.4	0.81	9.2	167.0	0.83	7.9	171.7	0.83	5.4
15	182.7	0.82	11.6	179.3	0.81	10.1	183.8	0.82	7.4
16	194.8	0.83	13.6	191.8	0.80	12.4	204.3	0.49	10.1
17	206.8	0.83	15.4	203.9	0.82	14.5	208.4	2.44	12.5
18	219.2	0.81	17.0	216.2	0.82	16.2	220.5	0.82	14.7
19	231.3	0.83	18.1	228.7	0.80	17.1	232.6	0.83	16.4
20	243.7	0.81	18.5	241.3	0.79	17.7	244.8	0.82	17.4
21	256.2	0.80	18.8	253.7	0.81	18.0	257.1	0.81	17.8
22	268.5	0.81	18.4	266.1	0.81	18.3	269.4	0.81	18.3
23	282.1	0.74	19.0	278.4	0.81	18.4	281.7	0.82	18.9
25	307.3	0.79	19.0	305.2	0.70	18.6	308.2	0.80	18.7
27	331.9	0.80	19.1	329.8	0.81	18.7	332.8	0.82	18.9
29	356.9	0.80	19.2	354.7	0.81	18.7	357.8	0.80	19.0
31	381.8	0.81	19.2	379.8	0.81	18.8	383.0	0.80	19.1
33	407.6	0.82	19.2	404.8	0.81	18.9	408.8	0.76	19.2

Table C-3.4 Uranium Breakthrough for Site 7 Columns

Pore Volumes	Column 7-1			Column 7-2			Column 7-3		
	Time (d)	Flow (mL/min)	U ($\mu\text{g/L}$)	Time (d)	Flow (mL/min)	U ($\mu\text{g/L}$)	Time (d)	Flow (mL/min)	U ($\mu\text{g/L}$)
10	0.9	0.82	2.3	0.9	0.82	2.2	0.9	0.82	2.2
20	1.8	0.80	2.3	1.7	0.80	2.5	1.8	0.80	2.2
30	2.6	0.81	2.2	2.6	0.80	2.5	2.6	0.79	2.4
40	3.5	0.76	10.8	3.5	0.77	7.8	3.5	0.79	5.7
50	4.4	0.80	46.8	4.3	0.81	41.5	4.3	0.83	34.6
60	5.2	0.81	92.8	5.2	0.82	92.1	5.2	0.82	74.7
70	6.1	0.73	144	6.1	0.81	152	6.1	0.77	127
80	7.0	0.80	182	6.9	0.81	193	6.9	0.80	179
90	7.9	0.82	214	7.8	0.78	224	7.8	0.79	219
100	8.7	0.81	262	8.7	0.79	259	8.6	0.80	260
110	9.6	0.82	279	9.5	0.82	283	9.7	0.61	281
120	10.6	0.81	310	10.4	0.79	305	10.8	0.62	294
130	11.4	0.81	313	11.2	0.80	315	11.9	0.62	299
140	12.2	0.85	318	12.1	0.77	314	13.1	0.60	316
150	13.1	0.80	329	13.0	0.80	341	14.4	0.41	312
160	14.0	0.80	334	13.8	0.79	325	16.2	0.41	321
170	14.9	0.83	325	14.7	0.79	330	18.0	0.33	309
180	15.8	0.80	330	15.6	0.80	328			ns
190	16.6	0.79	332	16.4	0.80	330			ns
200	17.5	0.79	357	17.6	0.57	365			ns

ns = not sampled

Table C-3.5 Bromide Breakthrough for Site 1 Column

Sample	Column 1-2		
	Time (min)	Flow (mL/min)	Br (ppm)
2	31.7	0.63	0.1
4	64.6	0.61	0.3
6	96.9	0.63	0.3
8	131.8	0.61	0.3
10	165.6	0.60	0.2
12	199.0	0.60	1.7
13	215.1	0.62	4.0
14	231.1	0.63	8.1
15	247.4	0.61	11.4
16	264.0	0.60	13.5
17	281.1	0.58	15.9
18	296.8	0.64	16.9
19	313.0	0.62	17.8
20	329.0	0.63	18.2
21	345.3	0.61	18.4
22	361.8	0.61	18.6
23	378.0	0.62	18.7
25	410.6	0.62	18.7
27	443.2	0.62	18.8
29	475.4	0.62	18.9
31	507.8	0.62	19.0
33	540.4	0.61	19.0

Table C-3.6 Uranium Breakthrough for Site 1 Columns

Pore Volumes	Column 1-2		
	Time (d)	Flow (mL/min)	U (µg/L)
4	0.5	0.59	1.8
10	1.2	0.46	1.8
19	2.4	0.49	1.8
24	3.1	0.51	1.9
30	4.0	0.49	1.9
46	6.1	0.51	2.8
52	7.0	0.50	7.3
60	8.4	0.41	17.9
70	10.1	0.40	50.7
80	11.8	0.41	79.8
88	13.2	0.39	92.9
93	14.1	0.38	118
100	15.3	0.40	144
110	17.1	0.39	207
116	18.1	0.40	180
121	19.0	0.40	208
128	20.2	0.39	203
134	21.2	0.39	248
140	22.3	0.39	265
151	24.2	0.40	302
157	25.2	0.41	331
163	26.3	0.40	341
169	27.3	0.40	350
173	28.0	0.39	348
182	29.6	0.42	366
190	31.0	0.40	371
197	32.2	0.40	364
202	33.0	0.40	367